The Role of Nitric Oxide in Lacrimal Gland Hypofunction and the Antisecretory Action of Anti-Muscarinic Autoantibodies Associated with Sjögren's Syndrome.

Thesis submitted in accordance with the requirements of the University of Liverpool for the degree of Doctor in Philosophy

By

John Charles Malone

January 2012

Acknowledgements

My most sincere thanks must go to my primary supervisor, Dr. Pete Smith, for his guidance, wisdom, and most of all, patience. Without those, and more, this thesis would not even exist.

Likewise, my thanks go to Dr. Luke Dawson, my second supervisor. For always taking the time whenever needed to offer guidance, cruelly taken from us in the move from the Edwards Building.

Thanks also to Dr. John Stanbury, for his technical support, and everyone else at the lab who helped me maintain what little is left of my sanity, or at least stayed out of my way.

Special mention will have to go to my good friend Mr. Robert Clarke who put a roof over my head for a year and asked for nothing in return.

And to Sarah, who has had to put up with me while I wrote the thesis and never complained once. Okay, maybe a little bit.

Also my thanks to the British Sjögren's syndrome association (BSSA) for funding the research and the Arthritis Research Council (ARC) for the grant.

Abstract

Sjögren's syndrome (SjS) is a systemic autoimmune disorder specifically targeting the exocrine glands, primarily the salivary and lacrimal glands. The autoimmune attack upon these organs is characterised by lymphocytic infiltration of the salivary and lacrimal glands, leading to an impairment of secretory function. Little is known about the mechanisms underlying glandular hypofunction, because the condition is very difficult to detect at an early stage, rendering treatment difficult.

Recent studies in salivary glands have identified a mechanism whereby the inflammatory mediator NO, acting through cGMP and cADPr, can modulate the fluid secretory process. Thus NO production may contribute to the glandular hypofunction associated with SjS. The likelihood that NO plays a key role in the aetiology of SjS would be greatly increased if it may be demonstrated that NO perturbed fluid secretion in lacrimal, as well as salivary gland acinar cells.

Using microfluorimetric and patch clamp techniques I have shown that the acute response of lacrimal acinar cells exposed to NO is an amplification of the muscarinic agonist evoked Ca^{2+} signal. Also, that this amplification is probably mediated through increased ryanodine receptor sensitivity. Chronic exposure to NO in salivary gland acinar cells has been shown to inhibit the response to muscarinic agonist. Observation of the same effect in lacrimal gland cells would suggest that increased levels of NO may be a unifying factor between two separate secretory organs for the glandular hypofunction associated with SjS.

Inhibition of secretion by anti-muscarinic receptor autoantibodies represents a complimentary mechanism of glandular hypofunction and one which also has the potential to aid in early detection of the condition. These autoantibodies are very difficult to detect using conventional immunological techniques, but represent an attractive target for being the basis of a diagnostic test.

My data demonstrate a similar pattern of response in lacrimal to salivary gland acinar cells, but also demonstrate that lacrimal acinar cells are capable of endogenous NO production. The mechanism by which NO modulates secretory mechanisms appears to be a universal feature of the exocrine glands affected by SjS. However, my data suggest at least quantitative differences in the role of NO in glandular function. These data represent further elucidation of the role of NO in glandular hypofunction in SjS, highlighting fundamental differences between two similar gland systems affected by SjS, potentially affecting avenues of treatment.

I have also demonstrated that anti-muscarinic receptor autoantibodies may be detected using conventional microfluorimetric techniques and I have developed a semi-automated fluorimetric tool that allows rapid screening and detection of autoantibodies within the isolated IgG fraction of patient serum. Preliminary data indicate that the sensitivity and specificity of detection of antimuscarinic autoantibodies was not sufficiently high enough to offer significant improvement over current methods for detecting SjS.

Abreviations

$[Ca^{2+}]_i$	intracellular free Ca^{2+} activity
7NI	7 nitroindazole
ACh	acetylcholine
ADMA	asymmetric dimethylarginine
AM *(as suffix)*	acetoxymethyl ester
AQP	aquaporin
Asp	aspartate
ATP	adenosine trisphosphate
AUC	area under the curve
BH_4	tetrahydrobiopterin
cADPr	cyclic adenosine diphosphate ribose
CaM	calmodulin
cAMP	cyclic adenosine monophosphate
CCh	Carbachol, carbamylcholine chloride
cDNA	complimentary deoxyribonucleic acid
cGMP	cyclic guanosine monophosphate
CHO-M3	chinese hamster ovary cells stably transfected with M3R
CICR	calcium-induced-calcium release
CNS	central nervous system
Da	dalton
DA *(as suffix)*	diacetate
DAF2	diaminofluorescein –2
DAG	diacylglycerol
dH_2O	deionized water
DMEM : F12	Dulbecco's Modified Eagle's Medium/Nutrient F-12 Ham
DMSO	dimethyl sulfoxide
DNA	deoxyribonucleic acid
DPI	diphenyleneiodonium chloride
EDRF	endothelial derived relaxing factor
EDTA	Ethylenediaminetetraacetic acid
EGTA	ethylene glycerol bis(b-aminoethyl ether)-N,N,N',N',-tetraacetic acid
EHS	Engelbreth-Holm-Swarm
ELISA	enzyme-linked immunosorbent assay

eNOS	endothelial nitric oxide synthase
ER	endoplasmic reticulum
ER	endoplasmic reticulum
FAD	flavin adenine dinucleotide
FMN	flavin mononucleotide
G protein	guanosine triphosphate -binding protein
GAP	guanosine trisphosphate activating protein
GDP	guanosine diphosphate
GTP	guanosine trisphosphate
Gαq	GTP-binding protein α subunit type q
HEPES	N-2 hydroxyethyl-piperazine-N'2-ethanesulfonic acid
HLA	human leukocyte antigen
HSG	human salivary gland epithelial cell line
IgG	Immunoglobulin G
IL-1 β	Interleukin-1 β
iNOS	inducible nitric oxide synthase
IP_3	inositol 1,4,5 triphosphate
IP_3R	inositol 1,4,5 triphosphate receptor
JNK	c-Jun N-terminal kinase
KCS	keratoconjunctivitis sicca
KEK-M3	human embryonic kidney 293 cells stably transfected with M3R
L-NAME	L-N^G-Nitroarginine methyl ester
LPS	lipopolysaccharide
M1R	type 1 muscarinic acetylcholine receptor
M3R	type 3 muscarinic acetylcholine receptor
M5R	type 5 muscarinic acetylcholine receptor
mAChR	muscarinic acetylcholine receptor
MALToma	mucosa associated lymphoid tissue lymphoma
MEM	Modified Eagle's Medium
MS	multiple sclerosis
mtNOS	mitochondrial nitric oxide synthase
NAD^+	nicotinamide adenine dinucleotide
NADPH	nicotinamide adenine dinucleotide phosphate
NFκB	nuclear factor-κB

nNOS	neuronal nitric oxide synthase
NOD	non-obese diabetic
NOS	nitric oxide synthase
ODQ	1H-[1,2,4]Oxadiazolo[4,3]quinoxalin-1-one
PBS	Dulbecco's Phosphate Saline Buffer
PIP_2	phosphotidylinositol 4, 5, bisphosphate
PKC	protein kinase C
PMCA4b	plasma membrane calcium ATPase
PNS	peripheral nervous system
pSjS	primary Sjögren's syndrome
RA	rheumatoid arthritis
RNA	ribonucleic acid
RNS	reactive nitrogen species
ROC	receiver-operating characteristic
ROS	reactive oxygen species
RyR	ryanodine receptor
sGC	soluble guanylyl cyclase
SH-SY5Y	human derived neuroblastoma cell line
SjS	Sjögren's syndrome
SLE	systemic lupus erythematosus
SM	submandibular
SMT	S-methyl isothio urea
SNAP	S-nitrosothiol, S- nitroso-N-acetyl-penicillamine
SOC	store operated Ca^{2+} channel/current
SS-A	anti-Ro autoantibody
SS-B	anti-La autoantibody
SSDI	Sjogren's syndrome damage index
sSjS	Secondary Sjogren's syndrome
SSNA-1	Sjogren's syndrome nuclear antigen-1
TM	trans-membrane domain
TNFα	Tumour Necrosis Factor α
Tyr	tyrosine
βPLC	β phosphoinositide specific phospholipase C enzyme

1 INTRODUCTION

1.1 Lacrimal gland anatomy, structure and function

The Role of tears in ocular health

The major function of precorneal film is, at its most basic level, is to keep the surface of the eye moist. The tear film acts to protect the eye surface, supplying nutrients, providing lubrication, and allowing for cleaning of the ocular surface. The tear film itself consists of 3 layers, lipid (0.1–0.2 μm thick), aqueous (7–8 μm thick) and mucous layers (30 μm thick) (Walcott 1998), each serving distinct functions.

Outermost on the eye surface, the lipid layer, which is secreted by the meibomian glands, primarily functions to provide a smooth optical surface and prevent evaporation of the tear film (Bron, Tiffany et al. 2004). The mid layer of the tear film, the aqueous layer, is secreted by the lacrimal gland and serves several functions: allowing for gaseous exchange- providing the eye surface epithelium with oxygen and provides a smooth surface for the eye – allowing not only a smooth movement of the lid over the eye surface, but also allows for a sharper image to be formed on the retina. The aqueous layer also allows for the removal of bacteria and dead cells from the eye surface (Walcott 1998). Closest to the corneal epithelium is the mucous layer, secreted by conjunctival goblet cells, which allows for the even spreading of the tear film.

The tear film shows a large degree of variation, dependent upon factors including age, environment, and emotional state. When the eye is closed for a prolonged time (such as sleep) IgA becomes a predominant protein present in the tear film, yet is near absent in reflex tearing (Sack, Tan et al. 1992). Quality of the tear film has also been shown to

decrease with advancing age (Ozdemir and Temizdemir 2010), and is associated with a decline in sex steroids (Krenzer, Dana et al. 2000; Sullivan, Sullivan et al. 2000).

Gross anatomy

The Lacrimal gland is responsible for the secretion of water, proteins, mucins and electrolytes (referred to as lacrimal gland fluid) maintaining the integrity and composition of the tear film. In many species, most notably humans, the lacrimal gland is an almond shaped gland situated just above the eye, within the bony orbit. Connecting the exorbital lacrimal gland to ocular surface is the excretory duct, which runs forward across the temporal muscle to the outer part of the upper eyelid (See figure 1.1.1). The gland consists mainly of lobules separated from each other by loose connective tissue (Iwamoto and Jakobiec 1982; Obata 2006). The gland's gross structure is almond shaped, and is tubuloacinar- consisting of about 80% acinar cells and 10-12% ductal cells. Both of these cell types are polarized, with the apical pole responsible for exocytosis and ion secretion. The basolateral membrane of the cell is host to the neurotransmitter receptors responsible for the initiation of secretion, as well as ion pumps required for the transcellular movement of electrolytes that drive fluid secretion (Walcott 1998).

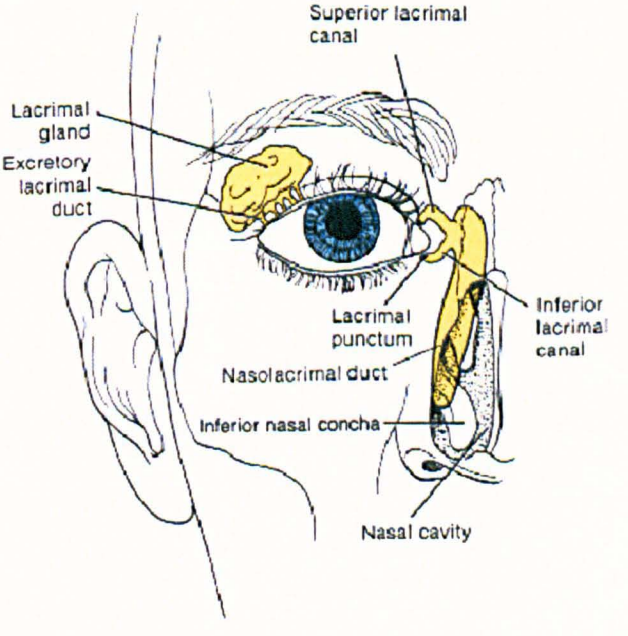

Figure 1.1.1 Anterior view of the human lacrimal apparatus

Lacrimal Gland Innervation

The lacrimal gland is innervated by sympathetic and parasympathetic nerves, although the latter predominate. It has been demonstrated via immunofluorescence microscopy, that there is dense innervation of the lacrimal gland by parasympathetic nerves in all species (Ruskell 1969; Ruskell 1971; Dartt, Baker et al. 1984; Dartt, Donowitz et al. 1984). The density of sympathetic innervations is subject to some controversy, having been shown to be dependant upon species, as well as differences in distinct areas of the lacrimal gland (Ding, Walcott et al. 2003). Where there are differing findings regarding the sympathetic innervation of the lacrimal gland, data consistently shows that loss of either pre, or post-ganglionic parasympathetic (but not sympathetic) innervations results in a drastic drop in secretion (Meneray et al. 1998) Sympathetic denervation of the rabbit lacrimal gland did not alter acinar morphology, nor induced denervation hypersensitivity of protein secretion (Meneray, Bennett et al. 1998). Pre and post-ganglionic denervation resulted in alteration of acinar morphology and loss of lacrimal gland function (Ruskell 1969; Butler, Ruskell et al. 1984; Toda, Ayajiki et al. 2000; Toshida, Nguyen et al. 2007). Overall, the nervous supply to the lacrimal gland serves the purpose of delivering neurotransmitter to receptors on the gland and initiating the intracellular signal cascade resulting in secretion.

Signal transduction in secretory glands

Acetylcholine is a neurotransmitter active in both the peripheral and central nervous systems. In the PNS acetylcholine has a role in skeletal muscle movement, and in the activation of cardiac and smooth muscle. In the CNS, acetylcholine is implicated in mood and memory (Pepeu and Giovannini 2010). ACh was the first neurotransmitter to be identified, initially by Henry Hallett Dale in 1914 for its actions upon heart tissue, and confirmed as such by Otto Loewi in 1929. It was this work for which both would receive the Nobel Prize in Medicine or Physiology in 1936.

ACh is secreted from axons into the synaptic cleft; from here it diffuses a small distance to its target receptors. In the salivary and lacrimal glands, those target receptors are the muscarinic acetylcholine receptors (mAChR).

Muscarinic Receptors

The mAChR belong to a class of metabotrophic (non pore forming) receptors which are bound to G proteins (heterotrimeric guanine nucleotide binding proteins) as part of their signaling process (Wess, Blin et al. 1995). The mAChR family is made up of 5 subtypes, designated M1- M5 (Hulme, Birdsall et al. 1990), identified by data from cDNA cloning, their coupled G proteins and their interactions with agonists and antagonists (Caulfield and Birdsall 1998). All 5 muscarinic receptors share a similar 3 dimensional structure, comprising of seven trans-membrane domains (TM I-VII), three extracellular loops, and three intracellular loops (i1- i3) (Wess, Blin et al. 1995). While secretion in salivary and lacrimal glands is predominantly governed by the M3R, evidence suggests that the M1R, acting through Gαq, may also be important in salivary secretion (Culp, Luo et al. 1996) The binding of ACh to the M3R is the first step in a signal cascade, with the final step being the secretion

of fluid and proteins. Data suggest that ACh binds to the M3R within a narrow cleft formed by the ring arrangement formed by the 7 transmembrane domains. The use of site directed mutagenesis upon rat M3R suggested that the ACh binding domain is formed by a series of hydrophilic amino acids that are located within the upper half of the transmembrane domains between TMs III, V,VI and VII, that likely consist of aspartate (Asp) and Tyrosine (Tyr). The negatively charged TM III aspartate residue, highly conserved between biogenic amine receptors, is most likely the site for the interaction due to ACh being positively charged (Wess, Blin et al. 1995).

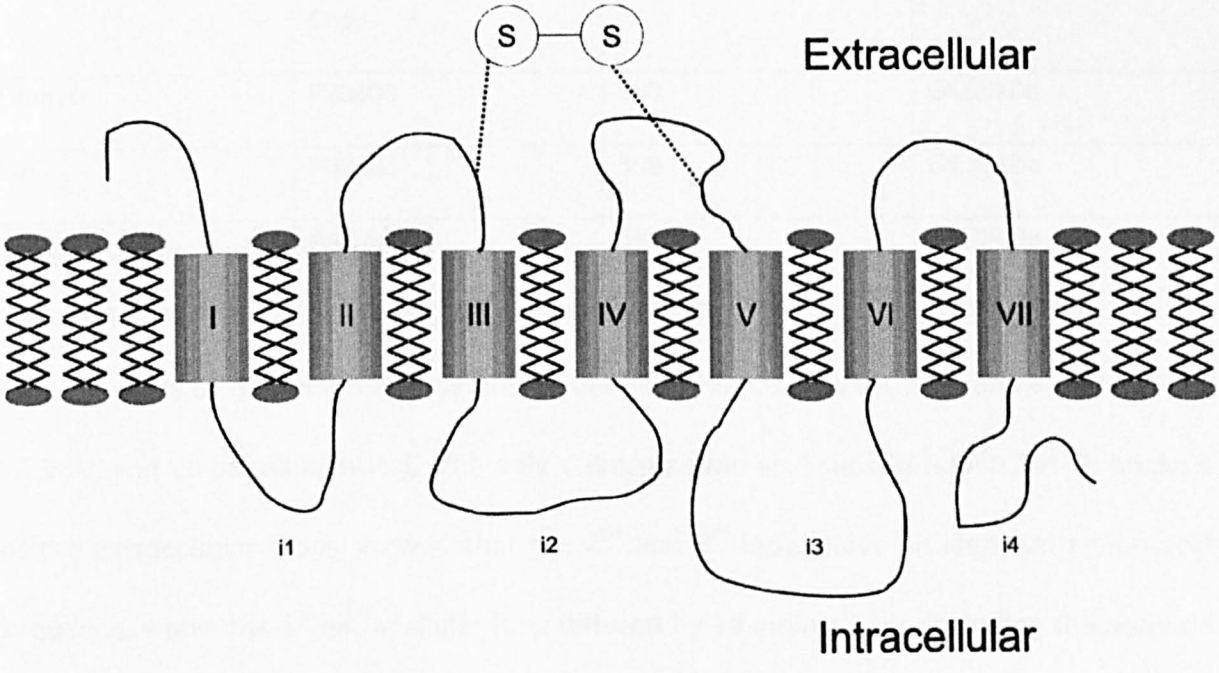

Figure 1.1.2 Diagrammatic representation of the components of muscarinic receptors in the cell membrane. I-VII represent transmembrane domains. i1- i4 represent the intracellular loops.

Based upon their pharmacological profiles there does not seem to be any significant difference between M3Rs between species (Caulfield and Birdsall 1998). The M3R retains a highly conserved sequence and structure across species, rat and mouse M3R both comprise of a 589 amino acid sequence, have a molecular mass of 64.78 kDa and have an amino acid sequence differing only by 16 amino acids. Human M3R comprises of 590 amino acids with a molecular mass of 64.90 kDa. Allowing for conservative changes in amino acid sequence there is still a 94.4% homology between the human and rat M3R.

Species	GenPet Accession Code	Amino Acid No.	Molecular Mass
Human	P20309	590	64.90kDa
Rat	P08483	589	64.79kDa
Mouse	AAG14344	589	64.79kDa

Table 1.1.1 Basic data for mouse, human and rat M3R.

Close analysis of the amino acid sequence between human and rat M3R show that TMI, II, IV, V, VI and VII are all identical, with only a single amino acid substitution in TM III. Analysis of the extracellular loops showed that the 2nd and 3rd loops have an identical amino acid sequence, whilst the 1st extracellular loop differed by 14 amino acids, including the addition of a glycine residue at position 54 of the human M3R.

G proteins

Binding of the ACh to the M3R allows for a conformational change in the receptor, resulting in the activation of the coupled G protein. The exact nature of the conformational change is still under investigation, but current data suggest that agonist binding results in an increase in proximity of the extracellular segments of TM III and VII (Han, Hamdan et al. 2005), allowing further conformational change, including rotation of the cytoplasmic end of TM VI (Ward, Hamdan et al. 2002; Ward, Hamdan et al. 2006) and an increase in proximity of the cytoplasmic ends of TM I and VII (Han, Hamdan et al. 2005). These conformational changes may allow for G protein access to previously inaccessible M3R residues and allow for G protein/ receptor coupling, with a recent study implicating an interaction between the i2 loop on the M3R and the Gα subunit (Hu, Wang et al. 2010).

The coupled G protein family has a heterotrimeric structure, consisting of α, β, and γ subunits. Upon the basis of their α subunits, the G proteins are divided into 4 families: s, i, q and 12/13 (Morris and Malbon 1999). In the salivary and lacrimal glands the M3R is coupled to G αq protein. Activation of the G protein is brought about by the release of GDP from the guanine nucleotide binding site of the α-subunit. Following the GDP release, GTP rapidly binds to the α-subunit, causing dissociation of the heterotrimer into a GTP bound α-subunit, and a β γ heterodimer. The length of time of the activation is governed by the GTP-ase activity of the α-subunit, since the hydrolysis of GTP to GDP releases the α subunit and the αβγ heterotrimer re-associates ready for another round of activation (Morris and Malbon 1999). It is the dissociation of the G protein into its subunits that provides the next link in the signal cascade- the β phosphoinositide specific phospholipase C enzyme (βPLC).

βPLC is targeted by the dissociated Gαq subunit, interacting and regulating βPLC's activity, although the βγ dimer is also active in this process (Berstein, Blank et al. 1992; Boyer, Waldo et al. 1992). βPLC itself is also active in this process, acting as a GTP activating protein (GAP) (Berstein, Blank et al. 1992). PLCs are soluble multidomain proteins, the βPLC having 4 isoforms (Rebecchi and Pentyala 2000). Activation of the βPLC by the G protein α subunit allows the βPLC to cleave the polar head group from inositol phospholipids and hydrolyse the membrane bound phosphotidylinositol 4, 5, bisphosphate (PIP_2), generating two 2^{nd} messenger signaling molecules 1,4,5 inositol triphosphate (IP_3) and diacylglycerol (DAG). The role of IP_3 is to activate the release of Ca^{2+} from intracellular stores, whereas DAG is required for the activation of protein kinase C (PKC) (Rebecchi and Pentyala 2000).

1,4,5 inositol triphosphate (IP_3)

Intracellular calcium is the driving force of fluid secretion in secretory cells, and there is little doubt that IP_3 is the primary intracellular messenger triggering the release of intracellular calcium in salivary gland acinar cells (Ambudkar 2000) and lacrimal gland acinar cells (Dartt, Dicker et al. 1990; Putney and Bird 1994). Upon production, IP_3 rapidly diffuses through the cytosol and binds to the IP_3 receptor (IP_3R). The IP_3R are located on the endoplasmic reticulum, accepted to be the primary intracellular store of Ca^{2+}, with the IP_3R predominately located towards the basolateral pole of the acinar cell (Lee, Xu et al. 1997; Zhang, Wen et al. 1999). The IP_3R itself is a homo or heterotrimeric Ca^{2+} release channel, its monomers having a molecular mass of approximately 313kDa. The IP_3R has 3 distinct domains: the ligand binding, regulatory, and Ca^{2+} channel domains. (Devogelaere, Verbert et al. 2008). Three isoforms have been identified in mammalian tissues (IP_3R 1-3) (Patel, Joseph et al. 1999) and are related both structurally and functionally (Gallacher and Smith 1999; Ambudkar 2000). All three IP_3 isoforms have been identified in the salivary and lacrimal acinar cells, with mainly IP_3R2 and IP_3R3 being expressed in lacrimal acinar cells (Mikoshiba, Hisatsune et al. 2008).

Ca^{2+} acts as a complex regulator of IP3Rs, as high concentrations of Ca^{2+} inhibit the IP_3R, whilst inversely low concentrations of Ca^{2+} stimulate IP_3R activity (Bezprozvanny, Watras et al. 1991; Finch, Turner et al. 1991). The sensitivity of the IP_3R is regulated not only by Ca^{2+}, but also IP_3, calmodulin and phosphorylation sites (Berridge 1997; Gallacher and Smith 1999; Ambudkar 2000). This arrangement offers considerable scope for the dynamic regulation of IP_3R sensitivity. It is considered most likely that the activation of the IP_3R is, by and large, due to the direct binding of Ca^{2+} to the receptor itself (Miyakawa, Mizushima et al. 2001; Mak, McBride et al. 2003). The mechanism of deactivation of IP_3R mediated by Ca^{2+}

remains unclear, but data suggest that the calcium binding protein calmodulin (CaM) is essential for full function of the IP_3R (Nadif Kasri, Bultynck et al. 2002; Kasri, Torok et al. 2006).

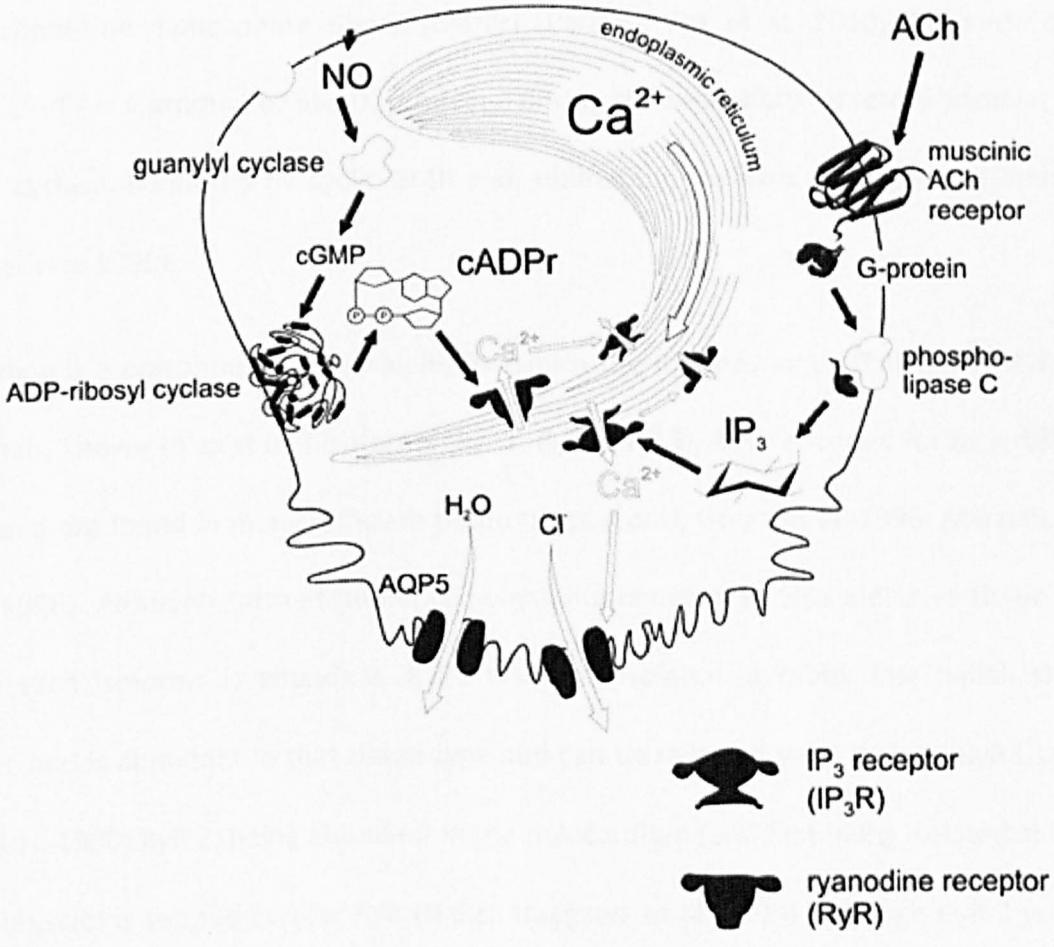

Figure 1.1.3 Diagrammatic representation of the key elements seen in salivary and lacrimal secretion. Acetylcholine binds to the muscarinic receptor, activating Gαq which binds GTP. The Gα subunit goes on to activate βPLC splitting PIP2 into DAG and IP3.IP3 activates IP3R releasing Ca^{2+}. NO acts upon sGC creating cGMP which activates ADPr cyclase. cADPr is formed and activates the RyR releasing Ca^{2+}. The increase in Ca^{2+} activates ion pumps which create the osmotic potential gradient allowing the movement of water (Diagram courtesy of Dr. Pete Smith).

Ryanodine receptors (RyR)

Calcium release from the ER is not entirely dependent upon the IP_3R, with a second set of receptors also being important in Ca^{2+} mobilisation from the ER- the ryanodine receptor (RyR). Similarly to the IP_3R, RyRs are involved in calcium induced calcium release (CICR), but RyR's sensitivity to intracellular Ca^{2+} is mediated by the concentration of the 2nd messenger cyclic adenosine diphosphate ribose (cADPr) (Venturi, Pitt et al. 2010) (Fill and Copello 2002). cADPr is a product of βNAD, produced during the secondary secretory pathway from ribosyl cyclase, mediated by cyclic GMP and, ultimately, by nitric oxide levels (Denninger and Marletta 1999).

Ryanodine is a poisonous plant alkaloid, for which the RyR has high affinity. The RyR is, in mammals, known to exist in 3 isoforms (RyR1, RyR2, RyR3), each encoded for by a different gene, and are found in many different tissue types (Conti, Gorza et al. 1996; Marziali, Rossi et al. 1996). Although termed numerically, naming convention also indicates tissue types where each isoforms is abundant, RyR1 was first isolated in rabbit fast twitch skeletal muscle, and is abundant in that tissue type and can be referred to as skeletal RyR (Zorzato, Fujii et al. 1990).RyR 2, being abundant in the myocardium (and first being isolated in canine heart muscle) is termed cardiac RyR (Nakai, Imagawa et al. 1990) Although RyR 3 was first isolated in bovine diaphragm tissue, it is widely expressed, although at higher concentrations in the brain, and therefore named as brain RyR (Hakamata, Nakai et al. 1992; Jeyakumar, Copello et al. 1998). Presence of all three RyR isoforms has been demonstrated in adult and post-natal mouse lacrimal acinar gland cells with expression dependent upon intracellular location (Medina-Ortiz, Gregg et al. 2007).

RyR Structure

The functional RyR unit itself is a homotetramer (Lai, Misra et al. 1989), with each subunit forming a quatrefoil shape. Most of the mass of RyR forms a large cytoplasmic assembly (Ludtke, Serysheva et al. 2005) measuring 280x280x120 Å each side (Hamilton and Serysheva 2009), forming a cation selective channel for the release of Ca^{2+} from the ER (Zucchi and Ronca-Testoni 1997). The receptor has a mass of 2.3 ±0.3 MDa, with each polypeptide subunit estimated to be approx. 500 kda (Marks, Tempst et al. 1989) with the RyR1 subunit having a mass of 565 kDa (Takeshima, Nishimura et al. 1989). Mutations of the RyR are associated with a number of human diseases: RyR1 mutations are associated with central core disease and malignant hypothermia and RyR2 with arrhythmogenic right ventricular dysplasia and stress-induced polymorphic ventricular tachycardia (Zucchi and Ronca-Testoni 1997).

RyR's are the principal mediator of CICR in excitable tissues, illustrated by the lack of channel activation by other ligands in the absence of Ca^{2+} (Zucchi and Ronca-Testoni 1997). In parotid glands, RyRs are primarily located towards the basolateral pole, with the IP_3R primarily at the apical end. (Lee, Xu et al. 1997; Zhang, Wen et al. 1999). Thus, the Ca^{2+} signal is initiated by the activation of the IP_3R towards the apical end of the cell, then propagates across the cell by CICR following the activation of both IP_3R and RyR (Harmer, Smith et al. 2005).

Cyclic Adenosine diphosphate ribose (cADPr)

Cyclic Adenosine diphosphate ribose (cADPr) is a second messenger shown to have an active role in calcium mobilisation in the cell. Originally identified by Lee et al in 1989 during work on sea urchin eggs (Lee, Walseth et al. 1989), cADPr has been shown to have a role in Ca^{2+} mobilisation in both sea urchin eggs (Galione, McDougall et al. 1993; Galione, White et al. 1993) and pancreatic acinar cells (Thorn, Gerasimenko et al. 1994). The Ca^{2+} mobilizing effect of cADPr has been shown to be blocked by the RyR inhibitors ruthenium red, ryanodine, and 8-amino-cADP-ribose in sea urchin eggs, pancreatic, and salivary acinar cells (Galione, White et al. 1993; Thorn, Gerasimenko et al. 1994; Yamaki, Morita et al. 1998; Harmer, Gallacher et al. 2001). Production of cADPr was found to be governed by the catalysis of NAD^+ to cADPr and nicotinimide (Lee and Aarhus 1991) by an enzyme originally purified from the ovotestis of the mollusk *Aplysia californica* (Hellmich and Strumwasser 1991). This specific enzyme, in order to distinguish it from other NAD-ases, was renamed ADP-ribosyl cyclase.

The mechanism of cADPr as in the mobilisation of $Ca^{2+}$was originally thought to be part of an alternative receptor system pathway, or have a higher affinity for the IP_3 receptors than IP_3 itself (Worley, Baraban et al. 1987). However, it was determined that cADPr was binding to a different receptor, shown by the use of heparin, a competitive inhibitor of IP_3 binding, still allowing cADPr to function (Worley, Baraban et al. 1987; Dargie, Agre et al. 1990).

Comparison of the ability of cADPr and IP_3 to mobilize calcium showed that when the calcium mobilized by one activator (cADPr or IP_3) was low, the response induced by the other, at maximal dose, would be great, although there was no change in the total amount of releasable calcium (Dargie, Agre et al. 1990) strongly suggesting that the two mobilized

Ca^{2+} from overlapping stores. This lack of synergy, along with the rest of the available data showed that, *in vivo,* the two second messengers were comparable in their ability to mobilize Ca^{2+}, and that cADPr 's mechanism for calcium mobilisation was independent of IP^3 (Dargie, Agre et al. 1990).

The idea that cADPr was mobilising Ca^{2+} came later, since the presence of a cADPr specific binding site was determined to exist (Lee 1991), yet it's exact nature was unknown. However, the identification of a second class of intracellular Ca^{2+} release channel, the RyR, in sea urchin eggs (Galione, Lee et al. 1991), allowed for the development of the theory that the RyR was the target of the cADPr second messenger.

cADPr has been shown to be capable of mobilising Ca^{2+} in salivary gland acinar cells from rats, dogs and mice (Yamaki, Morita et al. 1998; Masuda and Noguchi 2000; Harmer, Gallacher et al. 2001). The action of cADPr as a second messenger has also been demonstrated in rat lacrimal gland acinar cells (Gromada, Jorgensen et al. 1995; Gromada, Jorgensen et al. 1995).

Since the IP3 mediated Ca^{2+} release pathway seemed to fulfill all the requirement for it's role in signal transduction, it was suggested that the cADPr/ RyR pathway was "redundant" (Galione, McDougall et al. 1993). However it has since been shown that the level of cADPr within salivary gland acinar cells possesses the ability to alter the cell's magnitude of response to ACh stimulation (Harmer, Gallacher et al. 2001). These findings suggest that acinar cells may have an alternative mechanism of shaping response to agonist.

1.2 Nitric Oxide

Nitric Oxide Discovery

Nitric oxide (NO) is a small, gaseous molecule, comprising of one molecule of nitrogen bonded to one of oxygen. It has been shown to be produced in virtually all cell types in mammals, and plays a host of important roles within mammals, including cell signalling, immune response, neurotransmission and vasodilation amongst others (Chen, Tsai et al. 1996; Clementi 1998; Benencia and Courreges 1999; Ignarro 2002).

The discovery of NO's importance in cell signalling came about initially from Robert Furchgott's work investigating the mechanism of vasodilation (Furchgott and Zawadzki 1980). This work showed that the neurotransmitter acetylcholine (ACh) could only induce blood vessel relaxation in the presence of endothelial cells. The relaxation of the smooth muscles in blood vessels demonstrated that endothelial cells were releasing a vasodilating agent upon agonist invoked stimulation. This substance, initially believed to be a protein, like most other signalling molecules, was termed Endothelial Derived Relaxing Factor (EDRF). Following this discovery, research to discover the identity of EDRF intensified. During a similar period, Ferid Murad was investigating the mechanism of nitroglycerin function, demonstrating that nitroglycerin releases NO, which caused the relaxation of smooth muscle cells (Murad 1986). It wasn't until 1986 that Louis Ignarro took these two facts and correctly identified EDRF as nitric oxide (Ignarro, Buga et al. 1987). This discovery led to an explosion of interest in the subject and led to Furchgott, Ignarro and Murad being awarded the Nobel Prize in medicine or physiology in 1998.

Functions of NO

The role of NO as a signalling molecule is of great importance, in part, due to its properties: (i) a gaseous signalling molecule, (ii) requiring no specialised transport system by virtue of it being small and hydrophobic; and (iii) it being able to affect sites away from its point of synthesis (NO is able to diffuse several hundred microns/ a few cell diameters from its point of origin (Taha, Kiechle et al. 1992).

At physiological levels of NO and O_2 the half life of NO is measured in minutes (Taha, Kiechle et al. 1992), but the presence of metal ions in cells allows for the rapid oxidisation of NO to NO_2^- and NO_3^- (Denninger and Marletta 1999). At low concentrations of NO, and in the absence of metals and proteins contributing to NO's destruction, oxidisation of NO is much slower, allowing NO to accumulate. At higher concentrations NO is known to react with oxygen to form the powerful nitrosylating agent N_2O_3 (Denninger and Marletta 1999).

High NO concentrations have a vital role in the immune response. Production of NO by macrophages and lymphocytes has been shown to be important in the host defence of bacteria, parasites and viruses (Rajan, Porte et al. 1996; Benencia and Courreges 1999). Increased concentrations of NO can also have detrimental effects upon host cells, and has implicated in the pathogenesis of rheumatoid arthritis, asthma and Sjögren's syndrome (Grabowski, England et al. 1996) (Lundberg, Nordvall et al. 1996) (Ludviksdottir, Janson et al. 1999).

NO appears to play a role in the central and peripheral nervous system, promoting signal transference from neuron to neuron, and has been implicated in diseases affecting the nervous system, such as Parkinsons, Alzheimers and Huntingdon's diseases (Deckel, Tang et al. 2002; Togo, Katsuse et al. 2004; Aquilano, Baldelli et al. 2008).

Thus, NO function is of great interest due to its involvement as a signalling molecule acting in many tissues, regulating a diverse range of cellular and physiological processes.

Production Of Nitric Oxide

NO is produced in a reaction catalysed by the family of enzymes known as Nitric Oxide Synthases (NOS). All NOS isoforms catalyse the oxidation reaction of L-Arginine to citrulline (Marletta, Hurshman et al. 1998). This process involves 2 sequential monoxidase reactions requiring the presence of reduced nicotinamide adenine dinucleotide phosphate (NADPH), flavin adenine dinucleotide (FAD) , flavin mononucleotide (FMN) , tetrahydrobiopterin (BH_4) and oxygen as cofactors (Forstermann, Gath et al. 1995; Chen, Tsai et al. 1996), ultimately yielding NADP, citrulline and NO (Blaise, Gauvin et al. 2005). The known isoforms of NOS follow the naming convention of the type of tissue they were first described in (or mode of action in the case of iNOS): neuronal NOS (nNOS/ Type 1 NOS), inducible NOS (iNOS/ Type 2 NOS) and endothelial NOS (eNOS/ Type 3 NOS) (Forstermann, Gath et al. 1995) although all three isoforms are widely distributed throughout tissue types. Mitochondria also possess a NO producing enzyme known as mtNOS (Haynes, Elfering et al. 2004).

NOS Isoforms, control of action, location and expression

Whilst NO molecules produced by one NOS isoform are identical to NO molecules produced by any other isoform, the three NOS isoforms differ in their amino acid sequence, post-translational modifications, cellular location and regulation by Ca^{2+}/CaM.

Endothelial NOS (eNOS/ Type 3 NOS), first described in blood vessel endothelial cells (Forstermann, Gath et al. 1995) has also seen expressed in cardiac myocytes (Feron, Han et al. 1999), mouse pancreatic (Hegyi and Rakonczay Jr 2011) submandibular and parotid salivary glands, human salivary glands and mouse (Looms, Tritsaris et al. 2002) and rat

lacrimal glands (Hodges, Shatos et al. 2005). Endothelial NOS, has been described as being dependent upon calcium activated binding of calmodulin (CaM) to the eNOS molecule, however, this view may be considered over simplistic, since eNOS function can also be dependent upon co- and post-translational modification, as well as its spatial position within the cell (Shaul, Smart et al. 1996; Liu, Hughes et al. 1997; Shaul 2002). Post translational modification of eNOS, specifically N-myristoylation and S-palmitoylation, affect subcellular localisation (Michel, Li et al. 1993) (Busconi and Michel 1993; Sessa, Barber et al. 1993; Liu, Garcia-Cardena et al. 1996; Shaul, Smart et al. 1996; Liu, Hughes et al. 1997). Localisation of eNOS has been demonstrated, with many studies confirming that eNOS is mostly localised to caveolae (Feron, Belhassen et al. 1996; Goligorsky, Li et al. 2002; Solomonson 2003; Sullivan and Pollock 2003) with Hodges *et al* showing the colocalisation of eNOS with caveolin-1 (Hodges, Shatos et al. 2005) in unstimulated lacrimal acinar cells. The interaction of eNOS and caveolin-1 has been seen, *in vitro*, to result in the inhibition of eNOS activity (Ortiz and Garvin 2003). eNOS (like nNOS) is known to be calcium dependent, with the role of calmodulin well known. Calmodulin (CaM) was the first protein to be shown to interact with NOS (Bredt and Snyder 1990).

Neuronal NOS (nNOS/ Type 1 NOS), was the first NOS to be cloned and purified (Hence NOS1), with neuronal tissue being a rich source (Bredt and Snyder 1989; Bredt, Hwang et al. 1990; Bredt and Snyder 1990). Similarly to eNOS, nNOS is constitutively expressed and is dependent upon Ca^{2+}/calmodulin. Unlike the other isoforms of NOS, nNOS possesses a unique N terminal PDZ domain (Govers and Oess 2004) which allows for protein/protein interactions, since, unlike the other NOS isoforms, nNOS does not undergo acylation directly (Mungrue and Bredt 2004). Through its PDZ domain, nNOS interacts with the Ca^{2+}-efflux

pump PMCA4b at caveolae of different cell types (Schuh, Uldrijan et al. 2001). Subcellular targeting has been demonstrated for the nNOS isoform in cardiac myocytes with the interaction with RyR 1 being hypothesised to play a role (Barouch, Harrison et al. 2002). nNOS is a complicated protein, having multiple splice variants although data showing which are prevalent in the salivary or lacrimal glands, and any relevance to Sjögren's syndrome, remain to be published.

Unlike its constitutively expressed counterparts, inducible NOS (iNOS/ Type 2 NOS) is not constitutively expressed. iNOS expression is considered to be the main regulatory factor in control of iNOS activity, with iNOS synthesising NO until the enzyme is degraded (MacMicking, Xie et al. 1997) (Geller and Billiar 1998). However, iNOS activity has also been shown to be regulated, at least in part, by substrate availability (Closs, Scheld et al. 2000; Mori and Gotoh 2000) (Mori 2007) iNOS is considered to be calcium independent, since it forms an active complex with CaM even at low concentrations of intracellular Ca^{2+} (Alderton, Cooper et al. 2001). iNOS catalyses the same reaction as the other isoforms, although iNOS is responsible for micromolar increases in NO, compared to the more modest nanomolar concentrations produced by the constitutive forms. Induction of iNOS has been shown in lacrimal acinar glands, with increase in both measured nitrites and iNOS mRNA being evoked by incubation with the pro-inflammatory cytokine interleukin-1β (IL-1 β) (Beauregard, Brandt et al. 2003).

Effects of NO in Biological Systems

The effects of NO upon biological systems are mediated mainly via 3 definable methods:

The mediation of Ca^{2+} response via the NO dependent sGC pathway- resulting in activation of RyR by cADPr.

The action of reactive nitrogen species (RNS), nitrates, nitrites, and peroxynitrite, produced by the reaction of ROS with NO. These reactive species are highly unstable, and can result in damage to cells.

The reaction with the sulfhydryl group present in the cysteine residues in proteins- a process known as S- Nitrosylation. Such an action can conceivably result in conformational change in a protein, resulting in the alteration of action.

NO mediation of Ca^{2+} signalling via NO sensitive sGC and concomitant increase in cADPr.

Data obtained from salivary gland acinar cells show that activation of sGC by NO results in the production of cGMP from GTP (Michikawa, Mitsui et al. 1998; Denninger and Marletta 1999; Looms, Dissing et al. 2000) as a result of the conformational change in the sGC protein catalytic site. This increase in cGMP activates ribosyl cyclase, resulting in the formation of βNAD which is followed by the formation of cADPr. The cADPr produced has been demonstrated to increase $[Ca^{2+}]_i$ by activation of RyRs– modulating the calcium induced calcium release (CICR) observed upon cell stimulation (Looms, Tritsaris et al. 2001) (Smith and Gallacher 1992; Yamaki, Morita et al. 1998) (Harmer, Gallacher et al. 2001; Harmer, Smith et al. 2005).

The activation of sGC by NO may be inhibited by use of the potent and selective sGC inhibitor 1H-[1,2,4]oxadiazolo[4,3]quinoxalin-1-one (ODQ). ODQ has been demonstrated to

inhibit the NO activated sGC in a variety of tissue types (Brunner, Stessel et al. 1995; Garthwaite, Southam et al. 1995; Moro, Russel et al. 1996; Abi-Gerges, Hove-Madsen et al. 1997), and has been shown to be capable of inhibiting the sGC activating action of NO supplied by NO donors (Caulfield, Balmer et al. 2009). ODQ has no effect upon NO itself, rather it inhibits NO binding by oxidising the haem iron (from Fe^{2+} to Fe^{3+}) present in the sGC (Schrammel, Behrends et al. 1996). ODQ has no effect upon particulate guanyl cyclase (pGC)- which catalyses the same reaction as sGC, but is stimulated by small peptide hormones (Zhao, Brandish et al. 2000).

The effects of reactive nitrogen species (RNS) upon cell and tissue Function

Whilst the nature of NO as a signalling molecule is of primary concern to physiologists, the reaction products of NO with other molecules must also be considered. NO itself is considered to be cytotoxic in high concentrations, although there is sufficient evidence to allow for its oxidation products to be implicated in cellular damage. NO itself does not attack DNA, rather the effect relying upon NO conversion to nitrogen superoxides (Wink, Kasprzak et al. 1991). Reaction of NO with the superoxide ($O2^{\cdot-}$) can result in the generation of the strong oxidant peroxynitrite ($ONOO^-$). Peroxynitrite itself is shown to be a trigger of apoptosis, although the exact mechanism seems to be dependent upon the cell type and experimental protocol (Virág, Szabó et al. 2003). Nevertheless, peroxynitrite induction of apoptosis has been demonstrated in a wide variety of cells, including SH-SY5Y neuroblastoma cells (Saeki, Maeda et al. 2002), endothelial cells (Walford, Moussignac et al. 2004; Dickhout, Hossain et al. 2005) and pancreatic beta islet cells (Delaney, Tyrberg et al. 1996; Suarez-Pinzon, Szabo et al. 1997). Generation of peroxynitrite has previously been hypothesised to have a role in the propagation or pathogenesis of dry eye observed in SjS (Cejková, Ardan et al. 2007).

The effects of S-nitrosylation on cellular function.

S-Nitrosylation is the post translational modification of proteins by the transfer of an NO group to cysteine sulfhydryls in protein. Post translational modification of protein is a well known method of regulating protein action, influencing many aspects of cellular physiology. The most commonly thought of post-translational modification is phosphorylation, which is reversible and subject to tight spatial and temporal control. However, the role of NO in the post-translational modification of protein, and the effect of such modification, is becoming more apparent. NO's simple structure was initially thought of being incapable of possessing the control and specificity observed in other post translational modification systems. However, continued study has shown that S-nitrosylation, like phosphorylation, exhibits the required levels of spatio/temporal control, specificity and reversible nature required. The S-nitrosylation of proteins has been shown to either activate or inactivate protein function, with over a hundred proteins being identified as undergoing nitrosylation (Stamler, Lamas et al. 2001). Nitrosylation sites have been identified on the RyR1 subunit (Sun, Xin et al. 2001) resulting in an alteration of response profile, and on sGC (Sayed, Baskaran et al. 2007; Sayed, Kim et al. 2008), nitrosylation resulting in desensitisation of sGC to NO.

NO Donors

The use of NO as an experimental reagent in biological systems is rendered difficult by the fact that, in its natural state, NO is a gas. This has led to the development and use of NO donors- compounds which are capable of releasing NO *in situ* (Soff, Cornwell et al. 1997). Commonly used NO donors are of three different types: inorganic nitroso-compounds, S-nitrosothiols, and NONATES. NOCS/NONATES are newer compounds, similar in structure to amino acids (being zwitterions formed from polyamines) and are mooted as releasing fewer biologically active by-products than the other NO donors. SNP is one example of an inorganic nitroso-compound (Al-Sa'doni and Ferro 2000; Al-Sa'doni, Khan et al. 2000). Commonly used is the S-nitrosothiol, S-nitroso-N-acetyl-penicillamine (SNAP), with the modes of NO release from these compounds being well documented and understood (Marks, McLaughlin et al. 1995; Chipinda and Simoyi 2006).

Nitric oxide and the glandular hypofunction observed in Sjogren's syndrome

The constitutive forms of NOS (eNOS and iNOS) have been implicated in the aetiology of Sjogren's syndrome, with increased NO being found in the exhaled breath of sufferers, along with nitrites in patient derived sera (Konttinen, Platts et al. 1997; Ludviksdottir, Janson et al. 1999; Wanchu, Khullar et al. 2000). Exposure of submandibular acinar gland cells to increased concentrations of NO from NO donors has been observed to have a biphasic effect upon calcium signaling and thus secretion, with acute exposure increasing the magnitude of calcium signal and chronic exposure causing a decline and eventual abolition of signal (Caulfield, Balmer et al. 2009).

The exact cause of increased NO production observed in Sjögren's syndrome sufferers is unknown at present, although it is likely to be associated with the chronic inflammation

observed in the disease, although Reina et al have demonstrated that SjS antibodies can alter constitutive NOS expression (Reina, Sterin-Borda et al. 2004). The mode of attenuation of secretory gland cellular response (and subsequent loss of function) by the presence of increased NO concentrations is currently unidentified.

Ion Channel Activation and Water movement

The end result of the ACh-evoked mobilisation of intracellular Ca^{2+} is the net movement of water from the basolateral/ blood side of the cell to the gland lumen. The movement of water is achieved through the creation of an osmotic potential gradient between basolateral and luminal ends of the acinar cell. Establishment of this osmotic potential is achieved by the activation of Ca^{2+} dependent Cl^- and K^+ channels in the luminal and basolateral parts of the acinar cell plasma membrane respectively (Harmer, Smith et al. 2005). Activation of the luminal Cl^- channel allows Cl^- to enter the gland lumen along its electrochemical gradient. Unchecked, loss of Cl^- from the cell would result in a change of membrane potential. Maintenance of cell potential is brought about by the loss of K^+ ions through the Ca^{2+} dependent K^+ channels located at the basolateral end of the acinar cell. The continuous flow of Cl^- ions is maintained by the action of the Na^+ - K^+ - Cl^- triple co-transporter at the basolateral end of the acinar cell. Cl^- accumulation in the gland lumen is balanced by the flow of Na^+ ions into the lumen. This build up of NaCl provides the osmotic potential required for the net movement of water across the cell into the gland lumen (Harmer, Smith et al. 2005).

In acinar glands, water can either move by the paracellular route or the transcellular route. Due to the plasmamembrane being hydrophobic in nature, rapid movement of water via a transcellular path requires the presence of channels in the plasmamembrane. These channels, present in acinar cell plasmamembrane are called aquaporins (AQP). Aquaporin proteins are made up of six transmembrane domains, with the functional unit being a tetramer of these (Gonen and Walz 2006; Fu and Lu 2007). There are 13 aquaporins identified in humans (AQP 0- AQP 12) (Ishibashi, Hara et al. 2009), with this representing the

final number since the completion of the human genome project. AQP 5 is the most ubiquitously expressed in salivary glands (Borgnia, Nielsen et al. 1999).

1.3 Sjögren's Syndrome

Sjögren's Syndrome History

The original description of Sjögren's syndrome was made by surgeon, Johannes von Mikulicz in 1892, where he described a 42 year old man who presented with intermittent fever, bilateral enlargement of the parotid and lacrimal glands which was associated with a small round cell type (Piper 1990). Throughout his lifetime, the individual suffered recurrent episodes and upon his death, post-mortem examination revealed that the hypertrophied glands showed *"extensive lymphocytic infiltrations, but no evidence of malignancy or infection"*. The condition was thereafter termed Mikulicz's disease. Prior to the identification of this particular condition, the term "Mikulicz's syndrome" had already been used to describe a variety of conditions including lymphoma, sarcoidosis, tuberculosis and other infections, so due to the inadequacy of this term to provide prognostic or therapeutic data, the term fell into disuse (Daniels and Fox 1992). However, the term is occasionally used as a histological reference when focal lymphocytic infiltrates are observed on salivary gland biopsy samples (Morgan and Castleman 1953).

The Danish ophthalmologist, Henrik Sjögren, -after whom the disease is now named, first encountered the disease in 1930 when presented with a female patient suffering from dry and painful eyes. Sjögren's fascination with the case led to the documentation of clinical findings of 19 sufferers of dry eye and dry mouth (13 of which had probable rheumatoid arthritis) by 1933. Sjögren also characterised the histological appearance of the conjunctiva from biopsies obtained from each of the patients (Bell, Askari et al. 1999; Wollheim 1999). Submitted in 1933 in German, this work formed Sjögren's doctoral thesis, and thus, "Sjögren's syndrome" was born. Sjögren's work went largely unnoticed until 1953,

rediscovered by two American investigators: William Morgan and John Castleman, who presented a case study involving a patient presenting with Sjögren's syndrome. It was Morgan and Castleman who proposed that Sjögren's syndrome and Mikulicz's disease were one and the same (Morgan and Castleman 1953). This reignited interest in the disease, beginning with the outline of the clinical features of Sjögren's syndrome, still relevant today, by Bloch *et al* in 1956 (Bloch and Bunim 1963).

The study of Sjögren's syndrome is still of interest to this day, remaining the subject of intensive research as a model of systemic autoimmune disease.

Clinical Features and Incidence of Sjögren's Syndrome

Whilst relatively unheard of in the general population, Sjögren's syndrome has a prevalence similar to that of Rheumatoid Arthritis (Hazes and Silman 1990), with an estimated incidence of 3% of the population (Thomas, Hay et al. 1998; Jonsson, Haga et al. 2000), which makes it one of the most common of the autoimmune disorders (Pillemer, Matteson et al. 2001). Similarly to many of the autoimmune diseases, there is an obvious sexual dimorphism in the prevalence of the disease with a 9:1 female to male ratio in sufferers (Scully 1986). There appear to be 2 peaks of incidence with age of the sufferers: after menarche, and menopause (50-60 years of age) (Bowman, Ibrahim et al. 2004; Fox 2005). Juvenile Onset Sjögren's syndrome is rarer (though incidence is seen to be increasing), and symptoms are considerably less severe (Cimaz, Casadei et al. 2003; Singer, Tomanova-Soltys et al. 2008).

Sjögren's syndrome (SjS) is an autoimmune disorder which specifically targets the exocrine glands, primarily the salivary and lacrimal glands associated with a gradual and progressive decline in secretory function (resulting in dry eye and dry mouth) and can be characterised by lymphocytic infiltration of the salivary and lacrimal glands.

SjS is considered a "syndrome" rather than a disease. A syndrome is "a collection of symptoms which consistently occur together, or a condition which is characterised by a set of associated symptoms", whereas a disease is characterised by its cause, rather than symptoms. Symptoms vary in Sjögren's syndrome, but typically involve symptoms related to salivary gland hypofunction (dry mouth, difficulty eating/speaking, salivary gland enlargement, oral candidiasis and rampant caries), lacrimal gland hypofunction (dry eyes, blindness), other secretory dysfunction (vaginal dryness, skin dryness) (Scully 1986).

However, Sjögren's syndrome is a systemic autoimmune disorder, and not all symptoms are related to secretion. Other symptoms include chronic tiredness and peripheral neuropathies, (Delalande, de Seze et al. 2004; Mori, Iijima et al. 2005; Mandl, Granberg et al. 2008; Chai and Logigian 2010) as well as a significant (20-40 fold) (Theander, Henriksson et al. 2006) increase in incidence of malignant lymphoma- in nearly all cases, B cell mucosally associated lymphoid tissue tumors (MALTomas). One long term (10 year) study assessing a cohort of Sjögren's syndrome patients against the Sjögren's Syndrome Damage Index (SSDI) (Barry, Sutcliffe et al. 2008), reported that 55% of Sjogren's syndrome patients had suffered no damage after 10 years of the disease (Krylova and Isenberg 2010).

Diagnosis of Sjögren's syndrome

Diagnosis of SjS is rendered difficult due to the varying nature of its presentation from patient to patient. Coupled with this is the fact that many of the symptoms seen in SjS can be associated with other diseases, or the side effects from some medications. A total lack of specific or sensitive disease markers further complicates diagnosis, since without these there are no screening techniques for the disease. Further complication of disease diagnosis is caused by the fact that all studies so far have been performed upon subjects in which the disease is already established (from initial identification of illness to diagnosis takes, on average 6.5 years), which may lead to blurring of the lines of whether observed changes in patients are a cause or effect of the disease (Fox 2007).

The current method of diagnosis of SjS is that of satisfaction of a number of criteria based upon subjective and objective symptoms of lacrimal and salivary gland hypofunction in conjunction with immunological abnormalities, indicated by the presence of antibodies and/or lymphocytic infiltration of the labial salivary glands (Fox, Robinson et al. 1986; Vitali,

Bombardieri et al. 1993; Fox and Saito 1994; Vitali, Bombardieri et al. 1996). The current diagnostic criteria are summarized in Table 1.3.1 (Vitali, Bombardieri et al. 2002).

Table 1.3.1 Sjogren's syndrome classification criteria, part 1

Revised American-European classification criteria for Sjögren's syndrome (from *Vitali et al* 2002)

I. Ocular symptoms: a positive response to at least one of the following questions:

1. Have you had daily, persistent, troublesome dry eyes for more than 3 months?

2. Do you have a recurrent sensation of sand or gravel in the eyes?

3. Do you use tear substitutes more than 3 times a day?

II. Oral symptoms: a positive response to at least one of the following questions:

1. Have you had a daily feeling of dry mouth for more than 3 months?

2. Have you had recurrently or persistently swollen salivary glands as an adult?

3. Do you frequently drink liquids to aid in swallowing dry food?

III. Ocular signs—that is, objective evidence of ocular involvement defined as a positive result for at least one of the following two tests:

1. Schirmer's I test, performed without anaesthesia (<5 mm in 5 minutes)

2. Rose bengal score or other ocular dye score (>4 according to van Bijsterveld's scoring system)

IV. Histopathology: In minor salivary glands (obtained through normal-appearing mucosa) focal lymphocytic sialoadenitis, evaluated by an expert histopathologist, with a focus score >1, defined as a number of lymphocytic foci (which are adjacent to normal-appearing mucous acini and contain

more than 50 lymphocytes) per 4 mm2 of glandular tissue.

V. Salivary gland involvement: objective evidence of salivary gland involvement defined by a positive result for at least one of the following diagnostic tests:

1. Unstimulated whole salivary flow (<1.5 ml in 15 minutes)

2. Parotid sialography showing the presence of diffuse sialectasias (punctate, cavitary or destructive pattern), without evidence of obstruction in the major ducts

3. Salivary scintigraphy showing delayed uptake, reduced concentration and/or delayed excretion of tracer

VI. Autoantibodies: presence in the serum of the following autoantibodies:

1. Antibodies to Ro(SSA) or La(SSB) antigens, or both

Primary Vs Secondary SjS

Clinically, Sjögren's syndrome is considered primary (pSjS) if dry eye and dry mouth occur in isolation, but secondary (sSjS) if it occurs in conjunction with another connective disease (Scully 1986), for example rheumatoid arthritis, systemic lupus erythematosus and primary billiary cirrhosis (Jonsson, Haga et al. 2000). Criteria for the classification or exclusion of pSS and sSS are summarized in table 1.3.2 (Vitali, Bombardieri et al. 2002).

Comparison of the degree of glandular hypofunction experienced between sufferers of pSjS and sSjS shows no obvious difference (Dawson, Holt et al. 2001). However, striking differences between pSjS and sSjS are observed in HLA types (HLA DR and DQ) (Moutsopoulos, Mann et al. 1979; Moutsopoulos, Chused et al. 1980) and lymphocyte antigen expression (Kroneld, Halse et al. 1997). Overall, the available evidence suggests that primary and secondary Sjogren's syndrome represent conditions with different aetiologies, but share similar features and common mechanisms related to glandular hypofunction.

Table 1.3.2. Sjogren's syndrome classification criteria, part 2.

Revised rules for classification (from Vitali *et al* 2002)

For primary SS

In patients without any potentially associated disease, primary SS may be defined as follows:

a. The presence of any 4 of the 6 items is indicative of primary SS, as long as either item IV (Histopathology) or VI (Serology) is positive

b. The presence of any 3 of the 4 objective criteria items (that is, items III, IV, V, VI)

c. The classification tree procedure represents a valid alternative method for classification, although it should be more properly used in clinical-epidemiological survey

For secondary SS

In patients with a potentially associated disease (for instance, another well defined connective tissue disease), the presence of item I or item II plus any 2 from among items III, IV, and V may be considered as indicative of secondary S

Exclusion criteria:
Past head and neck radiation treatment
Hepatitis C infection
Acquired immunodeficiency disease (AIDS)
Pre-existing lymphoma
Sarcoidosis
Graft versus host disease
Use of anticholinergic drugs (since a time shorter than 4-fold the half life of the drug)

Traditional versus non-apoptotic models of the glandular hypofunction associated with Sjögren's syndrome

The traditional view of the glandular hypofunction associated with Sjögren's syndrome was attributed to the immune mediated destruction of the secretory cells in lacrimal and salivary glands (Fox and Saito 1994). However, the simplistic view of the glands being destroyed with a concomitant decline in secretion cannot explain more recent findings, which include:

Many patients who were showing symptoms of glandular hypofunction still possessed large quantities of apparently healthy tissue (Fox and Maruyama 1997; Fox, Tornwall et al. 1999; Humphreys-Beher, Brayer et al. 1999).

Immunohistochemical data demonstrating, that in glandular tissue of Sjögren's syndrome origin, both human and animal, showed neuronal innervations that remained intact subsequent to acinar cell loss (Konttinen, Platts et al. 1997) (Zoukhri, Hodges et al. 1998).

Experiments showing that the glandular hypofunction observed in Sjögren's patients could be reduced in some individuals by the administration of the immunomodulating drugs hydroxychloroquine (Tishler, Yaron et al. 1999) or interferon alpha (Shiozawa, Tanaka et al. 1998; Ship, Fox et al. 1999) which implied the involvement of inflammatory processes in the observed glandular hypofunction.

These data suggested that, contrary to the initial expectation of loss of function following tissue destruction, in many Sjögren's patients, loss of glandular function was not due to tissue destruction (Nakamura, Koji et al. 1998). The conclusion that followed was that the glandular hypofunction observed, rather than being due to a loss of secretory cells, was due to a loss in secretory cell function (Humphreys-Beher, Brayer et al. 1999).

1.4 Auto Antibodies in Sjögren's syndrome

There is still some debate that the glandular hypofunction observed is secondary to that of glandular destruction. However, it was eventually observed that Sjögren's sufferers still have substantial reserves of histologically normal acinar tissue (Fox and Maruyama 1997; Humphreys-Beher, Brayer et al. 1999). The remaining acinar tissue is functional, but with reduced sensitivity to muscarinic stimulation (Pedersen, Dissing et al. 2000; Dawson, Field et al. 2001). This non-apoptotic model follows a sequence of glandular atrophy following immune mediated inhibition of acinar glands. Other autoimmune disorders showing a defined target organ for autoimmune response, such as myasthenia gravis and Grave's disease, pathogenic autoantibodies have been identified (Drachman 1994; Weetman 2000). While Sjögren's syndrome is classed as an autoimmune disorder, no definitive antibody has been identified as the causal pathogen (Fox and Speight 1996; Gordon, Bolstad et al. 2001).

If an autoimmune condition is truly caused by an autoantibody, then it should satisfy the 5 criteria set out by Drachman:

> Autoantibodies are present in patients with the disease
>
> Antibody reacts with the target antigen
>
> Passive transfer of antibody reproduces features of the disease
>
> Immunisation with antigen produces a model disease
>
> Reduction in antibody levels ameliorates the disease (Drachman 1994)

Sjögren's syndrome has no shortage of candidates, with several autoantibodies being present in samples taken from Sjögren's syndrome sufferers, most commonly anti α-fodrin, anti-Ro and anti-La, and anti muscarinic type 3 receptor (M3R) antibodies.

Anti Ro/La

Anti Ro and Anti La (also known as SS-A and SS-B) are antibodies raised against the ribonuclear proteins (Wolin and Steitz 1984) Ro and La. The Ro (Ben-Chetrit, Gandy et al. 1989; McCauliffe, Lux et al. 1990) and La (Huhn, Pruijn et al. 1997)proteins are well characterised, and have been cloned and sequenced. Ro and La are usually sequestered inside the cell with data suggesting that Ro is involved in regulation of ribosomal protein mRNA translational fate and quality control in 5s rRNA production (O'Brien and Wolin 1994; Pellizzoni, Lotti et al. 1998). La ribonucleoprotein is involved in initiation and termination of RNA Polymerase III transcription, translational control and viral replication (Maraia 1996; Bachmann, Deister et al. 1998).

Anti-Ro and anti-La antibodies have been detected in the sera (Pourmand, Wahren-Herlenius et al. 1999), salivary glands (Tan 1989), saliva (Horsfall, Rose et al. 1989; Ben-Chetrit, Fischel et al. 1993; Halse, Marthinussen et al. 2000) and tear fluid (Toker, Yavuz et al. 2004) of Sjögren's syndrome patients. The high incidence (70-90%) of anti Ro and anti La autoantibodies observed in SjS sufferers (Whittingham, Mackay et al. 1983) is practically tautological due to the fact that these antibodies form part of the classification criteria for Sjögren's syndrome (Vitali, Bombardieri et al. 2002), although such a detection rate is dependent upon technique used. Detection of anti Ro/La is not limited to SjS, with a high incidence of anti Ro/La detected in SLE (Oshiro, Derbes et al. 1997).

Whilst being detected in SjS patients, data pertaining to a causal role of Anti Ro/La antibodies in SjS is lacking. However, a mechanism of anti Ro/La pathogenicity has been hypothesized, with internalization of anti-Ro and anti-La antibodies being demonstrated in the A-253 salivary gland cell line, triggering apoptosis (Lisi, Sisto et al. 2007; Sisto, Lisi et al.

2007). Presence of anti-Ro and anti-La antibodies has been associated with earlier onset of disease and an increased severity of symptoms (Toker, Yavuz et al. 2004).

Alpha Fodrin

Alpha fodrin (α-fodrin) is a 240kDa protein which is a fundamental constituent of the cell's cytoskeleton (Zhou, Ursitti et al. 1998), which anchor to the plasma membrane and bind to actin, calmodulin and microtubules (Bennett 1990). A role in secretion has been proposed, since α-fodrin has been demonstrated as associating with membrane ion channels and pumps (Perrin and Aunis 1985; Lukowski, Lecomte et al. 1996). Additionally, antibodies have been shown to block nerve conduction in salivary glands (Siman, Baudry et al. 1985; Perrin, Langley et al. 1987). These associations with the mechanisms of secretion provided the possibility of the identification of anti α-fodrin antibodies as having a possible role in the glandular hypofunction seen in Sjögren's syndrome(Miyazaki, Takeda et al. 2005). One early study showed great promise; in 1997 Haneji *et al* showed that anti α-fodrin antibodies were present in 95% of pSjS sufferers (as classified according to the Japanese criteria for SjS), 63% of sSjS sufferers, whilst being absent in associated diseases (SLE and RA) and healthy controls (Haneji, Nakamura et al. 1997). Consequently, a flurry of studies were performed to confirm such significant findings, with mixed results. IgG anti α-fodrin antibodies were detected in between 2 and 67% of SjS patients (Watanabe, Tsuchida et al. 1999; Witte, Matthias et al. 2000; Nordmark, Rorsman et al. 2003; Ruiz-Tiscar, Lopez-Longo et al. 2005). The initial reported specifity of anti α-fodrin is also open to debate, since anti α-fodrin antibodies have also been detected in 40% of Patients with RA, 20% of patients with MS (Ulbricht, Schmidt et al. 2003) and 47% of SLE sufferers not displaying sicca symptoms (Nordmark, Rorsman et al. 2003). The variance in reported incidence and specifity of anti α-fodrin antibodies led to the conclusion that detection and measurement of these antibodies

does not add much to the diagnosis of Sjögren's syndrome (Zandbelt, Vogelzangs et al. 2004; Turkcapar, Olmez et al. 2006). Similarly to anti-Ro and anti-La autoantibodies, increased anti α-fodrin antibody titer may be indicative disease progression, with one study showing a correlation between anti α-fodrin and levels of lymphocytic infiltration in salivary glands, and treatment of SjS patients with antimalarials or low-dose glucocorticosteroids may cause a decrease in anti α-fodrin within 3 months (Ulbricht, Schmidt et al. 2003).A recent study on the NOD mouse model of Sjögren's syndrome have indicated that nasally administering α-fodrin suppressed the production of inflammatory cytokines and prevented the decline of glandular function associated with this model of SjS (He, Zhao et al. 2008). Whilst the lack of specificity for Sjögren's syndrome may render the measurement of anti α-fodrin moot, its role disease progression may still render anti α-fodrin a viable target for treatment in Sjögren's syndrome.

Anti Muscarinic

Glandular secretion is brought about by the sequence of events explained earlier, with the signal cascade starting with the binding of the neurotransmitter acetylcholine (ACh) to the G protein-coupled muscarinic type 3 receptors (M3R), resulting in M3R's activation and subsequent secretion (Matsui, Motomura et al. 2000; Nakamura, Matsui et al. 2004). Previous work in detecting the putative anti M3R antibody has demonstrated the difficulties associated with the task, with standard ELISAs being shown to be ineffective at detecting the antibody (Dawson, Allison et al. 2004; Roescher, Kingman et al. 2011); however, in studies where antimuscarinic antibodies have been detected, they have been detected at an incidence of 80-90% (Bacman, Sterin-Borda et al. 1996; Waterman, Gordon et al. 2000; Kovacs, Marczinovits et al. 2005; Marczinovits, Kovacs et al. 2005). This high degree of

incidence satisfies Drachman's first criterion: "Autoantibodies are present in patients with the disease).

Since the events leading to secretion begin with the activation of M3R by ACh, it is safe to assume that prevention of ACh binding will prevent the normal sequence of events culminating in secretion. Until recently, the second of Drachman's criteria: "Antibody reacts with the target antigen" had not been definitively demonstrated, although implied by the blocking of cholinergic stimulation by M3R, altering contractilitiy in the smooth muscle of the bladder and intestine (Waterman, Gordon et al. 2000; Goldblatt, Gordon et al. 2002). The M3R autoantibody had also been implicated in the pathology of Sjogren's syndrome, with autoantibodies inhibiting secretion in isolated human salivary gland acinar cells (Dawson, Allison et al. 2004; Dawson, Stanbury et al. 2006) as well as salivary gland derived cell lines (Li, Ha et al. 2004). However, Kovács *et al* in 2008 showed that the anti M3R antibody, isolated from pSjS patients, bind to the M3R present on acinar cells in healthy labial salivary glands (Kovacs, Feher et al. 2008). The exact nature of the binding exhibited was not explained, although much data suggest that the target for anti-M3R is the second extracellular loop of the receptor (Bacman, Berra et al. 1998; Cavill, Waterman et al. 2004; Naito, Matsumoto et al. 2005; Dawson, Stanbury et al. 2006), although the third extracellular loop has recently become a target for study (Koo, Li et al. 2008).

Satisfaction of the next of Drachmann's autoantibody criteria, "Passive transfer of antibody reproduces features of the disease" has also been satisfied in a model animal. Transfer of IgG from the Non Obese Diabetic (NOD) mouse, a model animal for the development of SjS, resulted in dry mouth symptoms in healthy controls (Robinson, Brayer et al. 1998). Likewise, the healthy control mouse recipients of human SjS derived IgG developed bladder hyper-

responsiveness (Wang, Jackson et al. 2004). Satisfaction of the final criterion, "Reduction in antibody levels ameliorates the disease" has also been demonstrated. Neutralisation of circulating autoantibodies in SjS patients with intravenous immunoglobulin resulted in a reported improvement of SjS associated bladder symptoms (Smith, Jackson et al. 2005).

Anti M3R autoantibody has been found in other diseases, notably scleroderma (Goldblatt, Gordon et al. 2002), dermatomyositis (Dawson, Tobin et al. 2005) and narcolepsy (Dawson, Tobin et al. 2005; Jackson, Spencer et al. 2009).

1.5 Aims of the Study

The main aim of this study was to investigate the effect of NO upon lacrimal gland acinar cells, and to examine NO's effect upon fluid secretion. It has been shown that increased levels of NO are present in SjS sufferers, and that NO can have a biphasic effect upon salivary secretion, initially increasing response to agonist before resulting in attenuation of response. Demonstration of a similar effect in lacrimal gland acinar cells would lend credence to the hypothesised role of increased NO in SjS sufferers and possibly open up previously unexploited avenues for treatment.

Furthermore, identification of antimuscarinic action of IgG fraction from SjS patient sera has been described. Identitification of the anti M3R antibody as having an anti-secretory effect lends itself to be the basis of a diagnostic test for autoantibody involvement in SjS. Since previous work has been unable to detect the anti M3R antibody by standard methods, it was also the aim of this study to determine whether an assay based upon the effect of antiM3R upon agonist evoked stimulation could be constructed.

2 Materials and Methods

2.1 Solutions

Extracellular bathing solution (Na HEPES)

The extracellular bathing solution used for all experiments (Na HEPES) consisted of (in mM) : NaCl 140, KCl 4.7, MgCl 1.13, Glucose 10 and HEPES 10. The Na HEPES was constituted in deionised water and titrated to pH 7.4 with 1M NaOH and then stored at 4°C. The standard extracellular bathing solution was completed by adding $CaCl_2$ to 1mM immediately prior to the experimental run.

Standard intracellular solution (For Patch clamp)

The standard intracellular patch pipette solution used for all patch clamp experiments consisted of (in mM): KCl 140, $MgCl_2$ 1.13, Glucose 10, HEPES 10, ATP and EGTA.

Buffers for IgG isolation and preparation

Phosphate buffer was prepared by mixing 57.7ml of 0.1M, NaH_2PO_4 and 42.3 ml of 0.1M Na_2HPO_4 both titrated to pH 7.0 with 1M HCl. Elution buffer consisted of 0.1M glycine, titrated to pH 2.7 with 1M HCl. Neutralisation buffer consisted of 1M Tris, titrated to pH 9.0 with 1M HCl.

All buffers were made up using dH_20 and stored at 4°C until used.

Buffer Components and Supplier List

Reagent	Supplier and Code	Function
NaCl	BDH 10241	Buffer component
KCl	BDH 101985	Buffer component
MgCl	BDH 101494	Buffer component
Glucose	Sigma G7021	Buffer component
HEPES	Sigma H4034	Buffer component
ATP	Sigma A2383	Buffer component
EGTA	BDH E4378	Buffer component
NaH_2PO_4	BDH 307164T	Buffer component
Na_2HPO_4	BDH 102494C	Buffer component
glycine	BDH 101193C	Buffer component
Tris	BDH 103156X	Buffer Component

Test Solutions

Carbamylcholine chloride (Carbachol), CCh.

Carbamylcholine chloride (Sigma 4387), or carbachol, was used as a cholinergic agonist in these experiments. While not as potent as acetylcholine, carbachol is not as readily metabolised by acetylcholinesterase, which may still be present in serum or cell samples. Carbachol was made up as a 100nM stock in dH_20 and stored at 4°C until diluted with extracellular bathing solution to working concentrations.

S-Nitroso-N-acetyl penicillamine (SNAP)

S-nitroso-N-acetylpenicillamine stored as a powder at -20C, was used as a nitric oxide donor in these experiments. Each day a fresh 5mg vial was used, dissolving in DMSO to form a 100mM stock solution. This stock solution was then diluted with extracellular bathing solution to make a working solution of 100uM.

1H [1,2,4] oxadiazolo [4,3, alpha] quinoxaline-1- one (ODQ)

1H [1,2,4] oxadiazolo [4,3, alpha] quinoxaline-1- one is a highly selective inhibitor of NO sensitive soluble guanyl cyclase. It was initially made up to a 10mM stock solution with DMSO, then diluted with extracellular bathing solution to a working solution of 10uM.

L-N^G-Nitroarginine methyl ester (L-NAME)

L-N^G-Nitroarginine methyl ester was used as a non selective NOS inhibitor. A 100mM stock solution was made by dissolving the L-NAME in dH_20 and stored at 4°C. Experiments used a working solution of 10- 100µM L-NAME in the extracellular buffer.

S-methyl isothio urea (SMT)

S-methyl isothio urea is a highly selective inhibitor of iNOS. 100mM stock solution was prepared by dissolving SMT in dH_2O and storing at 4°C until diluted with extracellular bathing medium to form a 10μM working solution.

Diphenyleneiodonium chloride (DPI)

Diphenyleneiodonium chloride (Sigma D2926) is a potent, irreversible inhibitor of iNOS and eNOS. A 100mM stock solution was prepared by dissolving DPI in dH20 and storing at 4°C. A 10uM working solution was prepared by dilution of the stock solution with extracellular bathing medium.

Arginine

Arginine is the amino acid substrate of NOS, converted into citrulline and nitric oxide. A 100mM stock solution was prepared by dissolving Arginine in dH_20, and storing at 4°C. A 10uM working solution was prepared by dilution of the stock solution with extracellular bathing medium.

Note

When DMSO was used as a solvent, its final concentration was kept below 0.1% v/v in the experimental run. Previous studies have indicated that this concentration of DMSO did not significantly alter either Ca^{2+} or ion channel activity (Smith and Gallacher 1992).

List of Reagents

Reagent	Supplier and Product Code	Primary Vehicle	Secondary Vehicle	Stock Concentration	Working Concentration	Function
Carbamylcholine chloride	Sigma 4387	Water	Na HEPES	100µM – 100mM	100nM -100µM	Agonist
S-Nitroso-N-Acetylpenicillamine	Calbiochem 487910	DMSO	Na HEPES	50-100 mM	50100µM	NO donor
1H [1,2,4] oxadiazolo [4,3,alpha] quinoxaline-1- one	Calbiochem 495320	DMSO	Na HEPES	10mM	10µM	sGC inhibitor
L-N^G-Nitroarginine methyl ester	Sigma N5751	Water	Na HEPES	10mM-100mM	10 -100µM	NOS inhibitor
S-methyl Iso-Thio Urea	Sigma-Aldrich M8,444-5	Water	Na HEPES	10mM	10µM	NOS inhibitor
Diphenyleneiodonium chloride	Sigma D2926) is	Water	Na HEPES	50-100uM	50-100nM	NOS inhibitor
Arginine	Calbiochem 1820	Water	Na HEPES	10mM	10µM	NOS Substrate

Fluorescent Dyes for Microfluorimetry

Diaminofluorescein – 2 Diacetate (DAF-2- DA)

Diaminofluorescein – 2 Diacetate (DAF-2-DA) (Calbiochem 251505) was used to detect NOS activity in isolated cells. It is supplied as 2.22 mg/ml, dissolved in DMSO and stored away from light at 4°C until used.

Fura-2-acetoxymethyl ester (Fura 2 AM)

Fura-2-acetoxymethyl ester (Fura 2 AM) (Sigma F0888) was used to detect intracellular calcium release.

Primary Cell Culture Medium

Cells in primary culture were maintained in DMEM: F-12 (1:1) +L-glutamine + 15mM HEPES (GIBCO 31330-038). This was supplemented by antibiotic/ antimycotic (Sigma A5955) to 1% v/v. Primary cells were maintained serum free, limiting proliferation and reducing the risk of phenotypic change.

Gland Digestion Solution

To facilitate the release of small clusters of acinar cells from the gland in question, collagenase (Worthington Diagnostic, USA) was dissolved in calcium containing Na HEPES to a concentration of 200 U/ml. 1 ml aliquots of the digestion solution were stored at -20°C until used.

Cell Line Culture Medium

Cells in continuous culture were grown in MEM (GIBCO 10370) supplemented with penicillin (10,000 units), streptomycin (10mg/ml) and glutamine (200mM) 1%v/v (Sigma G6784) and (between 2 and 10 % v/v) fetal bovine serum (Gibco 10270) depending upon protocol.

Matrigel Basement Membrane Matrix

For use with the microfluorimetry rig, both cell lines and primary cultured cells were grown/maintained upon coverslips coated (c. 1mm thick) with Matrigel^{TM} Basement Membrane Matrix. Matrigel is a protein mixture secreted by Engelbreth-Holm-Swarm (EHS) mouse sarcoma cells and is used to form an adhesive basement membrane layer on the coverslips which prevents the cells washing away during perfusion.

2.2 Cell Culture

HSG Cell Line

The HSG cell line (a kind gift from I. S. Ambudkar, NIH Bethesda, USA) were cultured aseptically in cell line culture medium within 75cm^2, 250ml tissue culture flasks (Greiner 658/175) at 37°C in a humidified 95% air/ 5% CO_2 atmosphere until 75-85% confluent.

Cell Line Harvesting

Upon reaching the desired level of confluence the cells were subcultured and transferred to the relevant experimental vessel under aseptic conditions. This was achieved by first removing the exhausted culture medium using sterile 3ml pastettes. To ensure the complete removal of all dead cells and exhausted medium, the cells were washed with room temperature, sterile Dulbecco's Phosphate Saline Buffer (PBS) solution (D8537, Sigma). Detachment of the cells from the culture flask was achieved by incubating the cells with sterile 0.02% (0.5mM) EDTA solution (E8008, Sigma) at 37°C for 3 minutes followed by a vigorous lateral shake. A cell pellet was formed by centrifugation at 240g for 5 minutes at room temperature. The pellet was resuspended in fresh PBS and re-centrifuged at 240g for 5 minutes. The supernatant was removed again and the cells finally resuspended in cell line culture medium.

Mouse Acinar Cell Preparation

Lacrimal gland acinar cells are obtained from male CD-1 mice (Charles River UK Ltd, Margate, UK) between 5-8 weeks of age. These mice were maintained in the University of Liverpool's animal house for up to 3 weeks. The mice were stunned by concussion then euthanised by cervical dislocation and the salivary or lacrimal glands removed. Gland digestion solution was pre-warmed to 37°C and injected directly into the gland, facilitating

removal of the glandular capsule. The isolated gland was inflated with digestion solution and suspended in the remaining digestion solution. The inflated gland was then incubated for 15 minutes in a 37°C water bath with 30 second vigorous manual agitations every 5 minutes to break up the gland. After this incubation period, any large undigested sections of gland were removed from the digestion medium. The remaining small fragments in suspension were further broken up by repeated tritruations (c. 50) of the suspension with a 1ml Gilson pipette. This cell suspension was diluted by the addition of 3ml Primary Cell Culture Medium and centrifuged for 3 minutes at 200rpm at room temperature to obtain a pellet of acinar cells. The supernatant was discarded and the pellet resuspended in culture medium extinguishing residual collagenase activity by dilution. This procedure yielded individual acinar cells or small clumps of 2 to 10 acinar cells.

Human Salivary Gland Preparation

Following relevant local ethical committee approval and informed consent, small samples of human submandibular and parotid salivary glands were obtained from patients undergoing neck dissection surgery. Subjects were screened so as to avoid samples from patients who had undergone therapeutic irradiation to the head or neck.

Upon removal from the patient, the gland samples were placed in tissue culture fluid and immediately transported on ice to the laboratory within 60 minutes. Isolation of acinar cells proceeded in an identical fashion to that of the mouse acinar cells.

Cells in primary culture were maintained in DMEM: F-12 (1:1) +L-glutamine + 15mM HEPES (GIBCO 31330-038). This was supplemented by antibiotic/ antimycotic (Sigma A5955) to 1% v/v. Both mouse and human cells were used routinely after spending 4-48 hours in primary culture (humidified 5% CO_2/(95%O_2).

2.3 Microfluorimetry

Measurement of Ca^{2+} and NO were obtained by the use of a Cairn Spectrophotometer (Cairn Research, Cambridge). Light from a xenon arc lamp is filtered by a monochronometer, selecting for the required excitation wavelengths of the dyes being used (DAF 488nm, Fura 340nm and 380nm). The excitation wavelengths were passed down a quartz light guide to the Nikon Diaphot inverted binocular microscope (TMD 100. Nikon, Kingston, UK). This light was reflected by a dichroic mirror, which has a cut off of approximately 400nm. The excitation light is focused upon the dye loaded cells on the base of the perfusion chamber by a CF Fluor oil quartz objective lens. The light emitted by the dye laden cells is then passed through a 510 nm (Fura) or 515nm (DAF) long pass emission filter and the images captured by a CCD camera. The camera is linked to a computer running "Metafluor" software, allowing for data capture and visualisation.

Measurement of $[Ca^{2+}]_i$ by Fura-2 fluorescence

Fura 2 was used in all of the experiments to determine the change in $[Ca^{2+}]_i$. This dye allows for rapid loading and repeatable results whilst minimising alterations to cellular homeostasis; and, by virtue of its light emission in the presence and absence of Ca^{2+}, minimises artefacts caused by variations in cell thickness and loading concentration.

Fura-2 loading

Fura-2 itself is not readily permeable across cell membranes. For all experiments the membrane permeable, lipid soluble, acetomethoxy ester of Fura-2, Fura-2 AM (Sigma F0888) was used. Fura-2 AM diffuses easily across the cell membrane, where it is de-esterified by the cell, trapping the cell impermeable Fura-2 (Figure 2.3.1.1).

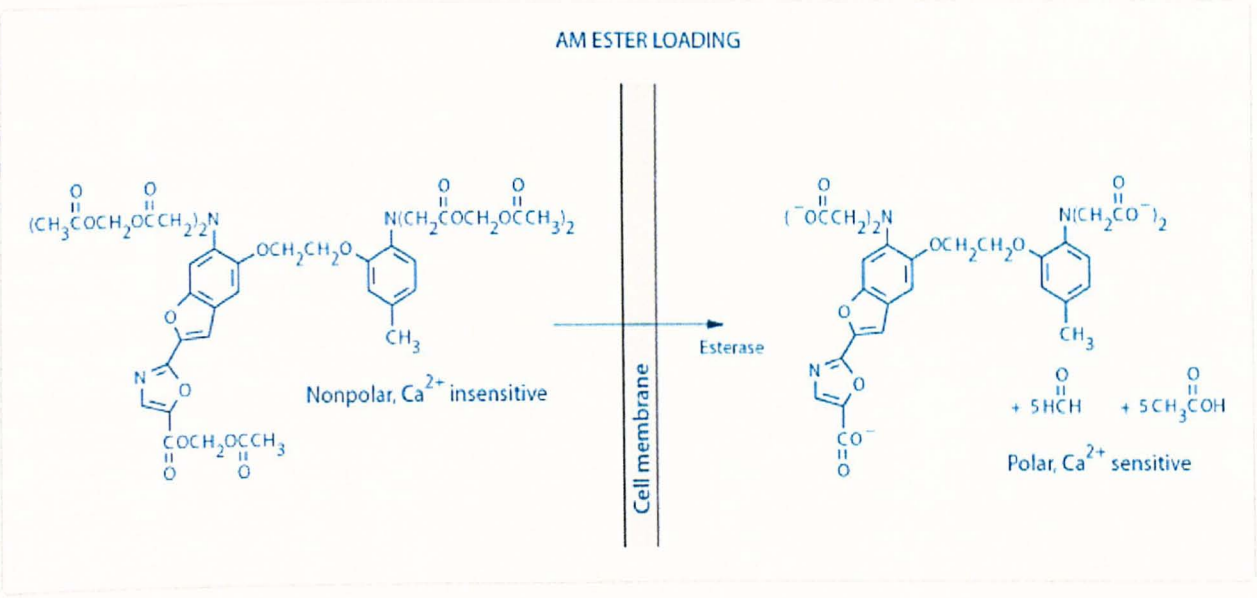

Figure 2.3.1.1 Diagrammatic representation showing the diffusion of Fura 2 AM and its consequent de-esterification to the fluorescent, cell impermeable Fura 2 (Source: Invitrogen).

Cell loading with Fura-2 was performed at 37°C for 10 minutes for primary isolated cells, and 15 minutes for cell lines.

The emission properties of Fura-2 are dependent upon the presence of free calcium, in its presence Fura-2 has an excitation maximum of 380nM but only 340nM in free calcium's absence. Maximal emission (following excitation at 340nM or 380nM) occurs at 510nM. The ratio of light emitted following excitation at these wavelengths is a function of the free calcium present in the cell. It is this ratiometric nature that minimises artefacts caused by variations in dye concentration and cell thickness.

Detection of Nitric Oxide using DAF-2

Detection of nitric oxide was achieved through the use of the NO reactive fluorescent dye 4,5 diaminofluorescein diacetate, or DAF-2DA (Calbiochem 251505). This compound is cell membrane permeable and, like Fura-2AM, is de-esterified upon entry to the cell. This generates diaminofluorescein (DAF-2) which, upon reaction with NO, forms the fluorescent triazolofluorescein (DAF-2 T) (Figure 2.3.2.1).

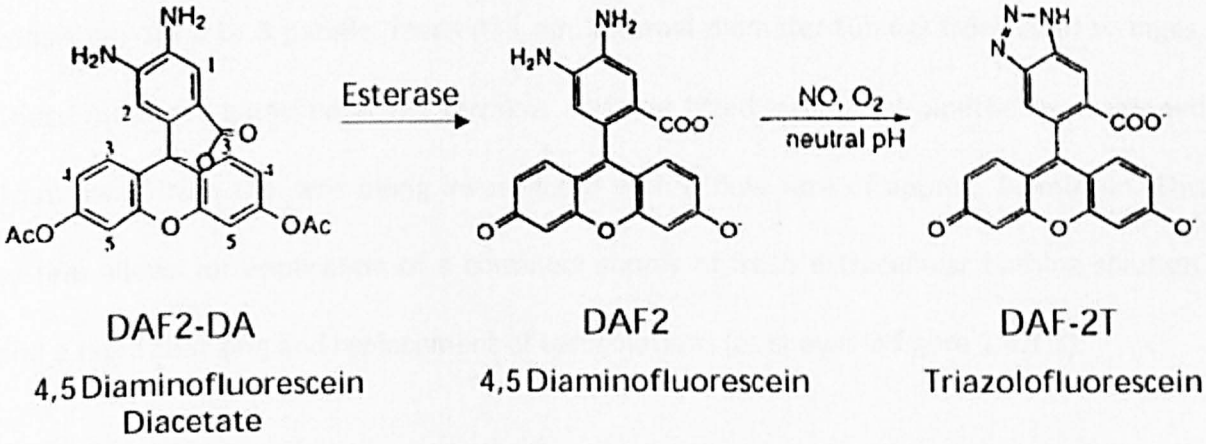

Figure 2.3.2.1 DAF 2-DA readily diffuses across the cell membrane and is de-esterified, leaving the cell- impermeable DAF 2. Under physiological conditions, only NO (rather than oxidised forms of NO) will react with DAF 2 to form the fluorescent DAF 2T (Source SigmaAldrich).

DAF loading

Lacrimal gland acinar cells on Matrigel coated coverslips were loaded in medium containing 5mM DAF-2DA for 10 minutes at 37°C in a humidified 5% CO2 atmosphere. The cells on coverslips were mounted as per the Fura microfluorimetry protocol. Fluorescence due to DAF was observed by excitation at 488nm and emission at 515nm.

2.4 Perfusion system.

Primary perfusion

The cell/Matrigel covered cover slips formed the base of the custom built perfusion chamber. This chamber is mounted upon the stage of an inverted binocular microscope attached to a video camera/ fluorimeter setup. The chamber is initially filled with extracellular bathing solution and has a suction tube attached for the purpose of removing excess solution. Continuous perfusion of the cells is achieved by a gravity fed system consisting of up to 8 parallel feeds (0.5 mm internal diameter tubing) from 20ml syringes. These tubes are gathered at the terminal end and fitted into a 1ml pipette tip positioned 1mm away from the cells being investigated with a flow rate of approx. 0.5ml/min. This system allows for application of a continual supply of fresh extracellular bathing solution, and a rapid changing and replacement of test solutions (as shown in figure 2.4.1.1).

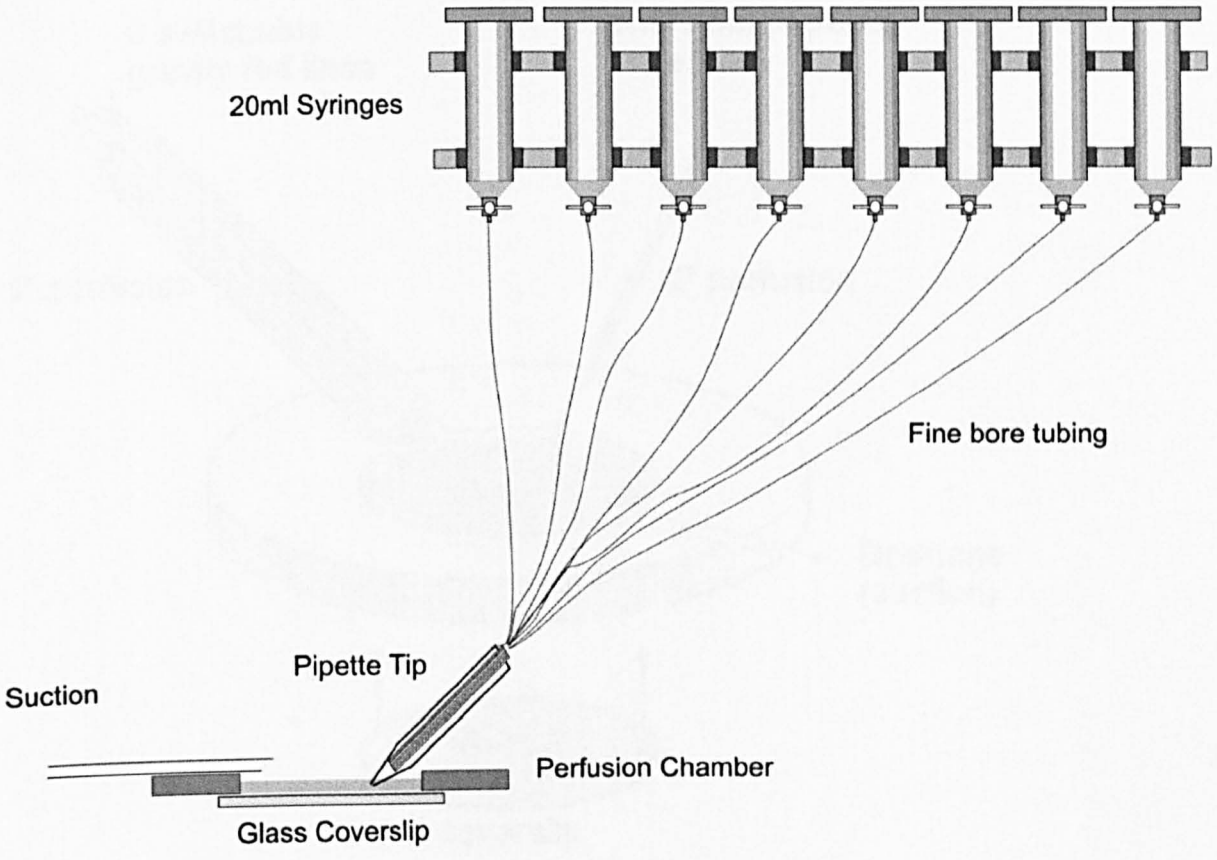

Figure2.4.1.1 Schematic diagram of the primary perfusion system. This system allows for the rapid changing between test solutions and removal of excess solution.

Secondary perfusion

In addition to the primary perfusion system, a secondary system was set up to assess the effects of IgG applications without the need for large amounts of IgG isolate. Interruption of the flow of the primary feed was achieved by the use of a secondary feed positioned 100-150um away from the cells being studied, with a flow rate of 5 ul/s. The secondary perfusion system consists of a No. 564 borosilicate capillary tube (Assistent, Denmark), pulled using a DMZ Universal Puller (Zeitz Instruments, Germany), and connected to a "Genie" syringe pump (Kent Scientific Corporation, USA) and backfilled with the solutions under investigation.

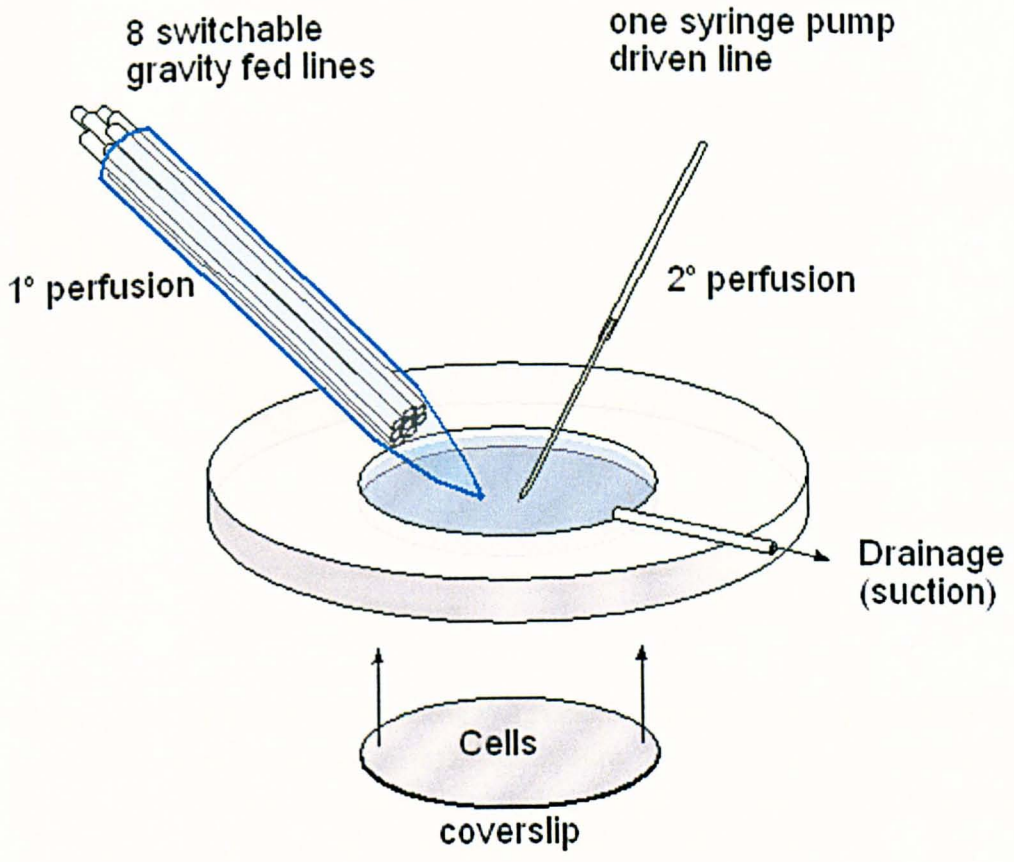

Figure 2.4.2.1 Schematic of the perfusion chamber with attached perfusion feeds and drainage system. Diagram courtesy of Dr. P. M. Smith.

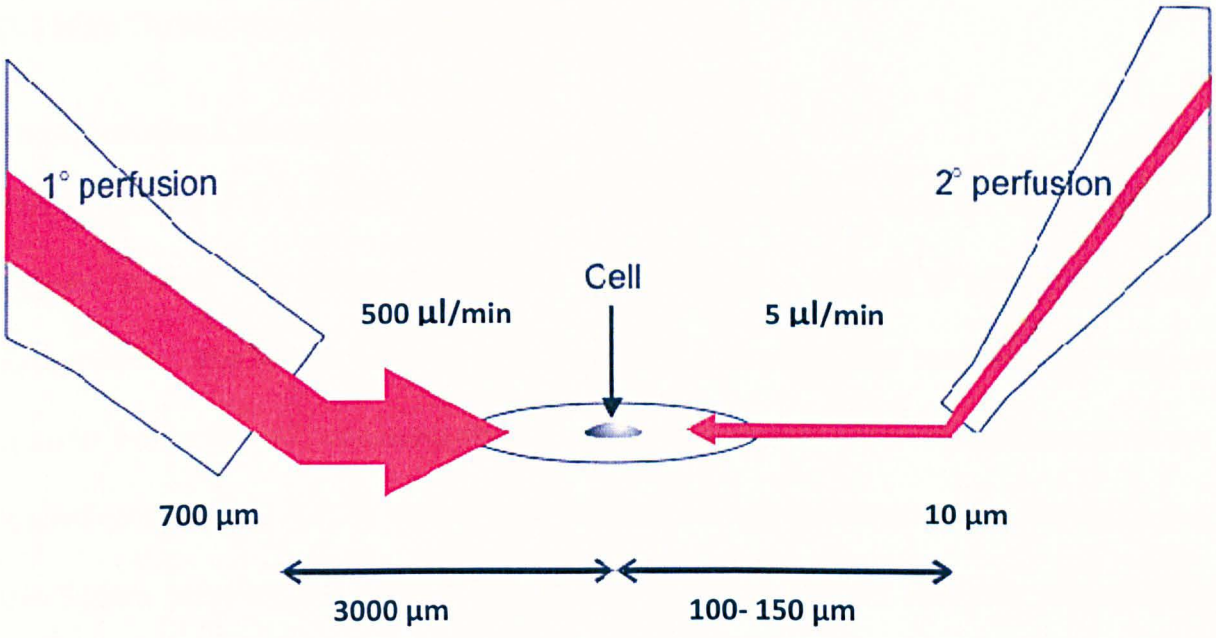

Figure 2.4.2.2 Illustration showing the positioning of the Primary and Secondary perfusion feeds. The smaller bore(10µm/2° vs 700µm 1°) and closer proximity(100-150µm/2° vs 3000µm/1°) of the secondary perfusion pipette allows the primary perfusion to be effectively overridden. Diagram courtesy of Dr. P. M. Smith.

2.5 High Throughtput Microfluorimetry

The Flexstation 3 Microplate Reader

The Flexstation 3 is a multi-mode microfluometric plate reader with an integrated fluid transfer system. This system allows for a high throughput method of screening agonist/ antagonists. The system employs an integrated 8 channel fluidics head to effect reagent transfer from a 96 well compound plate, to the black walled 96 well plate containing the dye loaded cells (Figure 2.5.1). In experiments fluorescence was read from below the plate using the 510nm wavelength emission light (with a cutoff of 455nm) following excitation at 340nm and 380nm wavelengths.

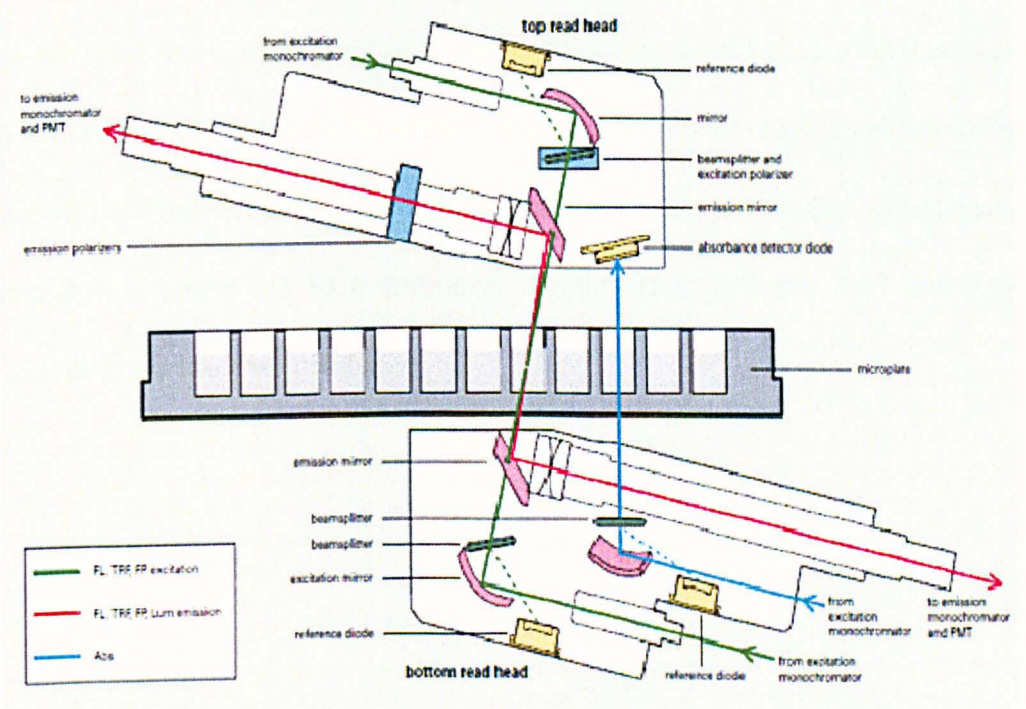

Figure 2.5.1 The integrated light reading unit in the Molecular Devices Flexstation 3, enabling a the development of a high throughput method of screening IgG fractions for antimuscarinic receptor activity. The principle is exactly the same as the microfluorimetry rig, but reads an area of plate, rather than individual cells and allows for a variety of test solutions to be run in parallel. (Source: Molecular Devices).

Cell culture and dye loading for high throughput method

Black walled 96 well plates were inoculated with HSG cells in 300uL of MEM supplemented with 10% FBS and incubated for 72 hours. Exhausted medium was aspirated and replaced with 100uL of dye loading medium, made up of standard extracellular bathing medium, 200nM Sulfinpyrazone (Sigma S9509), 0.0135% w/v Pluronic F127 (Sigma p2443) (Sulfinpyrazone and Pluronic were added here to aid in the loading of the Fura 2 into the HSG cells) and Fura 2 AM and incubated for 45 minutes at 37°C. After incubation, the loading medium was removed and replaced with 75uL of standard extracellular bathing medium and incubated at 37°C for an additional 10 minutes.

Experimental Protocol

Each experimental run consisted of an initial addition of carbachol to a final concentration of 50uM in each well. To measure the effect of IgG upon agonist evoked calcium release, the second addition contained carbachol and the IgG samples under investigation. The Flexstation 3 was connected to a computer running the "Softmax Pro" software which records and displays the data produced.

2.6 IgG Fraction Preparation

1ml of test serum (or saliva) was diluted with 4ml (2 ml for saliva) of 0.1M phosphate buffer. This was passed through a sterile 0.8uM Acrodisc syringe filter (PN 4618, Pall) to remove any debris or protein aggregations. This diluted solution was then passed through a High Trap Protein G column (GE Healthcare), using a peristaltic pump. The IgG fraction was subsequently eluted from the column with 0.1 M glycine-HCl buffer of pH 2.7. Collection of the IgG fraction was facilitated by the use of a U.V. Monitor (Pharmacia Biotech) connected to a chart recorder, allowing for the collection of the fraction as it was eluted. The fraction was collected into a tube with 400ul of the Tris-HCl buffer added to neutralise the pH. The eluted fraction in buffer was dialysed (size 8, 12-14kDa dialysis tubing) at 4°C for 24 hours against Na HEPES, to exchange the elution buffer for HEPES. Determination of the protein concentration (and therefore IgG content) was with use of the bichoninic acid assay kit (Sigma). The IgG fraction in Na-HEPES was then aliquotted and stored at -20°C until used.

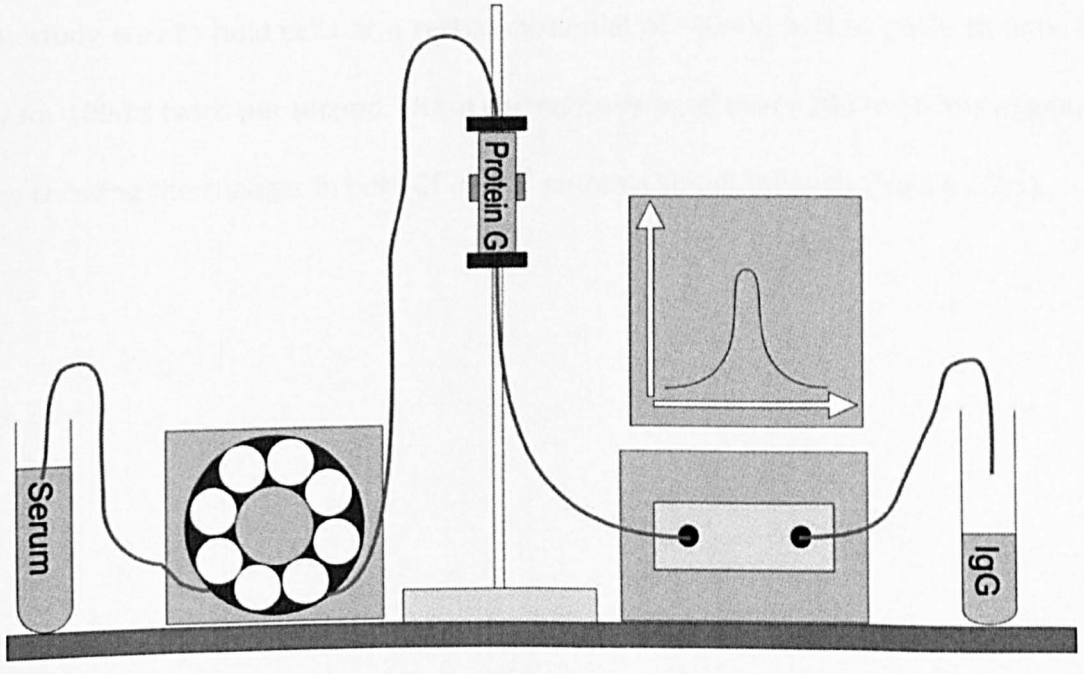

Figure 2.6.1 Schematic of apparatus for the extraction of the IgG fraction from human serum.

2.7 Whole cell patch clamp

Lacrimal gland secretion is dependent upon the mobilisation of Ca^{2+} from intracellular stores, which activate apical Cl^-, and basolateral K^+ channels. The opening of these channels drives NaCl into the lumen of the gland which, in turn, drags water with it along an osmotic gradient. The activation of these ion channels, and therefore, the movement of the ions across the membrane give rise to a measurable electrophysiological change in the cell, which is indicative of the change in intracellular calcium concentration. Making use of the Whole cell pulse protocol, it is possible to make near simultaneous measurements of K^+ and Cl^- currents.

With the standard extracellular and intracellular solutions, the reversal potential (the membrane potential at which there is no net movement of the ion in question) for Cl^- is 0mV and for K^+ is -80 mV. Thus, in a cell voltage clamped to 0mV, any current measured will be due to K^+, and any current measured at -80mV will be due to Cl^-. The pulse protocol used in this study was to hold cells at a resting potential of -40mV, and to pulse to 0mV and -80mV for 100ms twice per second. These currents averaged every 200 to 500ms to generate a trace showing the changes in both Cl^- and K^+ currents simultaneously (Figure 2.7.1).

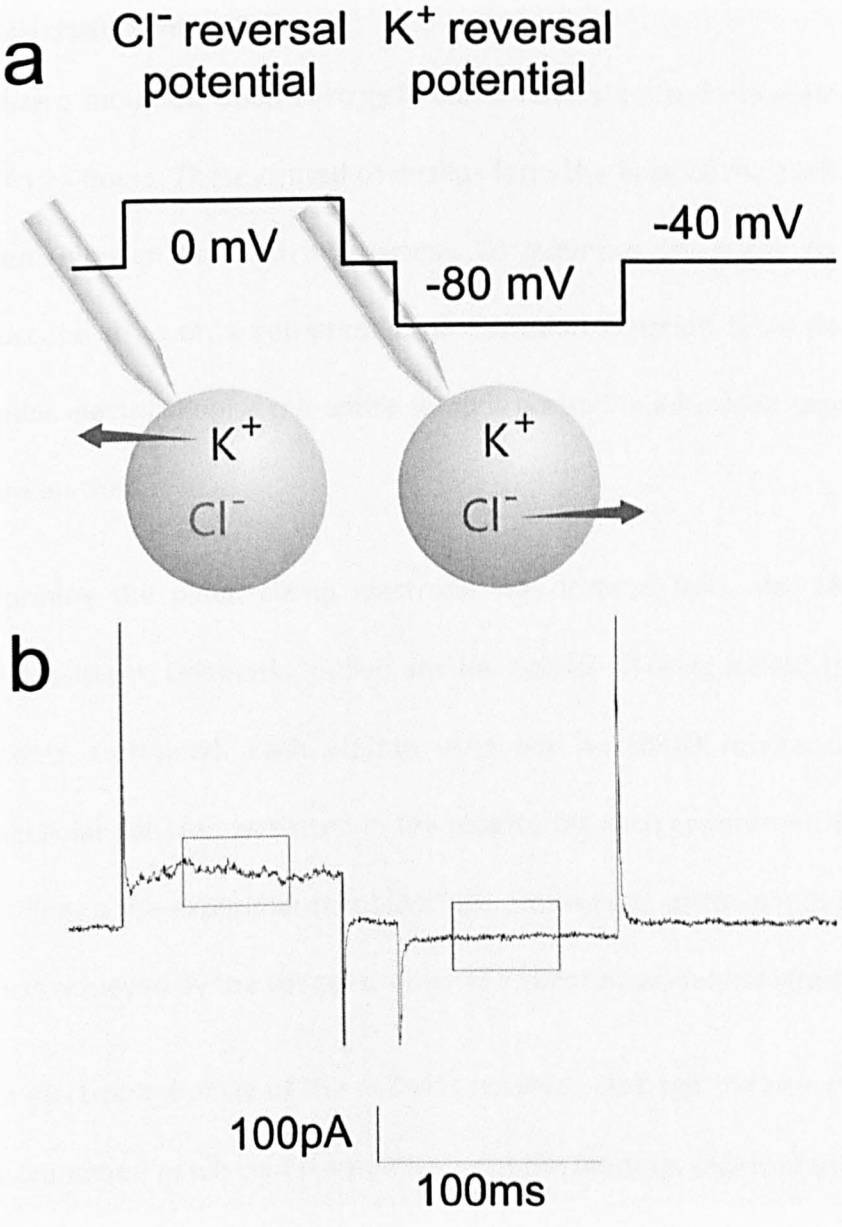

Figure 2.7.1 Whole-cell patchclamp pulse protocol of measurement of Ca^{2+} dependent ion currents

A) Lacrimal gland acinar cells were voltage clamped to -40mV using the whole-cell patch clamp technique. 100ms pulses were made at both the Cl^- (0mV) and K^+ (-80mV) reversal potentials.

B) The custom written "Holsel" software allows for the currents measured to be displayed on a computer screen. The Cl^- current was measured at the K^+ reversal potential and vice versa. Data was collected from a 50ms period in the middle of each voltage pulse (therefore avoiding on/ off transients) and averaged to give the mean current at that voltage. The averaged data was saved every 200-500ms and recorded and displayed via the "Holsel" software. (Diagram courtesy of Dr P. M. Smith).

Whole cell patch clamp protocol

Lacrimal cells were mounted upon Matrigel coated coverslips and maintained in primary culture for up to 24 hours. These coated coverslips form the base of the perfusion chamber and is mounted upon an inverted microscope. To minimise noise due to vibration the inverted microscope rests on a compressed air vibration isolation table (Newport, USA), whilst to minimise electrical noise the entire setup is housed in a Faraday cage and all metal components are earthed.

The pipette forming the patch clamp electrode was formed from No. 564 borosilicate capillary tubes (Assistent, Denmark), pulled and heat polished using a DMZ Universal Puller (Zeitz Instruments, Germany). Each pipette used had an initial resistance of 2-4 MΩ. Standard intracellular solution was used in the pipette for each experiment with additional reagents according to the experimental objectives. Positioning of the patch clamp pipettes onto the cell was achieved by the usage of a hydraulic micromanipulator (Narishige, Japan).

Measuring the electrophysiology of the cell was achieved through the use of the Axopatch 200a (Axon Instruments) patch clamp amplifier, with the readings digitised using a CED 1401 interface (Cambridge Electronic Design). Implementation of the patch clamp pulse protocol, data recording and analysis was performed by the custom written software package "HOLSEL" (Smith 1992)

A

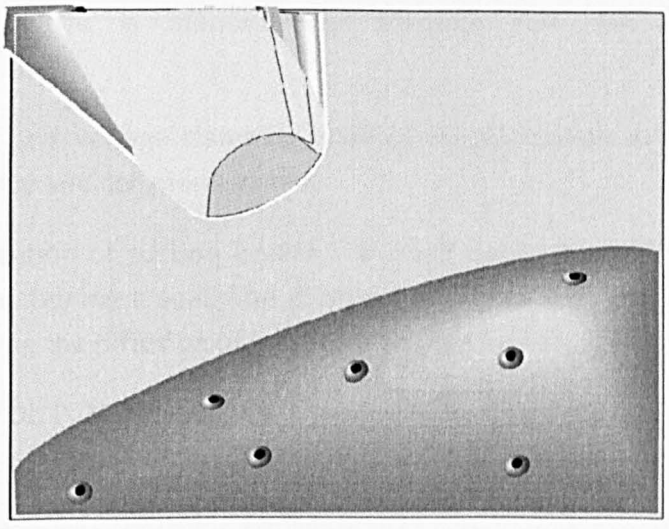

B

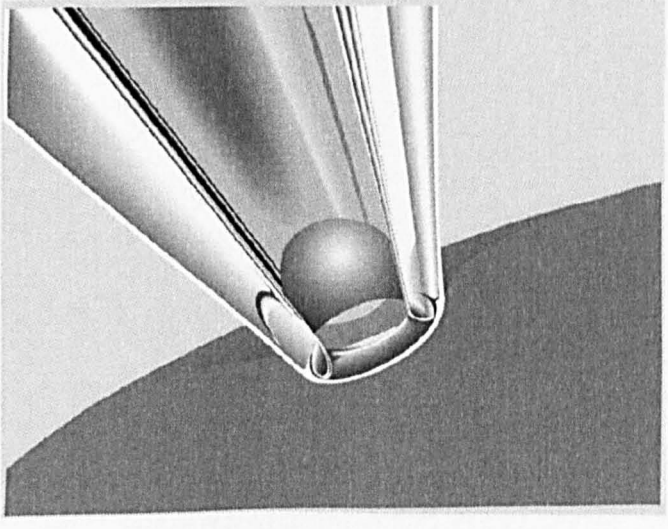

C

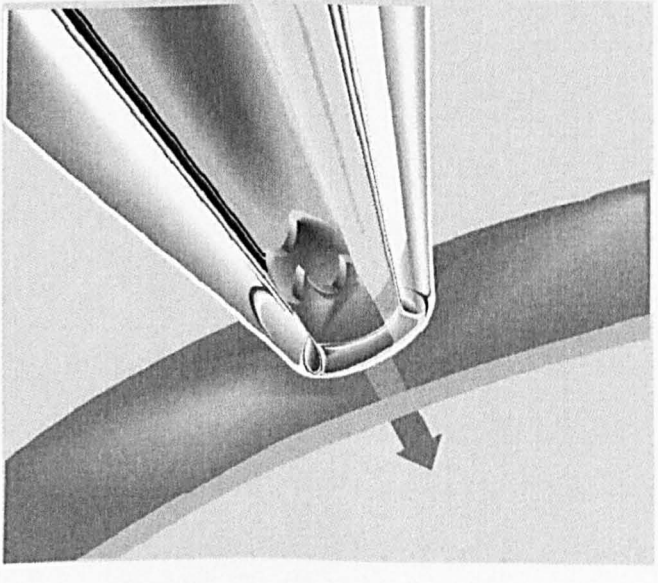

Figure 2.7.2 Illustration of Whole Cell Patch Clamp.

A) The patch pipette is manoeuvered towards the cell membrane with a micromanipulator

B) Slight suction and voltage clamping enables the formation of a tight (GigaΩ) seal between pipette and cell membrane

C) A sharp application of suction breaks the small patch of membrane at the pipette whilst still maintaining a seal. The pipette's contents are now contiguous with the cytosol, allowing the diffusion of test solutions to the cell interior.

Diagrams courtesy of Dr. P. M. Smith

3 Results

3.1 The effect of exogenous supply of NO from the NO donor SNAP upon Ca^{2+} signalling in mouse lacrimal gland acinar cells.

Aims and objesctives

The following results are an attempt to show whether increased NO from a donor has a similar mode of action upon lacrimal gland acinar cells to that described previously in submandibular gland acinar cells. The similarity of the biphasic effect of NO observed in mouse and human salivary gland tissue allows for the hypothesis that any effect seen in mouse lacrimal gland acinar cells would likely be similar in human lacrimal gland cells. The use of mice as a model organism removed the difficulty of obtaining healthy lacrimal gland tissue, which would be unnecessarily invasive (and unethical), and allowed for age/sex matched samples to be reliably sourced.

Introduction

Sjögren's syndrome sufferers exhibit a host of symptoms; most notable is the observed glandular hypofunction, and the role of nitric oxide (NO) in the signalling cascade involved in fluid secretion has been documented. There is circumstantial evidence for potential role for NO in the glandular hypofunction observed in SjS. Increased levels of NO have been measured in both the expired air of patients with SjS (Ludviksdottir, Janson et al. 1999) and saliva samples (Konttinen, Platts et al. 1997). It is well established that salivary and lacrimal secretion is dependant upon agonist evoked increase in $[Ca^{2+}]_i$, and any factors affecting the signal cascade may adversely affect cellular function, resulting in glandular hypofunction. Crucially, Caulfield *et al* demonstrated how NO from a donor has a biphasic effect upon agonist evoked intracellular calcium release, initially amplifying then diminishing calcium

release in mouse submandibular acinar cells, linking NO with fluid secretion (Caulfield, Balmer et al. 2009). Observation of the same effect of NO upon lacrimal gland acinar cells would suggest that increased levels of NO may be a unifying factor between the two separate secretory organs for the glandular hypofunction associated with SjS.

The agonist evoked secretory Ca^{2+} signal may be measured *in vitro* in both lacrimal and submandibular acinar cells using FURA 2 microfluorimetry (see methods). In both cell types a highly reproducible biphasic change in $[Ca^{2+}]_i$ follows stimulation with agonist. It is possible to elicit sequential responses to repeated agonist stimulation and, as we have previously shown (Caulfield, Balmer et al. 2009) in submandibular cells, these responses are consistent over the duration of the experiment. Thus it is possible to measure the response to agonist before and after treatment of the cells with NO donors, such as SNAP, and to use the response before exposure as a control against which to measure the response after exposure.

Figure 3.1.1A shows the change in $[Ca^{2+}]_i$ in lacrimal acinar cells evoked by a two minute exposure to low concentration of the cholinomimetic agonist carbamylcholine chloride (carbachol, CCh), followed by a two minute "rest" period. As may be seen, in this experiment, there was very little variation in the kinetics and magnitude of each response. The same protocol was used to obtain the data in figure 3.1.1B, except that in this experiment the cells were continuously exposed to SNAP (50μM) from approximately ten minutes after the start of the experiment, following the first two exposures to CCh. As may be seen, the magnitude of the response to CCh was increased acutely in the presence of SNAP, with the response increasing to 176% of the initial agonist exposure. On this occasion

there was also an alteration in the kinetics of the response in the form of an oscillatory component to the plateau phase of the response, although this was not observed in the majority of experiments. This observation is consistent with that previously reported using an identical protocol in submandibular cells (Caulfield, Balmer et al. 2009) where it was hypothesised that the amplification of the response followed NO-stimulated cGMP-mediated cADPr production and sensitisation of ryanodine receptors, thought to contribute to the spread of the Ca^{2+} signal in exocrine acinar cells. It is possible to test this hypothesis in lacrimal acinar cells by using the sGC inhibitor ODQ.

Figure 3.1.2 shows that the CCh-evoked Ca^{2+} signal was not amplified by SNAP (50μM) when ODQ was added at the same time; this is the same as the response previously seen in submandibular acinar cells.

Averaged data showing the amplifying effect of SNAP on the agonist evoked Ca^{2+} signal are shown in figure 3.1.3. These data show that, in mouse lacrimal acinar cells, 50uM SNAP induced a of 392% ± 51% (n=22) amplification of the CCh-evoked Ca^{2+} signal compared to the Ca^{2+} signal evoked in the same cell, prior to exposure to SNAP. This significant ($p=<0.05$) amplification was abolished by simultaneous exposure to the sGC inhibitor ODQ (10μM) where the mean response was found to be 194% ±26% (n=7, not significantly different *vs* control $p=>0.5$). However, it should also be noted that in the absence of stimulation by SNAP there was also, on average, an increase in the response to repeated stimulation by CCh to over twice the initial response, i.e. 216% ± 21% (n=10). However, there was no statistically significant difference when the magnitude of the first response to CCh was compared to that of the third response. While no statistically significant difference in response was observed between 1st and 3rd responses, all the experiments (n=10) showed

an increase in response at the 3rd application of agonist, this is in contrast to the observations made in submandibular cells, where the response to agonist was unchanged over this period. The CCh-evoked Ca^{2+} signal in the presence of SNAP was nevertheless significantly greater than the increased response seen in the absence of SNAP ($p=<0.05$ fig 3.1.1 B *vs* fig 3.1.1 A).

Together these data are similar to the previous observation of the stimulatory effect of exposure to NO donor made using mouse submandibular cells. In both cell types the action of ODQ makes it possible to hypothesise that NO amplifies the action of the Ca^{2+}-mobilising agonist by sensitising the ryanodine receptor to increased levels of $[Ca^{2+}]_i$.

In mouse submandibular cells, chronic exposure to NO donor resulted in an attenuation of the response to agonist (Caulfield, Balmer et al. 2009). Figure 3.1.4 shows the results of an experiment in which lacrimal acinar cells were exposed to NO for longer periods of time and the Ca^{2+} signal elicited by agonist was determined over this period, using the same protocol as previously shown in figure 3.1.1A (2 minutes agonist stimulation. 2 minutes rest).

The initial response to agonist are similar to those described previously in figure 3.1.1A, there is an amplification of the agonist evoked increase in $[Ca^{2+}]_i$ that persists for 10-12 minutes following exposure to SNAP (50μM). This amplification may be clearly observed in the first three responses to agonist following application of SNAP. The stimulatory effect of the NO donor was subsequently reduced over the following 10-12 minutes such that the response to CCh returned to the pre-SNAP-stimulus magnitude. Thereafter, the response to CCh continued to decline and 40 minutes after the initial exposure to NO donor, the lacrimal acinar cells no longer responded to agonist stimulation. This pattern of response is, in detail, similar to that reported previously in submandibular cells.

The data shown in figure 3.1.5 result from an identical experimental protocol to that shown in figure 3.1.4, except that ODQ was applied simultaneously with SNAP. Thus, the stimulatory action of NO was abolished and there is no amplification of the agonist-evoked Ca^{2+} signal. However, the attenuation of the response seen in the presence of SNAP alone was maintained. Thus, in both submandibular and in lacrimal acinar cells, the agonist-evoked Ca^{2+} signal was first amplified and then attenuated in the presence of SNAP and the amplification effect (but not the attenuation) was abolished by ODQ.

In the case of submandibular cells, the contrast in the pattern of response in the presence and in the absence of SNAP was very clear, not least because in the absence of SNAP, the cells responded consistently to agonist stimulation over the time course of the experiments. Whereas, lacrimal cells responded consistently to stimulus over a short experimental period (figure 3.1.1A), there was considerable variation in the pattern of response over a longer period. Whilst there were some experiments in which the response to agonist was maintained for the duration (figure 3.1.7). Another common pattern is shown in figure 3.1.7 C, where the signal first increased over time and then diminished. The averaged data shown in figure 3.1.6 are comprised of all the different patterns of response and this variability between individual traces goes some way to explaining the large standard error of the mean shown in figure 3.1.6.

Figure 3.1.6b represents the cumulative data for the response to agonist for all experiments. These cumulative data show the average trace obtained for the treatments with 50μM SNAP and 50μM SNAP/ 10μM ODQ against control data. Illustrated initial amplification then decline in response in the presence of SNAP, the inhibition of amplification by ODQ, and the

suggestion that the pattern of lacrimal gland acinar response in the absence of exogenous NO is similar to that when a NO donor is used.

In addition to the patterns of response already described, it was also observed that a number of cells did not respond at all to 100nM CCh. However, these cells were responsive to stimulation with 200nM. The patterns of response seen with 200nM CCh were indistinguishable from those elicited with 100nM CCh, following the same amplification/ attenuation of response. In an effort to increase efficiency, all further experiments were carried out using a 200nM concentration of CCh to evoke an increase in $[Ca^{2+}]_i$.

Upon exposure to NO donor, lacrimal gland acinar cells exhibit the same pattern of response amplification and rundown as observed in submandibular gland acinar cells. However, a similar pattern is observed in mouse lacrimal acinar in the absence of exogenous NO, the repeated stimulations with CCh having a use dependent pattern of amplification and attenuation. These observed similarities in response pattern lead to the hypothesis that mouse lacrimal acinar cells *in vitro* may be producing endogenous NO to a degree that it affects cellular function. As NO primarily exerts it's effect upon Ca^{2+} signalling via the cGMP mediated production of cADPr, the application of the sGC inhibitor ODQ (as figs 3.1.2 and 3.1.5) was used to show whether the amplification observed in mouse lacrimal acinar cells was due to the activation of this secondary pathway. Figure 3.1.9 shows the mean result (n=28, 7 expts, 4 animals) of repeat stimulations of mouse lacrimal acinar cells with 200nM CCh in the presence of 10uM ODQ, compared with that of stimulations with 200nM CCh in the absence of ODQ. The presence of 10uM ODQ suppresses the amplification to a significant degree ($p = < 0.05$) between 12 and 22 minutes (applications 4, 5 and 6).

Figure 3.1.1 100uM SNAP induced amplification of response to 100nM CCh in Lacrimal gland acinar cells.

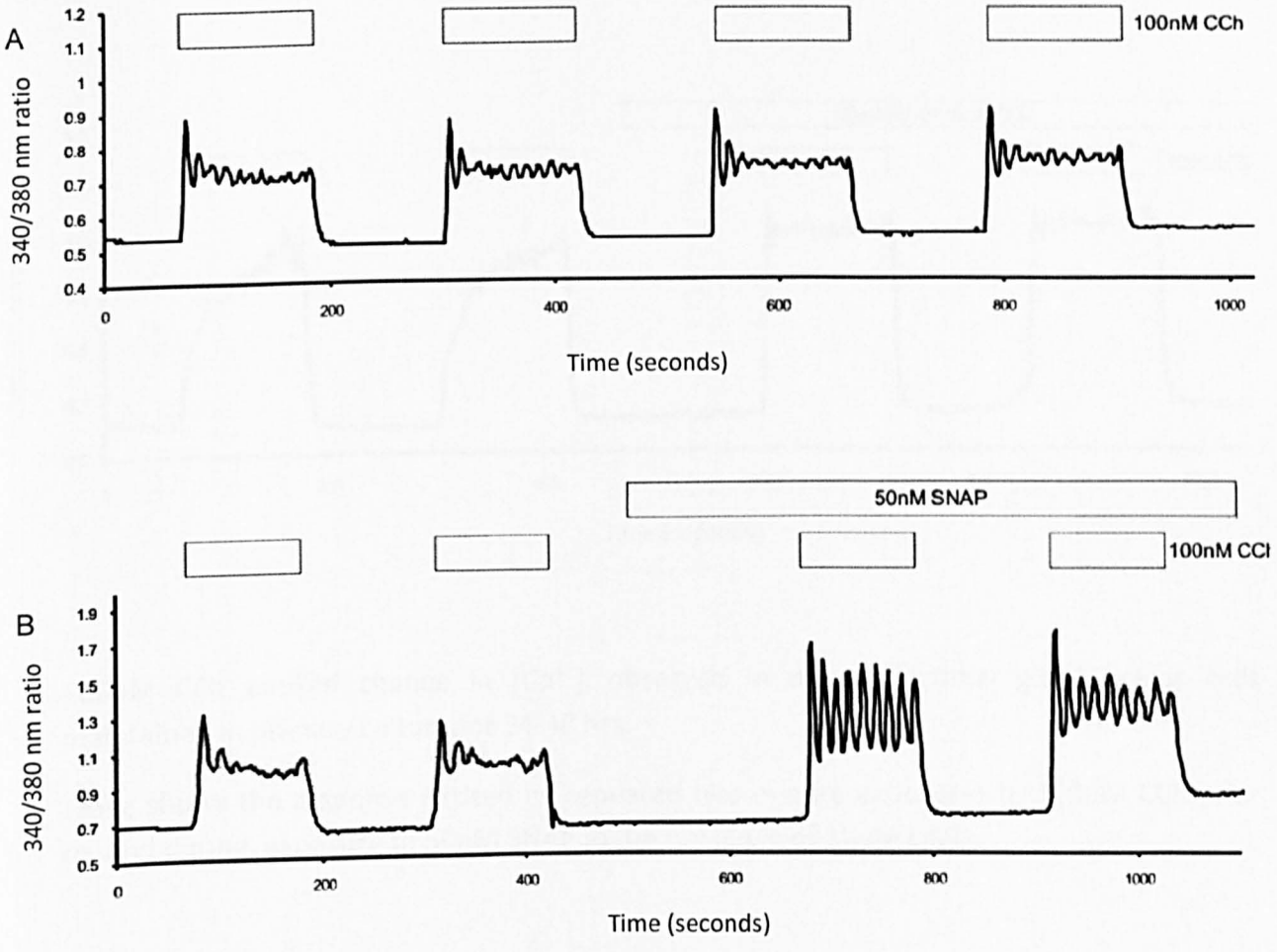

100nM CCh evoked change in $[Ca^{2+}]_i$ observed in mouse lacrimal gland acinar cells maintained in primary culture for 24-48 Hrs.

Trace A shows the response elicited by repeated two minute exposures to 100nM CCh.

Trace B shows the response elicited by repeated two minute exposures to 100nM CCh prior to, and during, exposure to 50µM SNAP.

Figure 3.1.2 100µM SNAP induced amplification of response to 100nM CCh is blocked by 10uM ODQ in Lacrimal gland acinar cells.

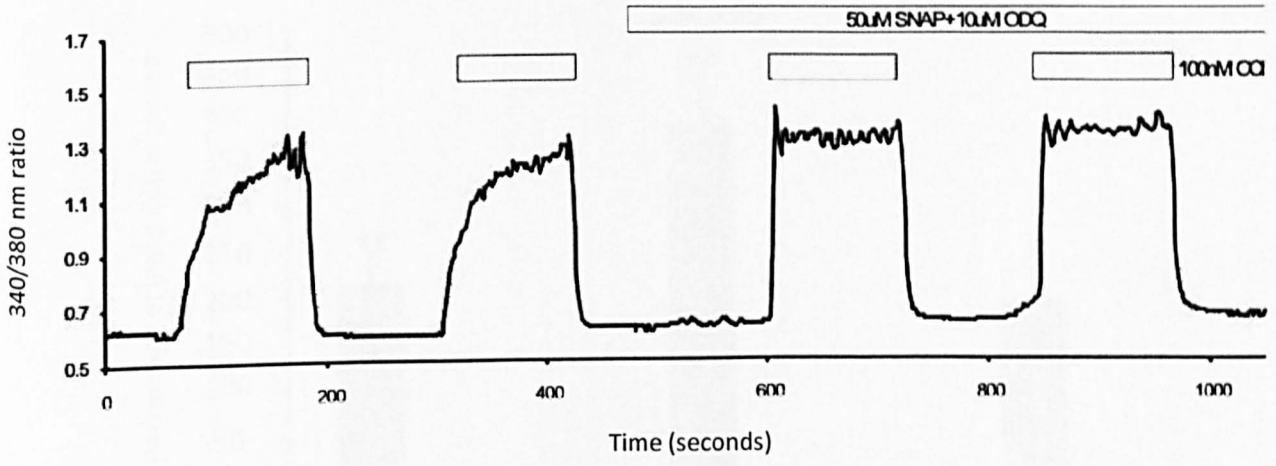

100nM CCh evoked change in $[Ca^{2+}]_i$ observed in mouse lacrimal gland acinar cells maintained in primary culture for 24-48 hrs.

Trace shows the response elicited by repeated two minute exposures to 100nM CCh prior to, and during, exposure to 50nM SNAP in the presence of 10µM ODQ.

Figure 3.1.3 Average agonist evoked change in $[Ca^{2+}]_i$ on 3rd application of 100nM CCh and the effect of 50µM SNAP and 50µM SNAP/10µM ODQ upon response.

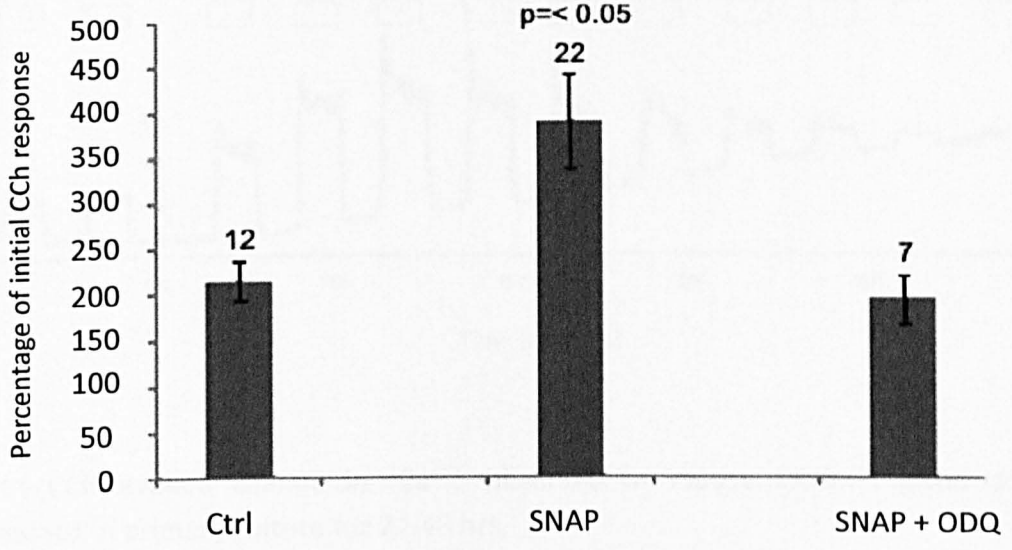

Histogram representing the cumulative data obtained for the third application (t= 6 minutes-control, 7 minutes SNAP and SNAP/ODQ) of 100nM CCh upon mouse lacrimal acinar cells. Data are expressed as a percentage of the response elicited during the first application (t= 1-3 minutes) of agonist.

Figure 3.1.4 The effect of chronic exposure of 50uM SNAP upon 100nM CCh evoked $[Ca^{2+}]_i$ in mouse lacrimal gland acinar cells.

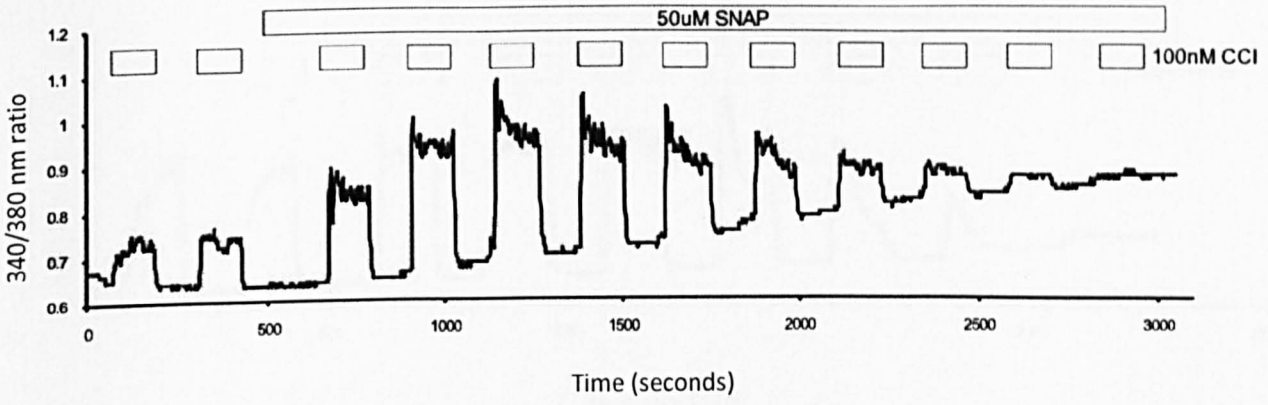

100nM CCh evoked change in $[Ca^{2+}]_i$ observed in mouse lacrimal gland acinar cells maintained in primary culture for 24-48 hrs.

Trace shows initial amplification of response to 100nM CCh after application of 50μM SNAP, followed by rundown to near abolition of response by the end of the experiment (t=50 minutes).

Figure 3.1.5 The effect of chronic exposure of 50µM SNAP in the presence of 10µM ODQ upon 100nM CCh evoked $[Ca^{2+}]_i$ in Lacrimal gland acinar cells.

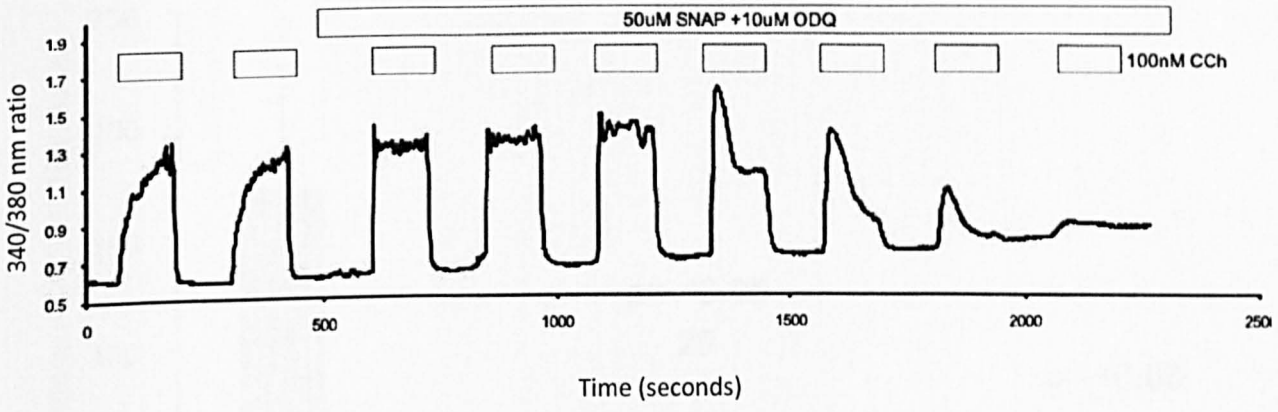

100nM CCh evoked change in $[Ca^{2+}]_i$ observed in mouse lacrimal gland acinar cells maintained in primary culture for 24-48 Hrs.

Trace shows the abolition of the 50µM SNAP induced amplification of response to 100nM CCh by 10µM ODQ, yet still shows the decline in response attributed to the presence of NO.

Figure 3.1.6 Average agonist evoked change in $[Ca^{2+}]_i$ observed at the end of experimental run and the effect of 50µM SNAP and 50µM SNAP/10µM ODQ upon response.

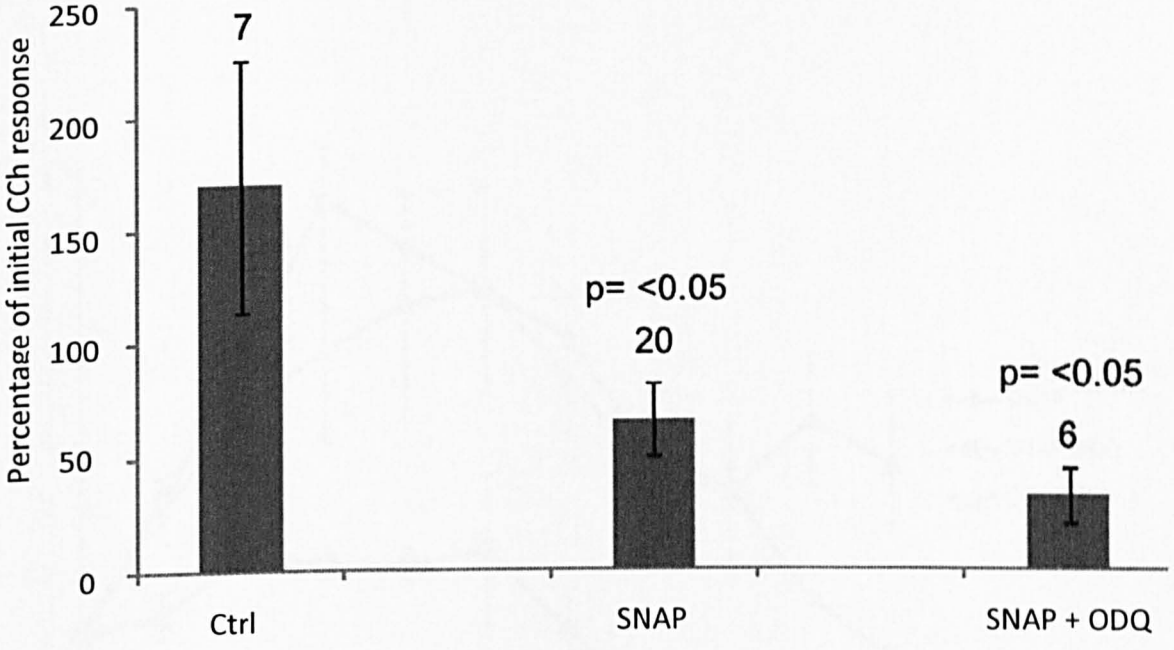

Histogram representing the cumulative data obtained for the final application 100nM CCh upon mouse lacrimal acinar cells. Data are expressed as a percentage of the response to the first 2 minute application (t= 1-3 minute) of agonist.

Figure 3.1.7 Average agonist evoked change in $[Ca^{2+}]_i$ observed for repeat stimulations with 100nM CCh and the effect of 50µM SNAP and 50µM SNAP/10µM ODQ upon response.

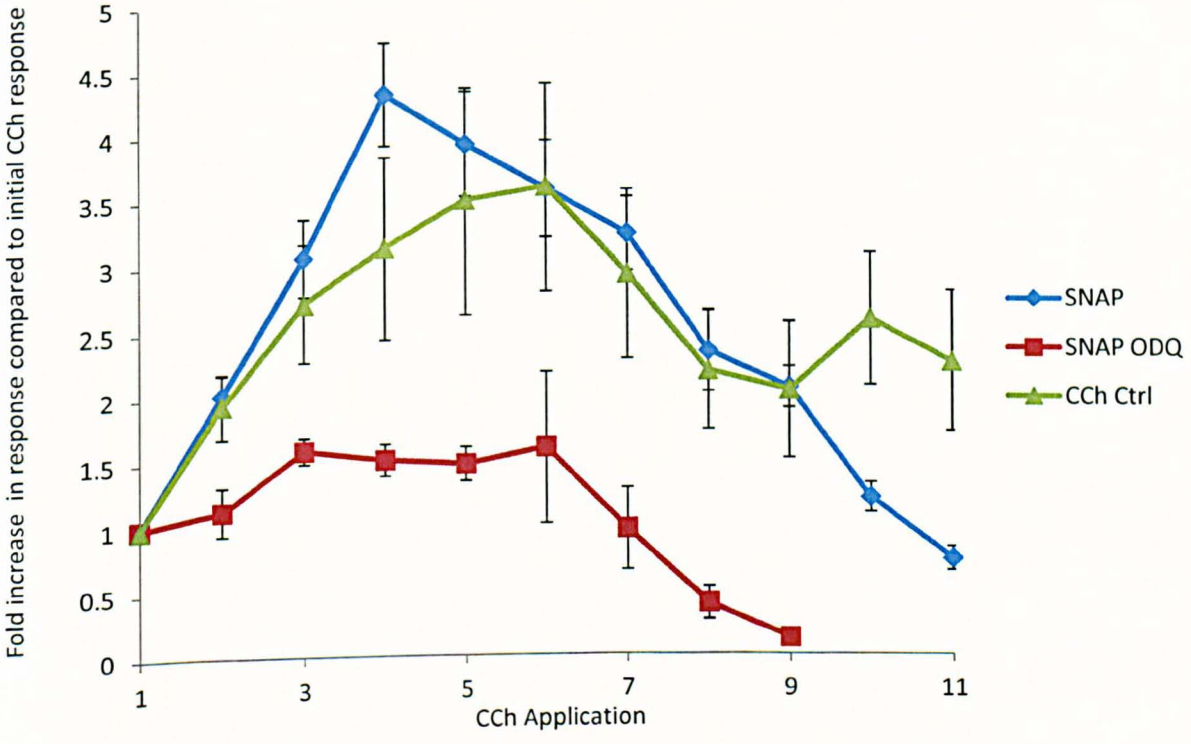

Trace showing the cumulative data for the result of 2 minute stimulations with 100nM CCh in the presence of 50µM SNAP and 50µM SNAP / 10µM ODQ, compared to control data obtained. Y axis representing response level as a function of the initial response to agonist and X axis representing agonist application number.

Figure 3.1.8 Change in $[Ca^{2+}]_i$ in mouse lacrimal acinar cells in response to repeat stimulations with 100nM CCh illustrating variability in control response.

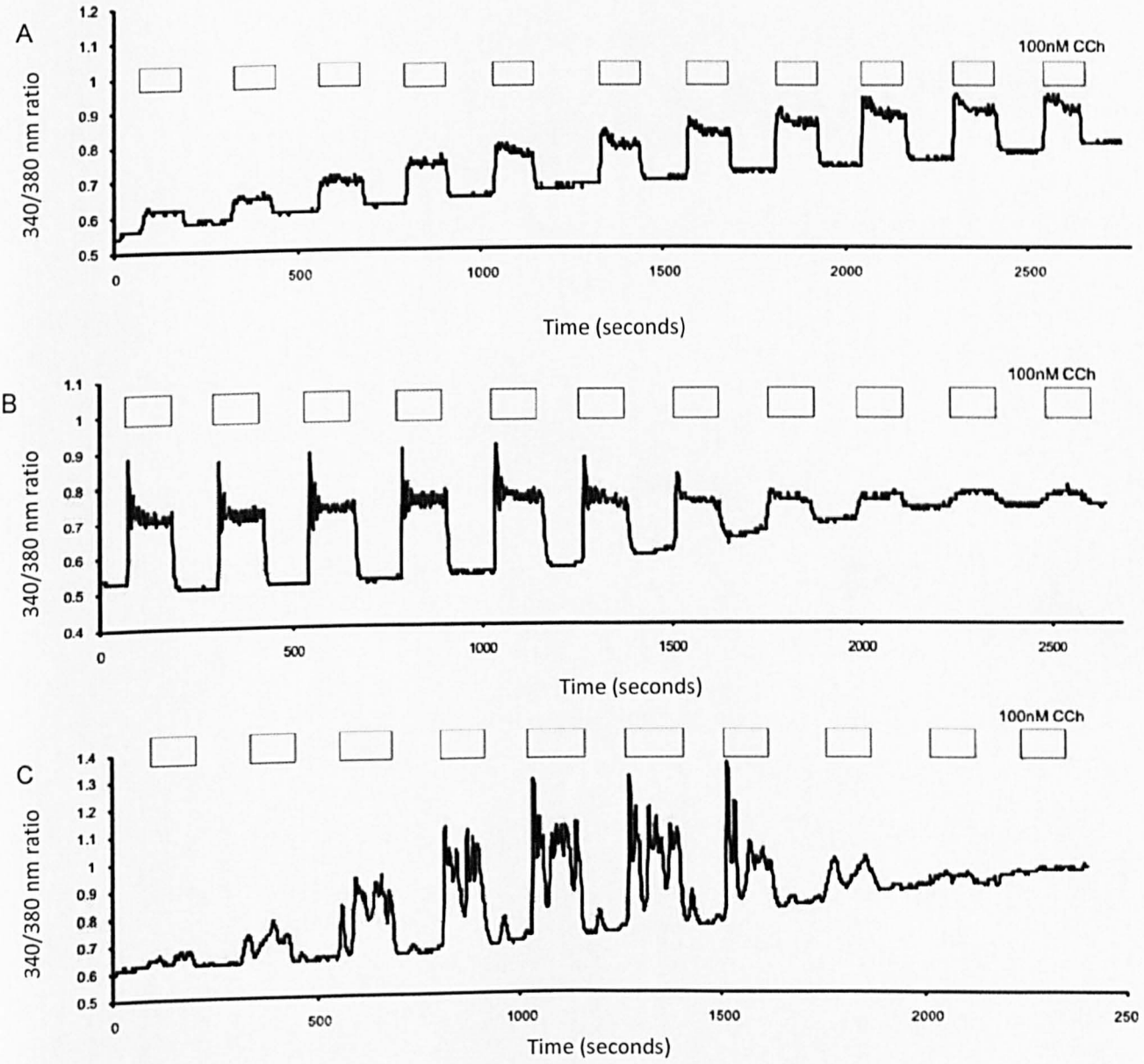

Traces A,B and C show 100nM CCh evoked change in $[Ca^{2+}]_i$ observed in mouse lacrimal gland acinar cells maintained in primary culture for 24-48 hrs. Traces show the response elicited by repeated two minute exposures to 100nM CCh over the course of the experimental run. Traces A, B and C illustrate the inherent variability of response observed in mouse lacrimal acinar cells.

Fig 3.1.9 Change in Fura fluorescence observed in mouse lacrimal acinar cells in response to repeat applications of 200 nM CCh.

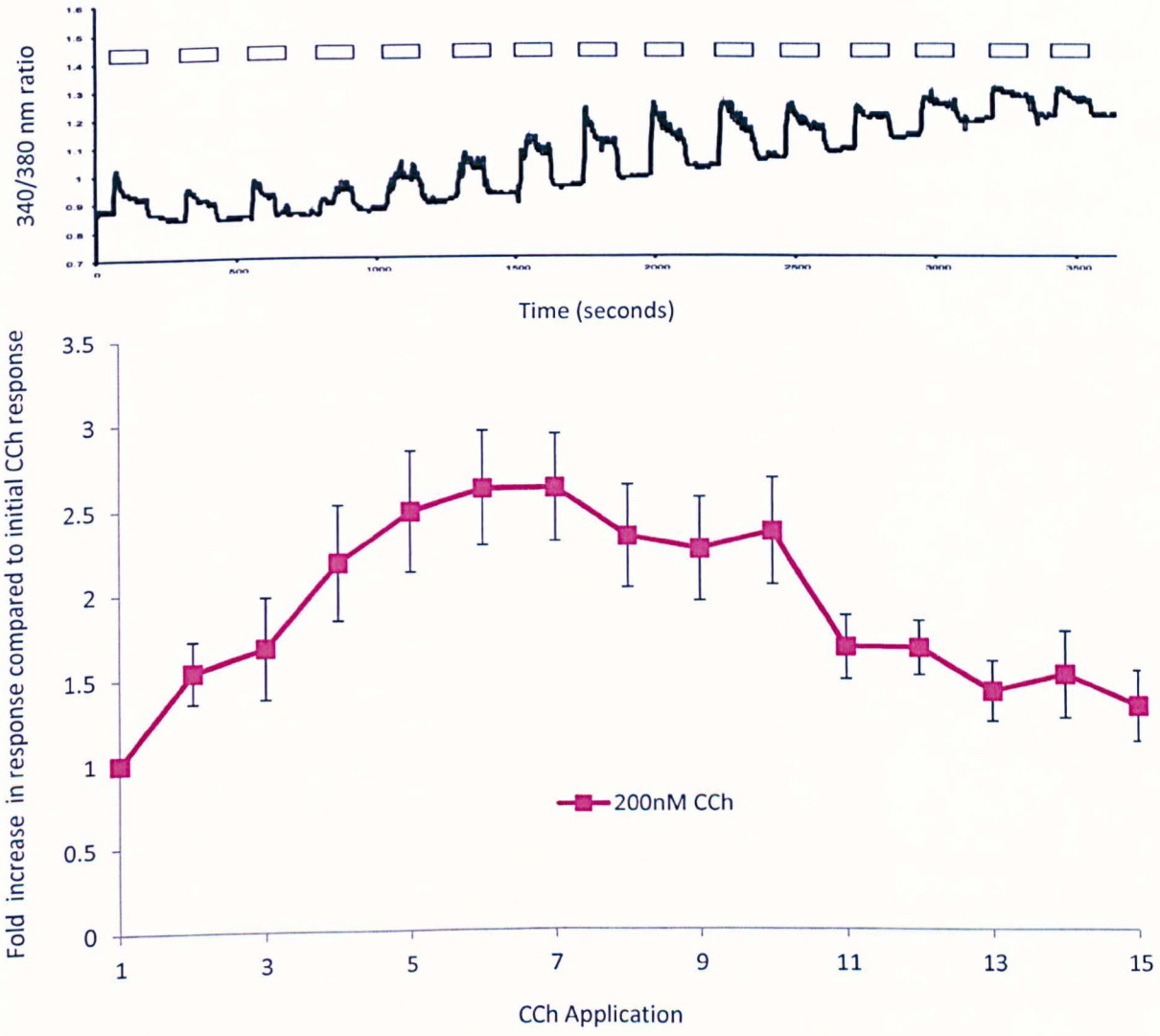

Trace A shows a representative trace of repeated 2 minute stimulations with 200nM CCh. The observed response is biphasic, initially showing an increase in response followed by a rundown to levels similar to that in response to the initial application.

Trace B shows cumulative data (n= 35 cells, 8 experiments, 7 animals) for the repeated application of 200nM CCh to mouse lacrimal acinar cells. Data is represented as a function of the response to the first application of agonist. Response to agonist peaked at 260% that of the initial response ($p < 0.001$) to 200nM CCh after 22-28 minutes, with a rundown to 130% ($p < 0.001$) of first response by t=60 minutes.

Figure 3.1.10 The amplification of Ca^{2+} response initially observed in mouse lacrimal gland is blocked by 10μM ODQ.

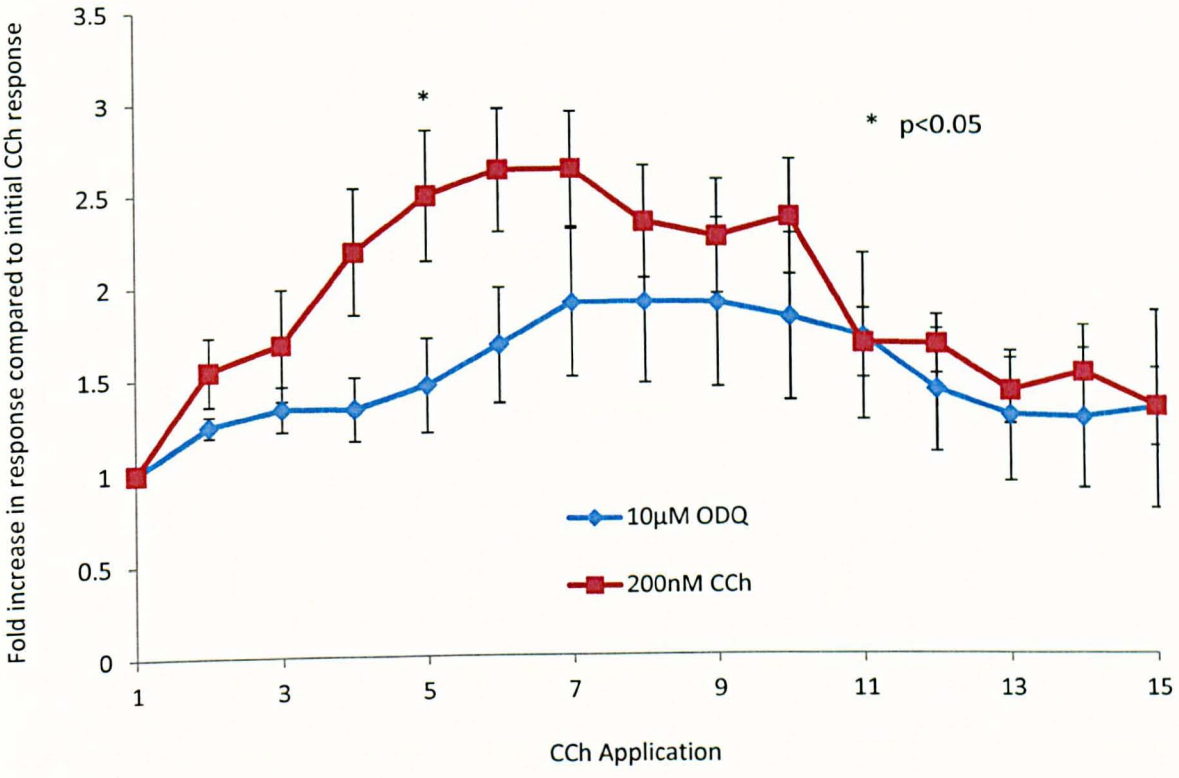

Cumulative averaged data for the 200nM CCh evoked change in $[Ca^{2+}]_i$ observed in mouse lacrimal gland acinar cells in the presence (blue) and absence (red) of 10μM ODQ. (n=25, 6 expts, 4 animals).Data are presented as a fold increase in response to agonist compared to the initial response (CCh application 1, t=2-4 minutes). Two tailed t-test shows a significant ($p<0.05$) inhibition of the amplification aspect at stimulation 5 (minutes 19-21).

Discussion

These results represent confirmation that an exogenous supply of NO from a donor has a similar effect upon mouse lacrimal gland acinar cells as it does upon mouse submandibular gland acinar cells, previously demonstrated by Caulfield *et al* (Caulfield, Balmer et al. 2009). Furthermore, these results also show that the amplification is cGMP dependent , shown by the prevention NO's amplification of response to agonist by the sGC inhibitor ODQ (figure 3.1.5). The decline in response caused by chronic exposure to NO is unaffected by the presence of ODQ (figure 3.1.6) and can therefore be considered as being independent of cGMP.

However, differences between mouse lacrimal and submandibular acinar cells have also been highlighted by this series of experiments, with mouse lacrimal gland acinar cells showing Ca^{2+} signal amplification even in the absence of NO donor. Also, this automatic amplification can be prevented by the presence of the sGC inhibitor ODQ. This suggests that this automatic amplification of agonist evoked Ca^{2+} release is a result of the sensitisation of ryanodine receptors by cADPr production, mediated by cGMP increase brought about by NO activation of sGC. These data therefore indirectly suggest that mouse lacrimal acinar cells are capable of producing amounts of NO that can significantly alter the response profile.

4 Results

4.1 The effect of cyclic ADP-ribose upon calcium mobilisation in mouse lacrimal gland acinar cells.

Aims and objesctives

Demonstration of the calcium mobilising effect of cADPr would confirm that RyR are present in mouse lacrimal gland acinar cells and that the cGMP mediated response pathway, of which NO is a part, plays a role in the calcium signal evoked by stimulation with agonist. Furthermore, any differences in sensitivity to cADPr between secretory organs would likely have implications upon any potential treatments for the secretory hypofunction observed in SjS.

Introduction

The majority of data concerning exocrine gland secretion was gleaned from salivary gland acinar cells, with relatively little literature concerning the potential differences between these and the lacrimal gland acinar cells. Recently some work has been undertaken to redress this balance. Medina-Ortiz *et al* successfully identified the presence and subcellular location of IP_3R and RyR in mouse lacrimal cells (Medina-Ortiz, Gregg et al. 2007).

The overall sequence of events has been shown to be very similar regarding the cholinergic stimulation of secretion, requiring cholinergic agonist to bind with the G-coupled M3 receptor generating IP_3 and resulting in calcium mobilisation from intracellular stores.

NO acts along the cGMP mediated secondary pathway in calcium response, resulting in the production of cADPr, activating the RyR, which in turn mediates the calcium signal in response to agonist.

In submandibular gland acinar cells it has been shown that cADPr acts to mobilise Ca^{2+} as well as act to amplify agonist evoked Ca^{2+} response.

Whole cell patch clamp electrophysiology was performed on mouse lacrimal acinar cells to elicit the effect of increasing concentration of the second messenger cADPr upon the stimulation observed in response to 200nM CCh as an agonist.

Figure 4.1.1 represents a whole cell patch clamp experiment to determine the basal level of response to agonist. Using a repeat 2 minute stimulation/ 2 minute rest protocol, it was observed that stimulation resulted in a small steady state increase in Ca^{2+} as shown by the activity measured in the K^+ channel, which returned to basal upon removal of agonist.

Figure 4.1.2 represents the repeated stimulation of mouse lacrimal gland acinar cells with 200nM CCh whilst simultaneously subjected to intracellular perfusion with 5μM cADPr. Initial breakthrough of the patch pipette was accompanied with a rapid increase then recovery of signal. Application of 200nM CCh showed no significant amplification of the response to agonist in the K^+ current, compared to control, but there was an agonist-dependent increase in the Cl^- current which was not observed in the absence of cADPr.

Figure 4.1.3 represents the repeated stimulation of mouse lacrimal gland acinar cells with 200nM CCh whilst simultaneously subjected to intracellular perfusion with 10μM cADPr. This trace was typical of a few experiments where application of 200nM CCh showed no significant amplification of the response to agonist in the K^+ current, compared to control, but there was an agonist-dependent increase in the Cl^- current which was not observed in the absence of cADPr. These data are very similar to that observed in the presence of 5 μM cADPr. Previous studies have indicated that the Cl^- current in mouse lacrimal acinar cells is

less Ca^{2+} sensitive than is the K^+ current (Smith 1992). Therefore these data may indicate a small additional increase in Ca^{2+} mobilisation in the presence of cADPr.

Figure 4.1.4 represents the intracellular perfusion of mouse lacrimal gland acinar cells with 10μM cADPr. Upon breakthrough the was a very large transient increase in the amplitude of both the K^+ and Cl^- currents. Both currents plateaued at levels considerably greater than that seen under control conditions and there was no subsequent response to stimulation with 200nM CCh. This was the most typical response of the lacrimal cells to exposure to 10μM cADPr.

Similar experiments were performed with 50 μM and 100 μM cADPr in the patch clamp pipette (data not shown). In every case, breakthough to the whole cell configuration resulted in very large K^+ and Cl^- currents, similar to those seen in figure 4.1.4. In the presence of 50 μM and 100 μM cADPr, mouse lacrimal gland acinar cells were unable to mobilise Ca^{2+} in response to 200nM CCh.

These data show that, at low concentrations, cADPr enhances the response of the mouse lacrimal gland acinar cells to agonist inasmuch as there is some activation of the Cl^- current on stimulation. Higher concentrations of cADPr were able to mobilise Ca^{2+} independently of agonist stimulation. The extent of the Ca^{2+} mobilisation in the presence of high concentration of cADPr was sufficiently large to preclude any additional effect of CCh.

Figure 4.1.1 The effect of 200nM CCh upon Ca^{2+} mobilisation in mouse lacrimal gland acinar cells as measured by patchclamp electrophysiology.

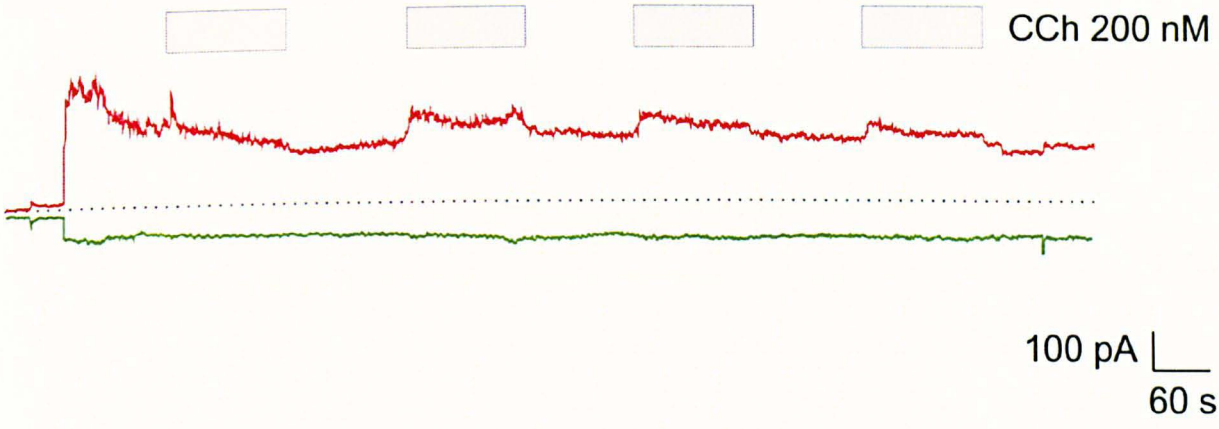

K^+ (upper trace, red) and Cl^- (lower trace, green) currents measured in single mouse lacrimal cell in response to intracellular perfusion with standard intracellular buffer and subsequent stimulation with 200 nM CCh. The dotted line indicates zero current. The data shown are typical of 3 similar experiments.

Figure 4.1.2 Patch clamp electrophysiology run on mouse lacrimal gland acinar cells.

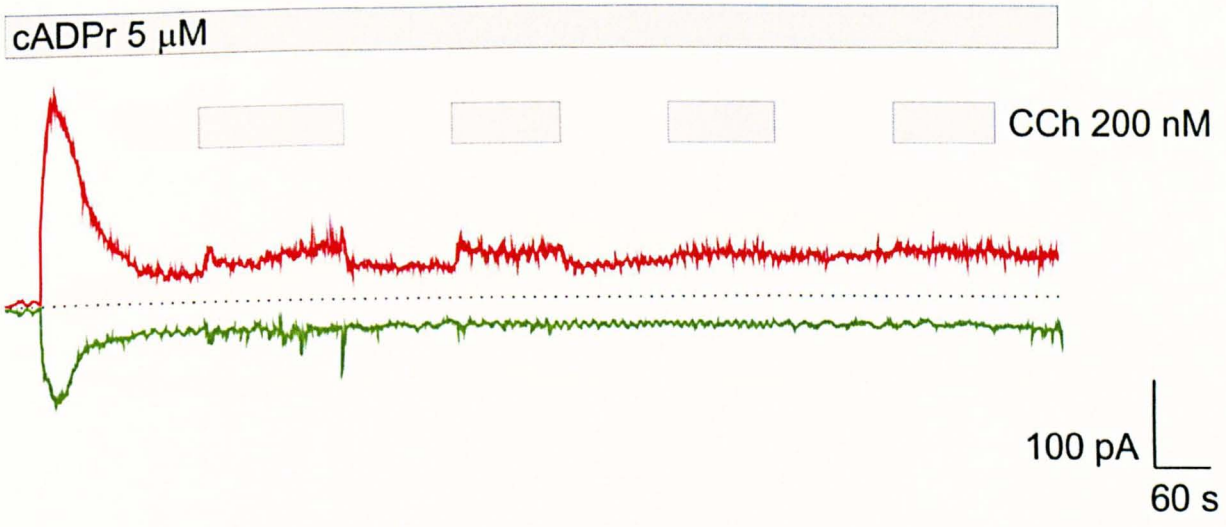

K^+ (upper trace, red) and Cl^- (lower trace, green) currents measured in single mouse lacrimal cell in response to intracellular perfusion with 5 µM cADPr and subsequent stimulation with 200 nM CCh. The dotted line indicates zero current. The data shown are typical of 3 similar experiments.

Figure 4.1.3 Patch clamp electrophysiology run on mouse lacrimal gland acinar cells.

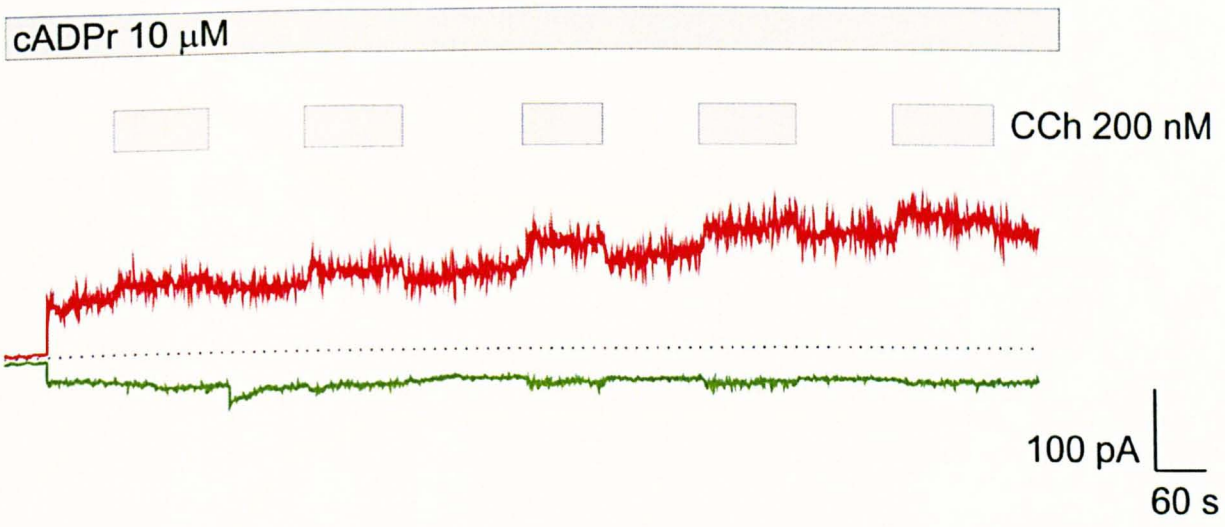

K^+ (upper trace, red) and Cl^- (lower trace, green) currents measured in single mouse lacrimal cell in response to intracellular perfusion with 10 μM cADPr and subsequent stimulation with 200 nM CCh. The dotted line indicates zero current. The data shown are typical of 2 similar experiments.

Figure 4.1.4 Patch clamp electrophysiology run on mouse lacrimal gland acinar cells.

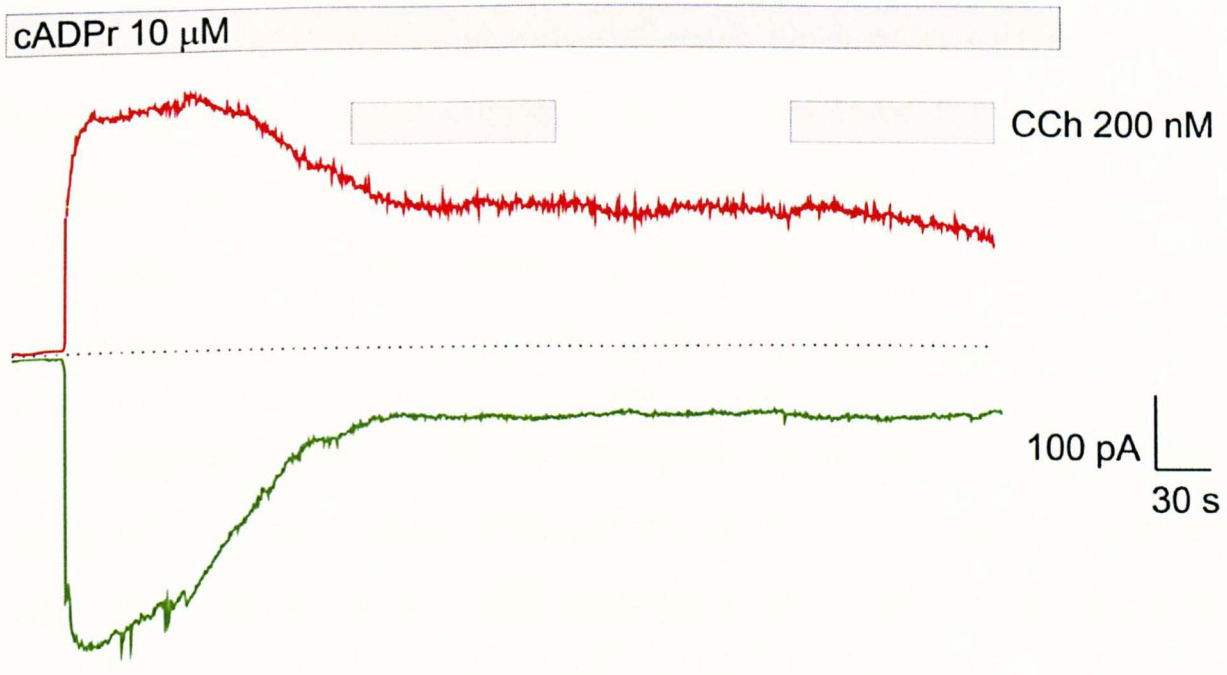

K^+ (upper trace, red) and Cl^- (lower trace, green) currents measured in single mouse lacrimal cell in response to intracellular perfusion with 10μM cADPr and subsequent stimulation with 200 nM CCh. The dotted line indicates zero current. The data shown are typical of 4 similar experiments.

Discussion

These results confirm that the cADPr dependent pathway of Ca^{2+} mobilization is present in mouse lacrimal gland acinar cells. The presence of low (5- 10μM) concentrations of cADPr in the patch pipette resulted in mobilization of Ca^{2+} from intracellular stores whilst showing negligible amplification upon agonist evoked Ca^{2+} mobilization (figures 4.1.2 and 4.1.3) with 10μM cADPr often independently mobilizing Ca^{2+} (figure 4.1.4). Higher doses (50-100μM) of cADPr independently mobilised Ca^{2+} and rendered the cells unable to respond to agonist.

These results demonstrate an inherent difference in response profile between mouse lacrimal and mouse submandibular acinar cells. Previous work upon mouse submandibular cells by Harmer *et al* (Harmer et al. 2001) shows that, in comparison to the data seen here for lacrimal gland acinar cells, mouse submandibular gland cells show a more graded response to intracellular perfusion with cADPr. The comparatively "all or nothing" response to cADPr seen in lacrimal gland acinar cells represents a significant difference between two separate secretory gland systems.

5 Results

5.1 The effect of inhibition of production of endogenous nitric oxide upon Ca^{2+} response in mouse lacrimal acinar gland cells.

Aims and objectives.

The aim of this sequence of experiments was to determine whether application of NOS inhibitors could alter the pattern of response to agonist observed in mouse lacrimal gland acinar cells. Demonstration of an alteration of calcium response by NOS inhibitors would show that endogenous production of NO in mouse lacrimal acinar can have a modulatory effect on calcium signaling and therefore upon secretion. Use of inhibitors with specific NOS isoform targets would identify the isoforms responsible Ca^{2+} signal modulation.

Introduction

The data from the previous chapter suggest that lacrimal gland acinar cells exhibit behavior similar to that of submandibular gland acinar cells exposed to NO from a donor (SNAP), and this behavior can be modulated by the sGC inhibitor ODQ. However, even in the absence of an exogenous source of NO, mouse lacrimal acinar cells still show similarities in response profile (amplification and decline in $[Ca^{2+}]_i$) to mouse SM acinar cells that are exposed to exogenous NO. The observed amplification observed in mouse lacrimal acinar cells in the absence of an external supply of NO can be modulated by ODQ, implicating the cADPr dependent pathway. A hypothesis to account for these observations is that, *in vitro*, mouse lacrimal acinar cells produce NO.

If the pattern of response to agonist previously observed in lacrimal acinar cells is dependent upon endogenously produced NO activity, then inhibition of NOS using NOS inhibitors should modulate the NO-dependent component of the Ca^{2+} response pattern

seen in mouse lacrimal acinar cells. The effect of increasing the availability of the NOS substrate, arginine, to the lacrimal gland acinar cells was also investigated, as increased levels of substrate may increase the rate or extent of NO production by lacrimal cells and thus alter response pattern. By chemical inhibition of the NOS isoforms and supply of arginine substrate we aim to show how endogenous NOS activity can alter the Ca^{2+} response in mouse lacrimal acinar cells and identify the isoform(s) responsible.

The effect of a series of NOS inhibitors was tested in an attempt to modulate the NO dependent component of the pattern of stimulation observed in mouse lacrimal acinar cells. 10μM L-NAME was used as a non-specific inhibitor as an attempt to inhibit NOS activity.

Figure 5.1.1 A shows a representative trace for the repeat 200nM CCh stimulation protocol in the presence of the non-specific NOS inhibitor 10 μM L-NAME. The averaged data from 23 cells from 4 separate animals over 6 experimental runs are shown in Figure 5.1.1 B. Similarly to the control data, a pattern of amplification and rundown was still present, with response to agonist peaking at the 7th application of agonist (minutes 27-29) at 280.7% (±50.2%) of the initial agonist response. The response continued to decline until the end of the experiment, responding at a mean value of 143.8% (±16.6%) of the initial response to 200nM CCh. Figure 5.1.2 shows the direct comparison of the averaged control data with data from the experiments performed using cells exposed to 10 μM L-NAME. A two tailed t-test revealed no significant difference in the levels of response obtained in the presence or absence of 10 μM L-NAME.

However, as shown in chapter 3 in figure 3.1.8, the response of lacrimal cells to repeated stimulation was diverse. This pattern was repeated in the presence of L-NAME, as shown in the examples in figure 5.1.3. However, there was a significant change in the number of cells

showing the pattern seen in figure 5.1.3 B. This was quantified as a count of the number of cells in which the final response to stimulus was <50% of the initial response to agonist exposure.

Table 5.1.1 Percentage of the total number of mouse lacrimal cells who's response to agonist declines to <50% of initial response to agonist- the effect of 10μM L-NAME.

	50% act by end	No 50% Drop	n	% drop by 50%
200nM control	9	26	35	25.7
10μM L-NAME	3	20	23	13.0

By this measure, the number of cells exhibiting attenuation of response was decreased in the presence of 10μM L-NAME (3 out of 23, or 13.0% in the presence of 10μM L-NAME, vs 9/35, or 25.7% of cells exposed to agonist only), an effect that was masked by averaging all of the data. These data are summarised in figure 5.1.14. Comparison of data obtained for 10μM and 100μM L-NAME (shown in figure 5.1.4) resulted in only one significantly different datapoint in the averaged data at agonist application 7 (minutes 27-29). At this point the response to agonist is only 183.1% (±30.3) with a p value of <0.05 vs the same point in the 10μM L-NAME data.

L-NAME is an analogue of the NOS substrate, arginine, and is a non-specific inhibitor for all 3 isoforms of NOS. Blanket inhibition of all three NOS isoforms may mask any effect caused by the inhibition of a single NOS isoform. A series of experiments were conducted using the same repeat stimulation protocol, measuring the effects of inhibitors specific to each of the NOS isoforms: S-methylisothiourea (SMT) –iNOS, diphenyleneiodonium chloride (DPI) – eNOS, 7 nitroindazole (7NI)-nNOS.

The experiments were repeated for each of the NOS inhibitors in question (L-NAME, 7 nitroindazole, S-methylisothiourea and diphenyleneiodonium chloride), using the same protocol used in the previous chapter, with the continuous presence of the NOS inhibitor in perfusion solutions after the 2nd agonist exposure and the data is presented as a function of the initial response (Application 1- t=2-4 minutes) of the mouse lacrimal acinar gland cells to 200nM CCh agonist.

Figure 5.1.5A shows a representative trace for the exposure of mouse lacrimal gland acinar cells to agonist in the presence of 10 μM of the iNOS inhibitor S-methylisothiourea (SMT). Figure 5.1.5B shows the averaged cumulative data for n=21 acinar cells, from 5 animals over 7 experiments of the repeat stimulation protocol for 10μM the SMT. Exposure to repeat applications of agonist resulted in the same pattern of amplification and rundown observed in the control data with peak response to agonist (300.8% of initial, ± 50.2%) recorded at the 7th application (minutes 27-29), before running down to 135.6% (±22.6%) at the last application. Figure 5.1.6 shows the direct comparison between the repeat stimulation data obtained in the presence and absence of 10uM SMT. Two tailed t-test showed there was no significant difference in mouse lacrimal gland acinar cell response to 200nM CCh in the presence or absence of 10μM SMT. However, as seen in the control and L-NAME data, the inherent variation in response may result in masking of deviation in response due to SMT's influence. Similarly to the LNAME experiments, the number of cells exhibiting a rundown in response to less than 50% of the initial response to agonist was noted.

Table 5.1.2 Percentage of the total number of mouse lacrimal cells who's response to agonist declines to <50% of initial response to agonist-the effect of 10μM SMT

	50% act by end	No 50% Drop	n	% drop by 50%
200nM control	9	26	35	25.7
10μM SMT	1	18	19	5.3

The number of cells exhibiting attenuation of response was decreased in the presence of 10μM SMT (1 out of 19, or 5.3% in the presence of 10μM SMT, vs 9/35, or 25.7% of cells exposed to agonist only), an effect that was masked by averaging all of the data. These data are summarised in Figure 5.1.14 The repeat stimulation protocol was carried out for the eNOS inhibitor 50nM DPI. Figure 5.1.7A shows a representative trace of a repeat 200nM CCh stimulation run, illustrating the pattern of stimulation observed. Figure 5.1.7B shows the averaged data for n=23 cells from 2 animals over 5 experiments, showing the cells in the presence of 50nM DPI follow a similar pattern of amplification and decline previously observed in mouse lacrimal acinar cells. In the presence of 50nM DPI the mouse lacrimal gland acinar cells peaked in response at the 7^{th} application of agonist (27-29 minutes) at 240.5% of initial response (±25.5%) before continually running down to 58.8% (±8.8%) of the initial response to agonist. Comparison of the 50nM DPI data with control data (Figure 5.1.8) shows the similarity in response profile, but a two tailed t-test revealed a significant ($p= <0.01$) decline in response of cells under the influence of 50nM DPI at last agonist application, compared to control. This difference is also borne out by the count of cells whose response decline to <50% of the initial response to agonist stimulation.

Table 5.1.3 Percentage of the total number of mouse lacrimal cells who's response to agonist declines to <50% of initial response to agonist-the effect of 50nM DPI.

	50% act by end	No 50% Drop	n	% drop by 50%
200nM control	9	26	35	25.7
50nM DPI	13	10	23	56.5

Compared to 25.7% (9/35) of control run cells declining in response to <50% of the initial response to agonist, cells run in the presence of the eNOS inhibitor, 50nM DPI, declined to <50% of the initial response in 13/23 cases (56.5%). Figure 5.1.14 illustrates the direct comparison with the results of the other NOS inhibitors.

The influence of nNOS was blocked by perfusing the mouse lacrimal gland acinar cells with 710nM 7NI. Representative data, showing the result of repeat 200nM CCh stimulations are seen in Figure 5.1.7. Averaged data for response of 25 cells from 3 animals (run over 10 experiments) to 200nM CCh is shown in Figure 5.1.7, where it is observed that a pattern of amplification and decline is still in evidence. In the presence of 710nM 7NI, the mouse lacrimal gland acinar cells peaked in response at the 6^{th} application of agonist (25-27 minutes) at 180.3.% (±4.5%) of initial response to 200nM CCh, before continually running down to 43.0% (±8.4%) of the initial response to agonist. Figure 5.1.10 shows the averaged 710nM 7NI response data compared to the control data for response to 200nM CCh. Compared to the control data, 710nM 7NI exposed mouse lacrimal gland acinar cells, representing the inhibition of nNOS activity, show a significant decrease in response to agonist from application 7 (27-29 minutes) $p<0.05$ vs control, and applications 10-15

(minutes 41-61) ($p<0.05$ for applications 7,10, 11 13 and 14. $P<0.01$ for applications 12 and 15).

Table 5.1.4 Percentage of the total number of mouse lacrimal cells who's response to agonist declines to <50% of initial response to agonist-the effect of 710 nM 7NI.

	50% act by end	No 50% Drop	n	% drop by 50%
200nM control	9	26	35	25.7
710nM 7NI	18	7	25	72.0

As summarised in. Figure 5.1.14 the 200nM CCh evoked Ca^{2+} response of 72% of mouse lacrimal gland acinar cells exposed to 710nM 7NI result in rundown to <50% of the initial response, compared to 25% of control cells.

The effect of increasing the availability of the NOS substrate, L-arginine, was tested by the inclusion of 10μM L-arginine in the perfusion solution from t=5 minutes as per the protocol previously used for the NOS inhibitors. Figure 5.1.11A shows a representative trace for the exposure of mouse lacrimal gland acinar cells to agonist in the presence of 10 μM L-arginine. Figure 5.1.11B shows the averaged cumulative data for n=25 acinar cells, from 3 animals obtained over 6 experiments. As shown in Figure 5.1.11B, the response of mouse lacrimal gland acinar cells follows a similar pattern of increase and decline seen in previous treatments. However, peak response of 168.6% (±19.0%) is achieved by the 5^{th} agonist stimulation (minutes 19-21), before declining to 69.3% (±9.9%) of initial response to 200nM CCh at t=60. Comparison of the data acquired for the repeat stimulation protocol in the presence of arginine with the control data is presented in Figure 5.1.12. The decline in response observed upon application of 10μM L-arginine is significantly greater than that seen in the control runs with two tailed ttests showing a p value of <0.05 for the decline of

response at applications 6 a and 15 (minutes 23-25 and 59-61) and $p<0.01$ for applications 7-14.

Table 5.1.5 Percentage of the total number of mouse lacrimal cells who's response to agonist declines to <50% of initial response to agonist-the effect of 10μM L-arginine.

	50% act by end	No 50% Drop	n	% drop by 50%
200nM control	9	26	35	25.7
Arginine 10μM	13	12	25	52.0

13/25 (52%) of arginine treated cells decreased to <50% responsiveness to 200nM CCh by the end of the experimental run, compared to only 25.7% of control cells.

Figure 3.1.10 in the chapter 3 showed that ODQ can significantly alter the automatic amplification component seen in mouse lacrimal gland acinar cells, yet did not significantly alter the decline. However, as seen previously, pooling and averaging of the data may obfuscate details of the response profile.

Table 5.1.6 Percentage of the total number of mouse lacrimal cells who's response to agonist declines to <50% of initial response to agonist -the effect of 10μM ODQ.

	50% act by end	No 50% Drop	n	% drop by 50%
200nM control	9	26	35	25.7
10μM ODQ	8	17	25	32.0

As seen here and summarised in Figure 5.1.14, 8/25 lacrimal glands tested (32.0%) were observed to rundown to <50% of their initial stimulation by 200nM CCh.

Figure 5.1.1 Change in Fura fluorescence observed in mouse lacrimal acinar cells in response to repeat applications of 200 nM CCh in the presence of the non specific NOS inhibitor 10μM L-NAME.

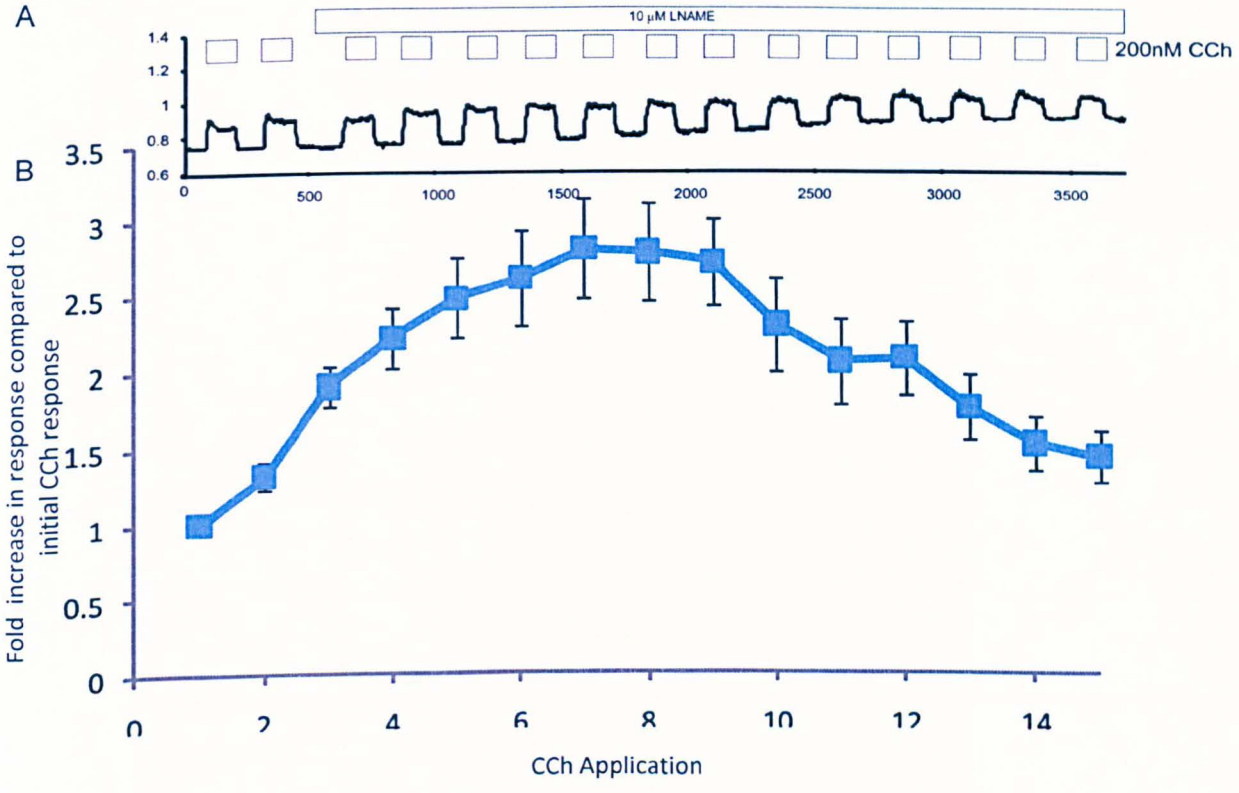

Trace A shows the result of repeat 2minute stimulations with 200nM CCh in the presence of the non-specific NOS inhibitor L-NAME. The first 2 applications of CCh were made in the absence of L-NAME, as a method of showing any effect of acute application of the NOS inhibitor upon $[Ca^{2+}]_i$. Subsequent applications of CCh were made while the cells were continually perfused with 10μM L-NAME.

Trace B represents cumulative data (n=23, 6 experiments, 4 animals) for the repeated application of 200nM CCh to mouse lacrimal acinar cell in the presence of 10μM L-NAME. Data is represented as a function of the response to the first application of agonist. Response to agonist peaked at 280% that of the initial response to 200nM CCh after 26-28 minutes/ 7^{th} application before running down to 130% of initial response at t=60.

Figure 5.1.2 Change in Fura fluorescence observed in mouse lacrimal acinar cells in response to repeat applications of 200 nM CCh in the presence and absence of the non specific NOS inhibitor 10μM L-NAME.

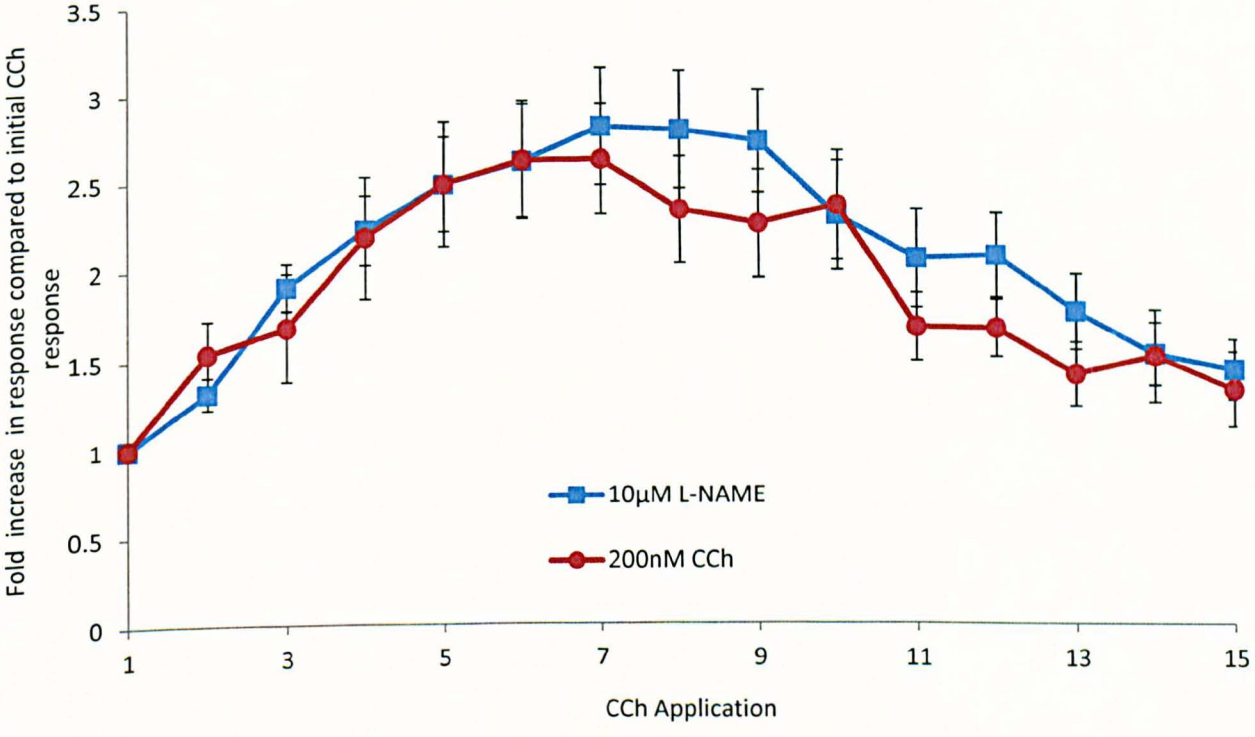

Direct comparison of the cumulative data for repeat applications of 200nM CCh in the presence (Blue) of 10μM L-NAME (n=23, 6 experiments, 4 animals) compared to the control data for repeat applications of 200nM CCh (Red) in the absence of 10μM L-NAME (n=35, 8 experiments, 7 animals). Performance of a 2 tailed t-test revealed no statistically significant difference between treatments.

Figure 5.1.3 Change in $[Ca^{2+}]_i$ in mouse lacrimal acinar cells in response to repeat stimulations with 200nM CCh illustrating variability in control response

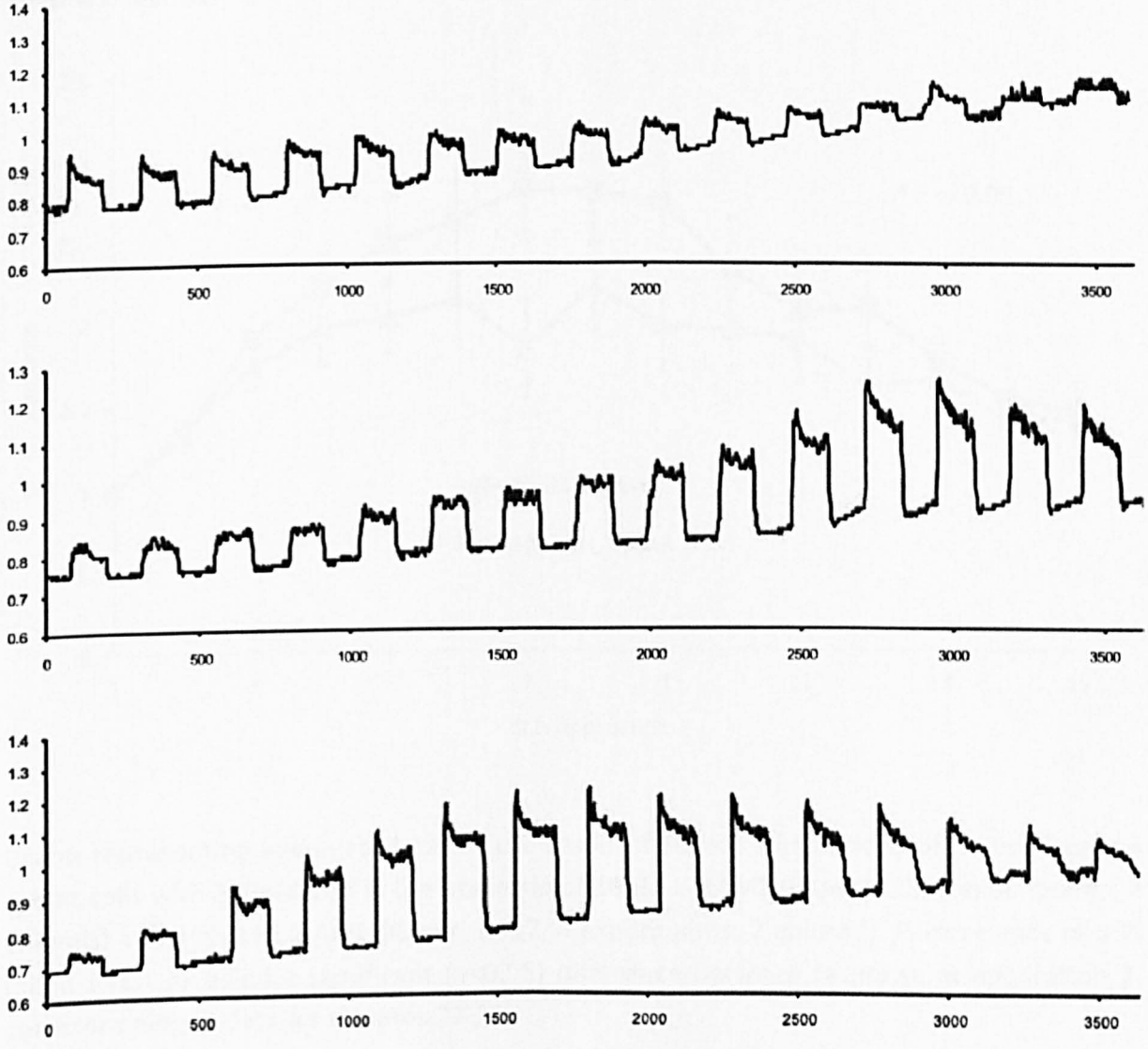

Traces A, B and C show the result of repeat stimulations of mouse lacrimal acinar cells with 200nM CCh in the presence of 10µM L-NAME and illustrate the continued diversity of lacrimal gland acinar cell response to agonist in the presence of 10µM L-NAME

Figure 5.1.4 Comparison of effect upon change in Fura fluorescence observed in mouse lacrimal acinar cells in response to repeat applications of 200 nM CCh between 10μM and 100μM L-NAME.

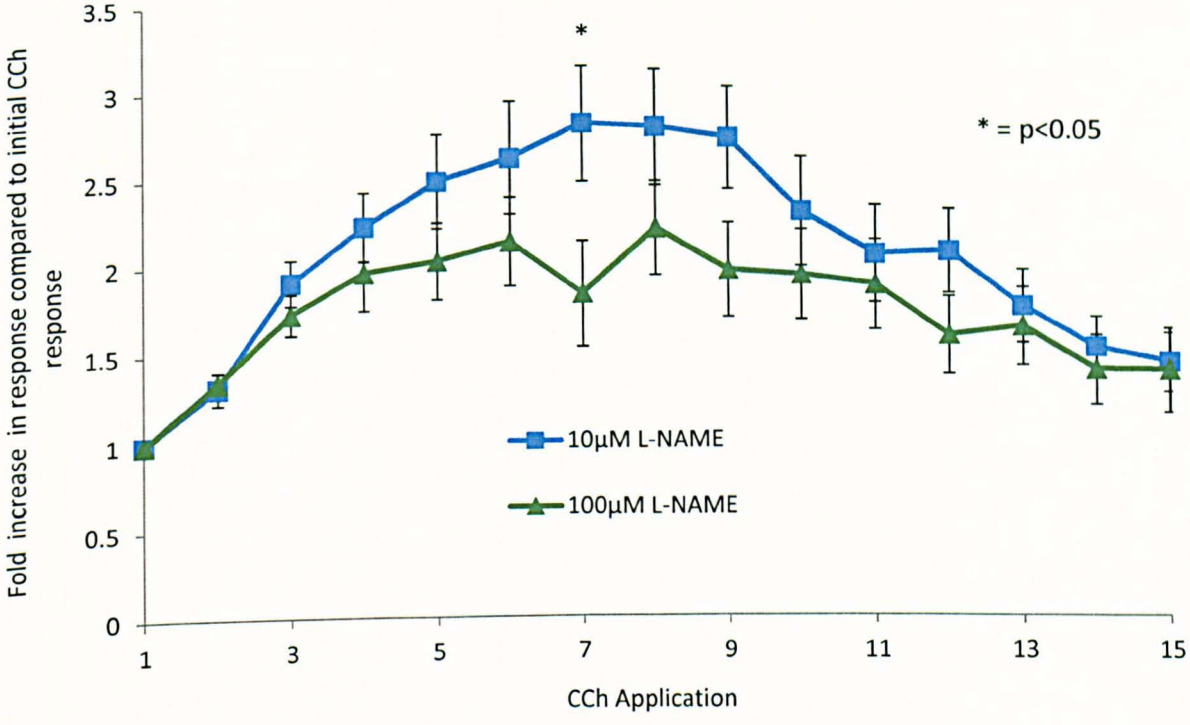

Graph representing averaged data for the result of repeat stimulations of mouse lacrimal acinar cells with 200nM CCh in the presence of 10μM L-NAME (Blue, n=23, 6 experiments, 4 animals) and 100μM L-NAME (Green, n=17, 4 experiments, 2 animals). Performance of a 2-tailed t-test revealed a significant ($p<0.05$) difference between response at application 7- corresponding to data for minutes 27-29.

Figure 5.1.5 Change in Fura fluorescence observed in mouse lacrimal acinar cells in response to repeat applications of 200 nM CCh in the presence of the specific iNOS inhibitor 10µM SMT.

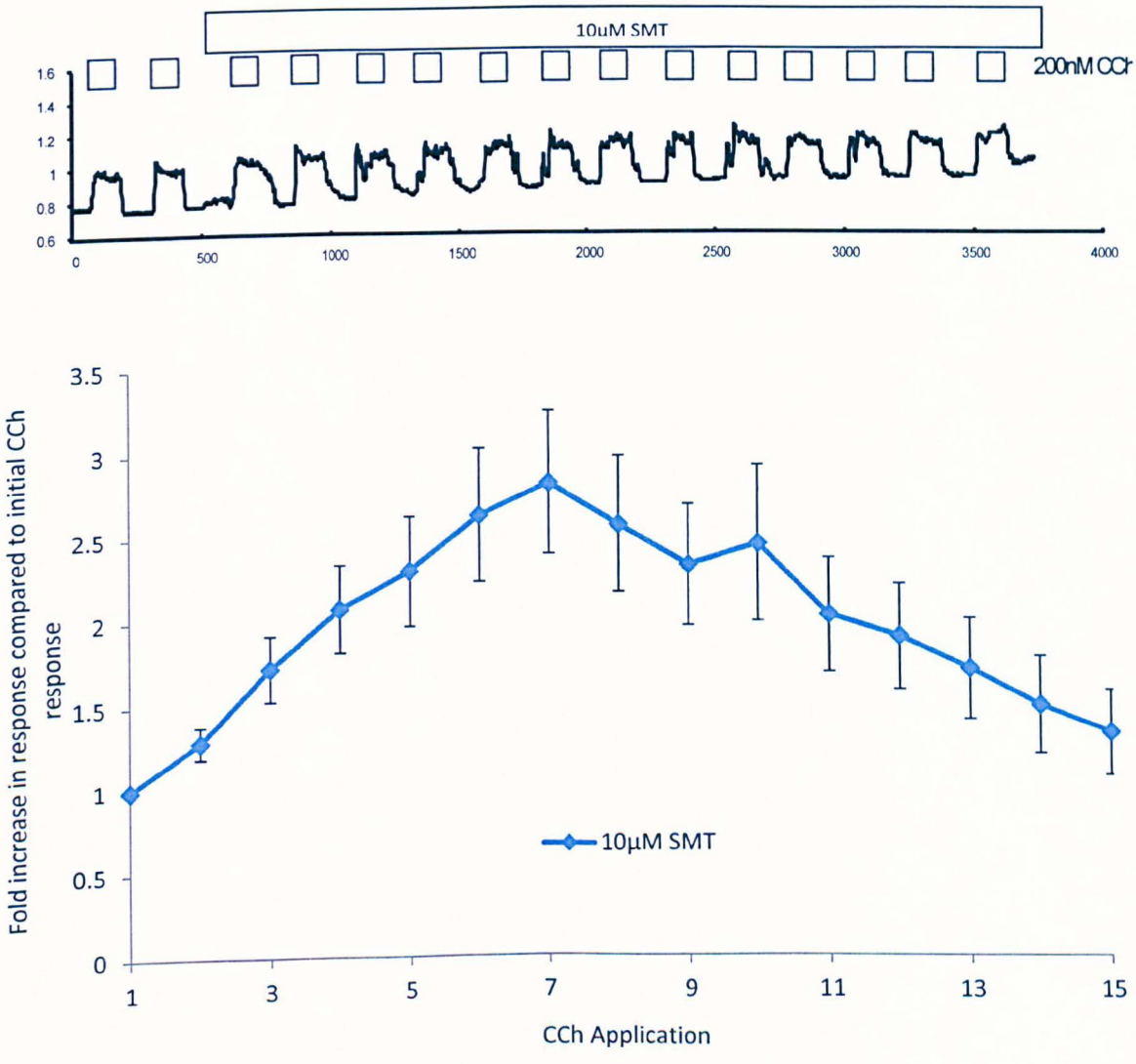

Trace A shows the result of repeat 2 minute stimulations with 200nM CCh in the presence of the specific iNOS inhibitor 10µM SMT. The first 2 applications of CCh were made in the absence of SMT, as a method of showing any effect of acute application of the iNOS inhibitor upon $[Ca^{2+}]_i$. Subsequent applications of CCh were made while the cells were continually perfused with 10µM SMT. The presence of 10µM SMT did not alter the pattern of response to 200nM CCh, the cells still responding in a manner consistent with the control applications of CCh (i.e. peak-plateau). This pattern of basal-plateau-basal was repeatable throughout the course of the experimental run, with the cells maintaining an elevated response to 200nM CCh.

Trace B represents cumulative data (n=19, 6 experiments, 4 animals) for the repeated application of 200nM CCh to mouse lacrimal acinar cell in the presence of 10µM SMT. Data

is represented as a function of the response to the first application of agonist. Response to agonist peaked at 282.5% of the initial stimulation (±4.3%) at application 7 (minutes 25-29), and run down to 133% (±25.2) by t=60. The response profile still follows the amplification/ rundown pattern, as observed in the control and L-NAME experiments.

Figure 5.1.6 Comparison of effect upon change in Fura fluorescence observed in mouse lacrimal acinar cells in response to repeat applications of 200 nM CCh in the presence and absence of 10μM SMT.

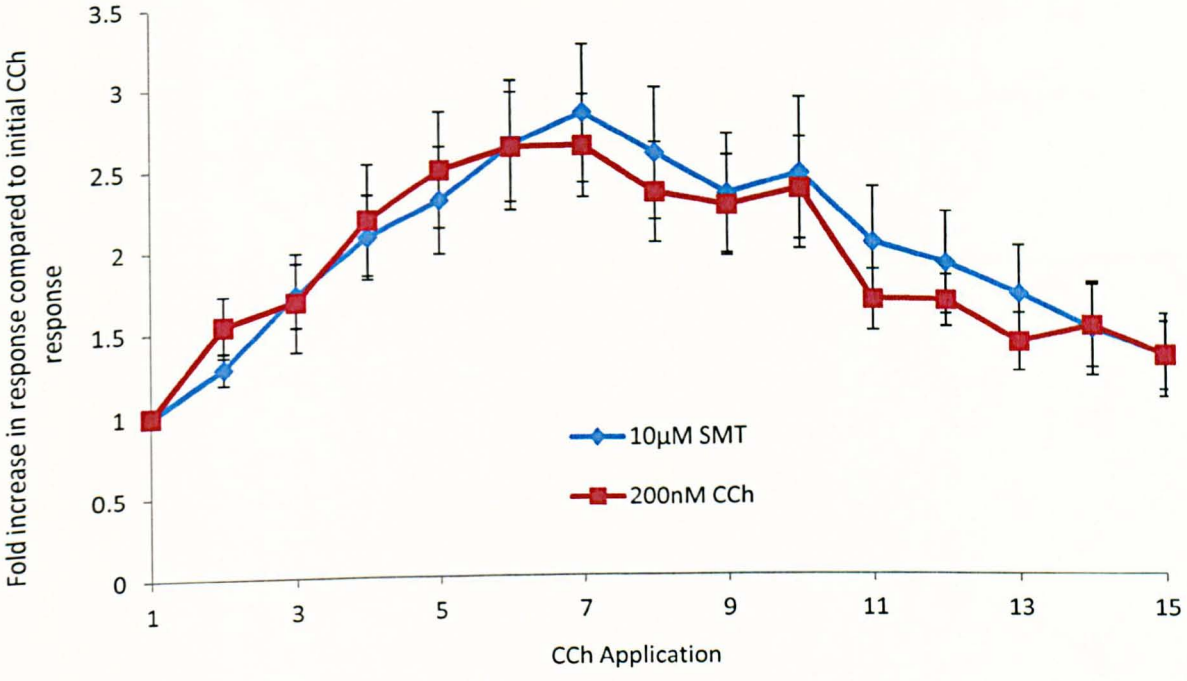

Direct comparison of the cumulative data for repeat applications of 200nM CCh in the presence (Blue) of 10 μM SMT (n=19, 6 experiments, 4 animals) compared to the control data for repeat applications of 200nM CCh (Red) in the absence of 10 μM SMT (n=35, 8 experiments, 7 animals). Performance of a 2 tailed t-test revealed no statistically significant difference between the data obtained for the control and treatment with 10 μM SMT.

Figure 5.1.7 Change in Fura fluorescence observed in mouse lacrimal acinar cells in response to repeat applications of 200 nM CCh in the presence of the eNOS inhibitor 50nM DPI.

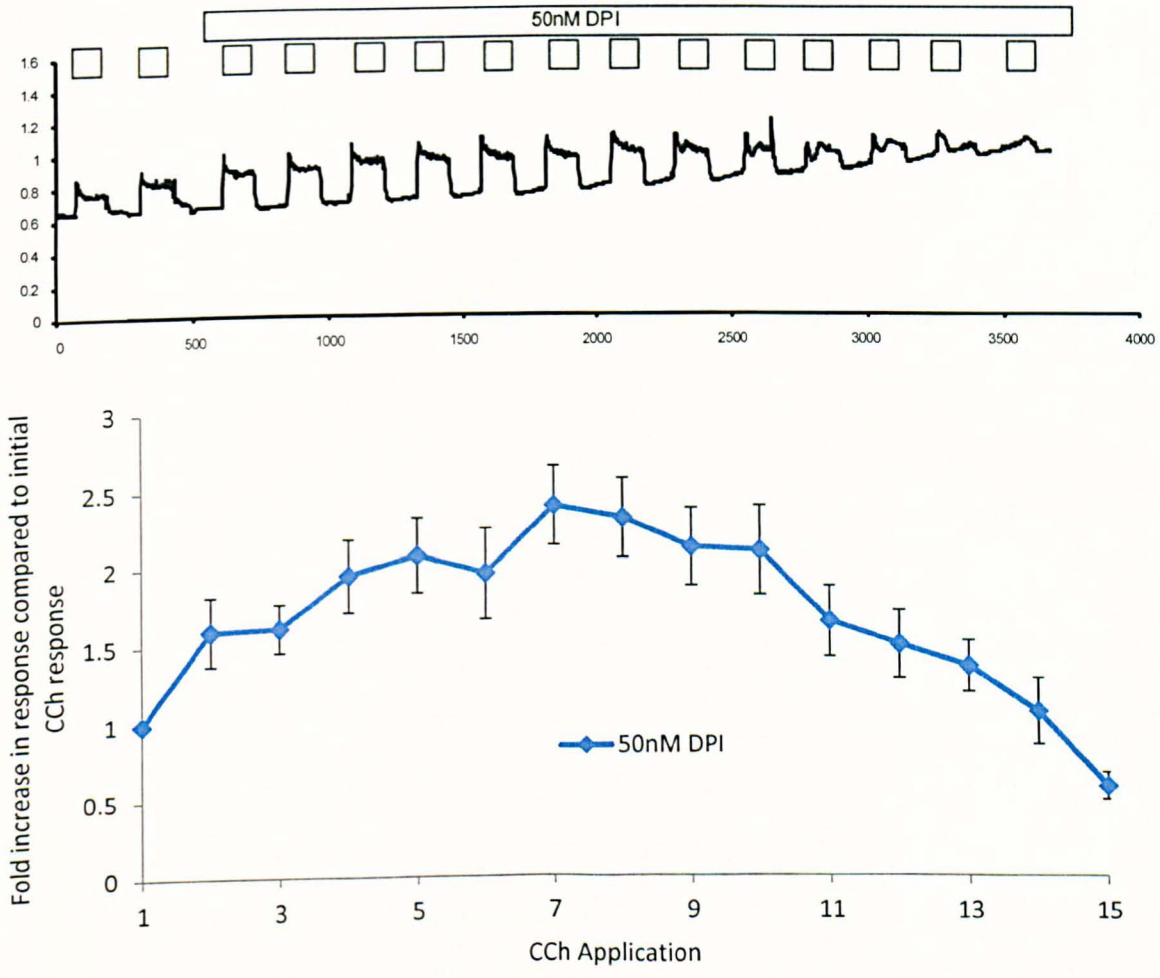

Trace A shows the result of repeat 2 minute stimulations with 200nM CCh in the presence of 50nM of the eNOS inhibitor DPI. The first 2 applications of CCh were made in the absence of DPI, as a method of showing any effect of acute application of the eNOS inhibitor upon $[Ca^{2+}]_i$. Subsequent applications of CCh were made while the cells were continually perfused with 50nM DPI.

Trace B shows the cumulative data for the repeated application of 200nM CCh to mouse lacrimal acinar cell in the presence of 50nM DPI. Data is represented as a function of the response to the first application of agonist. Response to agonist peaked at 2-2.5 fold that of the initial response to 200nM CCh after 26 minutes/ 7th application, and suffers a distinct rundown in response.

Figure 5.1.8 Comparison of effect upon change in Fura fluorescence observed in mouse lacrimal acinar cells in response to repeat applications of 200 nM CCh in the presence and absence of 50nM DPI.

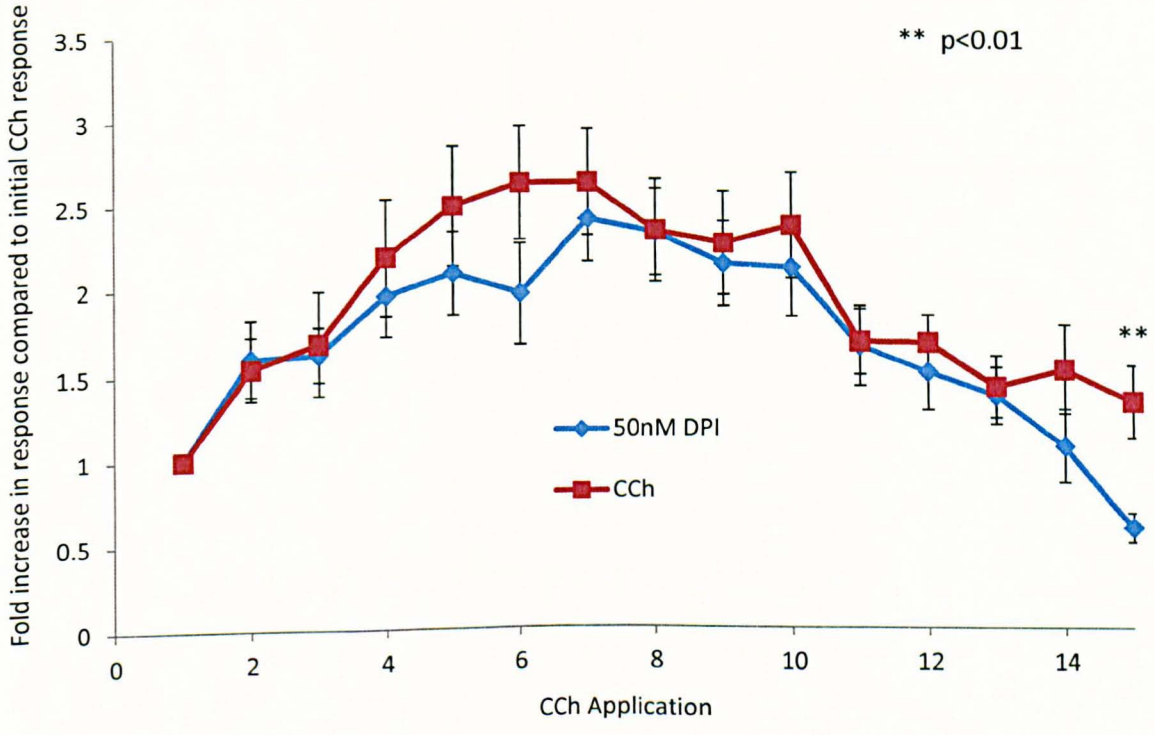

Direct comparison of the cumulative data for repeat applications of 200nM CCh in the presence (Blue) of 50nM DPI (n=23, 5 experiments, 2 animals) compared to the control data for repeat applications of 200nM CCh (Red) in the absence of 50nM DPI (n=35, 8 experiments, 7 animals). Performance of a 2 tailed t-test revealed significant ($p < 0.01$) decrease in DPI exposed cell response to 200nM CCh at t=60.

Figure 5.1.9 Change in Fura fluorescence observed in mouse lacrimal acinar cells in response to repeat applications of 200 nM CCh in the presence of the nNOS inhibitor 710nM 7NI.

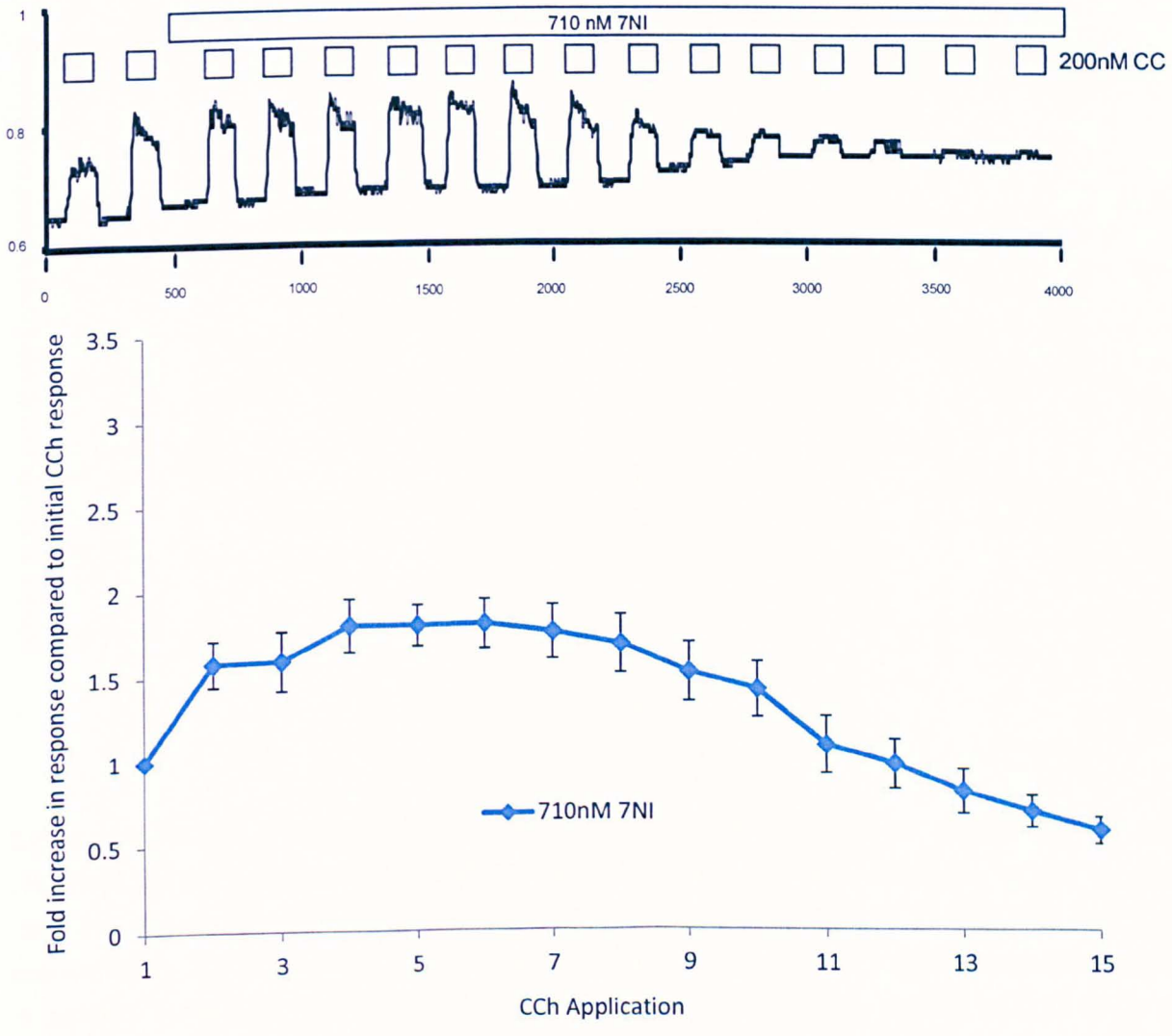

Trace A shows the result of repeat 2 minute stimulations with 200nM CCh in the presence of 710nM of the nNOS inhibitor 7NI. The first 2 applications of CCh were made in the absence of 7NI, as a method of showing any effect of acute application of the nNOS inhibitor upon $[Ca^{2+}]_i$. Subsequent applications of CCh were made while the cells were continually perfused with 710nM 7NI.

Trace B shows the cumulative data for the repeated application of 200nM CCh to mouse lacrimal acinar cell in the presence of 710nM 7NI for n=25 cells from 3 animals, 10 experiments.

Cumulative averaged data for the repeated application of 200nM CCh to mouse lacrimal acinar cell in the presence 710nM 7NI. Data is represented as a function of the response to the first application of agonist.

Figure 5.1.10 Comparison of effect upon change in Fura fluorescence observed in mouse lacrimal acinar cells in response to repeat applications of 200 nM CCh in the presence and absence of 710nM 7NI.

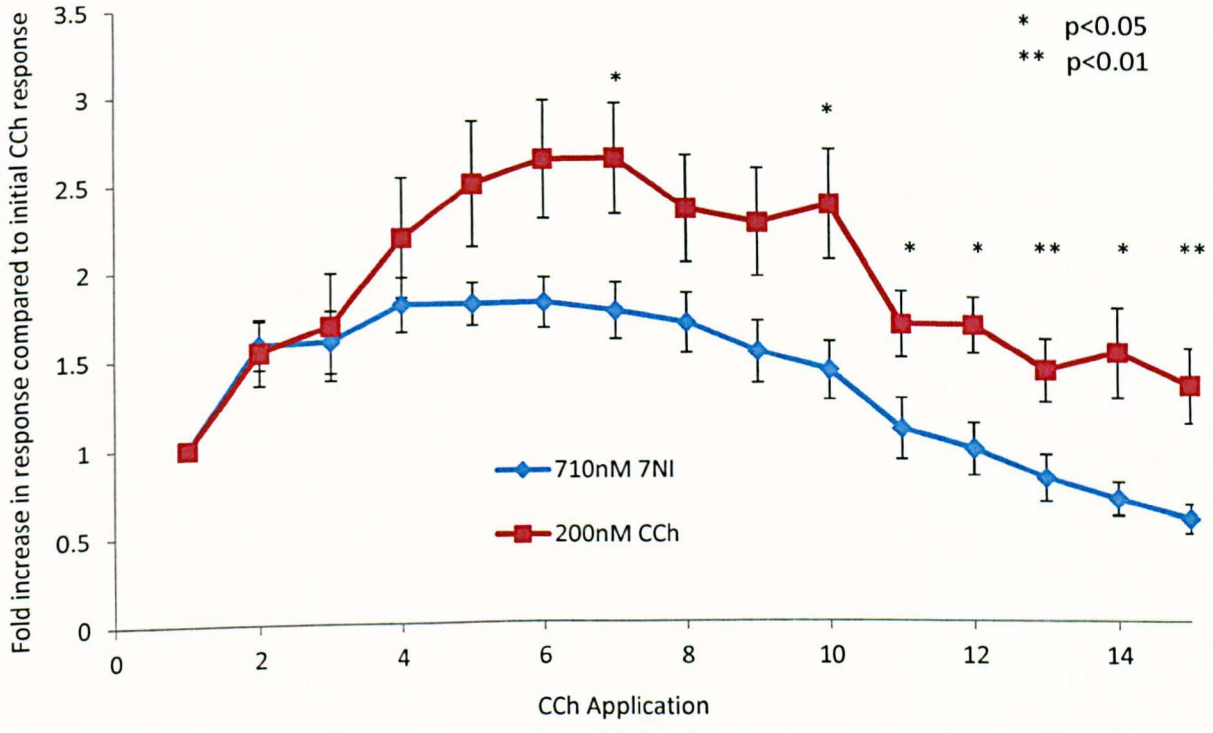

Direct comparison of the cumulative data for repeat applications of 200nM CCh in the presence (Blue) of 710nM 7NI (n=35, 10 experiments, 3 animals) compared to the control data for repeat applications of 200nM CCh (Red) in the absence of 710nM 7NI (n=35, 8 experiments, 7 animals). Performance of a 2 tailed t-test revealed a significant attenuation in agonist evoked Ca^{2+} response in the presence of 710nM 7NI. $p<0.05$ vs control, and applications 10-15 (minutes 41-61) ($p<0.05$ for applications 7,10, 11 13 and 14. $P<0.01$ for applications 12 and 15).

Figure 5.1.11 Comparison of effect upon change in Fura fluorescence observed in mouse lacrimal acinar cells in response to repeat applications of 200 nM CCh in the presence and absence of 10µM L-arginine.

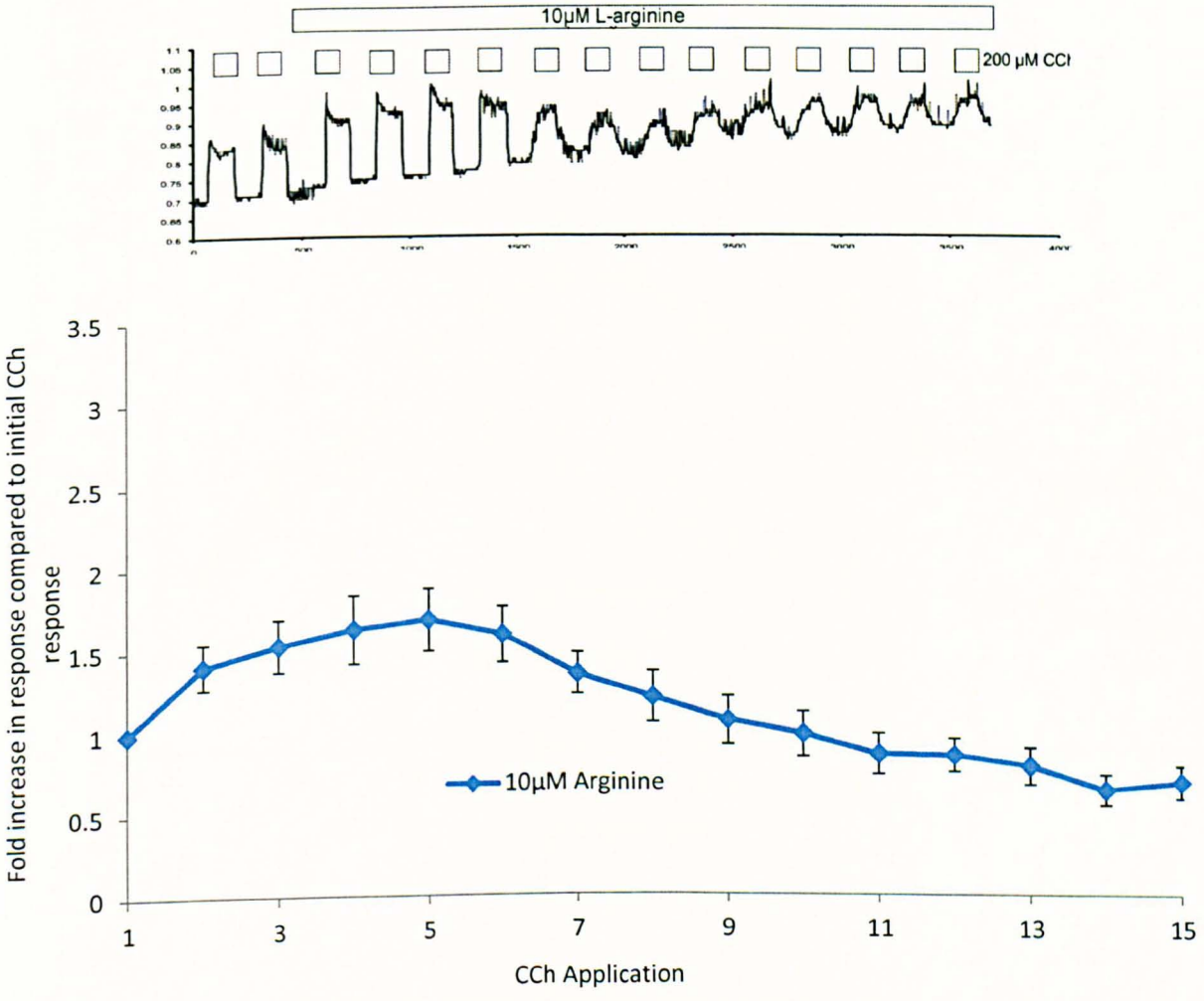

Trace A shows the result of repeat 2 minute stimulations with 200nM CCh in the presence of 10µM of the NOS substrate L-arginine. The first 2 applications of CCh were made in the absence of arginine, as a method of showing any effect of acute application of the NOS substrate upon $[Ca^{2+}]_i$. Subsequent applications of CCh were made while the cells were continually perfused with 10µM of L-arginine

Trace B shows the cumulative data for the repeated application of 200nM CCh to mouse lacrimal acinar cell in the presence of 10µM L-arginine for n=25 cells from 3 animals, 10 experiments peak response of 168.6% (±19.0%) is achieved by the 5th agonist stimulation (minutes 19-21) declining to 69.3% (±9.9%) of initial response t=60.

Figure 5.1.12 Comparison of effect upon change in Fura fluorescence observed in mouse lacrimal acinar cells in response to repeat applications of 200 nM CCh in the presence and absence of 10μM L-arginine.

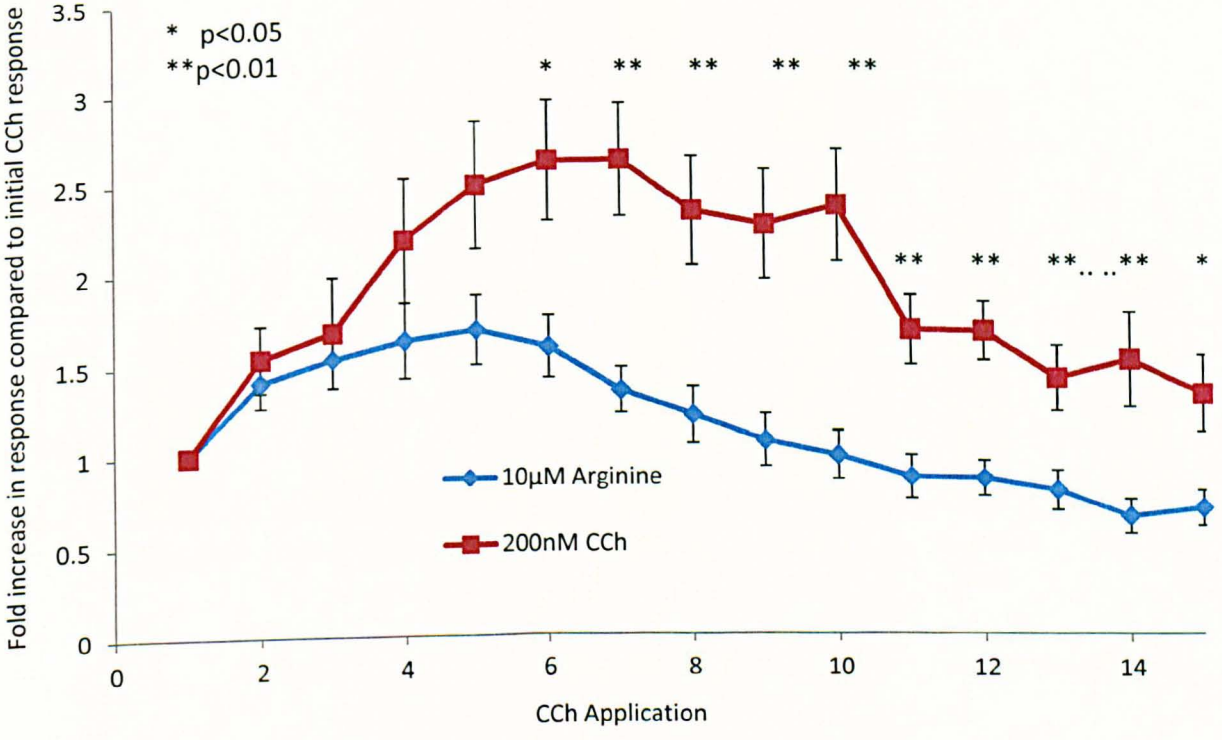

Direct comparison of the cumulative data for repeat applications of 200nM CCh in the presence (Blue) of the NOS substrate 10μM L-arginine (n=25, 5 experiments, 3 animals) compared to the control data for repeat applications of 200nM CCh (Red) in the absence of 10μM L-arginine (n=35, 8 experiments, 7 animals). Performance of a 2 tailed t-test revealed application significant decline in response to agonist during perfusion with arginine $p<0.05$ at applications 6 and 15 (minutes 23-25 and 59-61) and $p<0.01$ for applications 7-14.

Figure 5.1.13 Percentage of the total number of mouse lacrimal cells who's response to agonist declines to <50% of initial response to agonist.

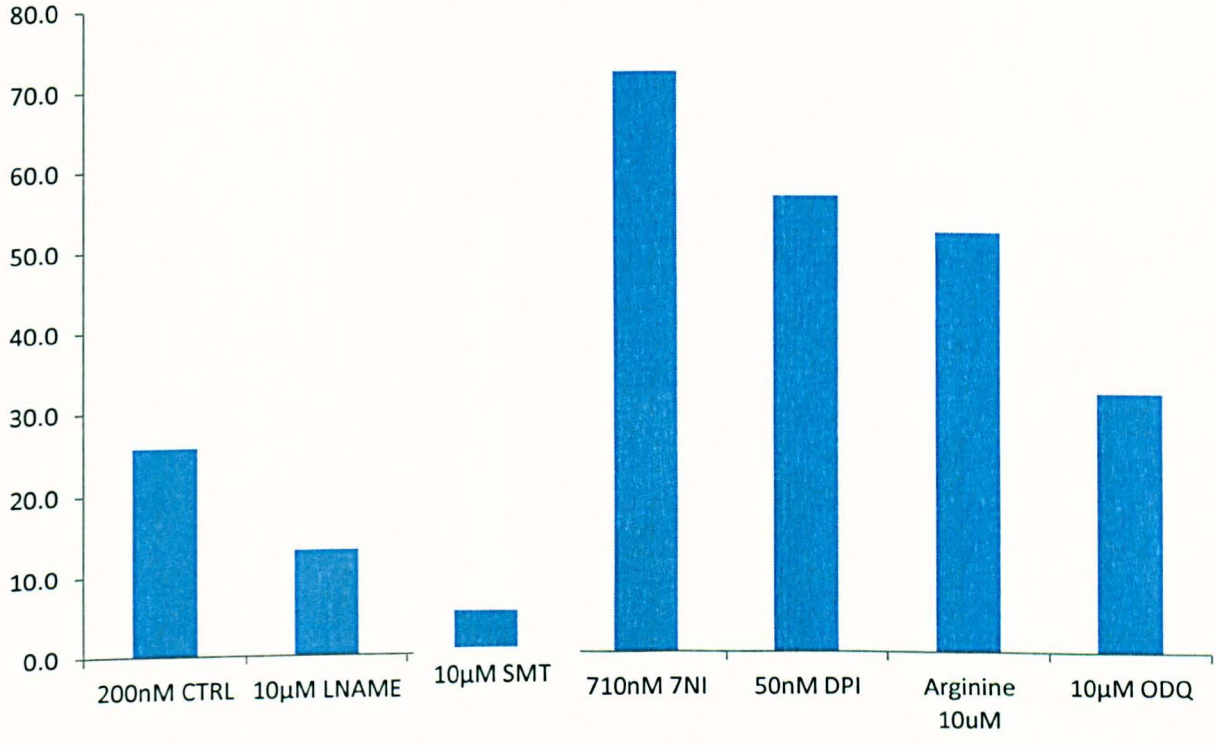

	50% act by end	No 50% Drop	n	% drop by 50%
200nM control	9	26	35	25.7
10µM LNAME	3	20	23	13.0
10µM SMT	1	18	19	5.3
710nM 7NI	18	7	25	72.0
50nM DPI	13	10	23	56.5
Arginine 10uM	13	12	25	52.0
10µM ODQ	8	17	25	32.0

Histogram and table summarizing the observations for the t=60 (end of experiment response) to 200nM CCh compared to their initial, pre treatment response to agonist. Cells were classified to have suffered significant rundown (<50% of initial response) or to have maintained function (>50% of initial response to agonist).

Figure 5.1.14 Average final response (± S.E.M.) of mouse lacrimal gland acinar cells to 200nM CCh in the presence of NOS inhibitors, L-arginine and ODQ

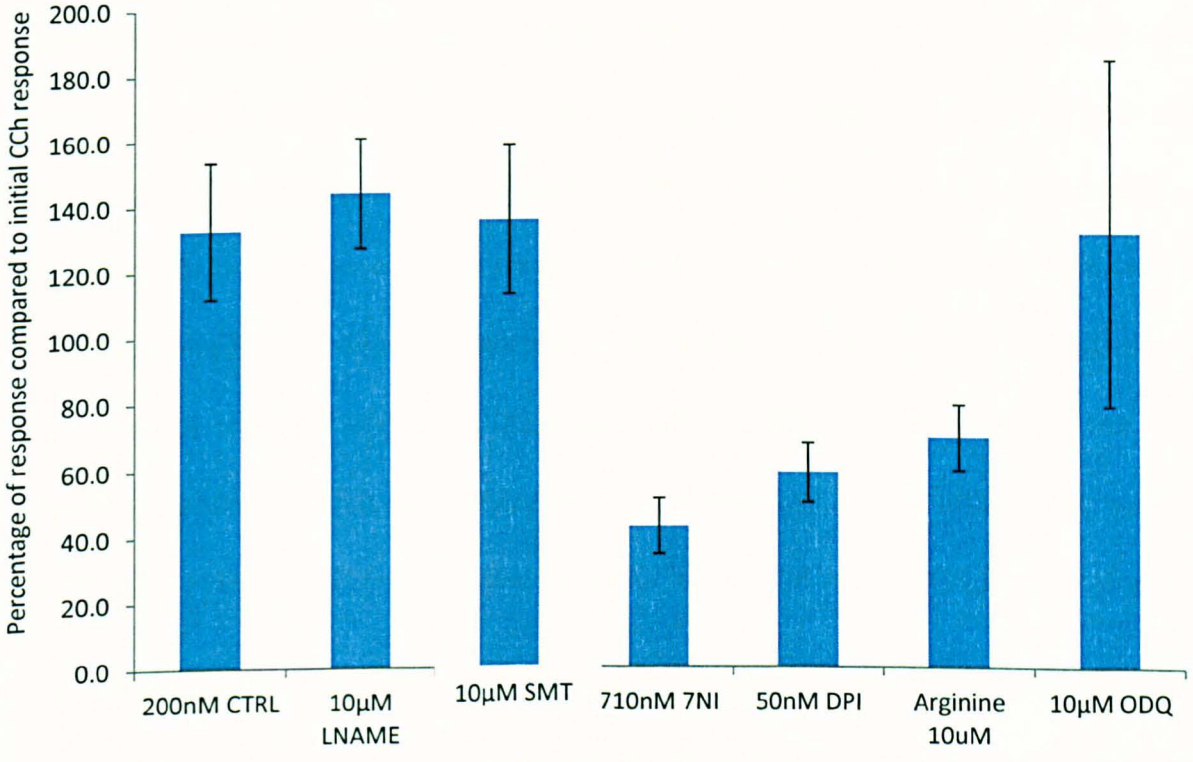

Treatment	n	Average response at t=60	SEM
200nM control	35	132.7	20.8
L-NAME 10μM	23	143.8	16.6
SMT 10μM	19	133.0	25.2
7NI 710nM	25	43.0	8.4
DPI 50nM	23	58.8	8.8
Arginine 10uM	25	69.3	9.9
ODQ 10μM	25	131.8	52.9

Histogram and table summarizing the findings for the magnitude of decline in mouse lacrimal gland acinar cells measured at t=60 (end of experiment) to 200nM CCh compared to their initial, pre treatment response to agonist.

Conclusions.

The response profile established using repeat stimulations with 200nM CCh of mouse lacrimal acinar cells provides a basis for testing the effect of NOS inhibitors upon the agonist evoked change in $[Ca^{2+}]_i$. Previously I have shown that exogenous NO supply from a donor affects mouse lacrimal acinar cells similarly to mouse submandibular gland acinar cells. Yet differences in the response profile of mouse lacrimal gland acinar cells to submandibular acinar cells imply an endogenous production of NO. This hypothesis was strengthened by the effect of the sGC inhibitor ODQ Figure 3.1.10., effectively left shifting the curve, affecting the amplification component of the response yet having little effect upon the decline of the response (Control declining to 132.7%, ±20.8% *vs* ODQ 131.8%, ±52.9%).

The averaged data for 10μM L-NAME (figure 5.1.2) show no significant alteration of the decline of response (Control declining to 132.7%, ±20.8% *vs* 10μM L-NAME 143.8%, ±16.6%). Since L-NAME was used in an attempt to inhibit all NOS activity, the lack of effect upon the change in $[Ca^{2+}]_i$ evoked by 200nM CCh can imply that 10μM L-NAME was ineffective, was not a high enough concentration to affect the NOS isoforms, or that simultaneous inhibition of NOS isoforms somehow results in a lack of change of response. Some protective effect against response rundown may have been conferred by 10μM L-NAME however, since the amount of cells declining in response to <50% represented only 13% *vs* control cells declining 25.7%. Figure 5.1.4 demonstrates the effect of increasing the concentration of L-NAME to 100 μM upon the Ca^{2+} response evoked by 200nM CCh. Little significant difference is seen using this higher concentration, although the peak activity at application 7 (t=27-29 minutes) is significantly ($p = <0.05$) reduced.

The effect of targeted inhibition of the iNOS isoform with 10μM SMT (figure 5.1.6) showed similar results to the use of 10μM L-NAME, inasmuch that the averaged response did not significantly differ from the control (Control declining to 132.7%, ±20.8% *vs* 10μM SMT 133.0% ±25.2). However, upon analysis of the amount of cells running down to <50% of initial response showed that the presence of the iNOS inhibitor, 10 μM SMT, had resulted in only 1/19 (5.3%) of cells showing that magnitude of decline *vs* 25.7% of control cells. This result raises the possibility that inhibition of iNOS by SMT, whilst not altering the average pattern of response, prevented the cells from declining to the 50% of initial activity threshold value- implying that iNOS may be responsible for the greater magnitude decline in response.

Inhibition of the constitutive eNOS isoform with 50nM DPI (figure 5.1.8) did not show any significant alteration of response to agonist until the very end of the experimental run (Control declining to 132.7%, ±20.8% *vs* 50nM DPI 58.8% ±8.8 ($p<0.01$)). The significant decline in response implies that NO production by eNOS is not responsible for the decline in response to agonist, and that the action of eNOS may be required to maintain cellular response- this hypothesis is strengthened by the fact that use of DPI resulted in the decline to <50% response of 13/23 (56.5%) cells compared to 25.7% of control cells.

The other constitutive NOS isoform, nNOS, inhibited with 710nM 7NI exhibited a significant shift in the response of the mouse lacrimal acinar cells (figure 5.1.10). Inhibition of nNOS resulted in the left shift of response profile and the sustained significant decline ($p<0.01$-<0.05) in response from application 10 (t=39minutes) onwards. 72% of the 7NI treated cells run down to <50% response (*vs* 25.7% in control) averaging only 43.0%, ±8.4% of initial activity at t=60. This was the most extreme of the NOS inhibitor effects. These results imply

that the constitutive nNOS isoform is paramount in maintaining normal cell function in response to muscarinic agonist, and that perturbation of this system can result in the rapid decline of cell response.

In an attempt to measure the effect of an increase in NO on a physiological scale, rather than the exogenous supply from an NO donor, the NOS substrate, 10 μM L-arginine was supplied to the cells. The result of this was an even more extreme left shift of response profile than observed with the NOS inhibitors, as shown in (figure 5.1.12). The significant decline ($p < 0.01$- $p < 0.05$) was sustained from agonist application 6 (t=23 minutes onwards) ending at t=60 with 69.3%, ±9.9%, with 13/25 (52%) of cells declining to <50% of initial activity. If addition of arginine would have increased endogenous NO production, then it would have been expected that there would have been at least a transient amplification effect, as per NO donor effects. However, the sustained decline- similar in curve to that observed for nNOS inhibition, and similar to the response magnitudes observed for eNOS inhibition (69.3%, ±9.9% and 52.0% responding at<50% response at t=60 for arginine *vs* 58.8% ±8.8 and 56.5% responding at<50% response at t=60 for DPI) may imply that this initial view of "increased substrate=increased NO= nil effect" may be simplistic.

These results show the effect upon agonist evoked change in $[Ca^{2+}]_I$, and therefore an effect upon secretion.

6 Results

6.1 The effect of NOS inhibitors upon endogenous NO production in mouse lacrimal acinar gland cells as visualised with DAF-2-DA.

Aims and objectives

The following series of experiments are an attempt to observe directly the change in NO levels during the repeat stimulation protocol outlined previously. Furthermore, through the use of NOS inhibitors, the effect upon NO generation by specific NOS isoform inhibition can be shown. Identification of specific NOS isoform activity in lacrimal gland acinar cells would further elucidate the pathways involved in lacrimal secretion and identify possible targets for treatment in NO mediated lacrimal gland disfunction potentially associated with SjS.

Introduction

NOS inhibitors were used previously (chapter 5) to demonstrate the effect of NOS isoform inhibition upon the agonist evoked calcium signal measured by Fura microfluorimetry in mouse lacrimal gland acinar cells. However, these data only show the effect of NOS inhibition on the Ca^{2+}signal secondary to any modulation of NO production, and therefore do not directly show changes in NO production. This shortcoming was resolved using the fluorescent NO indicator, DAF-2 to monitor the amount of NO produced by mouse lacrimal gland acinar cells in the absence and presence of specific NOS isoform inhibitors.DAF-2-DA is loaded into the cells as a non-fluorescent, membrane permeable reagent, which is then hydrolysed by cytosolic esterases to release cell impermeable active form, DAF-2. The DAF-2 becomes fluorescent upon reaction with NO and O_2 (Kojima, Nakatsubo et al. 1998).

The DAF-2 fluorescence data presented in this chapter were obtained in parallel with the FURA data (Chapter 5) collected by loading of the cells with FURA-2-AM and DAF-2-DA simultaneously, representing a matched set of data, thus, the changes in NO production may be directly correlated with modification of the Ca^{2+} signal. The DAF fluorescence data is presented as a percentage value of the initial DAF fluorescence measured in the lacrimal gland cells. Presentation of the data as a function of the starting condition combats the inherent variability in dye loading and allows each cell's response to be measured against its own starting conditions.

Whilst Fura-2-AM is a dual excitation ratiometric dye, DAF-2-DA has only a single excitation wavelength, thus DAF fluorescence is dependent on both NO activity and on dye concentration. Variation in DAF loading into the cells makes both aggregation of data and absolute calibration of NO levels difficult. Data analysis is further complicated by loss of fluorescence over the course of the experiment, most likely by a combination of dye leakage and photobleaching. Nevertheless, the effect of NOS inhibitors on NO levels may be assessed by directly comparing traces obtained under similar conditions.

The data below represent an attempt to visualise the change of NO levels in mouse lacrimal gland acinar cells undergoing repeat 2minute stimulations of 200nM CCh in the presence of the NOS inhibitors (L-NAME, DPI, 7NI, SMT), sGC inhibitor (ODQ) and the NOS substrate (arginine). These data for DAF2 fluorescence are not repeats of the experiments seen in the previous chapter, but are taken from the same cells simultaneously with the Fura 2 data , since prior to the experimental run, the cells were loaded with both DAF-2-DA and FURA-2-AM. This allows for a simultaneous and direct comparison of relative NO levels and the

effect upon agonist evoked Ca^{2+} signal. There is no evidence to suggest that there is any interaction between the DAF-2-DA and FURA-2-AM that may affect the obtained results.

Figure 6.1.1 shows the average (n=35 cell) change in mean DAF2 fluorescence over time in experiments where mouse lacrimal acinar gland cells were stimulated with 200nM CCh using the 2minute repeat stimulation protocol seen previously. (see Chapter 2: Methods for details of the protocol). This trace provides the baseline for comparison for the (CCh stimulated) endogenous production of NO in mouse lacrimal acinar gland cells against which the effects of NOS inhibitors will be compared. Each trace was normalised to the starting fluorescence level (100%) to compensate for variation in dye loading and initial fluorescence. On average, relative fluorescence declined during the initial 20.2 minutes of the experiment, to a minimum of 70.2% (±2.5%) ($p = <0.001$ vs starting fluorescence) before continually rising to a maximum fluorescence of 103.9% (±2.5) by 60 minutes which was not found to be statistically significantly different from the initial fluorescence reading. The decline in fluorescence observed is most likely a consequence of dye leakage and photobleaching of the DAF-2. Nevertheless, against what is assumed to be a constant loss of dye, fluorescence increased during the latter stages of the experiment, showing a continuous production of NO at a rate which overcame the loss of DAF-2 fluorescence. There was no immediate/ acute change in DAF fluorescence observed in response to 200nM CCh stimulation.

Shown in figure 6.1.2 is "proof of concept" data, demonstrating that DAF fluorescence does increase in the presence of NO. Exposure of the DAF loaded cells to 100μM of the NO donor, SNAP, resulted in a dramatic increase in the rate of fluorescence increase. At t=50 minutes,

the DAF fluorescence was 425% (±4.9%) of the starting fluorescence, compared to 94.9% (±5.6%) recorded in the control data at the same timepoint.

Comparing the rate of change of DAF fluorescence in stimulated cells against unstimulated cells would determine how capable mouse lacrimal gland acinar cells are at producing endogenous NO. Figure 6.1.3 represents the comparison between the repeat stimulation control data and cells not being subjected to challenge with agonist (n=33). DAF fluorescence in unstimulated cells decreased significantly ($p < 0.01$ vs start) to a minimum of 82.2% (±2.7%) of start at t= 24.8 minutes. Despite being subject to no stimulation with agonist, DAF fluorescence increased from this point to a maximum of 94.8% (±3.4%) at t= 59.6 minutes implying that the production of NO is not dependent upon agonist evoked response. There were statistically significant differences between unstimulated and control data, albeit the control data did recover (i.e. decline=/< increase) earlier, 20.2 minutes vs 24.8 minutes unstimulated.

The non specific NOS inhibitor, 10μM L-NAME, was used to determine whether this basal NO production could be attenuated, Figure 6.1.4 represents the data obtained for n=23 cells during the repeat stimulation of mouse lacrimal acinar glands with 200nM CCh in the presence of 10μM L-NAME. DAF fluorescence underwent a short-lived decline, reaching its minimum of 92.0% (±1.7) at t=9.3 minutes, significantly higher ($p<0.01$) and sooner (vs control at 24,8 minutes), implying that the 10μM L-NAME increased NO production. This increase was continuous and significant, reaching 161.2% (±11.6%) ($p< 0.01$ vs control maximum). This increase in DAF fluorescence represented an unexpected increase in NO production.

Targeting specific NOS isoforms with inhibitors particular to each followed, with figure 6.1.5 showing the result of 6 experiments (n=19 cells) obtained for the iNOS inhibitor, 10μM SMT, obtained in parallel with the FURA data seen earlier. Similarly to the previous DAF experiments, fluorescence initially declined before leveling out and increasing. For 10μM SMT the fluorescence nadir was reached at t=19.0 minutes (88.6%, ±1.7%. $p<0.05$ vs control minimum). However, the subsequent maximum (106.2% of start, ± 3.9% at=60) was statistically insignificant from the control data.

Attempted inhibition of the eNOS isoform with 50nM DPI during the repeat stimulation protocol (n=23) yielded results showing statistically insignificant differences from the DAF control data. Similarities in the trace obtained (figure 6.1.6) are confirmed with the endpoint maximum (108.8%, ±6.4%, *vs.* 103.9%, ±6.6% for the control), and a similar magnitude of decline: to 72.8% (±1.3%) at 18.5 minutes compared to the decline to 79.2% (±2.5%) seen at 20.2 minutes in the control data.

Figure 6.1.7 represents the data obtained during repeat stimulation of mouse lacrimal gland acinar cells during perfusion with the nNOS inhibitor 710nM 7NI (n=25), as outlined in the earlier protocol. The equilibrium point between DAF fluorescence decline and increase was reached significantly earlier at 6.9 minutes (and therefore significantly ($p<0.01$) higher, 97.2% (±1.1%) of start vs. control). DAF fluorescence went on to increase to a maximum of 141.9% (±5.2%) of the average initial fluorescence by t=60. This increase represents the second of the NOS inhibitors to result in a significant ($p<0.01$) increase in DAF fluorescence (and therefore NO production).

The effect of supplying mouse lacrimal gland acinar cells with the NOS substrate L-arginine (10μM) was determined for the agonist evoked change in $[Ca^{2+}]_i$ in Chapter 5.1. In figure

6.1.8 the data obtained for the DAF emission wavelengths are shown. The graph shows a significant ($p < 0.01$) increase in DAF fluorescence, peaking at 59.9 minutes with a value of 132.9% (±6.3%) of starting fluorescence. This upturn in fluorescence began at 10.4 minutes after decreasing to only 93.2% (±6.3%) of the initial DAF fluorescence value, significantly ($p < 0.01$) higher than data obtained for the control protocol. This data indicates that external supply of NOS substrate can result in an increase in NO production.

The sGC inhibitor, 10μM ODQ, was used in the previous chapter to determine whether the automatic amplification of Ca^{2+} response to agonist was modulated via cADPr. DAF data was simultaneously obtained during those experiments and are shown in figure 6.1.9. Whereas the rundown is similar to that seen in the 10μM L-arginine (to 91.9% ,±2.0%, at 10.5 minutes $p< 0.01$) there is a dramatic increase in the DAF fluorescence reading obtained, steadily increasing to 214% (±13.4), representing a significant ($p < 0.01$) increase in NO production.

The data obtained for the DAF maxima and minima are summarised in the histogram in figure 6.1.10.

Figure 6.1.1 DAF-2 Fluorescence measured in mouse lacrimal gland acinar cells during repeat stimulations with 200nM CCh.

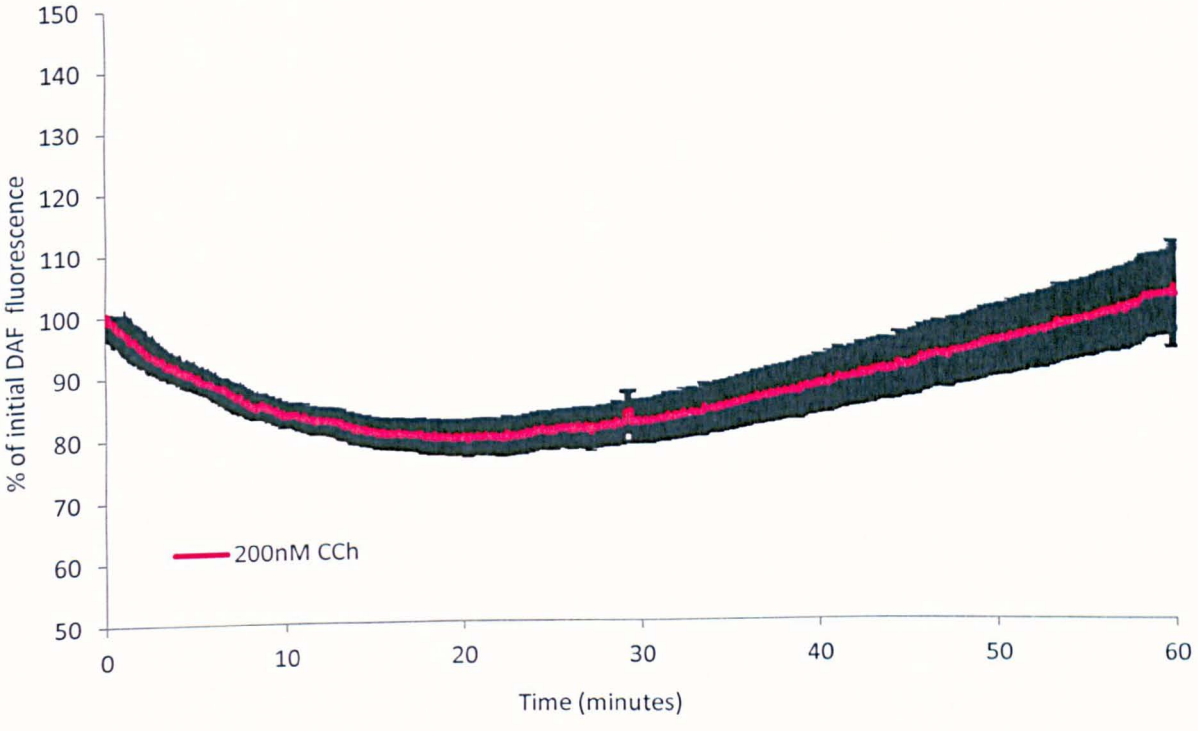

Timecourse showing the measured DAF fluorescence for the averaged data of 35 cells from 7 animals over 8 experiments for the repeated 2 minute stimulation of mouse lacrimal acinar gland cells with 200nM CCh. Data are presented as a percentage value of the starting fluorescence value. Fluorescence dipped to a minimum of 70.2% (±2.5%) of the starting value at 20.2minutes before continuously climbing to a maximum of 103.9 % (±6.6%) at t= 50.9 minutes.

Figure 6.1.2 DAF-2 Fluorescence measured in mouse lacrimal gland acinar cells during repeat stimulations with 200nM CCh in the presence of 100uM SNAP.

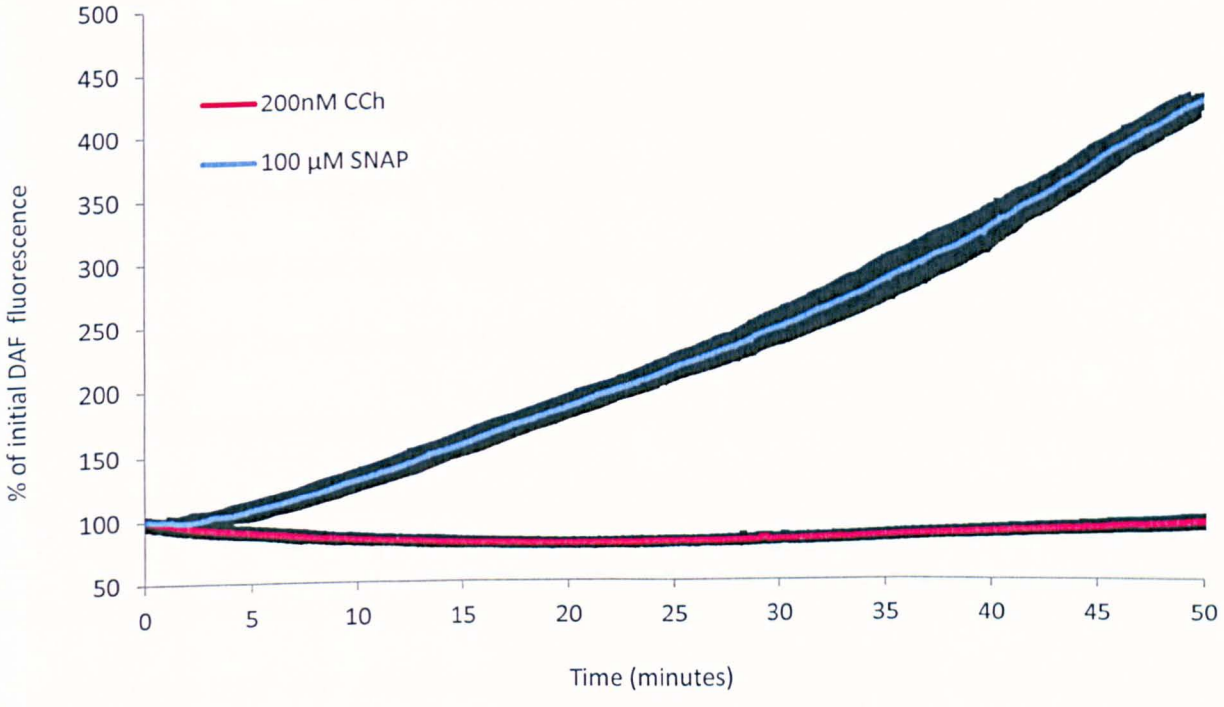

Graph represents the increase in DAF fluorescence (Blue) observed in mouse lacrimal gland acinar cells (n=2) when exposed to the NO donor (SNAP 100µM). The cells were exposed to 100.µM SNAP from t= 2 minutes resulting in a rapid and continuous increase in DAF fluorescence to a maximum of 425% (±4.9%) of the initial starting fluorescence by t=50. In comparison is the result of mouse lacrimals subjected to the 2min repeat 200nM CCh stimulation protocol, which exhibit a fluorescence value of 94.9% (±5.6) in the same period (n=35).

The following data represent an attempt to visualise the change of NO levels in mouse lacrimal gland acinar cells undergoing repeat 2minute stimulations of 200nM CCh in the presence of the NOS inhibitors (LNAME, DPI, 7NI, SMT), sGC inhibitor (ODQ) and the NOS substrate (arginine). These data for DAF2 fluorescence are not repeats of the experiments seen in the previous chapter, but are taken from the same cells simultaneously with the Fura 2 data , since prior to the experimental run, the cells were loaded with both DAF2DA and Fura 2 AM. This allows for a simultaneous and direct comparison of relative NO levels and the effect upon agonist evoked Ca^{2+} signal. There is no evidence to suggest that there is any interaction between the DAF2DA and FURA 2 AM that may affect the obtained result.

Whilst Fura 2 AM is a dual excitation ratiometric dye, DAF 2 DA has only a single excitation wavelength, thus DAF fluorescence is dependent on both NO activity and on dye concentration. Variation in DAF loading into the cells makes both aggregation of data and absolute calibration of NO levels difficult. Data analysis is further complicated by loss of fluorescence over the course of the experiment, most likely by a by a combination of dye leakage and photobleaching. Nevertheless, the effect of NOS inhibitors on NO levels may be assessed by directly comparing traces obtained under similar conditions.

Figure 6.1.1 shows the average (n=35 cell) change in mean DAF2 fluorescence over time in experiments where mouse lacrimal acinar gland cells were stimulated with 200nM CCh using the 2minute repeat stimulation protocol seen previously. (see Chapter 5 for details of the protocol). This trace provides the baseline for comparison for the (CCh stimulated) endogenous production of NO in mouse lacrimal acinar gland cells against which the effects of NOS inhibitors will be compared. Each trace was normalised to the starting fluorescence level (100%) to compensate for variation in dye loading and initial fluorescence. On average,

relative fluorescence declined during the initial 20.2 minutes of the experiment, to a minimum of 70.2% (±2.5%) ($p = <0.001$ vs starting fluorescence) before continually rising to a maximum fluorescence of 103.9% (±2.5) by 60 minutes which was not found to be statistically significantly different from the initial fluorescence reading. The decline in fluorescence observed is most likely a consequence of dye leakage and photobleaching of the DAF2. Nevertheless, against what is assumed to be a constant loss of dye, fluorescence increased during the latter stages of the experiment, showing a continuous production of NO at a rate which overcame the loss of DAF2 fluorescence. There was no immediate/ acute change in DAF fluorescence observed in response to 200nM CCh stimulation.

Shown in figure 6.1.2 is "proof of concept" data, demonstrating that DAF fluorescence does increase in the presence of NO. Exposure of the DAF loaded cells to 100μM of the NO donor, SNAP, resulted in a dramatic increase in the rate of fluorescence increase. At t=50 minutes, the DAF fluorescence was 425% (±4.9%) of the starting fluorescence, compared to 94.9% (±5.6%) recorded in the control data at the same timepoint.

Comparing the rate of change of DAF fluorescence in stimulated cells against unstimulated cells would determine how capable mouse lacrimal gland acinar cells are at producing endogenous NO. Figure 6.1.3 represents the comparison between the repeat stimulation control data and cells not being subjected to challenge with agonist (n=33). DAF fluorescence in unstimulated cells decreased significantly ($p <0.01$ vs start) t o a minimum of 82.2% (±2.7%) of start at t= 24.8 minutes. Despite being subject to no stimulation with agonist, DAF fluorescence increased from this point to a maximum of 94.8% (±3.4%) at t= 59.6 minutes implying that the production of NO is not dependent upon agonist evoked response. There were statistically significant differences between unstimulated and control

data, albeit the control cells did recover (i.e. increase in fluorescence equal to or greater than the rate of decline) earlier, 20.2 minutes *vs* 24.8 minutes unstimulated.

The non specific NOS inhibitor, 10μM L-NAME, was used to determine whether this basal NO production could be attenuated, Figure 6.1..4 represents the data obtained for n=23 cells during the repeat stimulation of mouse lacrimal acinar glands with 200nM CCh in the presence of 10μM L-NAME. DAF fluorescence underwent a short-lived decline, reaching its minimum of 92.0% (±1.7) at t=9.3 minutes, significantly higher ($p<0.01$) and sooner (vs control at 24,8 minutes), implying that the 10μM L-NAME increased NO production. This increase was continuous and significant, reaching 161.2% (±11.6%) ($p< 0.01$ vs control maximum). This increase in DAF fluorescence represented an unexpected increase in NO production.

Targeting specific NOS isoforms with inhibitors particular to each followed, with figure 6.1.5 showing the result of 6 experiments (n=19 cells) obtained for the iNOS inhibitor, 10μM SMT, obtained in parallel with the FURA data seen earlier. Similarly to the previous DAF experiments, fluorescence initially declined before leveling out and increasing. For 10μM SMT the fluorescence nadir was reached at t=19.0 minutes (88.6%, ±1.7%. $p<0.05$ vs control minimum). However, the subsequent maximum (106.2% of start, ± 3.9% at=60) was statistically insignificant from the control data.

Attempted inhibition of the eNOS isoform with 50nM DPI during the repeat stimulation protocol (n=23) yielded results showing statistically insignificant differences from the DAF control data. Similarities in the trace obtained (figure 6.1.6) are confirmed with the endpoint maximum (108.8%, ±6.4%, *vs.* 103.9%, ±6.6% for the control), and a similar magnitude of

decline: to 72.8% (±1.3%) at 18.5 minutes compared to the decline to 79.2% (±2.5%) seen at 20.2 minutes in the control data. .

Figure 6.1.7 represents the data obtained during repeat stimulation of mouse lacrimal gland acinar cells during perfusion with the nNOS inhibitor 710nM 7NI (n=25), as outlined in the earlier protocol. The equilibrium point between DAF fluorescence decline and increase was reached significantly earlier at 6.9 minutes (and therefore significantly ($p<0.01$) higher, 97.2% (±1.1%) of start vs. control). DAF fluorescence went on to increase to a maximum of 141.9% (±5.2%) of the average initial fluorescence by t=60. This increase represents the second of the NOS inhibitors to result in a significant ($p <0.01$) increase in DAF fluorescence (and therefore NO production).

The effect of supplying mouse lacrimal gland acinar cells with a supply of the NOS substrate L-arginine (10μM) was determined for the agonist evoked change in $[Ca^{2+}]_i$ in Chapter 5.1. In fig.6.1.8 the data obtained for the DAF wavelengths is shown. The graph shows a significant ($p <0.01$) increase in DAF fluorescence, peaking at 59.9 minutes with a value of 132.9% (±6.3%) of starting fluorescence. This upturn in fluorescence began at 10.4 minutes after decreasing to only 93.2% (±6.3%) of the initial DAF fluorescence value, significantly ($p <0.01$) higher than data obtained for the control protocol. This data indicates that external supply of NOS substrate can result in an increase in NO production.

The sGC inhibitor, 10μM ODQ, was used in the previous chapter to determine whether the automatic amplification of Ca_{2+} response to agonist was modulated via cADPr. DAF data was simultaneously obtained during those experiments and are shown in figure 6.1.9. Whereas the rundown is similar to that seen in the 10μM L-arginine (to 91.9% ,±2.0%, at 10.5 minutes

$p< 0.01$) there is a dramatic increase in the DAF fluorescence read obtained, steadily increasing to 214% (±13.4), representing a significant ($p <0.01$) increase in NO production.

The data obtained for the DAF maxima and minima are summarised in the histogram in figure 6.1.10. These data indicate a change in NO production upon the use of NOS inhibitor over the period investigated, although the effects of the inhibitors are difficult to interpret.

Figure 6.1.3 Comparison of DAF fluorescence in mouse lacrimal gland acinar cells subjected to the 200nM CCh repeat stimulation protocol with unstimulated cells.

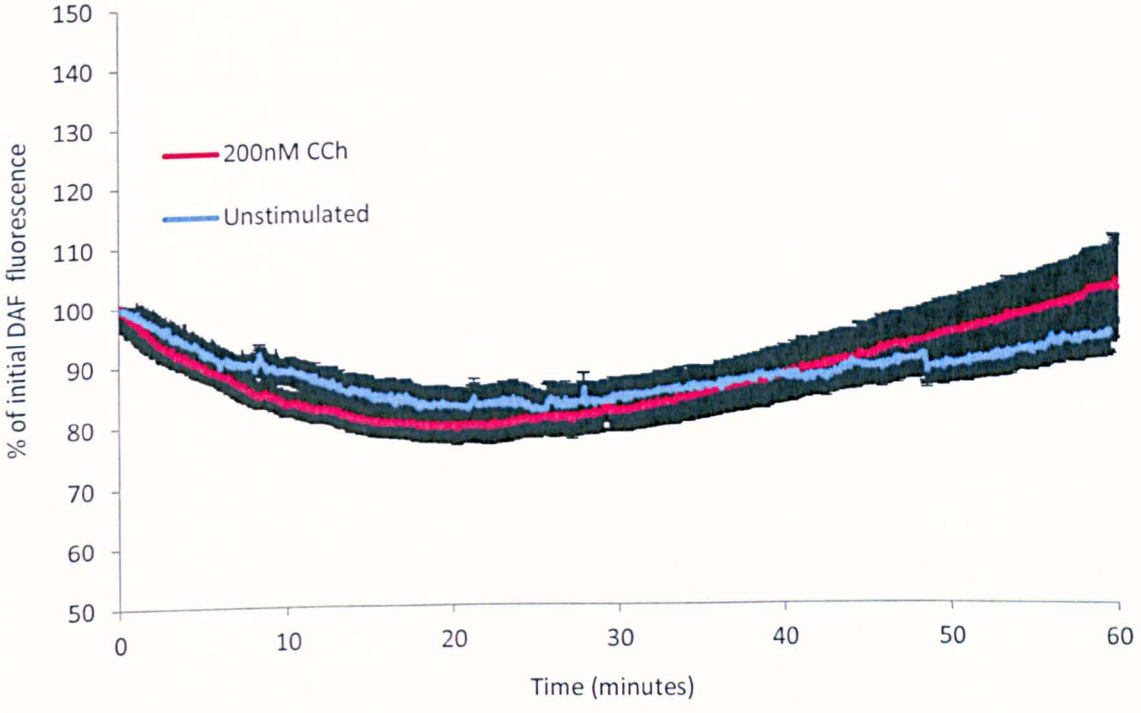

Comparison of DAF fluorescence for mouse lacrimal gland acinar cells subject to the 2 minute repeat 200nM CCh stimulation protocol (Red. n=35 cells, 8 experiments, 7 animals) with cells continuously perfused with extracellular bathing solution in the absence of agonist (Blue. n= 33cells, 8 experiments, 4 animals) Regardless of treatment, the data show a pattern of slow decline, to a minimum to 70.2% (±2.5%) of start at t=20.2 minutes (stimulated), and 82.2% (±2.6) of start at 24.8 minutes, followed by slow increase. Unstimulated cells fail to reach starting fluorescence, reaching 94.8% (±3.4%) at t=59.6 minutes, stimulated cells reach 102.8% (±6.6%) at the equivalent timepoint.

Figure 6.1.4 DAF 2 Fluorescence measured in mouse lacrimal gland acinar cells during repeat stimulations with 200nM CCh in the presence of 10μM L-NAME.

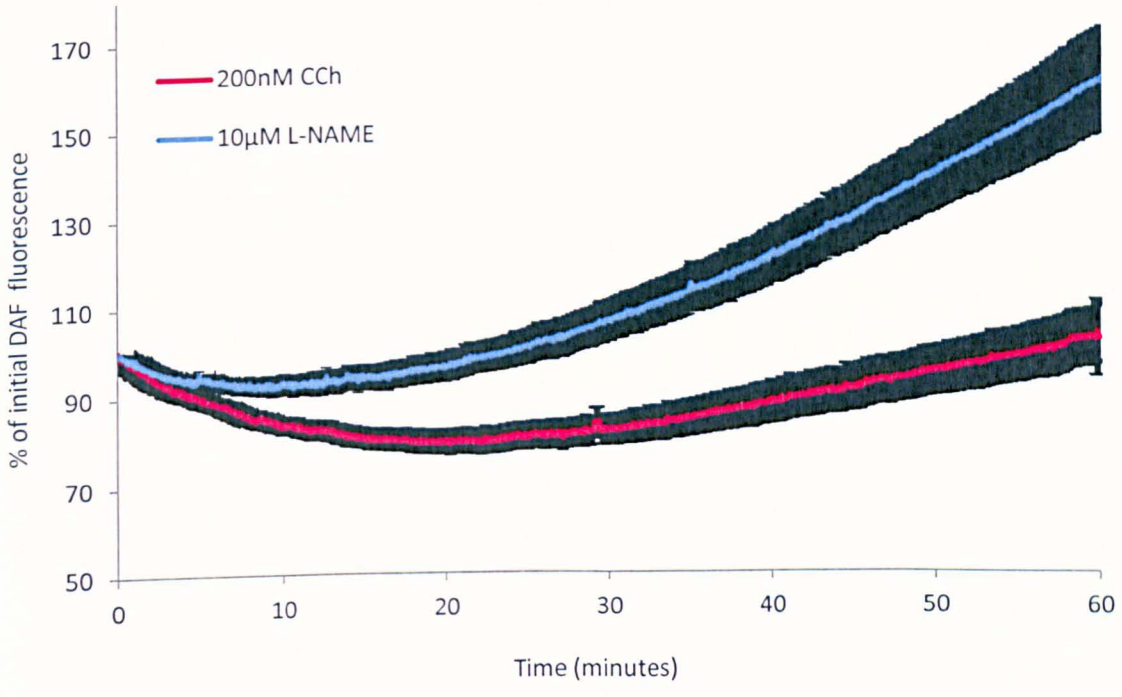

Averaged data for the DAF fluorescence measured in mouse lacrimal gland acinar cells (n=35, 6 experiments, 4 animals) undergoing the repeat 200nM CCh stimulation while exposed to the non-specific NOS inhibitor 10μM L-NAME (Blue). DAF fluorescence declined to a minimum of 92.0% (±1.7%) at 9.3 minutes before continually increasing to 161.3% (±11.7%) of initial fluorescence by the end of the experiment at t=60.

Figure 6.1.5 DAF 2 Fluorescence measured in mouse lacrimal gland acinar cells during repeat stimulations with 200nM CCh in the presence of 10µM SMT.

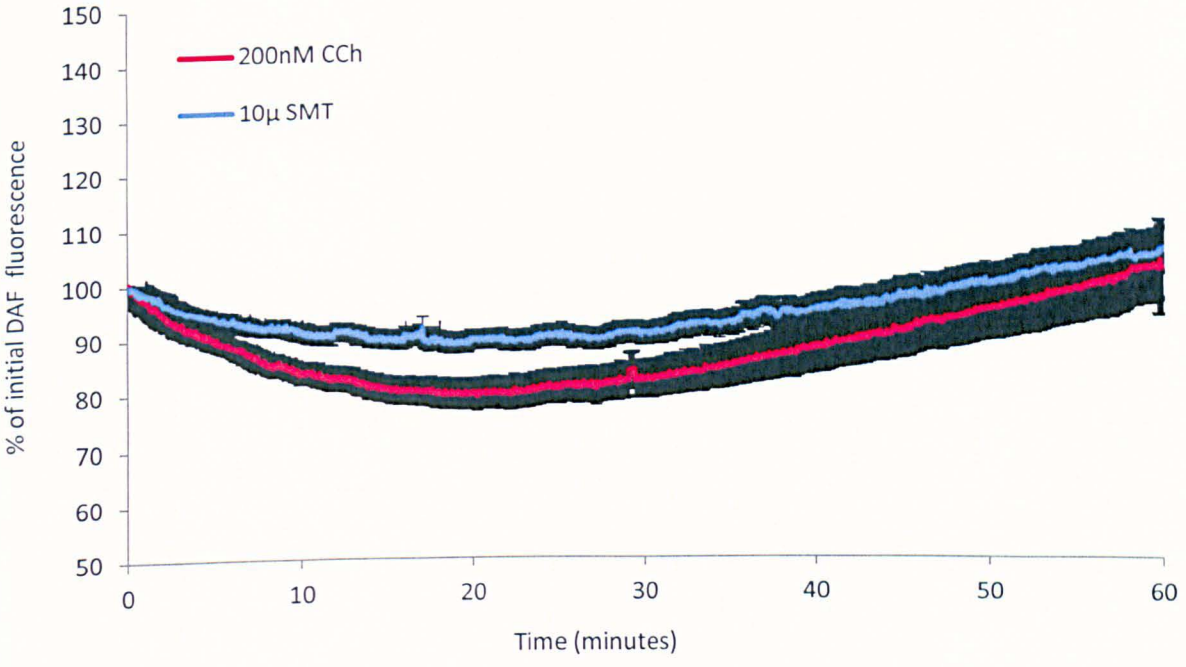

Averaged data for the DAF fluorescence measured in mouse lacrimal gland acinar cells (n=19, 6 experiments, 4 animals) undergoing the repeat 200nM CCh stimulation while exposed to the iNOS inhibitor 10µM SMT (Blue). DAF fluorescence declined to a minimum of 88.6% (±1.7%) at 19.0 minutes before continually increasing to 106.2% (±3.9%) of initial fluorescence by the end of the experiment at t=60.

Figure 6.1.6 DAF 2 Fluorescence measured in mouse lacrimal gland acinar cells during repeat stimulations with 200nM CCh in the presence of the eNOS inhibitor, 50nM DPI.

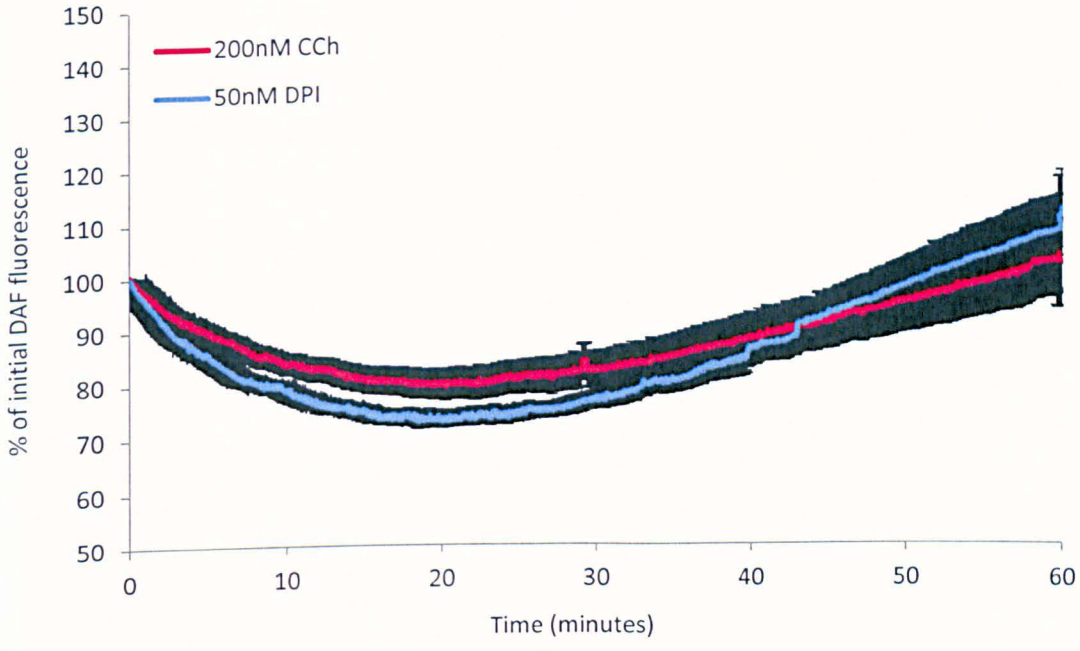

Averaged data for the DAF fluorescence measured in mouse lacrimal gland acinar cells (n=23, 5 experiments, 2 animals) undergoing the repeat 200nM CCh stimulation while exposed to the eNOS inhibitor 50nM DPI (Blue). DAF fluorescence declined to a minimum of 72.8% (±1.3%) at 18.5 minutes before continually increasing to 111.1% (±7.5%) of initial fluorescence by the end of the experiment at t=60.

Figure 6.1.7 DAF 2 Fluorescence measured in mouse lacrimal gland acinar cells during repeat stimulations with 200nM CCh in the presence of the nNOS inhibitor 710nM 7NI.

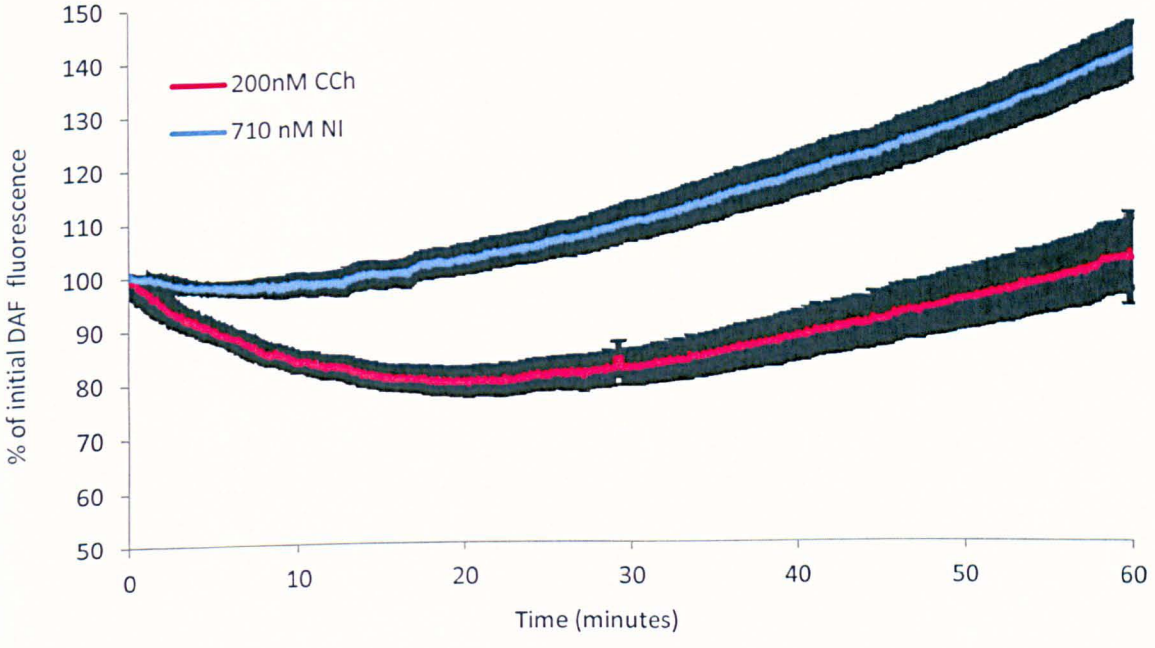

Averaged data for the DAF fluorescence measured in mouse lacrimal gland acinar cells (n=25, 10 experiments, 3 animals) undergoing the repeat 200nM CCh stimulation while exposed to the nNOS inhibitor 710nM 7NI (Blue). DAF fluorescence declined to a minimum of 97.2% (±1.1%) at 6.9 minutes before continually increasing to 142.0% (±5.2%) of initial fluorescence by the end of the experiment at t=60.

Figure 6.1.8 DAF 2 Fluorescence measured in mouse lacrimal gland acinar cells during repeat stimulations with 200nM CCh in the presence of 10µM Arginine.

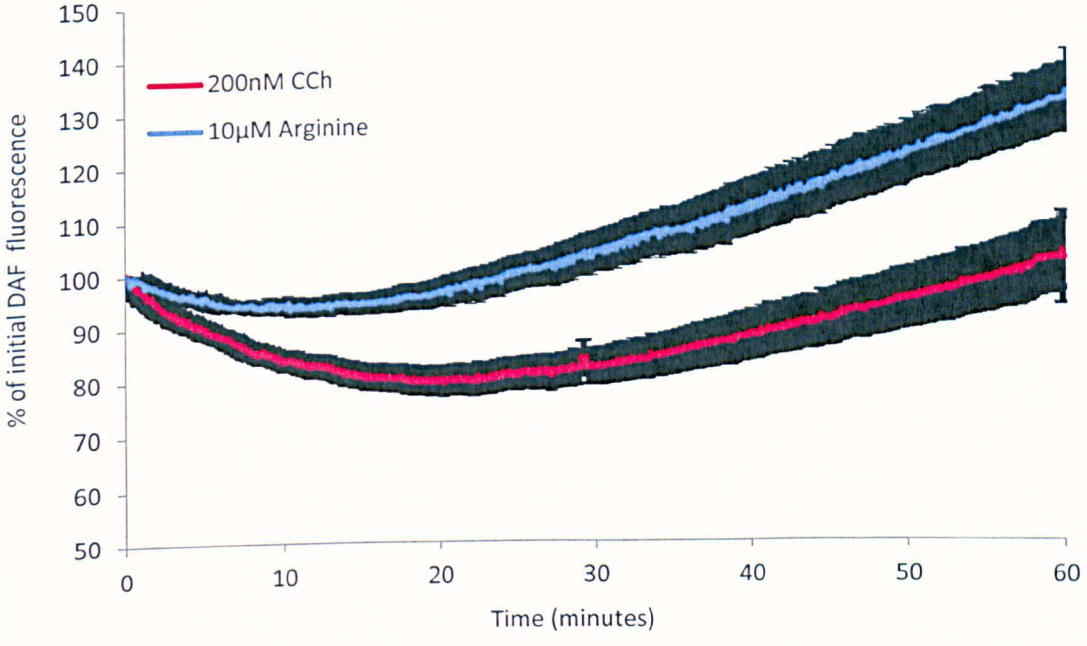

Averaged data for the DAF fluorescence measured in mouse lacrimal gland acinar cells (n= 25, 10 experiments, 3 animals) undergoing the repeat 200nM CCh stimulation while perfused with the NOS substrate 10µM L-arginine (Blue). DAF fluorescence declined to a minimum of 93.2% (±1.2%) at t=10.4 minutes before continually increasing to 132.9% (± 6.3 %) of initial fluorescence by the end of the experiment at t=59.9 minutes.

Figure 6.1.9 DAF 2 Fluorescence measured in mouse lacrimal gland acinar cells during repeat stimulations with 200nM CCh in the presence of 10μM ODQ.

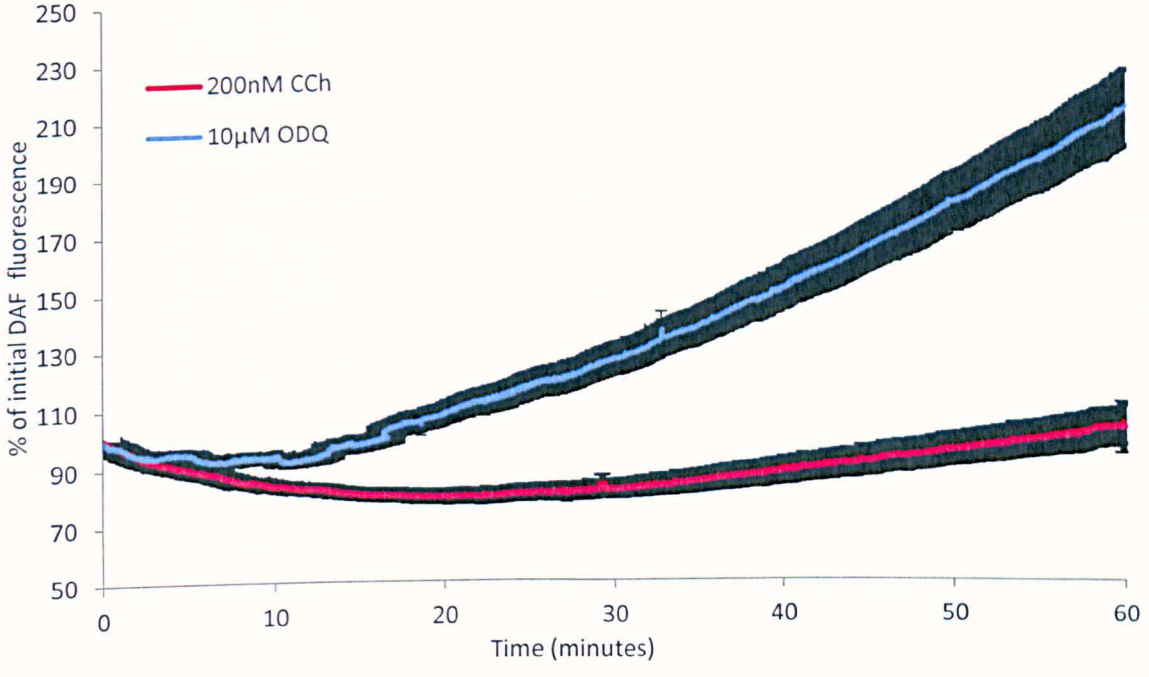

Averaged data for the DAF fluorescence measured in mouse lacrimal gland acinar cells (n= 25, 6 experiments , 4 animals) undergoing the repeat 200nM CCh stimulation while exposed to the sGC inhibitor 10μM ODQ (Blue). DAF fluorescence declined to a minimum of 91.9 % (± %) at 10.5 minutes before continually increasing to a maximum 214.6% (±13.4%) of initial fluorescence by the end of the experiment at t=60.

Figure 6.1.10 Summary of DAF-2 Fluorescence at maximum and minimum for all treatments on mouse lacrimal gland acinar cells.

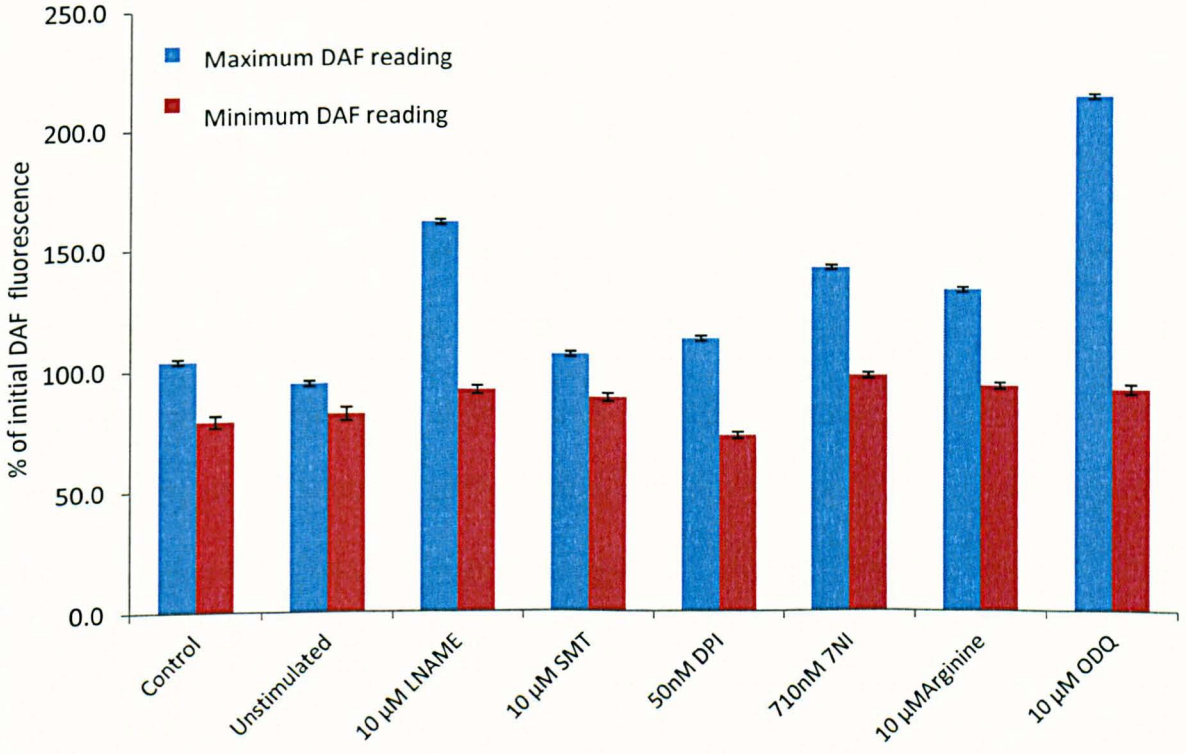

Histogram representing all data for the endpoint/maximum (Blue) and the minimum (Red) presented as percentage values of the DAF-2 fluorescence starting values of each experiment. Significant increases in DAF fluorescence were seen in L-NAME, 7NI, arginine and ODQ.($p<0.01$). The minima of SMT ($p<0.05$), L-NAME, 7NI, arginine and ODQ were also all significantly ($p<0.01$) higher than control.

Discussion

The aim of this experimental series was to directly show any change in intracellular concentration of NO using DAF microfluorimetry. It was hypothesized that the pattern of amplification and decline observed in the response to agonist in mouse lacrimal gland acinar cells was caused by endogenous production of NO.

Through DAF microfluorimetry, it was shown that mouse lacrimal gland acinar cells produce measurable endogenous NO and that this production can be modulated by the presence of NOS inhibitors (summarised in figure 6.1.10). Unexpectedly, some NOS isoform inhibition, most notably nNOS, inhibited by 7-nitroindazole (142.0% ± 5.2 of initial fluorescence) as shown in figure 6.1.7, resulted in an increase in NO production, as did exogenous supply of the NOS substrate L-arginine (figure 6.1.8) resulting in an increase to 132.9% ±6.3 of initial DAF fluorescence.

Furthermore, it was also shown that the sGC inhibitor, ODQ, whilst blocking the amplification of Ca^{2+} response to agonist (seen in chapters 4 and 5) resulted in an increase in NO production (214.6% ±13.4% of initial DAF fluorescence) shown in figure 6.1.9.

7 Results

7.1 Use of HSG as a Screening tool for Anti M3R activity in Sjögren's syndrome

Aims and objectives

Reliable detection of the anti M3R autoantibody has so far remained difficult, with the standard methods of detection failing to provide consistent results. Development of an assay based upon the anti secretory action of the anti-M3R could provide a more reliable method of detecting anti M3R autoantibodies. The primary aim of the following experiments was to ascertain whether the HSG cell line would be capable of reliably identifying anti M3R autoantibodies, and thus forming the first step towards creating a diagnostic test for anti M3R activity potentially associated with SjS.

Introduction

Despite the definition of Sjögren's syndrome as an autoimmune disorder, satisfactory demonstration of a pathogenic autoantibody has yet to be achieved. The identification of such a pathogenic autoantibody, similar to that observed in other autoimmune conditions, such as myasthenia gravis (Drachman 2003). The diagnosis of Sjögren's Syndrome currently relies upon the satisfaction of diagnostic criteria, reliant upon identification of clinical features and the results of a sequence of laboratory tests (Vitali, Bombardieri et al. 2002). This current methodology of diagnosis is expensive, time consuming and is of relatively little use to the patient, due to the current lack of treatment for the disease. Consequently, the diagnosis of Sjögren's syndrome can suffer long delay and will often only occur once the disease is well established and the damage to the salivary and lacrimal glands has already

occurred. This situation makes the development of a simple, rapid, yet accurate diagnostic test, an attractive prospect for researchers, clinicians and patients alike.

The glandular hypofunction observed in Sjögren's syndrome was previously thought to arise as a consequence of immune mediated glandular destruction (Scully 1986). However, current lines of research suggest an alternative, non apoptotic model for glandular hypofunction (Humphreys-Beher, Brayer et al. 1999; Nguyen, Brayer et al. 2000; Waterman, Gordon et al. 2000; Gordon, Bolstad et al. 2001; Fox and Stern 2002), that glandular atrophy is secondary to glandular hypofunction and that an autoimmune component is responsible for the initial glandular hypofunction (Dawson, Christmas et al. 2000; Dawson, Fox et al. 2006).

As outlined previously, glandular secretion follows the release of the neurotransmitter, acetylcholine, and the subsequent binding of ACh to the muscarinic type 3 receptor (M3R) on the acinar cell surface (Matsui, Motomura et al. 2000). It was hypothesised that putative antimuscarinic antibodies present in the IgG fraction from SjS patients may be responsible for glandular hypofunction (Bacman, Sterin-Borda et al. 1996; Dawson, Allison et al. 2004). This effect has been demonstrated, with putative antimuscarinic antibodies present in the IgG fraction from SjS patients causing a reversible inhibition of the CCh evoked Ca^{2+} in human and mouse salivary gland acinar cells (Dawson, Stanbury et al. 2006), providing the link between immune mechanism and physiological function. This represented the first demonstration of an antibody possessing a clearly defined pathological role, thus fulfilling Drachman's criteria (Drachman 1990).

Whilst this effect has been shown in isolated mouse salivary gland cells, it would be unfeasible to use this method as a screening tool due to the time and cost involved in the

preparation of the required cells. However, the use of a cultured cell line would allow for the adaptation of the protocol for the development of a cheaper, high throughput method of screening. The HSG cell line is a reasonably well characterised cell line (Patton, Pollack et al. 1991; Liu, Rojas et al. 1998; Liu, Liao et al. 2001), established from a neoplastic human salivary gland (Shirasuna, Sato et al. 1981).

Perturbation of cholinergic signalling may also be a factor in autoimmune diseases other than Sjögren's syndrome, Smith *et al* suggest that this may also be the case in narcolepsy (Smith, Jackson et al. 2004). The anticholinergic effect of a subset of antibodies associated with disease states present in more than one condition further increases the desirability of a rapid, high throughput diagnostic test.

The following sequence of experiments show the use of the HSG cell line as a model for the development of a diagnostic test for anti M3R autoantibodies as seen in Sjögren's syndrome and whether antibodies in the IgG fraction of narcolepsy patient sera can be detected using the perfusion protocol outlined in Figure 2.4.2.2 in chapter 2, methods.

Figure 7.1.1 illustrates proof of concept data, showing that the 2° perfusion system is capable of overriding the 1° perfusion flow. Also shown are the periods used to measure the effect.

Figure 7.1.2 describes a representative trace for the exposure of control IgG (1mg/ml) +10μM CCh upon HSG cells. Data were gathered for n=15 experiments using IgG isolated from the sera of healthy patients. Using the data analysis outlined in figure 7.1.1 the average test/recovery ratio, expressed as a percentage of pre vs post IgG exposure was calculated to be 134.1% (±17.3%). The fact that this ratio was above 100% indicates that the Ca^{2+} signal declined slightly over time. However, the decline observed was not caused by the presence of control IgG in the 2° perfusion, since replication of these experiments (n=5) using identical 10μM CCh solutions also showed a similar decline in response over time.

This experimental protocol was repeated for the IgG isolated from the sera of 3 Sjögren's syndrome patients. Figure 7.1.3B shows a representative trace of the effect of SjS IgG (1mg/ml) upon the agonist evoked change in $[Ca^{2+}]_i$. This experiment was repeated 9 times yielding an average test/recovery ratio of 70.1% (±11.8 %), consistently lower than the 134.1% (±17.3%) observed for the control IgG experiments representing a significant ($p<0.05$) decline in response.

Autoimmune perturbation of cholinergic signalling has been identified as a potential factor in narcolepsy. Using the same experimental protocol as for figures 7.1.1-3 to test IgG obtained from narcolepsy patients. Figure 7.1.4 shows that IgG from narcolepsy patients was at least as effective in causing reversible inhibition of the Ca^{2+} signal as was IgG from Sjögren's syndrome patients. Averaged data for 11 experiments, using IgG (1mg/ml) from 4 narcolepsy patients gave an average test/recovery ratio of 45.2% (±11.8%). This was highly

significantly different ($P < 0.01$) from the test/recovery ratio obtained for the use of IgG from control subjects.

Figure 7.1.1 The change of Fura 2 340/380nm ratio in HSG cells evoked by 10μM CCh and interruption of 1° perfusion flow by 2° perfusion system.

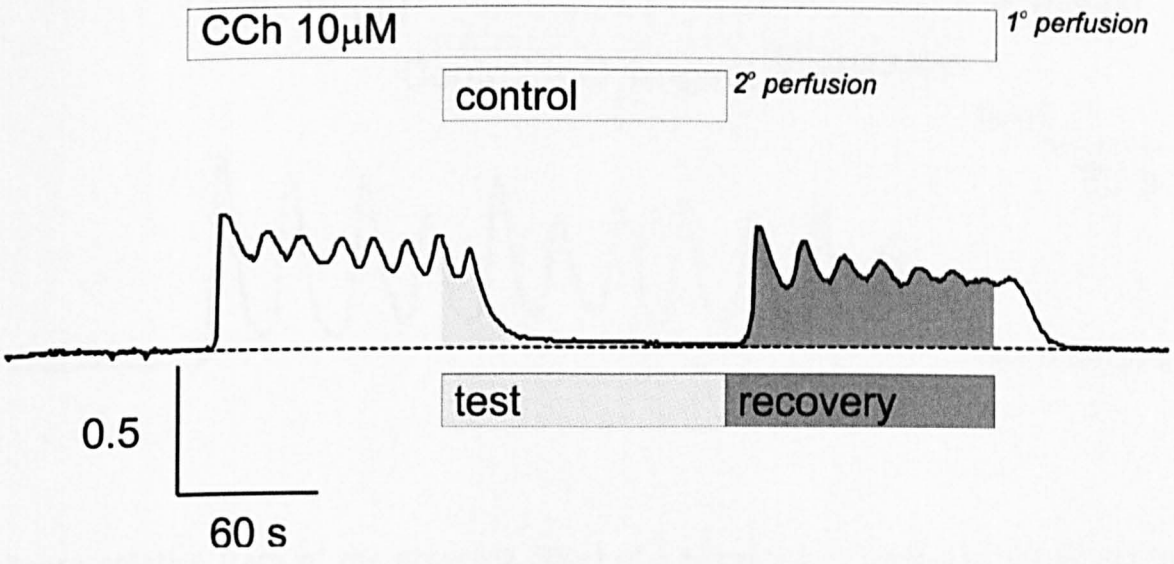

Trace represents the change in Fura 2 340/380nm wavelength ratio in a single HSG cell. Upon stimulation of the HSG cell with 10μM CCh via the 1° perfusion system this ratio increased. Upon activation, the 2° perfusion system, which did not contain CCh, overrode the flow from the 1° perfusion system was in operation for the duration of the experiment. The time period during which the 2° perfusion system was in operation was designated "test" and the subsequent period "recovery". The average ratio during each period was calculated from the area under the curve (test = light grey, recovery = dark grey) and data from the "test" period are presented as a percentage of that measured during the "recovery" period.

Figure 7.1.2 The effect of control IgG (1mg/ml) upon the 10μM evoked Ca2+ response in Fura loaded HSG cells.

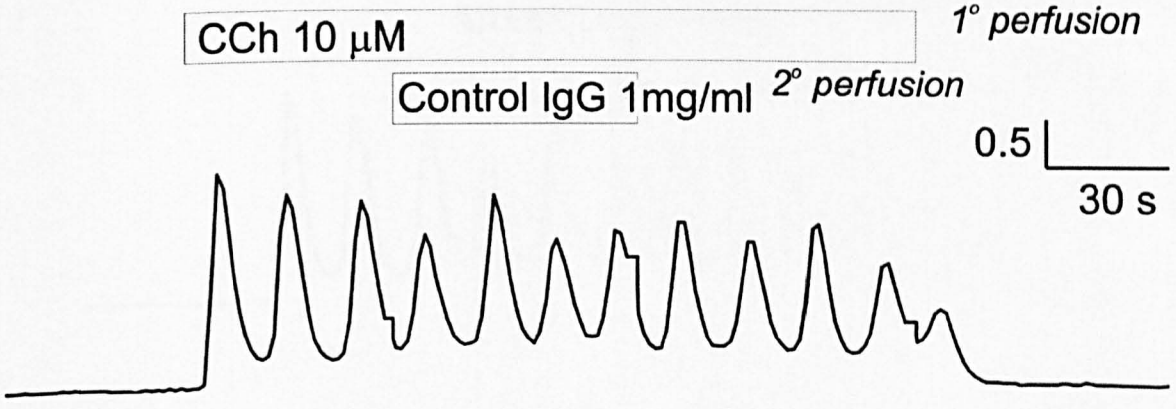

Representative trace of the observed effect of interrupting 1° perfusion 10μM CCh flow (upper bar) with solution containing control IgG (1mg/ml) and 10μM with the 2° perfusion system (lower bar) upon the Ca^{2+} response in HSG cells. The averaged data for n=15 experiments showed mean test to recovery value of 134.1% (±17.3%).

Figure 7.1.3 The effect of SjS IgG (1mg/ml) upon the 10μM evoked Ca2+ response in Fura loaded HSG cells.

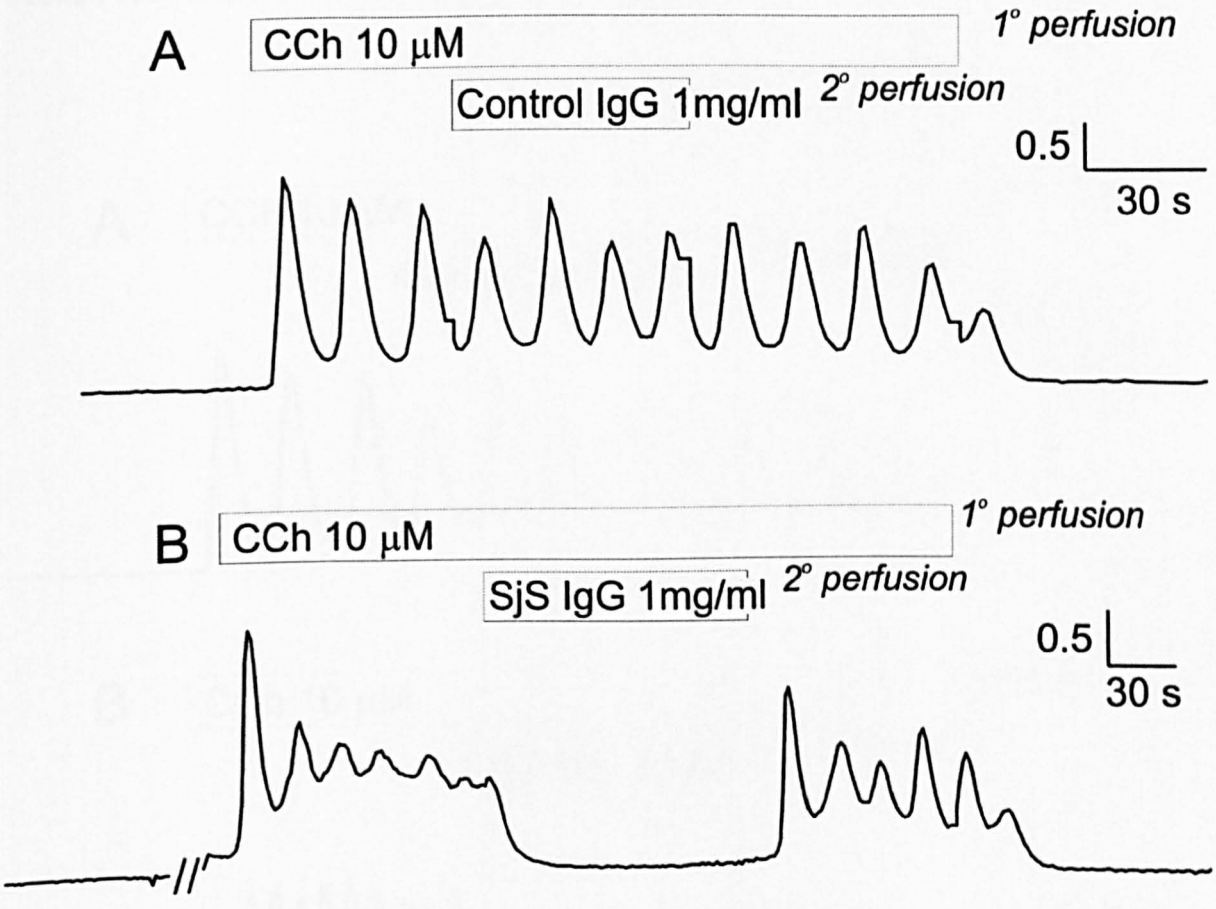

Trace A Representative trace obtained for the (1mg/ml) and 10μM with the 2° perfusion system (lower bar) upon the Ca^{2+} response in HSG cells. The averaged data for n=15 experiments showed mean test to recovery value of 134.1% (±17.3%).

Trace B shows a representative trace illustrating the effect of SjS IgG (1mg/ml) upon the 10μM CCh evoked change in $[Ca^{2+}]_i$. Averaged data for n=9 cells showed a significant ($p<0.05$) decline to a 70.1% (±11.8 %) test/recovery ratio compared to the control IgG.

.

Figure 7.1.4 The effect of IgG (1mg/ml) isolated from narcolepsy patients upon the 10μM evoked Ca2+ response in Fura loaded HSG cells.

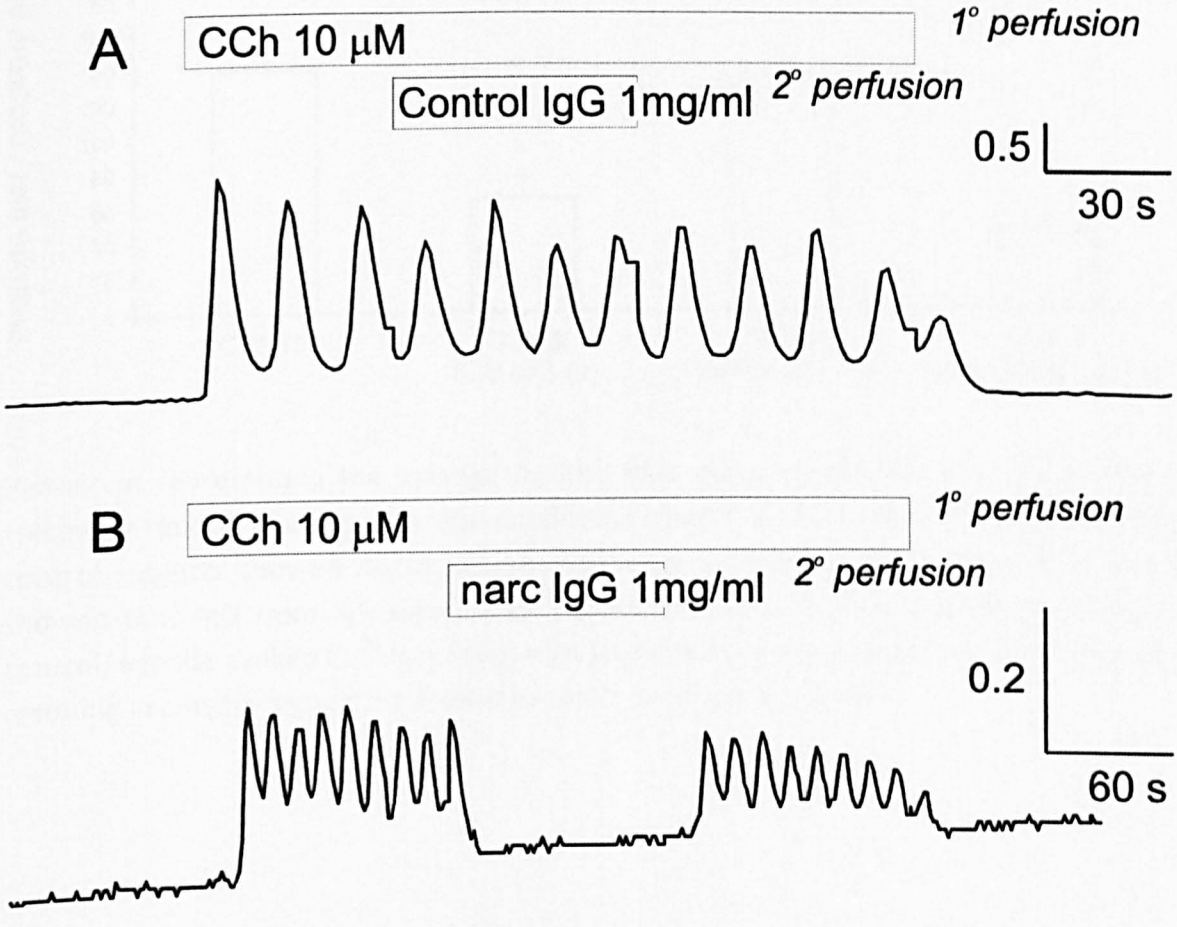

Trace A Representative trace obtained for the (1mg/ml) and 10μM with the 2° perfusion system (lower bar) upon the Ca^{2+} response in HSG cells. The averaged data for n=15 experiments showed mean test to recovery value of 134.1% (±17.3%).

Trace B demonstrates the effect of narcolepsy IgG (1mg/ml) upon the 10μM CCh evoked change in $[Ca^{2+}]_i$. Averaged data for 11 experiments, using IgG (1mg/ml) from 4 narcolepsy patients showed a significant attenuation of response, a test/recovery ratio of 45.2% (±11.8%), a significant ($P < 0.01$)decrease *vs* test/recovery ratio obtained for the use of IgG from control subjects.

Figure 7.1.5 Summary of data acquired for the test/recovery ratios for the effects of IgG upon Fura 2 fluorescence in HSG cells.

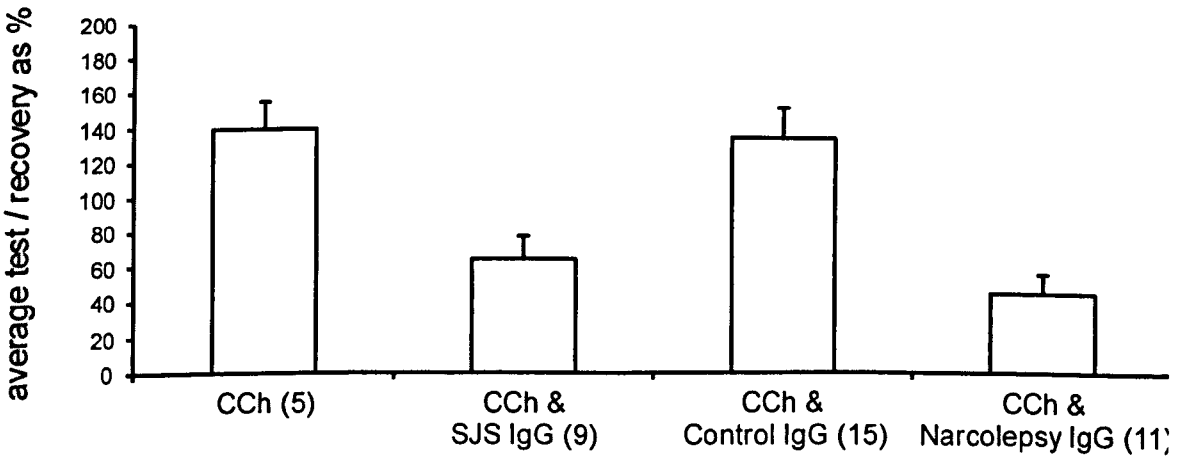

Histogram representing the average for the data acquired for the effect upon the test /recovery ratio of the experimental conditions described. Application of IgG from healthy control subjects showed no significant difference vs application of 10μM CCh. A t-test showed that IgG from SjS subjects (9 experiments) significantly decreased ($p < 0.05$ vs control) agonist evoked Ca^{2+} response, with application of narcolepsy patient derived serum resulting in a highly significant decline ($p < 0.01$) in reponse to agonist.

Discussion

Demonstration of the antimuscarinic effect of IgG derived from SjS patients is the first step in the construction of a diagnostic test for antisecretory autoantibodies. The experiments shown in this chapter represent the construction of a protocol that showed that SjS patient derived IgG serum fraction causes a significant ($p<0.05$) decrease in agonist evoked Ca^{2+} response (down to 70.1% (±11.8 %) compared to control IgG experiments (134.1% (±17.3%).

Furthermore, this protocol does not depend upon acutely isolated secretory cells from a human or model animal source, instead using the HSG model cell ine for salivary secretion. It was also shown that the hypothesised anti M3R activity of narcolepsy patient derived serum IgG fraction can be detected using the same protocol, and represented a significant decline in response (45.2% ±11.8%, $p<0.01$) compared to control (figure 7.1.5).

8 Results

8.1 High-Throughput detection of anti muscarinic autoantibodies.

Introduction

Fluid secretion is dependent upon acinar cells responding to neurotransmitter, initiating a signal cascade initiating release of intracellular calcium and consequent transport of Na and Cl ions across the cell membrane which in turn lowers osmotic potential in the gland lumen, forcing the movement of water. The Gq coupled muscarinic M3 receptor's role as an initiator of secretion, and its position on the cell surface renders it a candidate for involvement in autoantibody mediated secretory hypofunction. The neurotransmitter acetylcholine (ACh) binds to the M3R bringing about the release of the 2^{nd} messenger inositol 1,4,5 triphosphate (IP_3) which binds to ryanodine receptors on the endoplasmic reticulum, causing calcium release and subsequent calcium induced calcium release (CICR). Blockade of the M3R on the cell surface would prevent initiation of this sequence of events and therefore prevent fluid secretion. Identification of an active autoantibody in SjS would allow for a rapid screening protocol and possibly allow for earlier diagnosis of the disease, lessening the reliance upon a patient to fulfill the current criteria for SjS (Vitali, Bombardieri et al. 2002). As an autoimmune disorder, several autoantibodies have been implicated in the observed glandular dysfunction including antimuscarinic type 3 receptor autoantibodies, antibodies raised against the aquaporins, and anti Ro/ anti La.

Antibodies for the ribonuclear proteins Ro and La form part of the diagnostic criteria for the condition, showing a high (60-90%) incidence in Sjögren's patients. Antibodies for Ro and La, whilst being common in Sjögren's sufferers, are most likely a product of the disease rather than a causative agent. Ro and La are ribonuclear proteins, and therefore are usually

sequestered inside the cell, hidden from the immune system. Cell apoptosis releases cell contents and allows for antibodies to be raised against the previously hidden proteins. Whilst the full role anti Ro and anti La in the progression of the disease is currently unknown, their prevalence in sufferers renders them useful as a diagnostic marker.

Anti M3R have been demonstrated to bind to the salivary gland surface membrane and have been shown to reversibly inhibit secretion in salivary glands and cell lines. Whilst anti M3R may be prevalent in a sizeable proportion of Sjögren's sufferers, anti M3R have proven difficult to detect using standard immunological methods. The structure of the M3R is well understood, and there are data that suggest that the third extracellular loop of the M3R as being recognised by anti M3R.

Aims and objectives

The purpose of this sequence of experiments was to determine whether the anti M3 antibody activity observed in Sjögren's syndrome sufferers could be used as an aid in the diagnosis of the disease. Using the current microfluorimetry setup (see Methods) to observe this requires relatively large amounts (c. 200ul of IgG fraction) of patient serum per experimental run, time – for running the experiment, mounting cells on slides and confirmatory repeats, as well as training in microfluorimetry technique (which requires the constant presence of the operator to switch fluids and log the data correctly). These points effectively restrict the use of this method as a high throughput diagnostic tool for the screening of patient sera. The Flexstation 3 was chosen to help eliminate (or at least ameliorate) the problems associated with the microfluorimetry method, using smaller amounts of serum, the operator requiring less training, and each experimental run able to

screen up to 8 samples and yielding up to 6 repeats. Furthermore, since this system is highly automated it does not require the constant supervision by its operator.

The Flexstation 3 (and the SoftMax Pro software) provides data in a format similar to that of the microfluorimetry rig, showing data for the light emitted at 510nm after excitation at 340nm and 380nm (as per Fura 2 microfluorimetry). As with the standard microfluorimetry method, the ratio of the 510nm emission light after excitation was calculated and plotted. The data yielded was exported from SoftMax Pro (Fig 8.1.1) to a custom written Excel spreadsheet (courtesy of Dr Pete Smith) which takes the ratio of the light emitted at 510 nM after excitation by 340/380 nm, normalises to baseline and calculates the area under the curve produced at 3 key areas (fig 8.1.2): Baseline (the resting calcium level),maximum (initial response to agonist), and the effect upon the intracellular calcium concentration of the second addition (test IgG, agonist control, atropine etc.). The test value is calculated as a function of the initial response to agonist, meaning each test well acts as its own control. A mean value for each of the test treatments is obtained and presented in histogram format (fig 8.1.3). These experiments were repeated with IgG diluted to 20% of original strength to determine any dependency of anti M3R antibody activity upon IgG concentration. To help further elucidate the anti M3R status of an IgG further experiments were undertaken using a synthetic polypeptide (NTFCDSCIPKTFWN) corresponding to the 3rd extracellular loop of the M3R (Koo, 2008). The 3rd extracellular loop of the M3R has been inferred to as the target for anti M3R antibodies and therefore a polypeptide sequence corresponding to the 3rd extracellular loop should bind to the antibodies and thus prevent the inhibitory effect. This would act as confirmation of anti 3rd extracellular loop activity of the anti M3R antibodies expected in the SjS patient serum.

These experiments represent a first step into using live cells as a diagnostic tool in the high throughput, rapid screening of antibody status in sufferers of an autoimmune disease.

The techniques for collecting and analysing these data are sufficiently different from those used in the microfluorimetry experiments shown in Chapter 2.3 that the steps involved are introduced here.

Briefly

The setup of the flex station is shown in figure 8.1.1

The collection of data from single well is shown in figures 8.1.2 and 8.1.3

Normalisation and collation of data from replicates is shown in figures 8.1.4 and 8.1.5

The Flexstation protocol used records 6 replicates (1-6) of 8 different conditions (A-H), a total of 48 wells. The hardware is capable of recording twice that number of runs on a single 96 well plate, however such a protocol would double the duration of the experiment. Preliminary experiments indicated that the responsiveness of cells became more varied following a prolonged time in the flex station and therefore, to maximise consistency, only half the plate was seeded with cells.

The aim of these experiments was to measure the effect of IgG on CCh evoked signal, as a method of screening patients for anti M3R antibody activity. The measure of a diagnostic test is its ability to determine true positives (sensitivity) without incurring false negatives (specificity) The protocol was to evoke an increase in $[Ca^{2+}]_i$ and then monitor the effect of subsequent addition of IgG upon that response. A series of control experiments were

carried out in support of the test development including a) A positive (i.e. a definite decrease in response) control, consisting of 50uM (final well concentration) of the muscarinic antagonist atropine, b) a negative control where no second addition was performed and the natural rundown in response was observed, c) addition of 50uM CCh, showing the effect of the addition of solution that should have little of no effect upon the response.

As with any experiments involving whole cells, there is an inherent variability in response. This can be attributable to a number of factors including (but not limited to): the availability of agonist to the cell, subculture/ passage number, at what point any cell is at in the cell cycle etc. Cell density on the plate is not a factor in this case, since Fura 2 –AM is a ratiometric dye, and any drop in cell density will affect only the intensity of light emitted, not the ratio. Therefore, in an attempt to counter the natural variability in response, each resulting trace is normalised to the peak of CCh evoked response. This allows for the observation of the effect of the 2^{nd} addition seen against constant background. Unfortunately, the peak response seen upon the addition of CCh is not maintained, and suffers from a gradual rundown, potentially confusing an actual IgG effected decrease in response with that of the natural rundown. Additional experiments were carried out to identify a protocol which resulted in a sustainable maximum response rather than gradual decline. After experimenting with a variety of loading protocols (loading times, dye concentration, presence/ absence of loading facilitators) and cells (HSG, SHSY5Y, HEK-M3, CHO-M3), a protocol was finally determined that allowed for good dye loading, reproducible response and minimal decline in response over time.

Serum samples were collected from 9 healthy control donors and processed as per the IgG extraction protocol outlined in the methods. This was repeated for a cohort of Sjogren's syndrome sufferers (n=27) and the IgG concentration determined by BCA assay to be 1995.4 μmg/ml (± 108.7μmg/ml) for the SjS derived IgG and ±1335.7μmg/ml (±169μmg/ml) for the control group.

Figure 8.1.5 shows the mean results obtained from a single experimental run.

These IgG solutions were used to measure the effect of patient derived IgG upon the change in $[Ca^{2+}]_i$ evoked by 50 μM CCh. Figure 8.1.6 shows the averaged results obtained for the test period for each single patient IgG *vs.* the pooled group of control, presented as a percentage value of the "maximum" response. As the histogram shows, the effect was highly variable. Of the 27 SjS IgG samples tested, 5 showed statistically significant decreases in response. IgG NCL-007-1-S3 (n=21) showed the most pronounced negative effect upon the Ca^{2+} response, with an averaged test of 27.0% (±9.1%) of initial stimulation, significantly ($p<0.01$) below that of the 61.2% (±2.3%) remaining response for the pooled control IgG averages. IgG samples NCL-011-1-S6 (46.3%, ±3.5%, n=39), NCL-006-1-S6 (47.5%, ±3.5%, n=37), NCL-018-1-S6 (49.1%, ±3.9%, n=20) and NCL-009-1-S3 (50.0%, ±3.8%, n=42) also recorded significant ($p< 0.01$) diminution of agonist evoked response. 11/27 IgGs showed decline (although not statistically significant) in response. The remaining 10/27 IgG samples showed a test level of response to agonist above that of the control IgG, although not to a statistically significant degree. Since the Flexstation has no fluid removal apparatus, the final IgG concentration in the test well is diluted. This results in a final IgG concentration for this series of experiments of 399.1 μg/ml (±21.7) and 267.2 μg/ml (±32.6) for patient and control IgG respectively.

The average pooled response for control IgG, SjS IgG and related controls are shown in figure 8.1.7. As in figure .8.1.6, results are presented as the percentage of the "maximum" response remaining during the "test" period. Application of 50μM CCh as the test solution showed a decline to 67.7% (± 1.1% ,n= 375) of the initial "maximum". This decline is due to the rundown in response of the HSG cells over time. The inclusion of 50μM atropine in the test solution (n=58) resulted in a near complete ablation of agonist evoked change in $[Ca^{2+}]_i$, responding at only 1.3% (±2.6). Pooled results for all the SjS patient derived IgG (n=479), showed a mean test response of 55.1% (±0.9%). Compared to the pooled control IgG results, this represents a significant ($p < 0.01$) drop in muscarinic agonist evoked response in HSG cells.

To measure the dependency of the putative anti-muscarinic effect of SjS patient derived IgG a series of experiments were performed using the previous supplied IgG at a 20% dilution. Figure 8.1.8 shows the averaged results obtained for the test period for each single patient IgG vs the pooled group of control, with a final IgG concentration in the well at 79.8 μg/ml (±4.34) and 53.4 μg/ml (±6.5) for control and patient IgG respectively. At 20% of the initial IgG concentration 5/27 of the SjS derived IgG samples resulted in a significant decline of Ca^{2+} response compared to the 20% concentration IgG pooled data (72.3%, ±1.7, n= 128): IgGs NCL-009-1-S3(63.8%,± 3.8%, n=24), NCL-007-1-S3 (60.6%,± 3.4%, n=11) ($p< 0.05$), NCL-011-1-S6 (58.7%,± 4.3%, n=21), NCL-017-1-S6 (61.3%,± 3.2%, n=22), and NCL-019-1-S6 (52.0%,± 4.8%, n=13) ($p<0.01$). 12 SjS IgGs showed a decline in HSG response (although not significant), with the remaining 10 showing equal or greater response to agonist *vs.* control (not significant).

The averaged pooled response for the low concentration sequence are shown in Figure 8.1.9, in direct comparison with the previous high concentration pooled results. The effect of the low concentration SjS IgG vs the low concentration control IgG was also significant ($p<0.01$) The response observed in the cells exposed to control IgG was 72.6% (±1.7%) in the low concentration, compared to 61.2% (±1.9%) in the high. This difference was seen to be a significant ($p< 0.01$) dose dependent effect. The low dose control IgG was also significantly ($p<0.05$) lower than the 50μM CCh application. Comparing the two SjS IgG concentrations indicated that the difference in magnitude of the decline induced by the IgG (100% conc vs 20% conc) was also of significance ($p<0.01$).

Figure 8.1.10 represents pooled mean data for discerning any effect of 24 hour pre-incubation of putative anti M3R with a linear synthetic polypeptide corresponding to the 2nd extracellular loop of the M3R. As is shown by the histogram in figure 8.1.10, the presence of the 10μM of the synthetic polypeptide (pp) had a detrimental effect upon the Ca^{2+} response evoked by 50μM CCh. In the presence of the polypeptide, response to 50μM CCh itself dropped from 67.7% (±1.0% n=375) to 58.8% (±1.9% n=137). This 8.9% decrease in response was found by two tailed ttest to be statistically significant ($p<0.01$). For all treatments in the presence of the polypeptide, there was a decrease in response, but only statistically significant in high dose SjS IgG (n= 479 without pp, n=176 with pp. 9.8% response difference $p<0.01$), and low dose control IgG (n= 128 without pp, n=11 with pp. 15.2% response difference).

Figure 8.1.1 The Softmax Pro run screen.

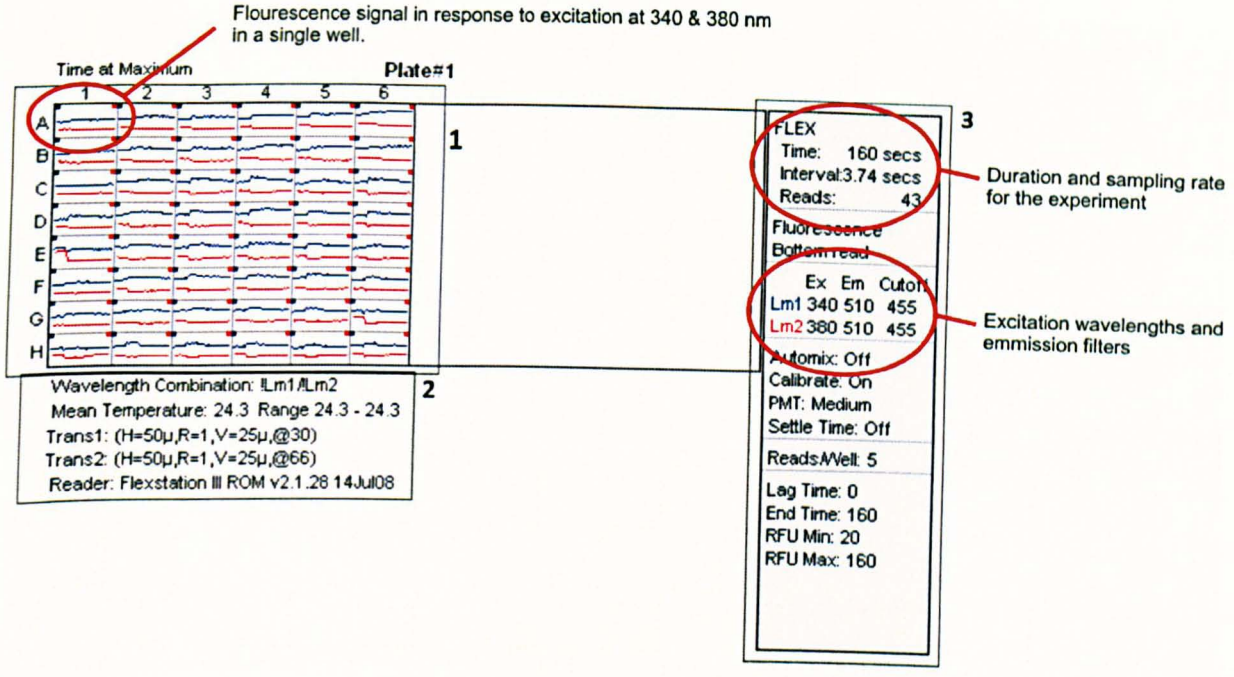

A-H being the different test solutions in question and 1-6 being experimental repeats. While a 96 well plate has 12 columns of wells, only 6 were used per run, to minimise deterioration of the cells over the duration of the experiment.

Experimental protocol details. Shown are wavelengths read, temperature at which the experiment was run and fluid transfer details (H=pipette height, R= fluid transfer rate, V= volume, @XX= time at which fluid transfer occurred (s).

Further experimental protocol details (Time= experimental runtime, Interval= time between each read of each well, Reads= No. of reads).

Figure 8.1.2 Fura wavelengths measured during the course of a Flexstation experimental run.

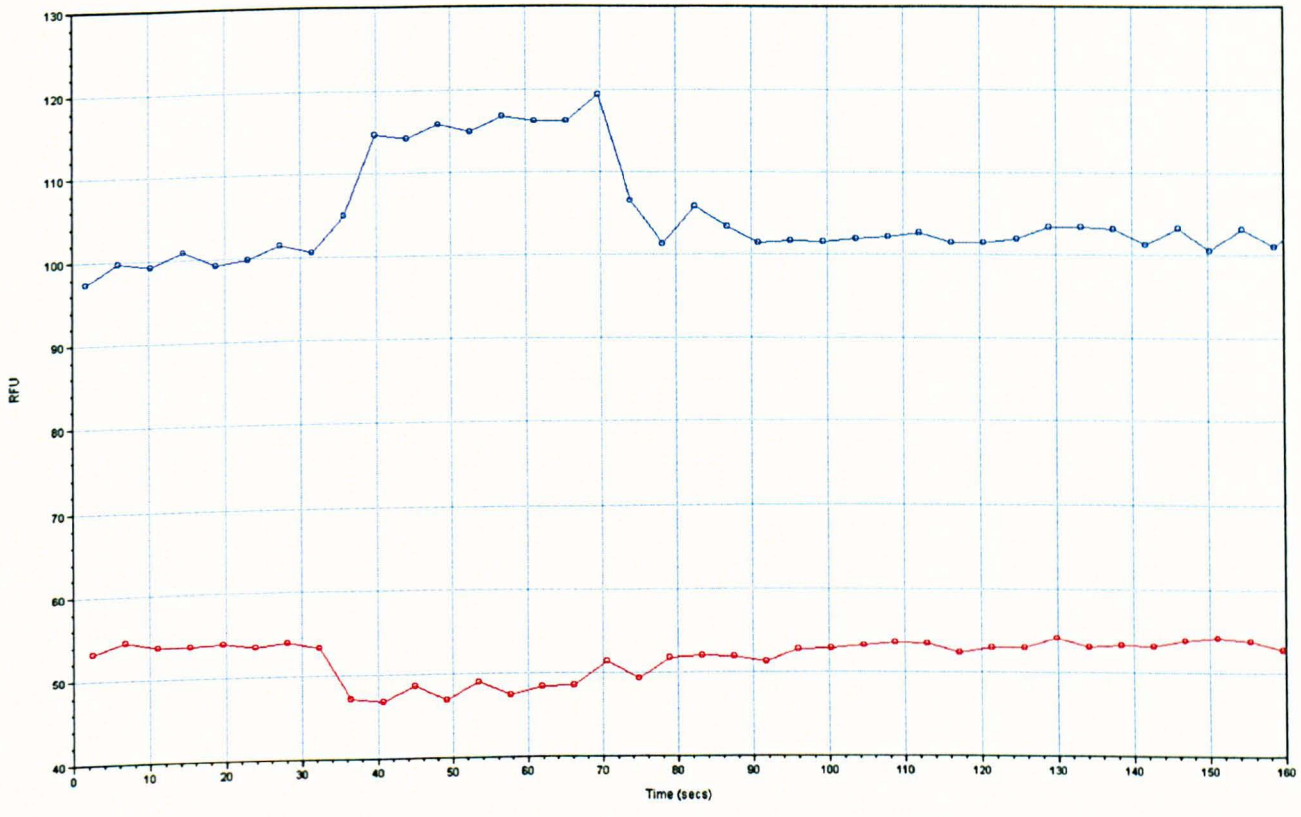

Expanded view of trace H2 as seen in fig 8.1.1. The upper (Blue) line represents light emitted by Fura 2 at 510 nm after excitation at 340nm. The lower (Red) line represents the emitted by Fura 2 at 510 nm after excitation at 380nm. The data represented by the upper trace are divided by that in the lower to give a ratiometric trace that represents changes in intracellular calcium concentration.

Fig 8.1.3 Fura 2 emitted light ratio obtained for a single well.

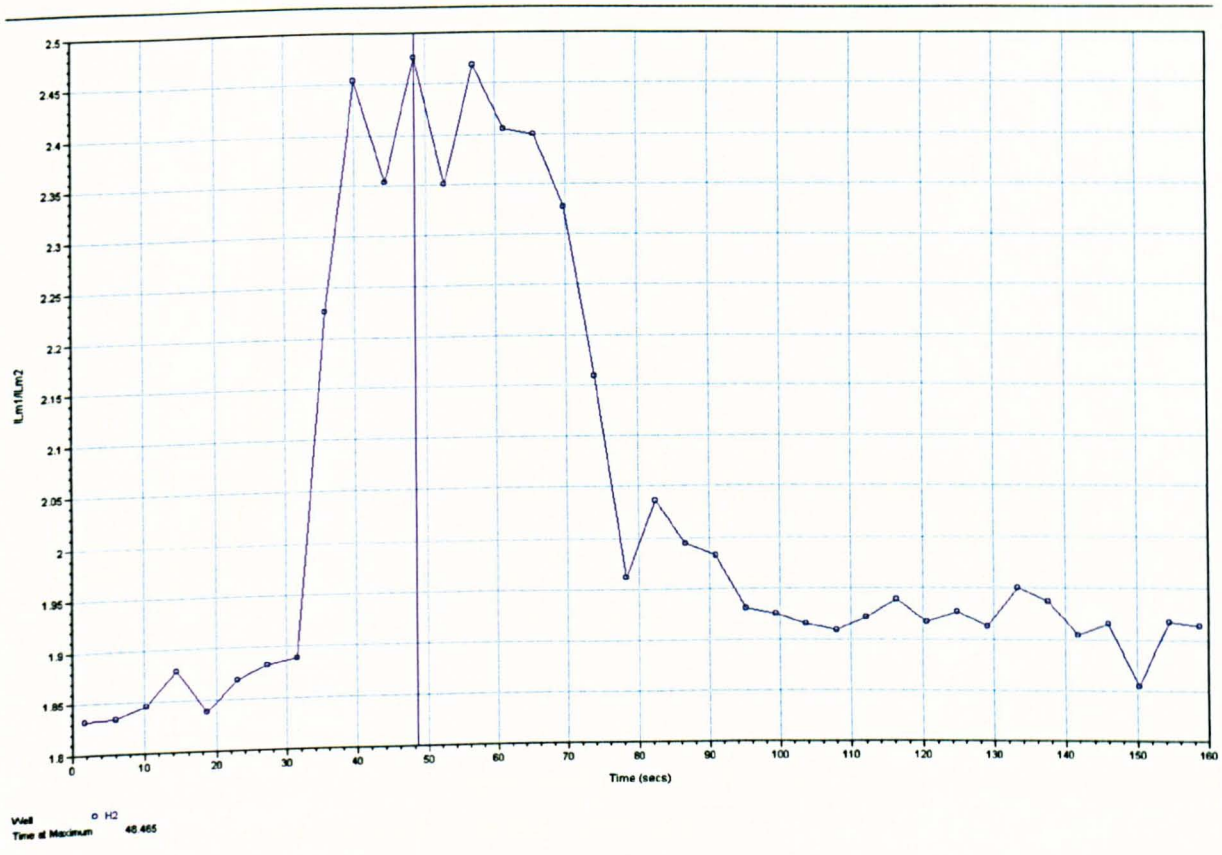

Ratiometric trace of the single well H2 (see Fig 8.1.1). This represents the ratio of light emitted at 510 nm after excitation at 340 and 380nM and is a direct correlation to the changes in $[Ca^{2+}]_i$. (From Softmax Pro software)

Figure 8.1.4 Calculation of the effect of second addition solution upon $[Ca^{2+}]_i$.

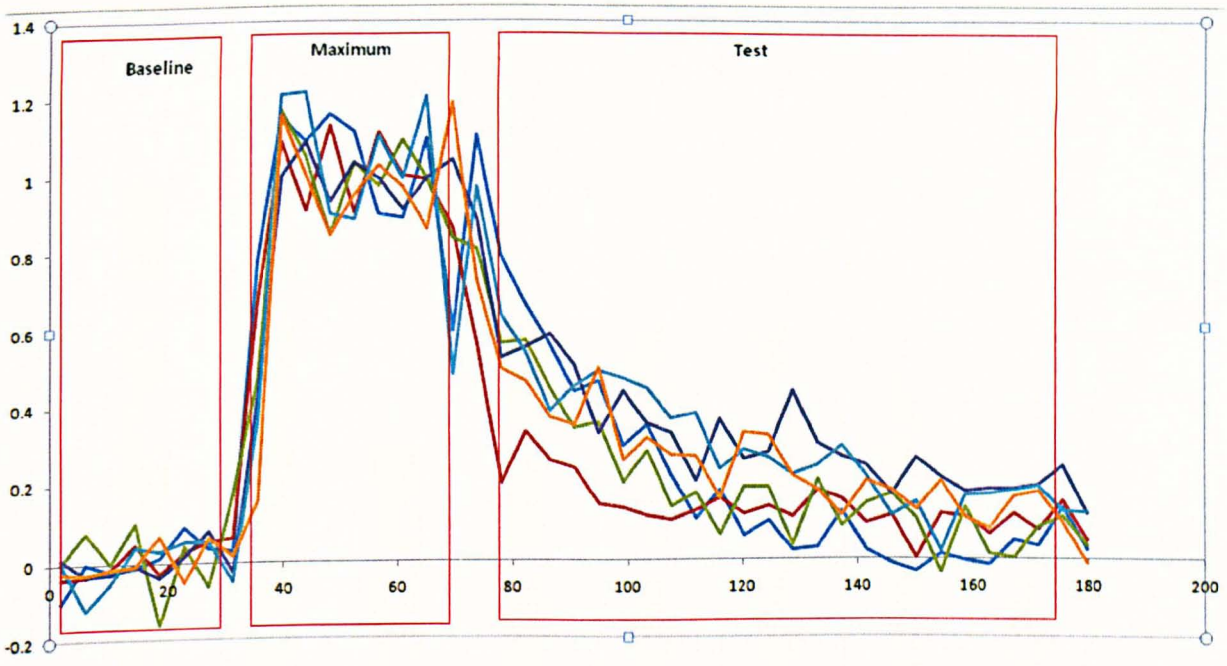

The resulting traces are normalised to baseline and show the result of the introduction of agonist (50uM CCh) - a rapid increase and plateau, followed by the test solution (in this case, a solution containing 50uM CCh and 50uM atropine).

Fig 8.1.5 Net output of a single Flexstation experiment run showing the averaged result for each treatment (n= 6 wells).

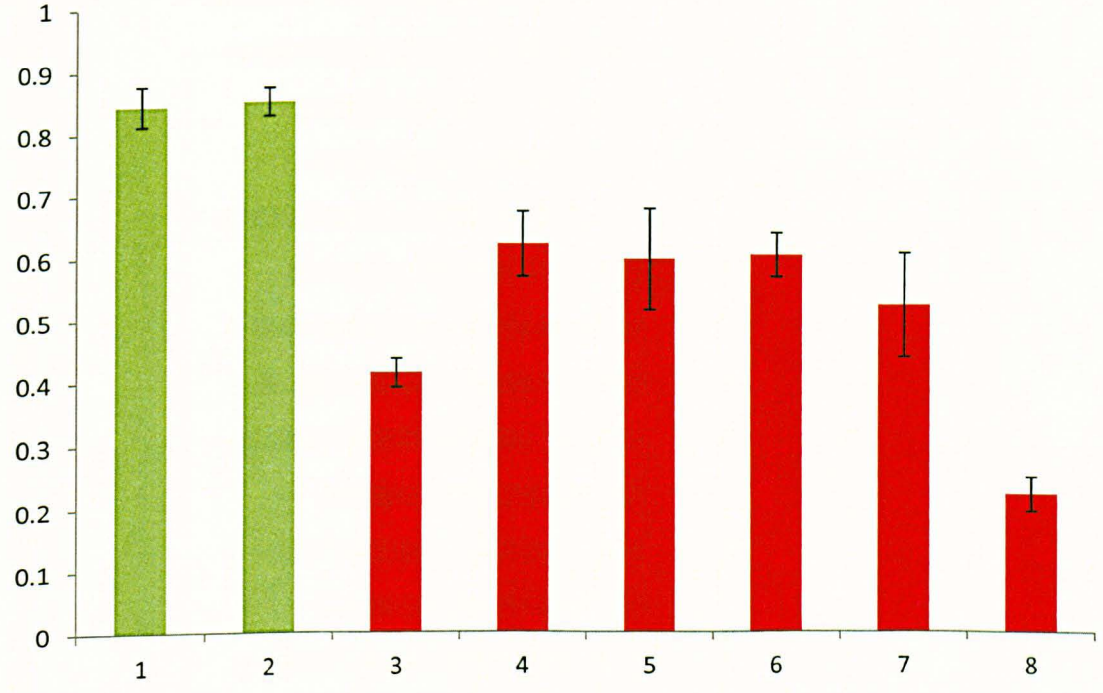

Each well's result is represented as a ratio of post treatment $[Ca^{2+}]_i$ vs. pre treatment $[Ca^{2+}]_i$.(1) and (2) : 50uM CCh, (3) IgG NCL-012-1-S6+50µM CCh, (4) IgG NCL-011-1-S6+50µM CCh, (5) IgG NCL-017-1-S6+50µM CCh, (6) IgG NCL-009-1-S3+50µM CCh, (7) IgG NCL-006-1-S6+50µM CCh and (8) 50uM CCh + 50µM atropine

Figure 8.1.6 Change in $[Ca^{2+}]i$ in the HSG cell line in response to 50uM CCh in the presence of IgG isolated from Sjögren's Syndrome patient and healthy control group sera.

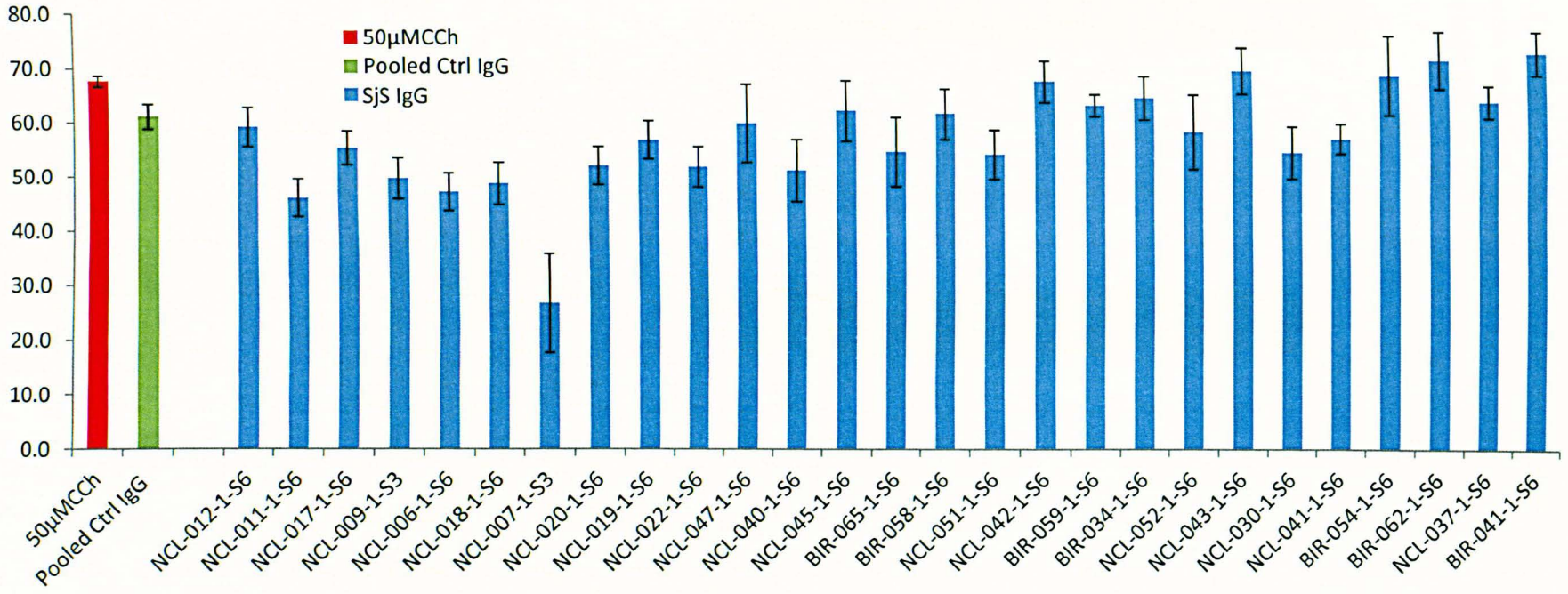

Histogram showing the mean effect of human serum IgG isolate from a control group (267 µg/ml +/- 33µg/ml) and IgG isolated from Sjögren's syndrome patients (399 µg/ml +/-22) upon the $[Ca^{2+}]_i$ evoked by 50µM CCh.

Figure 8.1.7 Changes in [Ca2+]i in the HSG cell line in response to 50uM CCh. The mean test response observed during application of 50µM CCh, non-SjS control IgG and SjS patient derived IgG.

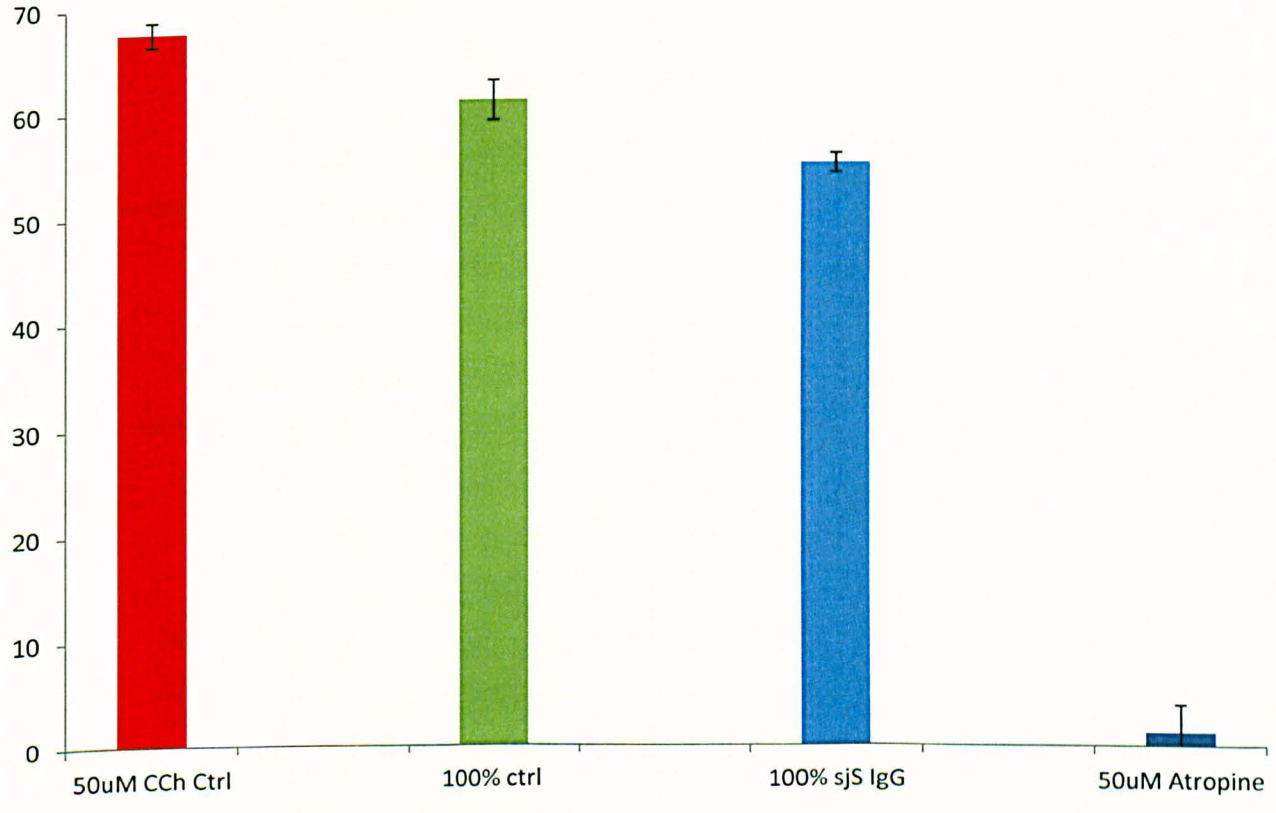

Mean response obtained for all treatments. 50µM CCh only 67.7% (± 1.1%, n= 375),Control IgG+ 50µM CCh6 1.2 (±1.9%, n=114), SjS IgG + 50µM CCh 55.1%(±0.9% n=479), and 50µM atropine 50µM CCh 1.3% (±2.6 n=58). Data represented as a percentage of "maximum" response as per protocol. Comparing the SjS IgG to Ctrl IgG, the decline in response observed in the SjS IgG treated cells is significantly (t-test p= <0.01) greater than seen in the control IgG. However, a significant (p= <0.01) decline in response is also seen in the control IgG treated cells when compared to the 50µM CCh only control runs.

Fig 8.1.8 The effect of dilution of the Control and Subject IgG upon the change in $[Ca^{2+}]_i$ response to 50uM CCh in the HSG cell line.

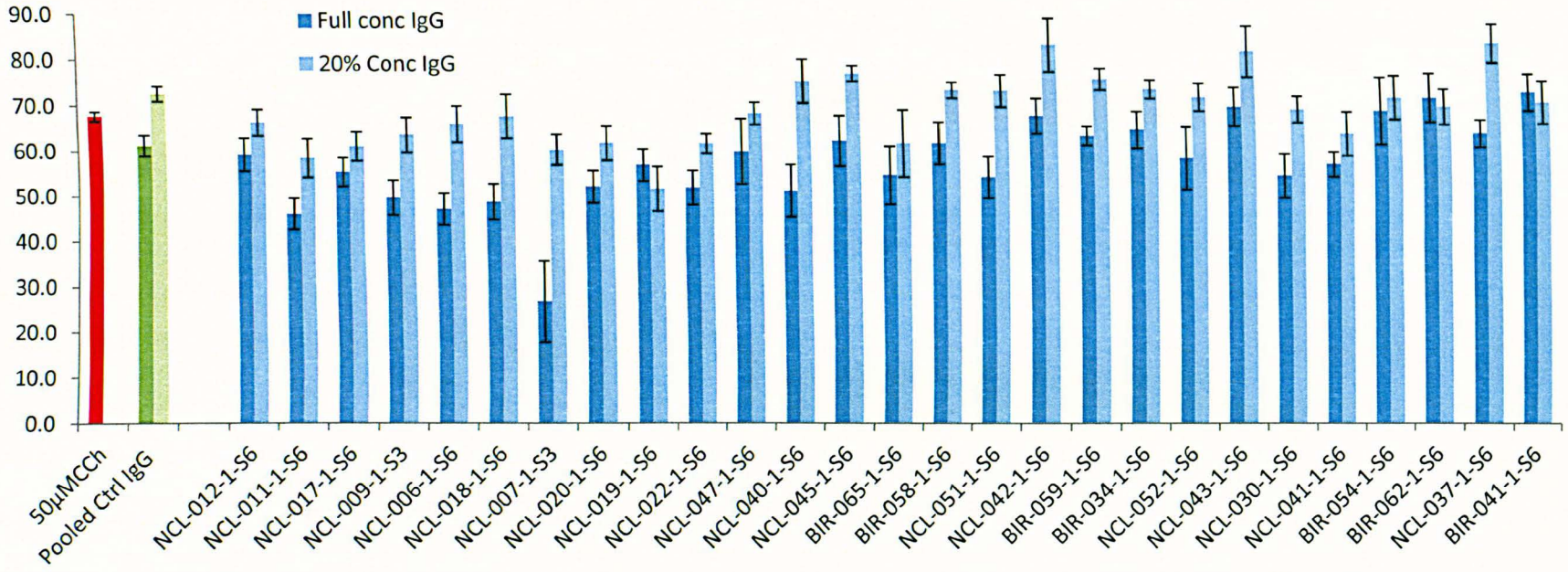

Histogram showing the mean effect of human serum IgG isolate from a control group (54 μg/ml +/- 6.6) and IgG isolate from Sjögren's syndrome patients (80 μg/ml +/-4.4) upon the $[Ca^{2+}]_i$ evoked by 50μM CCh

Fig 8.1.9 Changes in $[Ca^{2+}]_i$ in the HSG cell line in response to 50uM CCh. The mean test response observed during application of 50µM CCh, non-SjS control IgG and SjS patient derived IgG and comparison of dose dependency upon response.

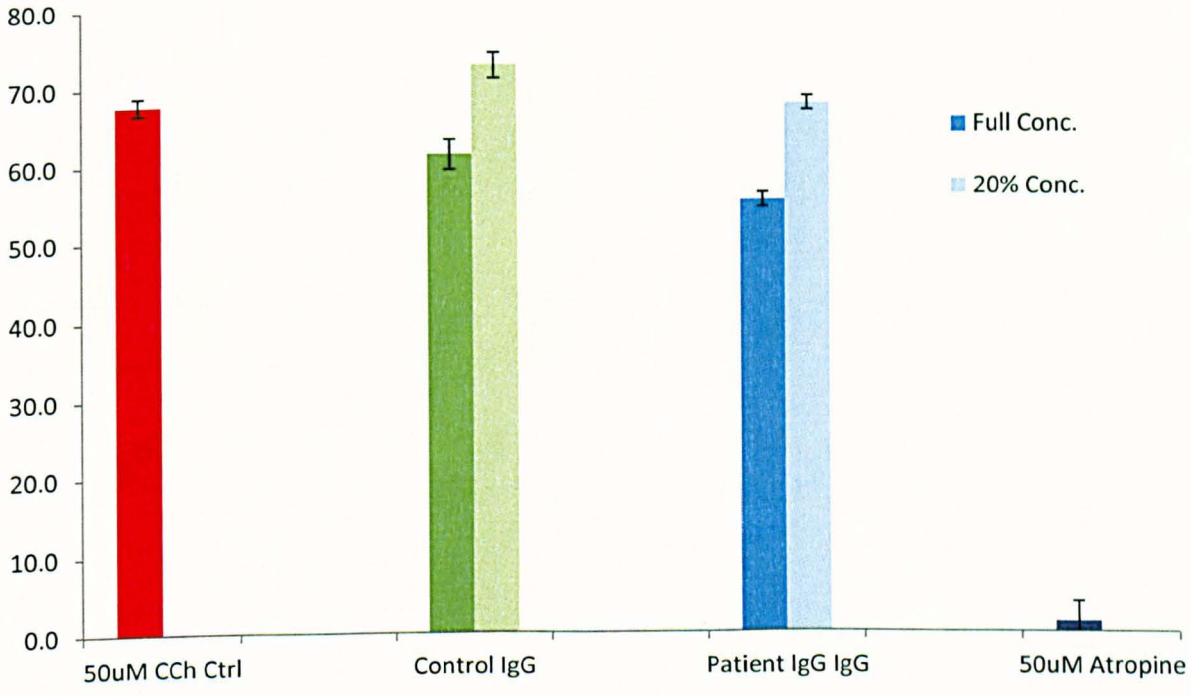

Mean response obtained for all treatments. 50µM CCh only 67.7% (± 1.1% ,n= 375),Control IgG+ 50µM CCh6 1.2 (±1.9%, n=114), SjS IgG + 50µM CCh 55.1%(±0.9% n=479), and 50µM atropine 50µM CCh 1.3% (±2.6 n=58). Data represented as a percentage of "maximum" response as per protocol.

Fig 8.1.10 Change in $[Ca^{2+}]_i$ in the HSG cell line in response to 50uM CCh in the presence of serum IgG fraction from Sjögren's Syndrome patients and a non SjS control group preincubated (24hours) with 10µM synthetic M3R 3rd extracellular loop polypeptide.

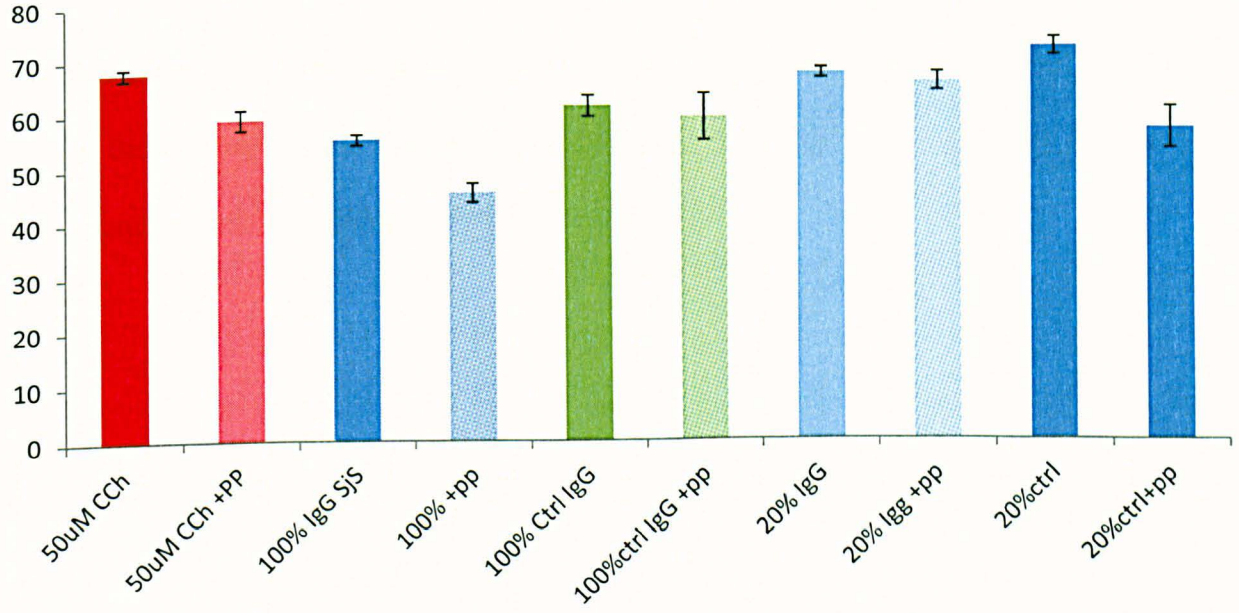

Average responses obtained for all treatments (50µM CCh in the presence/ absence of SjS IgG, Control IgG and 3rd extracellular loop polypeptide (pp)), representing the mean remaining percentage response of the "maximum" during the "test" phase.

Results in this format tell us that the addition of the IgG fraction is having an effect upon the agonist evoked calcium response, and even suggest which IgG's are more effective. For a diagnostic test to be successful it needs to be able to correctly identify actual positives for IgG action (Sensitivity), yet also be able to correctly identify negatives (Specificity). To measure the success of the putative diagnostic test, a graphical representation of how sensitive and specific was yielded by ROC curve analysis.

8.2 ROC Analysis of Sjogren's syndrome derived IgG vs. a healthy Control IgG.

The demonstration that IgG derived from SjS patients may enable the development of a rapid screening protocol for the detection of autoantibodies in SjS using a cell line. For such a test to be viable, it must be shown that A) autoantibodies should be detectable in sufferers, and B), autoantibodies should not detectable in non sufferers, i.e. the test must have both high sensitivity and high specificity.

ROC (Receiver-Operating Characteristic) curves are a statistical tool for the evaluation of a diagnostic test, providing an accurate demonstration of a test's ability to distinguish between two states: in this case, anti M3R activity (or lack thereof) of the IgG fraction of test subject sera. ROC curves plot Sensitivity (or True Positive Rate) against 1-Specificity (or False Positive Rate). The more accurate the test, the closer the curve will be to the upper left hand corner (or coordinate 0, 1; which represents 100% sensitivity and 100% specificity) of the plot area. A perfect test would give an area under the curve (AUC) result of 1.0, whilst a test showing no more than random variation will follow the left-to-right diagonal and give an AUC score of 0.5. This curve generates a range of cutoff values for test results indicating sensitivity and specificity values.

Using the Flexstation experimental protocol this would be the "test" percentage value that would determine whether a sample, based upon response to agonist, could be classed as coming from a sufferer.

ROC analysis was carried out on the previously collected data from the Flexstation IgG testing protocol and analysed with the SPSS 19 statistical software package.

Figure 8.2.1 shows proof of concept data, with the control addition containing 50μM CCh, representing the negative control, and the muscarinic antagonist atropine (50μM) being present in the test addition to provide an anti M3R effect. This curve is a near perfect discriminator between the decline in response shown in the "test "phase of 50μM CCh control and the decline shown upon addition of 50μM atropine, generating an area under the curve of near 1 (.985). The curve also generates the range of cutoff values for the determination of "disease" state.

Positive if <=	Sensitivity	1 - Specificity
29.86	0.9653	0.0345
30.52	0.9653	0.0172
31.00	0.9627	0.0172
31.86	0.9627	0.0000
33.17	0.9600	0.0000

Using the atropine as a simulation of positive action of anti M3R activity, taking these results as the basis of diagnosis, setting a cutoff value of 29.86% and above would determine that any unknown sample would be correctly detected 96.5% of the time whilst falsely giving a positive reading 3.5% of the time. A better cutoff point would, in this case, be 31.86% activity. This cutoff would correctly detect anti secretory activity 96.3% of the time whilst being 100% specific.

ROC analysis of the IgG moderated Ca^{2+} response to 50uM CCh in HSG cells is shown in figure 8.2.2. The AUC recorded for the high dose patient IgG vs CCh was 0.731 (95% CI, .647-.814).

Table 8.2.1 Generation of cut off values in ROC analysis

Cut off	Sensitivity	1-specificity
.6095	.604	.290
.6338	.703	.323
.6389	.723	.323

From the ROC analysis, it may be seen in the table above, that a cut off point of 0.6095 provides a sensitivity of approximately 60% and a selectivity of 71%.

The ROC analysis was repeated for the IgG obtained from the serum of control subjects. These data are shown in figure 8.2.3.

This analysis returns an AUC of 0. 630 (95%CI .496-.765). It should be noted that these data are not significantly different form a value of 0.5 which represents the line of non-discrimination, in other words the IgG from control subjects did not consistently reduce the response to CCh below that seen under control conditions.

Fig 8.2.1 ROC Analysis of the 50µM CCh control addition against 50µM CCh control addition in the presence of 50µ M of the muscarinic antagonist atropine.

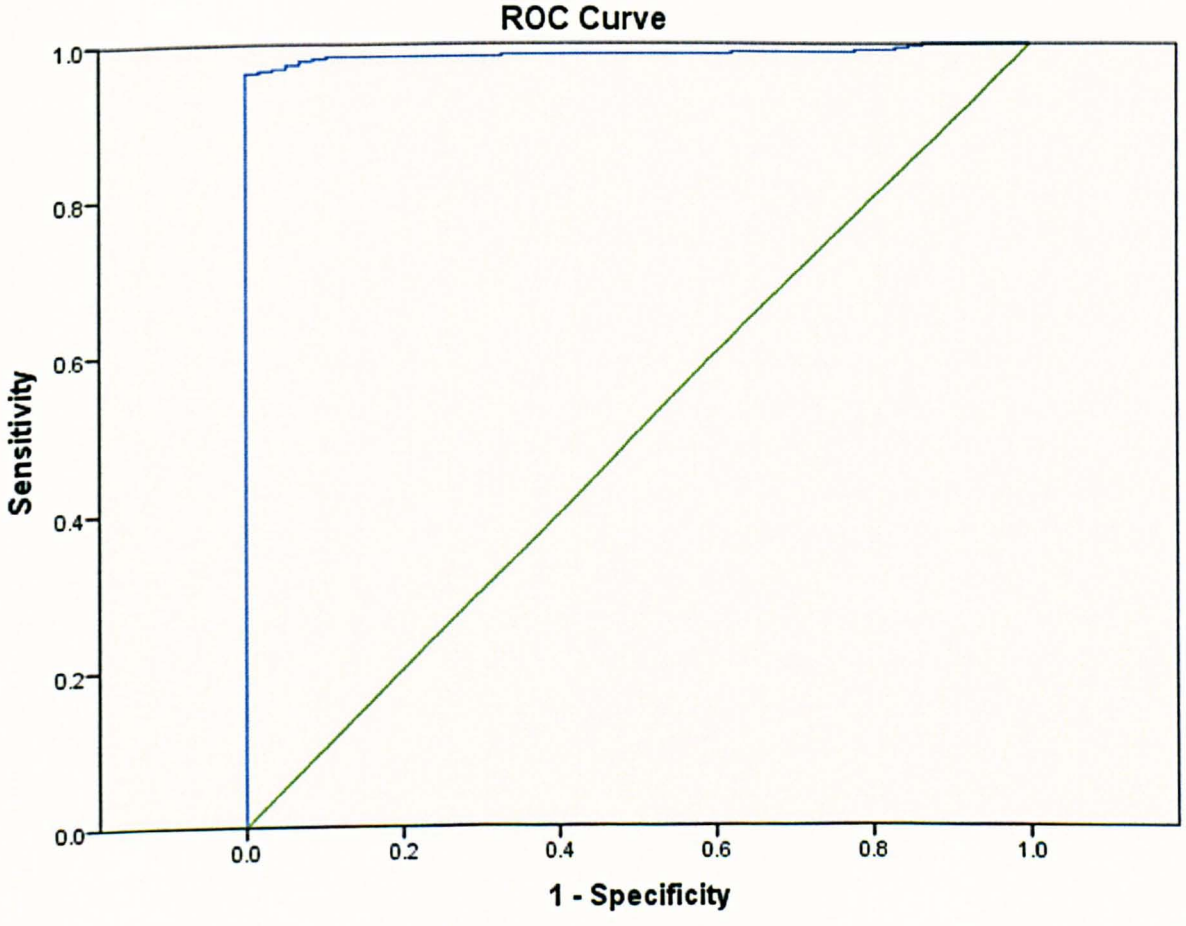

Test Result Variable(s) 50µM atropine +50µM CCh vs 50µM CCh

Area	Std. Error[a]	Asymptotic Sig.[b]	Asymptotic 95% Confidence Interval	
			Lower Bound	Upper Bound
.987	.005	.000	.978	.997

ROC curve for 50µM atropine+50µM CCh vs 50µM CCh demonstrating a near perfect ROC curve. The calculated ROC curve is represented by the blue line with the green line representing the null hypothesis area of 0.5.

Fig 8.2.2 ROC Analysis of 50μM CCh addition against 50μM CCh + high dose IgG from pSS patients.

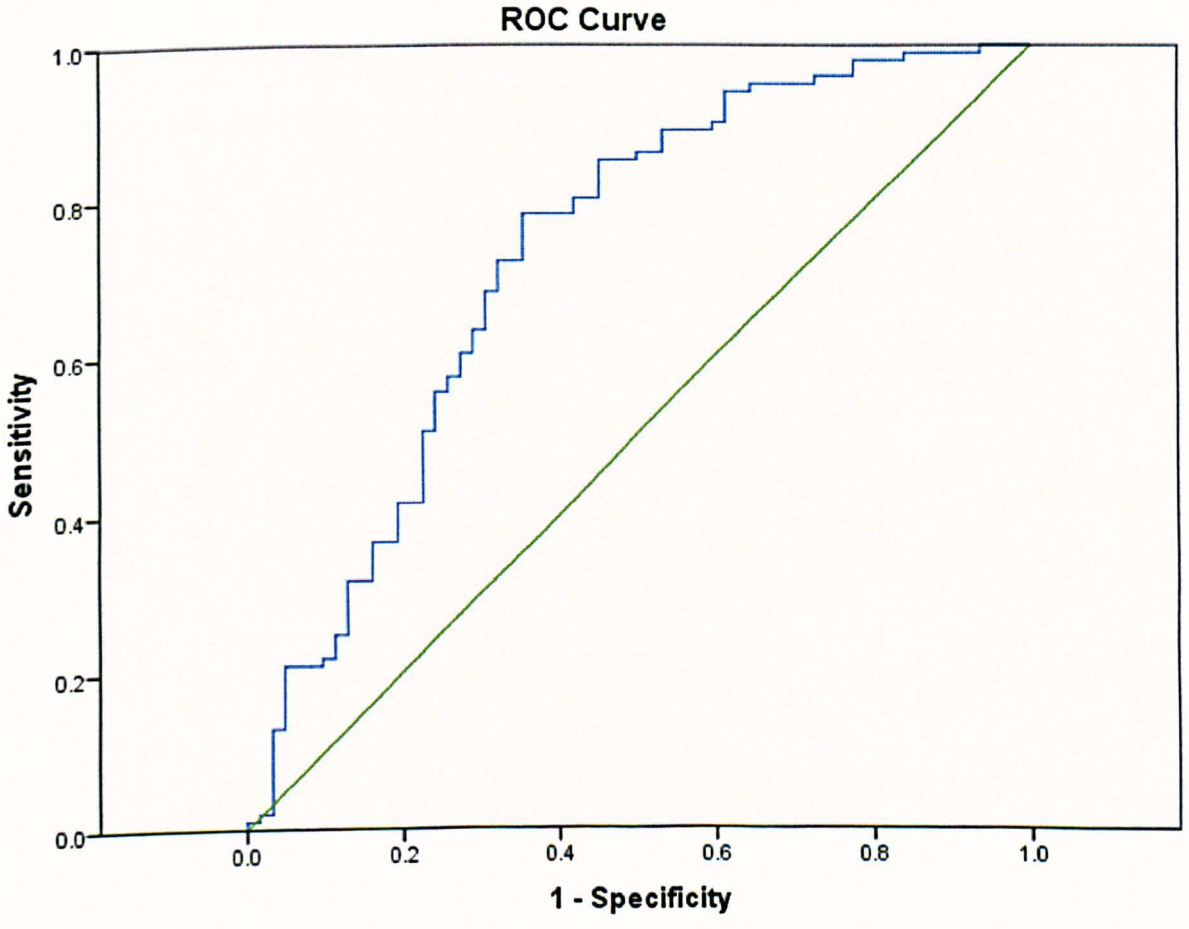

Area	Std. Error[a]	Asymptotic Sig.[b]	Asymptotic 95% Confidence Interval	
			Lower Bound	Upper Bound
.731	.043	.000	.647	.814

a. Under the nonparametric assumption
b. Null hypothesis: true area = 0.5

ROC analysis of the data collected for the effect of IgG isolate from Sjögren's syndrome patients (399 μg/ml ±22) upon the $[Ca^{2+}]_i$ evoked by 50μM CCh. The calculated ROC curve is represented by the blue line with the green line representing the null hypothesis area of 0.5.

Fig 8.2.3 ROC Analysis of 50µM CCh addition against 50µM CCh + high dose IgG from control subjects.

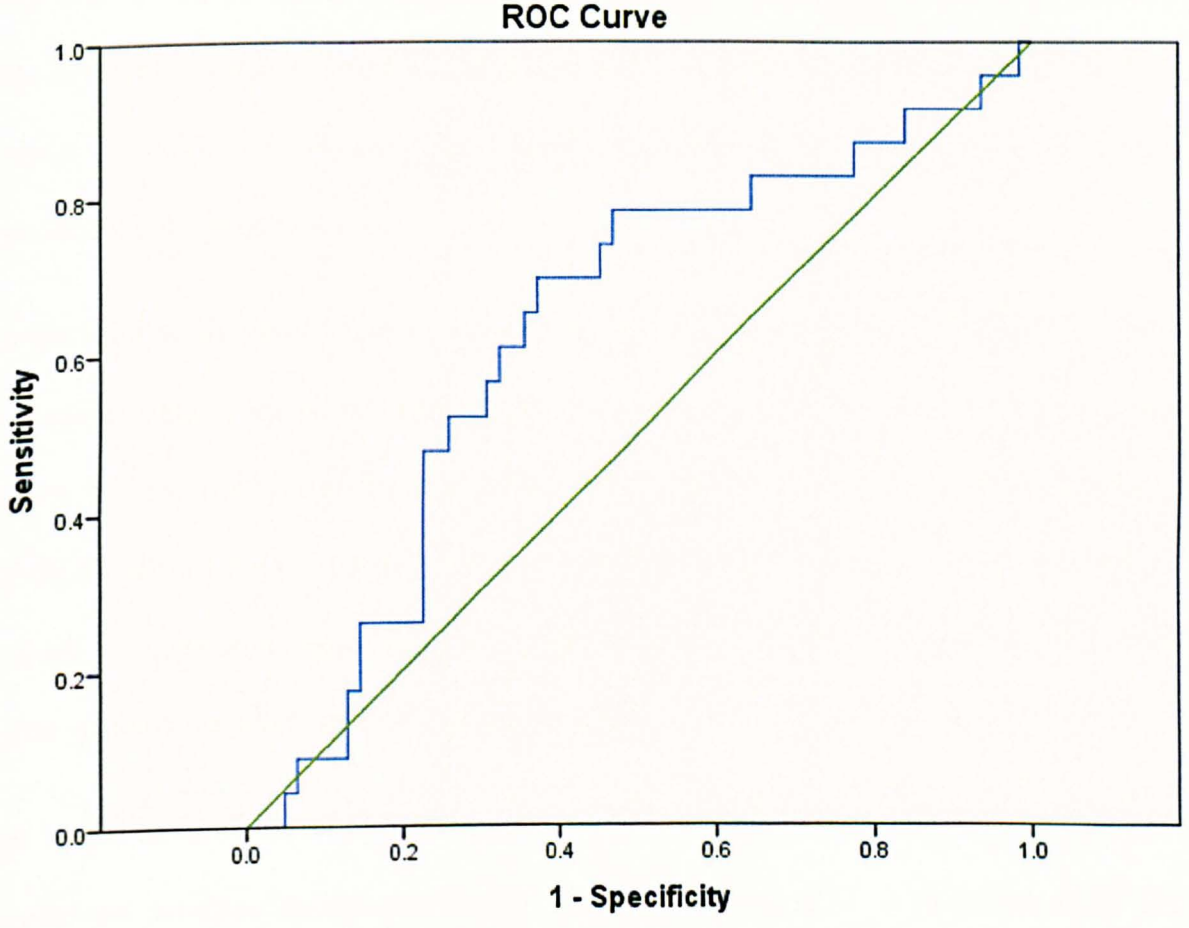

Area	Std. Error[a]	Asymptotic Sig.[b]	Asymptotic 95% Confidence Interval	
			Lower Bound	Upper Bound
.630	.069	.066	.496	.765

a. Under the nonparametric assumption

b. Null hypothesis: true area = 0.5

ROC analysis of the data collected for the effect of control human serum IgG isolate from a control group (267 µg/ml ± 33) upon the $[Ca^{2+}]_i$ evoked by 50µM CCh. The calculated ROC curve is represented by the blue line with the green line representing the null hypothesis area of 0.5.

Discussion

The previous microfluorimetry work performed with the SjS derived IgG has limitations when considered for use as a diagnostic test. The experiment is relatively slow, and uses large amounts of patient serum. The high throughput protocol using the Flexstation 3 was to address these issues, allowing for rapid IgG screening using the HSG cell based microfluorimetry protocol.

Comparision of the pooled results obtained for the high concentration (399 µg/ml ±22 final well concentration) SjS IgG and control IgG (267 µg/ml ± 33) (figure 8.1.9) show a significant decline in response caused by the patient IgG. However, the control IgG also shows a significant decline compared with the 50µM control. Also, the decline seen in response is also IgG concentration dependent, with significantly less decline observed in the low (54 µg/ml +/- 6.6-control IgG, and 80 µg/ml +/-4.4 SjS IgG).

Due to the variation in effect upon response (as can be seen in figue 8.1.8), ROC analysis was carried out upon the pooled data for the SjS IgG (figure 8.2.2) and control IgG (figure 8.2.3) vs 50µM CCh, giving an area under the curve (AUC) score of .731 and .630 respectively. Based upon these results, the Flexstation protocol in its current format is neither selective nor specific enough to be used as a diagnostic test.

In an attempt to confirm work by Koo *et al* (Koo, Li et al 2008) implicating the 3rd extracellular loop of the M3R in autoantibody binding, a linear polypeptide corresponding to this region was also included in some experimental runs (figure 8.1.10). As shown in figure 8.1.10, the polypeptide did not prevent the inhibition of response caused by the patient IgG, implying that the 3rd extracellular loop is not recognized by the anti M3R autoantibodies.

9 General Discussion and Conclusion

Sjogren's syndrome is an autoimmune disease characterised by salivary and lacrimal gland hypofunction, resulting in dry mouth and dry eye. Most of the research over the years has focused upon the mechanisms of salivary hypofunction.

Nitric Oxide and Lacrimal Gland hypofunction- a role for NO in SjS.

Lacrimal gland secretion is tightly regulated, with perturbation resulting in dry eye symptoms. Nitric oxide production is also tightly regulated, with large concentrations being potentially cytotoxic, while lower, physiological concentrations are required for normal cell function. Sjögren's syndrome has a well documented inflammatory aspect that includes elevated levels of NO.

This chronic inflammatory state endured by SjS patients is evidenced by the observation of increased levels of NO in expired air (Ludviksdottir, Janson et al. 1999) and saliva (Konttinen, Platts et al. 1997) of SjS patients. To determine whether NO could have a deleterious effect upon secretory gland function, Caulfield *et al* tested a number of NO donors on mouse and human salivary gland acinar cells in an attempt to reproduce *in vitro*, the acinar hypofunction seen in SjS *in vivo* (Caulfield, Balmer et al. 2009). They showed that acute application of NO donors amplified the Ca^{2+} response to cholinergic agonist in a manner consistent with the cADPr stimulation of RyR. This was shown to be mediated via NO stimulation of sGC and cGMP.In the same study, prolonged exposure to NO lead to a reduction in the agonist-stimulated secretory signal. The decline in response was shown to be independent of cGMP mediation and hypothesised to be a result of the action of NO via the action of reactive nitrogen species (RNS), or the nitrosylation of key cysteine residues, a process known as S-nitrosylation. Recently, an *in vivo* study conducted by Correia *et al*

demonstrated that induction of iNOS with lipopolysaccaride (LPS), and consequent increase in NO, resulted in an increase in cholinergically evoked salivary secretion (Correia, Carpenter et al. 2010), similar to the initial response seen *in vitro* .

My data show that exposure to NO caused a very similar biphasic pattern of response in mouse lacrimal gland acinar cells to that seen previously in mouse submandibular acinar cells. These data, which show an initial ODQ-sensitive amplification of the agonist-evoked Ca^{2+} signal, confirm that the cGMP dependent pathway, culminating with the production of cADPr and activation of RyR, acts to modulate the secretory signal. Furthermore, prolonged exposure to NO resulted in the loss of the agonist-evoked Ca^{2+} signal, in a very similar way to that seen previously in salivary acinar cells. In both cell types, the ODQ-insensitive rundown in the response appears to be independent of the cGMP/cADPr pathway. These data show, for the first time that lacrimal and submandibular glands share a similar NO-sensitive cADPr-mediated secretory pathway and thus that both acinar cells types are vulnerable to this potential mechanism of glandular hypofunction. The decrease in sensitivity to cholinergic stimulation is consistent with findings by Dawson *et al* who showed that SjS patients retain functioning acinar tissue that has a reduced sensitivity to cholinergic stimulation (Dawson, Field et al. 2001).The demonstration that two separate glands are affected in a similar fashion via the same mechanism reinforces the role of a chronic inflammatory state, characterised by increase in NO in the aetiology of the condition and also allows for the possibility that a common therapy for NO mediated glandular hypofunction in SjS might be developed.

Endogenous production of NO in mouse lacrimal gland acinar cells

One conspicuous difference between lacrimal and submandibular acinar cells was the variability in the responses seen under control conditions. Submandibular cells generally produced a consistent, steady response pattern in the absence of exogenous NO but lacrimal cells were capable of a variety of responses. Whilst a proportion of the cells tested showed a consistent response to stimulation over the duration of the experiment, many other cells instead showed first an increase and then a decline in response, similar to that seen following exposure to NO. This apparently spontaneous amplification of the Ca^{2+} response to agonist followed by rundown of the response is suggestive of endogenous NO production by the lacrimal acinar cells. This hypothesis is supported by the observation that the amplification of response to CCh stimulation was abolished by uncoupling of NO production to synthesis of cADPr by application of 10μM ODQ. Whilst the mechanism of fluid secretion has been well documented in salivary acinar cells, characterisation of lacrimal cells lags behind considerably. The demonstration of endogenous production of NO in mouse lacrimal acinar cells represents a hitherto unexplored aspect of lacrimal gland secretion.

Whilst the spontaneous amplification effect has been seen to be acting through the cGMP/cADPr pathway, which implies the action of NO, it is not proof that NOS is present in the lacrimal acinar cells to an appreciable degree. Modification of the pattern of response observed by the use of NOS inhibitors and the NOS substrate, L-NAME, would provide evidence for the involvement of NO in cellular hypofunction.

An increase in supply of the NOS substrate L- arginine was provided to the cells in an attempt to increase the NO production and amplify the NO mediated amplification and

rundown. Exogenous supply of L-arginine did not result in an amplification event, however the observed rundown was pronounced compared to the control data. Provision of L-arginine to the cells caused an increased incidence of cells running down to <50% response by the end of the experiment. Use of the non- specific NOS inhibitor, L-NAME was used in an attempt to prevent the NO mediated effects by preventing NO production. Whilst the average response to agonist over the course of the experiments was not significantly different to that seen in control, some protective effect was in evidence, since the incidence of cells running down to <50% halved compared to control (or quarter that in arginine). To identify the NOS isoform(s) responsible for the production of NO, inhibitors specific to each isoform were used. Inhibition of iNOS was achieved with SMT, and resulted in a similar response seen in the use of L-NAME- no significant difference in the average agonist evoked change in Ca^{2+} over the course of the experiment, but a significant decrease in the amount of cells suffering rundown to <50%. Inhibition of the constitutive NOS isoforms eNOS and nNOS with DPI and 7NI, respectively, showed a significant decline in lacrimal cell response to agonist, coupled with an increased incidence of cells running down to <50% of initial response comparable to that seen in the arginine results. These findings imply that each of the NOS isoforms is present and functional in mouse lacrimal gland acinar cells.

Measurement of NO and the effect of NOS inhibition

Use of the NO sensitive fluorescent dye, DAF 2 DA allowed for the direct measurement of NO production *in vitro*, and allows for the direct correlation of change in NO with effect upon cell response. Proof that we are capable of observing change in NO production via DAF microfluorimetry was shown by the application of the NO donor to mouse lacrimal acinar cells resulting in the steep increase in DAF fluorescence in comparison to control. A similar basal production of NO was observed in both unstimulated cells to those repeatedly

challenged with agonist. This is consistent with data suggesting that an increase in $[Ca^{2+}]_i$ alone is not responsible for larger increases in NO (Broillet, Randin et al. 2001). The fact that the measured DAF fluorescence levels out and increases after its initial decline suggests that the cells are producing appreciable levels of NO, enough to overcome the loss of fluorescence due to DAF 2 leakage/ photobleaching, although the NOS isoform(s) responsible remain unknown.

Supply of the NOS substrate arginine resulted in a sustained and significant increase in DAF fluorescence consistent with the increase in NO production. Inhibition of the iNOS isoform with SMT resulted in no significant difference in NO production compared to control. Similarly, DPI inhibition of eNOS showed no significant effect *vs.* control. Paradoxically, the use of L-NAME as a non specific NOS inhibitor resulted in the sustained increase in NO production. Such a paradoxical rise of NO after NOS inhibition was also demonstrated during the use of 7NI to inhibit nNOS.

The significant declines in agonist evoked change in $[Ca^{2+}]_i$ during the eNOS (DPI) and nNOS (7NI) inhibition experiments indicate that the constitutive NOS isoforms play an important role in the maintenance of Ca^{2+} response. DPI inhibition of eNOS showed a significant decline in agonist evoked Ca^{2+} response by t=60, yet showed no significant change in NO production. Decline in cell response coupled with no change in NO levels may indicate a more subtle role for eNOS, with the possibility that governed production of NO is produced locally to its site of action by eNOS or is too low to be shown by changes in DAF fluorescence.

Neuronal NOS has already been shown to be prevalent in the cytosolic fraction of rat parotid acinar cells, accounting for 74% of NOS activity (Mitsui and Furuyama 2000), as well

as nNOS antibodies cross reacting with cytosolic protein seen in rabbit parotid gland acinar cells (Sugiya, Mitsui et al. 2001). nNOS and eNOS have been shown to be present in lacrimal gland acinar cells, although data on their relative abundance is lacking. eNOS is expressed in a diverse array of epithelial cell types, and has been shown to be present in lacrimal gland acinar cells (Hodges, Shatos et al. 2005) with studies confirming that eNOS is located within caveolae (Ding, Walcott et al. 2003; Solomonson 2003; Sullivan and Pollock 2003). nNOS has been demonstrated to be present in the nerve fibres associated with lacrimal gland acini, as well as within the acinar cells themselves (Ding, Walcott et al. 2001);(Hodges, Shatos et al. 2005). In humans, however, it has been shown that a T>G polymorphism at amino acid position 894 has been associated with increased eNOS activity (Yoon, Song et al. 2000), and this has been seen to be associated with recurrent swelling of the salivary glands and early onset of SjS (Pertovaara, Antonen et al. 2007).

The arginine analogue, L-NAME, was used in an attempt to inhibit all endogenous NOS activity. 10μM L-NAME showed no significant effect the average pattern of Ca^{2+} mobilisation, yet seemed to have some measure of protective effect, with less lacrimal acinar cells declining in response to <50% of initial stimulation by the end of the experiment compared with control. Unexpectedly, the DAF fluorescence indicated a significant increase in NO production during 10μM L-NAME perfusion.

Compared to the constitutive NOS isoforms, iNOS is responsible for large, sustained production of NO, with regulation of iNOS activity primarily achieved by the regulation of iNOS expression. iNOS expression can be induced by a host of transcription factors, including nuclear factor-κB (NFκB) (Dinarello 2000) which in most cells, resides in the cytoplasm complexed with its inhibitor IκB (Baeuerle and Baltimore 1988). NFκB can be

activated by lipopolysaccaride (LPS), IL-1 Beta (IL1β), Tumour Necrosis Factor α (TNFα) (Xie and Nathan 1994; Xie, Kashiwabara et al. 1994; MacMicking, Xie et al. 1997). In mouse lacrimal cells it has also been shown that IL1-β also induces JNK, which in turn stimulated the expression of iNOS (Zoukhri, Macari et al. 2006).Under normal conditions, the physiological concentrations of NO, maintained by constitutive NOS, activation of NFκB is suppressed. Inhibition of constitutive NOS results in a decrease in NO which can result in activation of NFκB leading to expression of iNOS and a subsequent increase in NO production.

If this is the case, my data suggest that nNOS may be responsible for the production of the basal concentrations of NO maintaining NFκB inhibition, thus preventing expression of iNOS. This pattern of NO derived from nNOS inhibiting NFκB and consequently iNOS expression has already been seen in astrocytes (Togashi, Sasaki et al. 1997).

Use of L-NAME highlights one of the potential problems with NOS inhibition. Homology in NOS between isoforms renders it difficult to completely isolate a single isoform for inhibition, and selectivity and potency can vary between inhibitor/ isoform and even between species. The similarity in response observed between the non specific inhibition of NOS with L-NAME and the 7NI inhibition of nNOS, a paradoxical rise in NO during supposed blanket NOS inhibition, suggests that L-NAME could more effective at inhibiting nNOS than iNOS. This may be explained by the fact that to be truly effective against iNOS, L-NAME requires hydrolysis, occurring rapidly *in vivo*, but in the relatively short incubation times associated with *in vitro* experiments may only undergo only partial hydrolysis (Southan and Szabo 1996).

NFκB and SjS

The activity of iNOS is controlled primarily at the transcriptional level.iNOS transcription can be modulated by NFkB, with NFkB itself regulated by NO, forming a self regulatory pathway. Normal, physiological levels of NO act to inhibit NFkB by S-nitrosylation of NFkB's p50 subunit, with the S-nitrosylation by NO donors and subsequent attenuation of DNA binding being described *in vitro* (Matthews, Botting et al. 1996; delaTorre, Schroeder et al. 1998). Further work by Marshall and Stamler showed that S-nitrosylation inhibits NFkB *in vivo* (Marshall and Stamler 2001). A decrease in levels of NO in the cell could result in deactivation of NFkB resulting in an upregulation of iNOS transcription, resulting in increased production of NO.This could result in an increase in NO following constitutive NOS isoform inhibition. NFkB induces transcription of its inhibitor, establishing a regulatory mechanism of feedback inhibition (Cheng, Cant et al. 1994; Chiao, Miyamoto et al. 1994) and it has been demonstrated in mice with mutated κB enhancers in the IkBα gene develop lymphocytic infiltrations in lacrimal and salivary glands, as well as high levels of the SjS diagnostic markers: anti Ro/La (Peng, Ling et al. 2010). Another mouse model expressing constituvely active NFκB (Dong, Jimi et al. 2010) shows corneal inflammation and a gene expression profile similar to that seen in humans with KCS (Pflugfelder 2004). The similarities shown between mutant κB enhancer mice and SjS samples by Peng *et al* implicate a defective NFkB pathway in the observed pathology of SjS. The bias in gender seen in autoimmune disease may related to effect of sex steroids on NFkB, since several of the androgens have been shown to inhibit IL-1β induced NO production in rabbit lacrimal acini (Beauregard and Brandt 2004).

The data shown here represent a demonstration of the intricate nature of effect NO production has upon Ca^{2+}signalling and eventual fluid secretion. It has long been perceived

that NO has a dual nature, both protective and destructive. These data show that perturbation of the delicate balance of the NO produced in normal mouse lacrimal acinar glands can result in a decrease in cellular response potentially mimicking the acinar hypofunction observed in Sjögren's syndrome. Increased levels of NO have been observed in individuals diagnosed with SjS (with its inflammatory component well known), and NO's relationship with inflammation is well documented. These data suggest that an increase in NO, seen in a chronic inflammatory state, may contribute to glandular hypofunction. Furthermore, my data shows that a decrease in housekeeping levels of NO production by constitutive NOS isoforms could also bring about a rise to an increase in NO production, mimicking the chronic inflammatory disease state. Regardless of the causative agent of NO's increase in production, the fact remains that an alteration of NO generation could have serious consequences for cellular function. NO has such a wide spectrum of effects, that showing exactly how NO results in acinar gland hypofunction remains difficult. However, these data indicate that: (a) an exogenous supply of NO has a similar, biphasic effect upon lacrimal gland acinar cells as it does upon submandibular gland acinar cells; (b) lacrimal gland acinar cells are capable of generating a measurable endogenous supply of NO; (c) the endogenous supply of NO can be altered by use of NOS inhibitors; and (d) specific isoform inhibition can result in an unexpected increase in NO generation. Furthermore, for the first time, the so called "Arginine Paradox" has been demonstrated in mouse lacrimal acinar cells- implying that availability of the NOS substrate, arginine, may have some part to play.

A role for the NOS substrate, L-arginine.

An increase in availability of NOS substrate could conceivably result in an increase in the production of NO, with an expected effect upon Ca^{2+} signalling. Exogenous supply of the NOS substrate L-arginine also resulted in a significant rise in NO production. Whilst specific data for intracellular arginine concentration in lacrimal and submandibular glands is unavailable, for other tissues a range of 0.5-2 mmol l^{-1} have been reported (Colleluori, Morris et al. 2001), higher than the 10uM concentration of the exogenous arginine supply, and more than enough to saturate any of the NOS isoforms. The observed increase in endogenous NO production upon exogenous supply of subcellular concentration of arginine, dubbed "the arginine paradox", has been well documented although not completely explained. Several theories exist to explain how the addition of low concentrations of arginine can affect NO production, including the arginine regulation of iNOS induction in cultured astrocytes (Lee, Ryu et al. 2003), and the modulation of NO production by the endogenous NOS inhibitor, asymmetric dimethylarginine (ADMA), with particular importance upon the ratio of arginine to ADMA (Tsikas, Boger et al. 2000; Bode-Boger, Scalera et al. 2007). Increased levels of ADMA have been demonstrated in patients with Reynaud's Phenomenon secondary to Sjögren's syndrome (Rajagopalan, Pfenninger et al. 2003), and shown to induce an increase in expression of Sjögren's syndrome nuclear antigen-1 (SSNA-1) (Smith, Anthony et al. 2005). The role (if existent) of arginine itself in the pathology of Sjögren's syndrome has not been investigated, other than in relation to the production of NO, and the results presented here represent the first demonstration of the arginine paradox phenomenon in lacrimal gland acinar cells. No data has been published pertaining to any link between arginine availability and glandular hypofunction, although

anything that may perturb NO production (such as arginine/ ADMA ratio) and have a knock on effect upon Ca^{2+} signalling may have some part to play in the pathology of SjS.

ODQ

The results returned for the effect of the sGC inhibitor ODQ represent an unexpected effect of ODQ upon NO production as the sGC step in Ca^{2+} signal modulation is post-NO production. It is reasonable to suggest that the large sustained increase in DAF2 fluorescence may implicate the induction of iNOS. While precedent exists for the increase in NO production during NOS inhibition (see above), the results obtained for the sGC inhibitor ODQ are more difficult to explain. sGC represents a post-NO production step in signal modulation, with ODQ blocking the NO mediated amplification observed when SNAP is present during stimulation, in both lacrimal gland acinar cells (previous chapter) and in submandibular gland acinar cells (Caulfield, Balmer et al. 2009). ODQ is reported to have no effect upon NO production in platelets and vascular tissue (Moro, Russel et al. 1996), yet has been shown to potentially inhibit NO production in endothelium-intact aortic rings (Feelisch, Kotsonis et al. 1999). My data represent a previously unseen effect by ODQ, seemingly causing a sustained increase in NO production in mouse lacrimal acinar cells. ODQ functions as an inhibitor of sGC by targeting sGC's heme group, resulting in a change in oxidation state (Zhao, Brandish et al. 2000) with a concomitant inhibition of sGC function. The functional NOS enzyme consists of a homodimer each monomer having 2 distinct domains: reductase and oxygenase. It is the oxygenase domain that catalyses the conversion of arginine to citrulline (releasing NO) and contains the binding sites for arginine, tetrahydrobiopterin and heme. It is possible that ODQ may alter the oxidation state of the prosthetic heme group attaching to the NOS oxygenase domain. Should this occur to the nNOS isoform

preferentially over the iNOS, then that would account for the unexpected increase in NO production.

The mechanism of NO mediated decline of response

The high levels of NO associated with inflammation are potentially cytotoxic, with high levels of NO being implicated in the formation of the reactive nitrogen species (RNS), peroxynitrite. Peroxynitrite is formed rapidly in the reaction of NO with the superoxide anion (OO^-) (Gryglewski, Palmer et al. 1986). The highly reactive peroxynitrite anion ($ONOO^-$) is capable of modulating cell signalling as well as having direct cytotoxic effects (Ballinger, Patterson et al. 2000). Peroxynitrite can react directly with transition metal centres (Alvarez and Radi 2003), and can render NOS inactive by alteration of the prosthetic heme group (Huhmer, Nishida et al. 1997).

S-nitrosylation of important components of the signalling cascade could result in a decline in sensitivity to their ligands resulting in a decline in function. In sGC, cysteine 243 in the α subunit and, cysteine 122 in the β subunit have been shown to be targets for nitrosylation, becoming desensitized to NO in a time/ NO concentration dependent manner (Sayed, Baskaran et al. 2007; Sayed, Kim et al. 2008).

In RyR1 up to 1 in 50 cysteine residues are capable of undergoing S-nitrosylation with cysteine 3635 nitrosylation shown to have a modulatory effect on function (Sun, Xin et al. 2001).

The role of nitric oxide in the decline of secretory function is still very much a subject of debate, recent work by Correia *et al* showing that induction of iNOS and the associated increase in NO resulted in hypersecretion, even after prolonged and increased NO production (Correia, Carpenter et al. 2010). This was performed *in vivo*, whereas Caulfield

(Caulfield, Balmer et al. 2009) and myself used isolated acinar cells. It is plausible that the 24hr *in vivo* study showing glandular hyperfunction correlated to the early events seen in the *in vitro* isolated cell experiments – a NO modulated amplification of Ca^{2+} signal.

DAF Photobleaching/dye leakage

The averaged data for all of the DAF experiments show the same pattern, initial decline followed by a continual increase in fluorescence. The initial decline may be a result of photobleaching (Kojima, Nakatsubo et al. 1998), or leakage from the cell in question before an equilibrium between the rate of dye leakage and the rate of NO production is reached. DAF 2DA diffuses across the cell membrane where the ester bonds are hydrolysed by intracellular esterases, leaving the cell impermeable DAF2 dye. However, the retention of fluorescein based dyes can vary, depending not only upon membrane integrity, but upon the rate of fluorescein dye efflux by active transport (Prosperi, Croce et al. 1986). The observed increase in fluorescence measured at 488nm is a result of the DAF2 reacting with NO in the presence of O_2 (Kojima, Nakatsubo et al. 1998). Use of the DAF2 fluorescence to measure relative amounts of fluorescence, rather than absolute values of NO removes any concern that DAF fluorescence can be dependent upon the intensity of excitation (Looms, Dissing et al. 2000), and the influence of Ca^{2+} upon the DAF/NO reaction, although at physiological levels of $[Ca^{2+}]_i$,even the large concentrations of Ca^{2+} evoked by ionomycin exposure, has been shown to not significantly alter DAF 2 fluorescence (Broillet, Randin et al. 2001).

Since DAF 2 is a single wavelength fluorescent dye, it is plausible that some measure of the recorded increase in fluorescence may be attributed to cell shrinkage due to repeated stimulation. Since there was no significant difference between the DAF traces for stimulated

and unstimulated cells, this seems relatively unlikely. It may be possible to re-analyse the images obtained from Metafluor^{tm} using an image processing program such as "Imagej" in order to determine whether there were consistent changes in cell volume. However, due to the irregular shape of individual lacrimal gland acinar cells any measured change in the 2 dimensional cross section may not be truly representative of cell volume, as the relationship between 2 dimensional image and the 3 dimensional shape of the cell is not immediate. Since the same slow increase was seen in stimulated and unstimulated cells, it can still be reasoned that the significant differences in DAF 2 fluoresence in cells undergoing NOS inhibition is a real and significant effect.

Anti muscarinic autoantibodies as a mediator of glandular hypofunction seen in Sjögren's syndrome.

The M3R makes an attractive target for the study of the autoimmune component, since the high reported incidence of specific anti-M3R antibodies may act as a superior marker of SjS. Furthermore, these autoantibodies have been shown to replicate the secretory hypofunction by blocking the action of muscarinic agonists. In this thesis I have shown that the HSG cell line, shown to be a good model for salivary secretion (Nagy, Szlavik et al. 2007) exhibit behavior consistent with secretory hypofunction when exposed to SjS patient IgG. Furthermore, anti muscarinic antibody activity has been hypothesised to be responsible for narcolepsy, and my work with the HSG cell line has determined that this action is detectable using the same protocol for SjS.

Development of a rapid diagnostic test requires specificity and sensitivity. The Flexstation protocol developed here was able to show an average effect of SjS IgG upon the change in

agonist evoked $[Ca^{2+}]_i$. However, its use as a diagnostic tool would not currently add anything to the current methods of diagnosis. Figure 8.2.3 shows the ROC curve generated for the use of control IgG which has an AUC of 0.630, yet has a 95% lower confidence boundary of 0.496. This large variation in result is due to the amount of variation seen in the response of HSG cells to the control IgG. The ROC curve generated for the comparison of patient IgG (figure 8.2.2) to the response seen in 50μM CCh only, shows an AUC of 0.731 with a lower 95% confidence boundary of 0.647 allowing for the selection of a reasonable cutoff, in this case 65.9%. Generation of a ROC curve for the direct comparison of patient and control IgG masks any significant inhibitory effect of the patient IgG due to the "noise" generated by the greater level of variation response seen in the control data.

The limitations of the Flexstation protocol in its current format may be caused by several factors:

Concentration of IgG: The IgG samples under investigation were purified to 1995 4μg/ml. (± 108.7 μg/ml) for the SjS derived, and 1335.7μg/ml (± 108.7 μg/ml). The fluidics module on the Flexstation lacks a method of fluid removal, so, given that each experiment well will contain 40μL prior to a 10μl IgG addition, this renders the final test concentration of IgG to be 199.5μg/ml and 133.5 μg for SjS and healthy control respectively. Dawson *et al* showed how *in vitro* antimuscarinic activity is concentration dependent, rapidly declining at concentrations below 1μg/ml (Dawson, Stanbury et al. 2006). *In vivo* concentration dependency may be overcome by localised production of IgG within the diseased glands.

A diagnostic test based upon ROC will require a relatively accurate measure of prevalence. So far, anti muscarinic autoantibodies have been shown to be difficult to isolate by normal methods, leaving the reported prevalence of anti M3R open to debate, with reports varying, dependent upon methodology.

The reversible nature of the inhibition observed in anti M3R studies(Dawson, Stanbury et al. 2006) (and chapter 8) indicate that antibody and M3R binding is a transient event, which may have some bearing on the "noise" generated in the Flexstation protocol.

Much of the work conducted upon the mechanism of anti M3R activity has focused upon the importance of the 2nd intracellular loop. Koo *et al* (Koo, Li et al. 2008) hypothesised that the M3R 3rd extracellular loop may be important in the antisecretory effect of anti-M3R autoantibody. Koo *et al* went on to show that a synthetic linear polypeptide corresponding to the 3rd extracellular loop prevented the IgG mediated inhibition of Ca^{2+} response in HSG cells. In the protocol used here, the anti M3R antibody antisecretory effect was not shown to be affected by the presence of the polypeptide. My findings do not support those of Koo *et al*. I found no evidence of binding of anti-muscarinic receptor autoantibodies to this polypeptide.

IgG isolated from SjS patients has been shown to stimulate NO production in rat lacrimal glands (Bacman, Berra et al. 1998), and rat submandibular glands (Perez Leiros, Sterin-Borda et al. 1999). This represents an important overlap in the potential spectrum of causes for SjS.

The causes of the glandular hypofunction associated with SjS are varied, but all resulting in the spectrum of symptoms – the very definition of a "syndrome".

Conclusion

Prolonged exposure to NO results in the desensitisation of acinar cells to agonist, although the exact cause is unknown. Mouse lacrimal gland acinar cells exhibit a similar pattern of amplification and diminution of response to agonist when exposed to NO. However, mouse lacrimal acinar cells appear to produce endogenous NO, and perturbation of NO synthesis can significantly alter lacrimal cell functionality. Furthermore, the data in this thesis highlight some of the differences between lacrimal and salivary gland acinar cells in relation to NO mediated secretion. Development of any treatments for the glandular hypofunction would have to take into account any differences in cell behavior between secretory organs.

The putative anti-M3R activity IgG isolated from Sjögren's syndrome, and narcolepsy patients can be detected using the HSG cell line. The protocol developed here for the high-throughput detection of anti-M3R activity is neither sensitive nor specific enough in its current format to use as a screening tool in the diagnosis of anti-M3R activity in SjS.

Further Work

Throughout the reviewed literature there seems to be a large variation in the reported specificity/ potency of NOS inhibitors, potentially a variance between species in NOS isoform homology, and dependence upon experimental protocol. To further illustrate the effect upon specific NOS isoform inhibition, the experimental protocol deployed in this work could be repeated with other NOS isoform inhibitors.

NO may exert its antisecretory effect by s-nitrosylation of important components of the signal cascade. Investigation of likely targets for S-nitrosylation (such as the RyR and sGC) and demonstration of an effect upon secretory function would give some idea of the extent of NO's role in glandular hypofunction.

Further confirmation of glandular structure/function between human and model organisms by immunohistochemistry experiments could highlight any colocalisation between NOS isoforms/ caveolae/ nuclei in mouse lacrimals and any difference in humans.

Repetition of DAF/ FURA experiments with lacrimals from NOS isoform specific knockout mice may clarify the sequence of events leading to NO mediated glandular hypofunction. Whilst the use of a model organism (in this case, CD1 mice) enables a steady supply of sex/age matched cells, the use of human tissue would always be preferential, although obtaining lacrimal tissue from human subjects would be overly invasive, due to the lacrimal gland's location within the bony orbit. Investigation of the NOS isoform expression in Sjögren's patients' lacrimal gland acinar cells and comparison with healthy controls would also show if perturbation of NOS isoform expression has a role, although difficulties in obtaining tissue samples render this method unlikely.

Further development of the diagnostic protocol using the high throughput microfluorimetry method, using a greater concentration of IgG/ stringent screening of control subjects. Repeating the current Flexstation protocol with other cell types expressing M3R that may be more stable during the protocol and a repeat of the synthetic polypeptide experiments but with a polypeptide corresponding to the 2nd extracellular loop of the M3R to confirm whether 3rd extracellular loop binding occurs.

This fundamental difference between glands could render development of NO mediating treatment difficult. Such differences between glands may go some way to explain why current treatments for dry eye and dry mouth have been seen to be more effective at treating the dry mouth component over the dry eye.

10 References

Abi-Gerges, N., L. Hove-Madsen, et al. (1997). "A comparative study of the effects of three guanylyl cyclase inhibitors on the L-type Ca^{2+} and muscarinic K^{+} currents in frog cardiac myocytes." Br J Pharmacol **121**(7): 1369-1377.

Al-Sa'doni, H. and A. Ferro (2000). "S-Nitrosothiols: a class of nitric oxide-donor drugs." Clin Sci (Lond) **98**(5): 507-520.

Al-Sa'doni, H. H., I. Y. Khan, et al. (2000). "A novel family of S-nitrosothiols: chemical synthesis and biological actions." Nitric Oxide **4**(6): 550-560.

Alderton, W. K., C. E. Cooper, et al. (2001). "Nitric oxide synthases: structure, function and inhibition." Biochemical Journal **357**(Pt 3): 593.

Alvarez, B. and R. Radi (2003). "Peroxynitrite reactivity with amino acids and proteins." Amino Acids **25**(3-4): 295-311.

Ambudkar, I. S. (2000). "Regulation of calcium in salivary gland secretion." Crit Rev Oral Biol Med **11**(1): 4-25.

Aquilano, K., S. Baldelli, et al. (2008). "Role of nitric oxide synthases in Parkinson's disease: a review on the antioxidant and anti-inflammatory activity of polyphenols." Neurochemical research **33**(12): 2416-2426.

Bachmann, M., H. Deister, et al. (1998). "The human autoantigen La/SS-B accelerates herpes simplex virus type 1 replication in transfected mouse 3T3 cells." Clin Exp Immunol **112**(3): 482-489.

Bacman, S., L. Sterin-Borda, et al. (1996). "Circulating antibodies against rat parotid gland M3 muscarinic receptors in primary Sjogren's syndrome." Clin Exp Immunol **104**(3): 454-459.

Bacman, S. R., A. Berra, et al. (1998). "Human primary Sjogren's syndrome autoantibodies as mediators of nitric oxide release coupled to lacrimal gland muscarinic acetylcholine receptors." Curr Eye Res **17**(12): 1135-1142.

Baeuerle, P. A. and D. Baltimore (1988). "I kappa B: a specific inhibitor of the NF-kappa B transcription factor." Science **242**(4878): 540-546.

Ballinger, S. W., C. Patterson, et al. (2000). "Hydrogen peroxide- and peroxynitrite-induced mitochondrial DNA damage and dysfunction in vascular endothelial and smooth muscle cells." Circ Res **86**(9): 960-966.

Barouch, L. A., R. W. Harrison, et al. (2002). "Nitric oxide regulates the heart by spatial confinement of nitric oxide synthase isoforms." Nature **416**(6878): 337-339.

Barry, R. J., N. Sutcliffe, et al. (2008). "The Sjogren's Syndrome Damage Index--a damage index for use in clinical trials and observational studies in primary Sjogren's syndrome." Rheumatology (Oxford) **47**(8): 1193-1198.

Beauregard, C. and P. Brandt (2004). "Down regulation of interleukin-1beta-induced nitric oxide production in lacrimal gland acinar cells by sex steroids." Curr Eye Res **29**(1): 59-66.

Beauregard, C., P. C. Brandt, et al. (2003). "Induction of nitric oxide synthase and over-production of nitric oxide by interleukin-1 [beta] in cultured lacrimal gland acinar cells." Experimental eye research **77**(1): 109-114.

Bell, M., A. Askari, et al. (1999). "Sjogren's syndrome: a critical review of clinical management." J Rheumatol **26**(9): 2051-2061.

Ben-Chetrit, E., R. Fischel, et al. (1993). "Anti-SSA/Ro and anti-SSB/La antibodies in serum and saliva of patients with Sjogren's syndrome." Clin Rheumatol **12**(4): 471-474.

Ben-Chetrit, E., B. J. Gandy, et al. (1989). "Isolation and characterization of a cDNA clone encoding the 60-kD component of the human SS-A/Ro ribonucleoprotein autoantigen." J Clin Invest **83**(4): 1284-1292.

Benencia, F. and M. C. Courreges (1999). "Nitric oxide and macrophage antiviral extrinsic activity." Immunology **98**(3): 363-370.

Bennett, V. (1990). "Spectrin: a structural mediator between diverse plasma membrane proteins and the cytoplasm." Curr Opin Cell Biol **2**(1): 51-56.

Berridge, M. J. (1997). "Elementary and global aspects of calcium signalling." J Physiol **499 (Pt 2)**: 291-306.

Berstein, G., J. L. Blank, et al. (1992). "Phospholipase C-beta 1 is a GTPase-activating protein for Gq/11, its physiologic regulator." Cell **70**(3): 411-418.

Bezprozvanny, I., J. Watras, et al. (1991). "Bell-shaped calcium-response curves of Ins(1,4,5)P_3- and calcium-gated channels from endoplasmic reticulum of cerebellum." Nature **351**(6329): 751-754.

Blaise, G. A., D. Gauvin, et al. (2005). "Nitric oxide, cell signaling and cell death." Toxicology **208**(2): 177-192.

Bloch, K. J. and J. J. Bunim (1963). "Sjögren's syndrome and its relation to connective tissue diseases." Journal of chronic diseases **16**(8): 915-927.

Bode-Boger, S. M., F. Scalera, et al. (2007). "The L-arginine paradox: Importance of the L-arginine/asymmetrical dimethylarginine ratio." Pharmacol Ther **114**(3): 295-306.

Borgnia, M., S. Nielsen, et al. (1999). "Cellular and molecular biology of the aquaporin water channels." Annu Rev Biochem **68**: 425-458.

Bowman, S. J., G. H. Ibrahim, et al. (2004). "Estimating the prevalence among Caucasian women of primary Sjogren's syndrome in two general practices in Birmingham, UK." Scand J Rheumatol **33**(1): 39-43.

Boyer, J. L., G. L. Waldo, et al. (1992). "Beta gamma-subunit activation of G-protein-regulated phospholipase C." J Biol Chem **267**(35): 25451-25456.

Bredt, D. S., P. M. Hwang, et al. (1990). "Localization of nitric oxide synthase indicating a neural role for nitric oxide." Nature **347**(6295): 768-770.

Bredt, D. S. and S. H. Snyder (1989). "Nitric oxide mediates glutamate-linked enhancement of cGMP levels in the cerebellum." Proceedings of the National Academy of Sciences **86**(22): 9030.

Bredt, D. S. and S. H. Snyder (1990). "Isolation of nitric oxide synthetase, a calmodulin-requiring enzyme." Proceedings of the National Academy of Sciences **87**(2): 682.

Broillet, M., O. Randin, et al. (2001). "Photoactivation and calcium sensitivity of the fluorescent NO indicator 4,5-diaminofluorescein (DAF-2): implications for cellular NO imaging." FEBS Lett **491**(3): 227-232.

Bron, A. J., J. M. Tiffany, et al. (2004). "Functional aspects of the tear film lipid layer." Exp Eye Res **78**(3): 347-360.

Brunner, F., H. Stessel, et al. (1995). "Novel guanylyl cyclase inhibitor, ODQ reveals role of nitric oxide, but not of cyclic GMP in endothelin-1 secretion." FEBS Lett **376**(3): 262-266.

Busconi, L. and T. Michel (1993). "Endothelial nitric oxide synthase. N-terminal myristoylation determines subcellular localization." Journal of Biological Chemistry **268**(12): 8410.

Butler, J. M., G. L. Ruskell, et al. (1984). "Effects of VIIth (facial) nerve degeneration on vasoactive intestinal polypeptide and substance P levels in ocular and orbital tissues of the rabbit." Exp Eye Res **39**(4): 523-532.

Caulfield, M. P. and N. J. Birdsall (1998). "International Union of Pharmacology. XVII. Classification of muscarinic acetylcholine receptors." Pharmacol Rev **50**(2): 279-290.

Caulfield, V. L., C. Balmer, et al. (2009). "A role for nitric oxide-mediated glandular hypofunction in a non-apoptotic model for Sjogren's syndrome." Rheumatology (Oxford) **48**(7): 727-733.

Cavill, D., S. A. Waterman, et al. (2004). "Antibodies raised against the second extracellular loop of the human muscarinic M3 receptor mimic functional autoantibodies in Sjogren's syndrome." Scand J Immunol **59**(3): 261-266.

Cejková, J., T. Ardan, et al. (2007). "Nitric oxide synthase induction and cytotoxic nitrogen-related oxidant formation in conjunctival epithelium of dry eye (Sjögren [] s syndrome)." Nitric Oxide **17**(1): 10-17.

Chai, J. and E. L. Logigian (2010). "Neurological manifestations of primary Sjogren's syndrome." Curr Opin Neurol **23**(5): 509-513.

Chen, P. F., A. L. Tsai, et al. (1996). "Endothelial nitric-oxide synthase. Evidence for bidomain structure and successful reconstitution of catalytic activity from two separate domains generated by a baculovirus expression system." J Biol Chem **271**(24): 14631-14635.

Cheng, Q., C. A. Cant, et al. (1994). "NK-kappa B subunit-specific regulation of the I kappa B alpha promoter." J Biol Chem **269**(18): 13551-13557.

Chiao, P. J., S. Miyamoto, et al. (1994). "Autoregulation of I kappa B alpha activity." Proc Natl Acad Sci U S A **91**(1): 28-32.

Chipinda, I. and R. H. Simoyi (2006). "Formation and stability of a nitric oxide donor: S-nitroso-N-acetylpenicillamine." J Phys Chem B **110**(10): 5052-5061.

Cimaz, R., A. Casadei, et al. (2003). "Primary Sjogren syndrome in the paediatric age: a multicentre survey." Eur J Pediatr **162**(10): 661-665.

Clementi, E. (1998). "Role of nitric oxide and its intracellular signalling pathways in the control of Ca2+ homeostasis." Biochem Pharmacol **55**(6): 713-718.

Closs, E. I., J. S. Scheld, et al. (2000). "Substrate supply for nitric-oxide synthase in macrophages and endothelial cells: role of cationic amino acid transporters." Molecular pharmacology **57**(1): 68.

Colleluori, D. M., S. M. Morris, Jr., et al. (2001). "Expression, purification, and characterization of human type II arginase." Arch Biochem Biophys **389**(1): 135-143.

Conti, A., L. Gorza, et al. (1996). "Differential distribution of ryanodine receptor type 3 (RyR3) gene product in mammalian skeletal muscles." Biochem J **316 (Pt 1)**: 19-23.

Correia, P. N., G. H. Carpenter, et al. (2010). "Inducible nitric oxide synthase increases secretion from inflamed salivary glands." Rheumatology (Oxford) **49**(1): 48-56.

Culp, D. J., W. Luo, et al. (1996). "Both M1 and M3 receptors regulate exocrine secretion by mucous acini." Am J Physiol **271**(6 Pt 1): C1963-1972.

Daniels, T. E. and P. C. Fox (1992). "Salivary and oral components of Sjogren's syndrome." Rheum Dis Clin North Am **18**(3): 571-589.

Dargie, P. J., M. C. Agre, et al. (1990). "Comparison of Ca^{2+} mobilizing activities of cyclic ADP-ribose and inositol trisphosphate." Cell Regul **1**(3): 279-290.

Dartt, D. A., A. K. Baker, et al. (1984). "Vasoactive intestinal polypeptide stimulation of protein secretion from rat lacrimal gland acini." Am J Physiol **247**(5 Pt 1): G502-509.

Dartt, D. A., D. M. Dicker, et al. (1990). "Lacrimal gland inositol trisphosphate isomer and inositol tetrakisphosphate production." Am J Physiol **259**(2 Pt 1): G274-281.

Dartt, D. A., M. Donowitz, et al. (1984). "Cyclic nucleotide-dependent enzyme secretion in the rat lacrimal gland." J Physiol **352**: 375-384.

Dawson, L., A. Tobin, et al. (2005). "Antimuscarinic antibodies in Sjogren's syndrome: where are we, and where are we going?" Arthritis Rheum **52**(10): 2984-2995.

Dawson, L. J., H. E. Allison, et al. (2004). "Putative anti-muscarinic antibodies cannot be detected in patients with primary Sjogren's syndrome using conventional immunological approaches." Rheumatology (Oxford) **43**(12): 1488-1495.

Dawson, L. J., S. E. Christmas, et al. (2000). "An investigation of interactions between the immune system and stimulus-secretion coupling in mouse submandibular acinar cells. A possible mechanism to account for reduced salivary flow rates associated with the onset of Sjogren's syndrome." Rheumatology (Oxford) **39**(11): 1226-1233.

Dawson, L. J., E. A. Field, et al. (2001). "Acetylcholine-evoked calcium mobilization and ion channel activation in human labial gland acinar cells from patients with primary Sjogren's syndrome." Clin Exp Immunol **124**(3): 480-485.

Dawson, L. J., P. C. Fox, et al. (2006). "Sjogrens syndrome--the non-apoptotic model of glandular hypofunction." Rheumatology (Oxford) **45**(7): 792-798.

Dawson, L. J., D. J. Holt, et al. (2001). "A comparison of salivary gland hypofunction in primary and secondary Sjogren's syndrome." Oral Dis **7**(1): 28-30.

Dawson, L. J., J. Stanbury, et al. (2006). "Antimuscarinic antibodies in primary Sjogren's syndrome reversibly inhibit the mechanism of fluid secretion by human submandibular salivary acinar cells." Arthritis Rheum **54**(4): 1165-1173.

Deckel, A. W., V. Tang, et al. (2002). "Altered neuronal nitric oxide synthase expression contributes to disease progression in Huntington's disease transgenic mice." Brain research **939**(1-2): 76-86.

Delalande, S., J. de Seze, et al. (2004). "Neurologic manifestations in primary Sjogren syndrome: a study of 82 patients." Medicine (Baltimore) **83**(5): 280-291.

Delaney, C. A., B. Tyrberg, et al. (1996). "Sensitivity of human pancreatic islets to peroxynitrite-induced cell dysfunction and death." FEBS letters **394**(3): 300-306.

delaTorre, A., R. A. Schroeder, et al. (1998). "Differential effects of nitric oxide-mediated S-nitrosylation on p50 and c-jun DNA binding." Surgery **124**(2): 137-141; discussion 141-132.

Denninger, J. W. and M. A. Marletta (1999). "Guanylate cyclase and the NO/cGMP signaling pathway." Biochimica et Biophysica Acta (BBA)-Bioenergetics **1411**(2-3): 334-350.

Devogelaere, B., L. Verbert, et al. (2008). "The complex regulatory function of the ligand-binding domain of the inositol 1, 4, 5-trisphosphate receptor." Cell Calcium **43**(1): 17-27.

Dickhout, J. G., G. S. Hossain, et al. (2005). "Peroxynitrite Causes Endoplasmic Reticulum Stress and Apoptosis in Human Vascular Endothelium." Arteriosclerosis, thrombosis, and vascular biology **25**(12): 2623-2629.

Dinarello, C. A. (2000). "Proinflammatory cytokines." Chest **118**(2): 503-508.

Ding, C., B. Walcott, et al. (2001). "Neuronal nitric oxide synthase and the autonomic innervation of the mouse lacrimal gland." Investigative ophthalmology & visual science **42**(12): 2789.

Ding, C., B. Walcott, et al. (2003). "Sympathetic neural control of the mouse lacrimal gland." Investigative ophthalmology & visual science **44**(4): 1513.

Dong, J., E. Jimi, et al. (2010). "Constitutively active NF-kappaB triggers systemic TNFalpha-dependent inflammation and localized TNFalpha-independent inflammatory disease." Genes Dev **24**(16): 1709-1717.

Drachman, D. B. (1990). "How to recognize an antibody-mediated autoimmune disease: criteria." Res Publ Assoc Res Nerv Ment Dis **68**: 183-186.

Drachman, D. B. (1994). "Myasthenia gravis." N Engl J Med **330**(25): 1797-1810.

Drachman, D. B. (2003). "Autonomic "myasthenia": the case for an autoimmune pathogenesis." J Clin Invest **111**(6): 797-799.

Feelisch, M., P. Kotsonis, et al. (1999). "The soluble guanylyl cyclase inhibitor 1H-[1,2,4]oxadiazolo[4,3,-a] quinoxalin-1-one is a nonselective heme protein inhibitor of nitric oxide synthase and other cytochrome P-450 enzymes involved in nitric oxide donor bioactivation." Mol Pharmacol **56**(2): 243-253.

Feron, O., L. Belhassen, et al. (1996). "Endothelial nitric oxide synthase targeting to caveolae." Journal of Biological Chemistry **271**(37): 22810.

Feron, O., X. Han, et al. (1999). "Muscarinic cholinergic signaling in cardiac myocytes: dynamic targeting of M2AChR to sarcolemmal caveolae and eNOS activation." Life sciences **64**(6-7): 471-477.

Fill, M. and J. A. Copello (2002). "Ryanodine receptor calcium release channels." Physiological reviews **82**(4): 893-922.

Finch, E. A., T. J. Turner, et al. (1991). "Calcium as a coagonist of inositol 1,4,5-trisphosphate-induced calcium release." Science **252**(5004): 443-446.

Forstermann, U., I. Gath, et al. (1995). "Isoforms of nitric oxide synthase. Properties, cellular distribution and expressional control." Biochem Pharmacol **50**(9): 1321-1332.

Fox, P. C. (2007). "Autoimmune diseases and Sjogren's syndrome: an autoimmune exocrinopathy." Ann N Y Acad Sci **1098**: 15-21.

Fox, P. C. and P. M. Speight (1996). "Current concepts of autoimmune exocrinopathy: immunologic mechanisms in the salivary pathology of Sjogren's syndrome." Crit Rev Oral Biol Med **7**(2): 144-158.

Fox, R. I. (2005). "Sjogren's syndrome." Lancet **366**(9482): 321-331.

Fox, R. I. and T. Maruyama (1997). "Pathogenesis and treatment of Sjogren's syndrome." Curr Opin Rheumatol **9**(5): 393-399.

Fox, R. I., C. A. Robinson, et al. (1986). "Sjogren's syndrome. Proposed criteria for classification." Arthritis Rheum **29**(5): 577-585.

Fox, R. I. and I. Saito (1994). "Criteria for diagnosis of Sjogren's syndrome." Rheum Dis Clin North Am **20**(2): 391-407.

Fox, R. I. and M. Stern (2002). "Sjogren's syndrome: mechanisms of pathogenesis involve interaction of immune and neurosecretory systems." Scand J Rheumatol Suppl(116): 3-13.

Fox, R. I., J. Tornwall, et al. (1999). "Current issues in the diagnosis and treatment of Sjogren's syndrome." Curr Opin Rheumatol **11**(5): 364-371.

Fu, D. and M. Lu (2007). "The structural basis of water permeation and proton exclusion in aquaporins." Mol Membr Biol **24**(5-6): 366-374.

Furchgott, R. F. and J. V. Zawadzki (1980). "The obligatory role of endothelial cells in the relaxation of arterial smooth muscle by acetylcholine." Nature **288**(5789): 373-376.

Galione, A., H. C. Lee, et al. (1991). "Ca($^{2+}$)-induced Ca^{2+} release in sea urchin egg homogenates: modulation by cyclic ADP-ribose." Science **253**(5024): 1143-1146.

Galione, A., A. McDougall, et al. (1993). "Redundant mechanisms of calcium-induced calcium release underlying calcium waves during fertilization of sea urchin eggs." Science **261**(5119): 348-352.

Galione, A., A. White, et al. (1993). "cGMP mobilizes intracellular Ca^{2+} in sea urchin eggs by stimulating cyclic ADP-ribose synthesis." Nature **365**(6445): 456-459.

Gallacher, D. V. and P. M. Smith (1999). "Autonomic transmitters and Ca^{2+}-activated cellular responses in salivary glands in vitro." Neural mechanisms of salivary secretion. Karger, Basel: 80-93.

Garthwaite, J., E. Southam, et al. (1995). "Potent and selective inhibition of nitric oxide-sensitive guanylyl cyclase by 1H-[1,2,4]oxadiazolo[4,3-a]quinoxalin-1-one." Mol Pharmacol **48**(2): 184-188.

Geller, D. A. and T. R. Billiar (1998). "Molecular biology of nitric oxide synthases." Cancer and Metastasis Reviews **17**(1): 7-23.

Goldblatt, F., T. P. Gordon, et al. (2002). "Antibody-mediated gastrointestinal dysmotility in scleroderma." Gastroenterology **123**(4): 1144-1150.

Goligorsky, M. S., H. Li, et al. (2002). "Relationships between caveolae and eNOS: everything in proximity and the proximity of everything." American Journal of Physiology-Renal Physiology **283**(1): F1.

Gonen, T. and T. Walz (2006). "The structure of aquaporins." Q Rev Biophys **39**(4): 361-396.

Gordon, T. P., A. I. Bolstad, et al. (2001). "Autoantibodies in primary Sjogren's syndrome: new insights into mechanisms of autoantibody diversification and disease pathogenesis." Autoimmunity **34**(2): 123-132.

Govers, R. and S. Oess (2004). "To NO or not to NO:'where?'is the question." Histology and histopathology **19**(2): 585.

Grabowski, P. S., A. J. England, et al. (1996). "Elevated nitric oxide production in rheumatoid arthritis: detection using the fasting urinary nitrate: creatinine ratio." Arthritis & Rheumatism **39**(4): 643-647.

Gromada, J., T. D. Jorgensen, et al. (1995). "Cyclic ADP-ribose and inositol 1,4,5-triphosphate mobilizes Ca2+ from distinct intracellular pools in permeabilized lacrimal acinar cells." FEBS Lett **360**(3): 303-306.

Gromada, J., T. D. Jorgensen, et al. (1995). "The release of intracellular Ca2+ in lacrimal acinar cells by alpha-, beta-adrenergic and muscarinic cholinergic stimulation: the roles of inositol triphosphate and cyclic ADP-ribose." Pflugers Arch **429**(6): 751-761.

Gryglewski, R. J., R. M. Palmer, et al. (1986). "Superoxide anion is involved in the breakdown of endothelium-derived vascular relaxing factor." Nature **320**(6061): 454-456.

Hakamata, Y., J. Nakai, et al. (1992). "Primary structure and distribution of a novel ryanodine receptor/calcium release channel from rabbit brain." FEBS Lett **312**(2-3): 229-235.

Halse, A. K., M. C. Marthinussen, et al. (2000). "Isotype distribution of anti-Ro/SS-A and anti-La/SS-B antibodies in plasma and saliva of patients with Sjogren's syndrome." Scand J Rheumatol **29**(1): 13-19.

Hamilton, S. L. and Serysheva, II (2009). "Ryanodine receptor structure: progress and challenges." J Biol Chem **284**(7): 4047-4051.

Han, S. J., F. F. Hamdan, et al. (2005). "Pronounced conformational changes following agonist activation of the M(3) muscarinic acetylcholine receptor." J Biol Chem **280**(26): 24870-24879.

Haneji, N., T. Nakamura, et al. (1997). "Identification of alpha-fodrin as a candidate autoantigen in primary Sjogren's syndrome." Science **276**(5312): 604-607.

Harmer, A. R., D. V. Gallacher, et al. (2001). "Role of Ins(1,4,5)P3, cADP-ribose and nicotinic acid-adenine dinucleotide phosphate in Ca^{2+} signalling in mouse submandibular acinar cells." Biochem J **353**(Pt 3): 555-560.

Harmer, A. R., P. M. Smith, et al. (2005). "Local and global calcium signals and fluid and electrolyte secretion in mouse submandibular acinar cells." Am J Physiol Gastrointest Liver Physiol **288**(1): G118-124.

Haynes, V., S. Elfering, et al. (2004). "Mitochondrial nitric-oxide synthase: enzyme expression, characterization, and regulation." Journal of bioenergetics and biomembranes **36**(4): 341-346.

Hazes, J. M. and A. J. Silman (1990). "Review of UK data on the rheumatic diseases--2. Rheumatoid arthritis." Br J Rheumatol **29**(4): 310-312.

He, J., J. Zhao, et al. (2008). "Mucosal administration of alpha-fodrin inhibits experimental Sjogren's syndrome autoimmunity." Arthritis Res Ther **10**(2): R44.

Hegyi, P. and Z. Rakonczay Jr (2011). "The Role of Nitric Oxide in the Physiology and Pathophysiology of the Exocrine Pancreas." Antioxidants & Redox Signaling.

Hellmich, M. R. and F. Strumwasser (1991). "Purification and characterization of a molluscan egg-specific NADase, a second-messenger enzyme." Cell Regul **2**(3): 193-202.

Hodges, R. R., M. A. Shatos, et al. (2005). "Nitric Oxide and cGMP Mediate α1D-Adrenergic Receptor–Stimulated Protein Secretion and p42/p44 MAPK Activation in Rat Lacrimal Gland." Investigative ophthalmology & visual science **46**(8): 2781.

Horsfall, A. C., L. M. Rose, et al. (1989). "Autoantibody synthesis in salivary glands of Sjogren's syndrome patients." J Autoimmun **2**(4): 559-568.

Hu, J., Y. Wang, et al. (2010). "Structural basis of G protein-coupled receptor-G protein interactions." Nat Chem Biol **6**(7): 541-548.

Huhmer, A. F., C. R. Nishida, et al. (1997). "Inactivation of the inducible nitric oxide synthase by peroxynitrite." Chem Res Toxicol **10**(5): 618-626.

Huhn, P., G. J. Pruijn, et al. (1997). "Characterization of the autoantigen La (SS-B) as a dsRNA unwinding enzyme." Nucleic Acids Res **25**(2): 410-416.

Hulme, E. C., N. J. Birdsall, et al. (1990). "Muscarinic receptor subtypes." Annu Rev Pharmacol Toxicol **30**: 633-673.

Humphreys-Beher, M. G., J. Brayer, et al. (1999). "An alternative perspective to the immune response in autoimmune exocrinopathy: induction of functional quiescence rather than destructive autoaggression." Scand J Immunol **49**(1): 7-10.

Ignarro, L. J. (2002). "Nitric oxide as a unique signaling molecule in the vascular system: a historical overview." J Physiol Pharmacol **53**(4 Pt 1): 503-514.

Ignarro, L. J., G. M. Buga, et al. (1987). "Endothelium-derived relaxing factor produced and released from artery and vein is nitric oxide." Proceedings of the National Academy of Sciences **84**(24): 9265.

Ishibashi, K., S. Hara, et al. (2009). "Aquaporin water channels in mammals." Clin Exp Nephrol **13**(2): 107-117.

Iwamoto, T. and F. A. Jakobiec (1982). "A comparative ultrastructural study of the normal lacrimal gland and its epithelial tumors." Hum Pathol **13**(3): 236-262.

Jackson, M. W., N. J. Spencer, et al. (2009). "Potentiation of a functional autoantibody in narcolepsy by a cholinesterase inhibitor." Lab Invest **89**(12): 1332-1339.

Jeyakumar, L. H., J. A. Copello, et al. (1998). "Purification and characterization of ryanodine receptor 3 from mammalian tissue." J Biol Chem **273**(26): 16011-16020.

Jonsson, R., H. J. Haga, et al. (2000). "Current concepts on diagnosis, autoantibodies and therapy in Sjogren's syndrome." Scand J Rheumatol **29**(6): 341-348.

Kasri, N. N., K. Torok, et al. (2006). "Endogenously bound calmodulin is essential for the function of the inositol 1,4,5-trisphosphate receptor." J Biol Chem **281**(13): 8332-8338.

Kojima, H., N. Nakatsubo, et al. (1998). "Detection and imaging of nitric oxide with novel fluorescent indicators: diaminofluoresceins." Anal Chem **70**(13): 2446-2453.

Konttinen, Y. T., L. A. Platts, et al. (1997). "Role of nitric oxide in Sjogren's syndrome." Arthritis Rheum **40**(5): 875-883.

Koo, N. Y., J. Li, et al. (2008). "Functional epitope of muscarinic type 3 receptor which interacts with autoantibodies from Sjogren's syndrome patients." Rheumatology (Oxford) **47**(6): 828-833.

Kovacs, L., E. Feher, et al. (2008). "Demonstration of autoantibody binding to muscarinic acetylcholine receptors in the salivary gland in primary Sjogren's syndrome." Clin Immunol **128**(2): 269-276.

Kovacs, L., I. Marczinovits, et al. (2005). "Clinical associations of autoantibodies to human muscarinic acetylcholine receptor 3(213-228) in primary Sjogren's syndrome." Rheumatology (Oxford) **44**(8): 1021-1025.

Krenzer, K. L., M. R. Dana, et al. (2000). "Effect of androgen deficiency on the human meibomian gland and ocular surface." J Clin Endocrinol Metab **85**(12): 4874-4882.

Kroneld, U., A. K. Halse, et al. (1997). "Differential immunological aberrations in patients with primary and secondary Sjogren's syndrome." Scand J Immunol **45**(6): 698-705.

Krylova, L. and D. Isenberg (2010). "Assessment of patients with primary Sjogren's syndrome--outcome over 10 years using the Sjogren's Syndrome Damage Index." Rheumatology (Oxford) **49**(8): 1559-1562.

Lai, F. A., M. Misra, et al. (1989). "The ryanodine receptor-Ca^{2+} release channel complex of skeletal muscle sarcoplasmic reticulum. Evidence for a cooperatively coupled, negatively charged homotetramer." J Biol Chem **264**(28): 16776-16785.

Lee, H. C. (1991). "Specific binding of cyclic ADP-ribose to calcium-storing microsomes from sea urchin eggs." J Biol Chem **266**(4): 2276-2281.

Lee, H. C. and R. Aarhus (1991). "ADP-ribosyl cyclase: an enzyme that cyclizes NAD+ into a calcium-mobilizing metabolite." Cell Regul **2**(3): 203-209.

Lee, H. C., T. F. Walseth, et al. (1989). "Structural determination of a cyclic metabolite of NAD+ with intracellular Ca2+-mobilizing activity." J Biol Chem **264**(3): 1608-1615.

Lee, J., H. Ryu, et al. (2003). "Translational control of inducible nitric oxide synthase expression by arginine can explain the arginine paradox." Proc Natl Acad Sci U S A **100**(8): 4843-4848.

Lee, M. G., X. Xu, et al. (1997). "Polarized expression of Ca^{2+} channels in pancreatic and salivary gland cells. Correlation with initiation and propagation of $[Ca^{2+}]_i$ waves." J Biol Chem **272**(25): 15765-15770.

Li, J., Y. M. Ha, et al. (2004). "Inhibitory effects of autoantibodies on the muscarinic receptors in Sjogren's syndrome." Lab Invest **84**(11): 1430-1438.

Lisi, S., M. Sisto, et al. (2007). "Fcgamma receptors mediate internalization of anti-Ro and anti-La autoantibodies from Sjogren's syndrome and apoptosis in human salivary gland cell line A-253." J Oral Pathol Med **36**(9): 511-523.

Liu, J., G. Garcia-Cardena, et al. (1996). "Palmitoylation of endothelial nitric oxide synthase is necessary for optimal stimulated release of nitric oxide: implications for caveolae localization." Biochemistry **35**(41): 13277-13281.

Liu, J., T. E. Hughes, et al. (1997). "The first 35 amino acids and fatty acylation sites determine the molecular targeting of endothelial nitric oxide synthase into the Golgi region of cells: a green fluorescent protein study." J Cell Biol **137**(7): 1525-1535.

Liu, X., D. Liao, et al. (2001). "Distinct mechanisms of $[Ca^{2+}]_i$ oscillations in HSY and HSG cells: role of Ca2+ influx and internal Ca2+ store recycling." J Membr Biol **181**(3): 185-193.

Liu, X., E. Rojas, et al. (1998). "Regulation of KCa current by store-operated Ca2+ influx depends on internal Ca2+ release in HSG cells." Am J Physiol **275**(2 Pt 1): C571-580.

Looms, D., K. Tritsaris, et al. (2001). "Nitric oxide and cGMP activate Ca^{2+}-release processes in rat parotid acinar cells." Biochemical Journal **355**(Pt 1): 87.

Looms, D. K., S. Dissing, et al. (2000). "Adrenoceptor-activated nitric oxide synthesis in salivary acinar cells." Adv Dent Res **14**: 62-68.

Looms, D. K., K. Tritsaris, et al. (2002). "Nitric oxide-induced signalling in rat lacrimal acinar cells." Acta physiologica scandinavica **174**(2): 109-115.

Ludtke, S. J., I. I. Serysheva, et al. (2005). "The pore structure of the closed RyR1 channel." Structure **13**(8): 1203-1211.

Ludviksdottir, D., C. Janson, et al. (1999). "Increased nitric oxide in expired air in patients with Sjogren's syndrome. BHR study group. Bronchial hyperresponsiveness." Eur Respir J **13**(4): 739-743.

Lukowski, S., M. C. Lecomte, et al. (1996). "Inhibition of phospholipase D activity by fodrin. An active role for the cytoskeleton." J Biol Chem **271**(39): 24164-24171.

Lundberg, J., S. Nordvall, et al. (1996). "Exhaled nitric oxide in paediatric asthma and cystic fibrosis." Archives of disease in childhood **75**(4): 323-326.

MacMicking, J., Q. W. Xie, et al. (1997). "Nitric oxide and macrophage function." Annu Rev Immunol **15**: 323-350.

Mak, D. O., S. M. McBride, et al. (2003). "Spontaneous channel activity of the inositol 1,4,5-trisphosphate (InsP3) receptor (InsP3R). Application of allosteric modeling to calcium and InsP3 regulation of InsP3R single-channel gating." J Gen Physiol **122**(5): 583-603.

Mandl, T., V. Granberg, et al. (2008). "Autonomic nervous symptoms in primary Sjogren's syndrome." Rheumatology (Oxford) **47**(6): 914-919.

Maraia, R. J. (1996). "Transcription termination factor La is also an initiation factor for RNA polymerase III." Proc Natl Acad Sci U S A **93**(8): 3383-3387.

Marczinovits, I., L. Kovacs, et al. (2005). "A peptide of human muscarinic acetylcholine receptor 3 is antigenic in primary Sjogren's syndrome." J Autoimmun **24**(1): 47-54.

Marks, A. R., P. Tempst, et al. (1989). "Molecular cloning and characterization of the ryanodine receptor/junctional channel complex cDNA from skeletal muscle sarcoplasmic reticulum." Proc Natl Acad Sci U S A **86**(22): 8683-8687.

Marks, G. S., B. E. McLaughlin, et al. (1995). "Time-dependent increase in nitric oxide formation concurrent with vasodilation induced by sodium nitroprusside, 3-morpholinosydnonimine, and S-nitroso-N-acetylpenicillamine but not by glyceryl trinitrate." Drug Metab Dispos **23**(11): 1248-1252.

Marletta, M. A., A. R. Hurshman, et al. (1998). "Catalysis by nitric oxide synthase." Current opinion in chemical biology **2**(5): 656-663.

Marshall, H. E. and J. S. Stamler (2001). "Inhibition of NF-kappa B by S-nitrosylation." Biochemistry **40**(6): 1688-1693.

Marziali, G., D. Rossi, et al. (1996). "cDNA cloning reveals a tissue specific expression of alternatively spliced transcripts of the ryanodine receptor type 3 (RyR3) calcium release channel." FEBS Lett **394**(1): 76-82.

Masuda, W. and T. Noguchi (2000). "ADP-Ribosyl cyclase in rat salivary glands." Biochem Biophys Res Commun **270**(2): 469-472.

Matsui, M., D. Motomura, et al. (2000). "Multiple functional defects in peripheral autonomic organs in mice lacking muscarinic acetylcholine receptor gene for the M3 subtype." Proc Natl Acad Sci U S A **97**(17): 9579-9584.

Matthews, J. R., C. H. Botting, et al. (1996). "Inhibition of NF-kappaB DNA binding by nitric oxide." Nucleic Acids Res **24**(12): 2236-2242.

McCauliffe, D. P., F. A. Lux, et al. (1990). "Molecular cloning, expression, and chromosome 19 localization of a human Ro/SS-A autoantigen." J Clin Invest **85**(5): 1379-1391.

Medina-Ortiz, W. E., E. V. Gregg, et al. (2007). "Identification and functional distribution of intracellular ca channels in mouse lacrimal gland acinar cells." Open Ophthalmol J **1**: 8-16.

Meneray, M. A., D. J. Bennett, et al. (1998). "Effect of sensory denervation on the structure and physiologic responsiveness of rabbit lacrimal gland." Cornea **17**(1): 99-107.

Michel, T., G. K. Li, et al. (1993). "Phosphorylation and subcellular translocation of endothelial nitric oxide synthase." Proceedings of the National Academy of Sciences **90**(13): 6252.

Michikawa, H., Y. Mitsui, et al. (1998). "cGMP production is coupled to Ca2+-dependent nitric oxide generation in rabbit parotid acinar cells." Cell Calcium **23**(6): 405-412.

Mikoshiba, K., C. Hisatsune, et al. (2008). "The role of Ca^{2+} signaling in cell function with special reference to exocrine secretion." Cornea **27 Suppl 1**: S3-8.

Mitsui, Y. and S. Furuyama (2000). "Characterization of nitric oxide synthase in the rat parotid gland." Arch Oral Biol **45**(7): 531-536.

Miyakawa, T., A. Mizushima, et al. (2001). "$Ca(^{2+})$-sensor region of IP(3) receptor controls intracellular Ca(2+) signaling." EMBO J **20**(7): 1674-1680.

Miyazaki, K., N. Takeda, et al. (2005). "Analysis of in vivo role of alpha-fodrin autoantigen in primary Sjogren's syndrome." Am J Pathol **167**(4): 1051-1059.

Morgan, W. S. and B. Castleman (1953). "A clinicopathologic study of Mikulicz's disease." Am J Pathol **29**(3): 471-503.

Mori, K., M. Iijima, et al. (2005). "The wide spectrum of clinical manifestations in Sjogren's syndrome-associated neuropathy." Brain **128**(Pt 11): 2518-2534.

Mori, M. (2007). "Regulation of nitric oxide synthesis and apoptosis by arginase and arginine recycling." The Journal of nutrition **137**(6): 1616S.

Mori, M. and T. Gotoh (2000). "Regulation of nitric oxide production by arginine metabolic enzymes." Biochemical and biophysical research communications **275**(3): 715-719.

Moro, M. A., R. J. Russel, et al. (1996). "cGMP mediates the vascular and platelet actions of nitric oxide: confirmation using an inhibitor of the soluble guanylyl cyclase." Proc Natl Acad Sci U S A **93**(4): 1480-1485.

Morris, A. J. and C. C. Malbon (1999). "Physiological regulation of G protein-linked signaling." Physiol Rev **79**(4): 1373-1430.

Moutsopoulos, H. M., T. M. Chused, et al. (1980). "Sjogren's syndrome (Sicca syndrome): current issues." Ann Intern Med **92**(2 Pt 1): 212-226.

Moutsopoulos, H. M., D. L. Mann, et al. (1979). "Genetic differences between primary and secondary sicca syndrome." N Engl J Med **301**(14): 761-763.

Mungrue, I. N. and D. S. Bredt (2004). "nNOS at a glance: implications for brain and brawn." Journal of cell science **117**(13): 2627.

Murad, F. (1986). "Cyclic guanosine monophosphate as a mediator of vasodilation." Journal of Clinical Investigation **78**(1): 1.

Nadif Kasri, N., G. Bultynck, et al. (2002). "The role of calmodulin for inositol 1,4,5-trisphosphate receptor function." Biochim Biophys Acta **1600**(1-2): 19-31.

Nagy, K., V. Szlavik, et al. (2007). "Human submandibular gland (HSG) cell line as a model for studying salivary gland Ca^{2+} signalling mechanisms." Acta Physiol Hung **94**(4): 301-313.

Naito, Y., I. Matsumoto, et al. (2005). "Muscarinic acetylcholine receptor autoantibodies in patients with Sjogren's syndrome." Ann Rheum Dis **64**(3): 510-511.

Nakai, J., T. Imagawa, et al. (1990). "Primary structure and functional expression from cDNA of the cardiac ryanodine receptor/calcium release channel." FEBS Lett **271**(1-2): 169-177.

Nakamura, H., T. Koji, et al. (1998). "Apoptosis in labial salivary glands from Sjogren's syndrome (SS) patients: comparison with human T lymphotropic virus-I (HTLV-I)-seronegative and -seropositive SS patients." Clin Exp Immunol **114**(1): 106-112.

Nakamura, T., M. Matsui, et al. (2004). "M(3) muscarinic acetylcholine receptor plays a critical role in parasympathetic control of salivation in mice." J Physiol **558**(Pt 2): 561-575.

Nguyen, K. H., J. Brayer, et al. (2000). "Evidence for antimuscarinic acetylcholine receptor antibody-mediated secretory dysfunction in nod mice." Arthritis Rheum **43**(10): 2297-2306.

Nordmark, G., F. Rorsman, et al. (2003). "Autoantibodies to alpha-fodrin in primary Sjogren's syndrome and SLE detected by an in vitro transcription and translation assay." Clin Exp Rheumatol **21**(1): 49-56.

O'Brien, C. A. and S. L. Wolin (1994). "A possible role for the 60-kD Ro autoantigen in a discard pathway for defective 5S rRNA precursors." Genes Dev **8**(23): 2891-2903.

Obata, H. (2006). "Anatomy and histopathology of the human lacrimal gland." Cornea **25**(10 Suppl 1): S82-89.

Ortiz, P. and J. Garvin (2003). "Trafficking and activation of eNOS in epithelial cells." Acta physiologica scandinavica **179**(2): 107-114.

Oshiro, A. C., S. J. Derbes, et al. (1997). "Anti-Ro/SS-A and anti-La/SS-B antibodies associated with cardiac involvement in childhood systemic lupus erythematosus." Ann Rheum Dis **56**(4): 272-274.

Ozdemir, M. and H. Temizdemir (2010). "Age- and gender-related tear function changes in normal population." Eye (Lond) **24**(1): 79-83.

Patel, S., S. K. Joseph, et al. (1999). "Molecular properties of inositol 1,4,5-trisphosphate receptors." Cell Calcium **25**(3): 247-264.

Patton, L. L., S. Pollack, et al. (1991). "Responsiveness of a human parotid epithelial cell line (HSY) to autonomic stimulation: muscarinic control of K^+ transport." In Vitro Cell Dev Biol **27A**(10): 779-785.

Pedersen, A. M., S. Dissing, et al. (2000). "Innervation pattern and Ca^{2+} signalling in labial salivary glands of healthy individuals and patients with primary Sjogren's syndrome (pSS)." J Oral Pathol Med **29**(3): 97-109.

Pellizzoni, L., F. Lotti, et al. (1998). "Involvement of the Xenopus laevis Ro60 autoantigen in the alternative interaction of La and CNBP proteins with the 5'UTR of L4 ribosomal protein mRNA." J Mol Biol **281**(4): 593-608.

Peng, B., J. Ling, et al. (2010). "Defective feedback regulation of NF-kappaB underlies Sjogren's syndrome in mice with mutated kappaB enhancers of the IkappaBalpha promoter." Proc Natl Acad Sci U S A **107**(34): 15193-15198.

Pepeu, G. and M. G. Giovannini (2010). "Cholinesterase inhibitors and memory." Chem Biol Interact **187**(1-3): 403-408.

Perez Leiros, C., L. Sterin-Borda, et al. (1999). "Activation of nitric oxide signaling through muscarinic receptors in submandibular glands by primary Sjogren syndrome antibodies." Clin Immunol **90**(2): 190-195.

Perrin, D. and D. Aunis (1985). "Reorganization of alpha-fodrin induced by stimulation in secretory cells." Nature **315**(6020): 589-592.

Perrin, D., O. K. Langley, et al. (1987). "Anti-alpha-fodrin inhibits secretion from permeabilized chromaffin cells." Nature **326**(6112): 498-501.

Pertovaara, M., J. Antonen, et al. (2007). "Endothelial nitric oxide synthase +894 polymorphism is associated with recurrent salivary gland swelling and early onset in patients with primary Sjogren's syndrome." Ann Rheum Dis **66**(10): 1400-1401.

Pflugfelder, S. C. (2004). "Antiinflammatory therapy for dry eye." Am J Ophthalmol **137**(2): 337-342.

Pillemer, S. R., E. L. Matteson, et al. (2001). "Incidence of physician-diagnosed primary Sjogren syndrome in residents of Olmsted County, Minnesota." Mayo Clin Proc **76**(6): 593-599.

Piper, H. (1990). "100 years of the Mikulicz syndrome]." Gesnerus **47**: 83.

Pourmand, N., M. Wahren-Herlenius, et al. (1999). "Ro/SSA and La/SSB specific IgA autoantibodies in serum of patients with Sjogren's syndrome and systemic lupus erythematosus." Ann Rheum Dis **58**(10): 623-629.

Prosperi, E., A. C. Croce, et al. (1986). "Flow cytometric analysis of membrane permeability properties influencing intracellular accumulation and efflux of fluorescein." Cytometry **7**(1): 70-75.

Putney, J. W., Jr. and G. S. Bird (1994). "The inositol phosphate-calcium signalling system in lacrimal gland cells." Adv Exp Med Biol **350**: 115-119.

Rajagopalan, S., D. Pfenninger, et al. (2003). "Increased asymmetric dimethylarginine and endothelin 1 levels in secondary Raynaud's phenomenon: implications for vascular dysfunction and progression of disease." Arthritis Rheum **48**(7): 1992-2000.

Rajan, T., P. Porte, et al. (1996). "Role of nitric oxide in host defense against an extracellular, metazoan parasite, Brugia malayi." Infection and immunity **64**(8): 3351.

Rebecchi, M. J. and S. N. Pentyala (2000). "Structure, function, and control of phosphoinositide-specific phospholipase C." Physiol Rev **80**(4): 1291-1335.

Reina, S., L. Sterin-Borda, et al. (2004). "Human mAChR antibodies from Sjögren syndrome sera increase cerebral nitric oxide synthase activity and nitric oxide synthase mRNA level." Clinical Immunology **113**(2): 193-202.

Robinson, C. P., J. Brayer, et al. (1998). "Transfer of human serum IgG to nonobese diabetic Igmu null mice reveals a role for autoantibodies in the loss of secretory function of exocrine tissues in Sjogren's syndrome." Proc Natl Acad Sci U S A **95**(13): 7538-7543.

Roescher, N., A. Kingman, et al. (2011). "Peptide-based ELISAs are not sensitive and specific enough to detect muscarinic receptor type 3 autoantibodies in serum from patients with Sjogren's syndrome." Ann Rheum Dis **70**(1): 235-236.

Ruiz-Tiscar, J. L., F. J. Lopez-Longo, et al. (2005). "Prevalence of IgG anti-{alpha}-fodrin antibodies in Sjogren's syndrome." Ann N Y Acad Sci **1050**: 210-216.

Ruskell, G. L. (1969). "Changes in nerve terminals and acini of the lacrimal gland and changes in secretion induced by autonomic denervation." Z Zellforsch Mikrosk Anat **94**(2): 261-281.

Ruskell, G. L. (1971). "The distribution of autonomic post-ganglionic nerve fibres to the lacrimal gland in monkeys." J Anat **109**(Pt 2): 229-242.

Sack, R. A., K. O. Tan, et al. (1992). "Diurnal tear cycle: evidence for a nocturnal inflammatory constitutive tear fluid." Invest Ophthalmol Vis Sci **33**(3): 626-640.

Saeki, M., S. Maeda, et al. (2002). "Insulin-like growth factor-1 protects peroxynitrite-induced cell death by preventing cytochrome c-induced caspase-3 activation." Journal of cellular biochemistry **84**(4): 708-716.

Sayed, N., P. Baskaran, et al. (2007). "Desensitization of soluble guanylyl cyclase, the NO receptor, by S-nitrosylation." Proc Natl Acad Sci U S A **104**(30): 12312-12317.

Sayed, N., D. D. Kim, et al. (2008). "Nitroglycerin-induced S-nitrosylation and desensitization of soluble guanylyl cyclase contribute to nitrate tolerance." Circ Res **103**(6): 606-614.

Schrammel, A., S. Behrends, et al. (1996). "Characterization of 1H-[1, 2, 4] oxadiazolo [4, 3-a] *quinoxalin-1-one* as a heme-site inhibitor of nitric oxide-sensitive guanylyl cyclase." Molecular pharmacology **50**(1): 1.

Schuh, K., S. Uldrijan, et al. (2001). "The plasmamembrane calmodulin–dependent calcium pump." The Journal of cell biology **155**(2): 201.

Scully, C. (1986). "Sjogren's syndrome: clinical and laboratory features, immunopathogenesis, and management." Oral Surg Oral Med Oral Pathol **62**(5): 510-523.

Sessa, W. C., C. M. Barber, et al. (1993). "Mutation of N-myristoylation site converts endothelial cell nitric oxide synthase from a membrane to a cytosolic protein." Circulation research **72**(4): 921-924.

Shaul, P. W. (2002). "Regulation of endothelial nitric oxide synthase: location, location, location." Annu Rev Physiol **64**: 749-774.

Shaul, P. W., E. J. Smart, et al. (1996). "Acylation targets emdothelial nitric-oxide synthase to plasmalemmal caveolae." J Biol Chem **271**(11): 6518-6522.

Shiozawa, S., Y. Tanaka, et al. (1998). "Single-blinded controlled trial of low-dose oral IFN-alpha for the treatment of xerostomia in patients with Sjogren's syndrome." J Interferon Cytokine Res **18**(4): 255-262.

Ship, J. A., P. C. Fox, et al. (1999). "Treatment of primary Sjogren's syndrome with low-dose natural human interferon-alpha administered by the oral mucosal route: a phase II clinical trial. IFN Protocol Study Group." J Interferon Cytokine Res **19**(8): 943-951.

Shirasuna, K., M. Sato, et al. (1981). "A neoplastic epithelial duct cell line established from an irradiated human salivary gland." Cancer **48**(3): 745-752.

Siman, R., M. Baudry, et al. (1985). "Regulation of glutamate receptor binding by the cytoskeletal protein fodrin." Nature **313**(5999): 225-228.

Singer, N. G., I. Tomanova-Soltys, et al. (2008). "Sjogren's syndrome in childhood." Curr Rheumatol Rep **10**(2): 147-155.

Sisto, M., S. Lisi, et al. (2007). "Autoantibodies from Sjogren's syndrome trigger apoptosis in salivary gland cell line." Ann N Y Acad Sci **1108**: 418-425.

Smith, A. J., M. W. Jackson, et al. (2004). "A functional autoantibody in narcolepsy." Lancet **364**(9451): 2122-2124.

Smith, A. J., M. W. Jackson, et al. (2005). "Neutralization of muscarinic receptor autoantibodies by intravenous immunoglobulin in Sjogren syndrome." Hum Immunol **66**(4): 411-416.

Smith, C. L., S. Anthony, et al. (2005). "Effects of ADMA upon gene expression: an insight into the pathophysiological significance of raised plasma ADMA." PLoS Med **2**(10): e264.

Smith, P. M. (1992). "Ins(1,3,4,5)P_4 promotes sustained activation of the Ca^{2+}-dependent Cl^- current in isolated mouse lacrimal cells." Biochem J **283**(Pt 1): 27-30.

Smith, P. M. (1992). "Patch-clamp whole-cell pulse protocol measurements using a microcomputer." J Physiol (Lond) **446**: 72P.

Smith, P. M. and D. V. Gallacher (1992). "Acetylcholine- and caffeine-evoked repetitive transient Ca(2+)-activated K+ and C1- currents in mouse submandibular cells." J Physiol **449**: 109-120.

Soff, G. A., T. L. Cornwell, et al. (1997). "Smooth muscle cell expression of type I cyclic GMP-dependent protein kinase is suppressed by continuous exposure to nitrovasodilators, theophylline, cyclic GMP, and cyclic AMP." Journal of Clinical Investigation **100**(10): 2580.

Solomonson, L. P., Flam, B.R., Pendleton, L.C., Goodwin, B.L., Eichler, D.C. (2003). "The caveolar nitric oxide synthase/arginine regeneration system for NO production in endothelial cells." J Exp Biol **206**: 2083-2087.

Southan, G. J. and C. Szabo (1996). "Selective pharmacological inhibition of distinct nitric oxide synthase isoforms." Biochem Pharmacol **51**(4): 383-394.

Stamler, J. S., S. Lamas, et al. (2001). "Nitrosylation. the prototypic redox-based signaling mechanism." Cell **106**(6): 675.

Suarez-Pinzon, W. L., C. Szabo, et al. (1997). "Development of autoimmune diabetes in NOD mice is associated with the formation of peroxynitrite in pancreatic islet -cells." Diabetes-American Diabetes Association **46**(5): 907-911.

Sugiya, H., Y. Mitsui, et al. (2001). "$Ca^{(2+)}$-regulated nitric oxide generation in rabbit parotid acinar cells." Cell Calcium **30**(2): 107-116.

Sullivan, D. A., B. D. Sullivan, et al. (2000). "Androgen influence on the meibomian gland." Invest Ophthalmol Vis Sci **41**(12): 3732-3742.

Sullivan, J. and J. Pollock (2003). "NOS 3 subcellular localization in the regulation of nitric oxide production." Acta physiologica scandinavica **179**(2): 115-122.

Sun, J., C. Xin, et al. (2001). "Cysteine-3635 is responsible for skeletal muscle ryanodine receptor modulation by NO." Proc Natl Acad Sci U S A **98**(20): 11158-11162.

Taha, Z., F. Kiechle, et al. (1992). "Oxidation of nitric oxide by oxygen in biological systems monitored by porphyrinic sensor." Biochem Biophys Res Commun **188**(2): 734-739.

Takeshima, H., S. Nishimura, et al. (1989). "Primary structure and expression from complementary DNA of skeletal muscle ryanodine receptor." Nature **339**(6224): 439-445.

Tan, E. M. (1989). "Antinuclear antibodies: diagnostic markers for autoimmune diseases and probes for cell biology." Adv Immunol **44**: 93-151.

Theander, E., G. Henriksson, et al. (2006). "Lymphoma and other malignancies in primary Sjogren's syndrome: a cohort study on cancer incidence and lymphoma predictors." Ann Rheum Dis **65**(6): 796-803.

Thomas, E., E. M. Hay, et al. (1998). "Sjogren's syndrome: a community-based study of prevalence and impact." Br J Rheumatol **37**(10): 1069-1076.

Thorn, P., O. Gerasimenko, et al. (1994). "Cyclic ADP-ribose regulation of ryanodine receptors involved in agonist evoked cytosolic Ca^{2+} oscillations in pancreatic acinar cells." EMBO J **13**(9): 2038-2043.

Tishler, M., I. Yaron, et al. (1999). "Hydroxychloroquine treatment for primary Sjogren's syndrome: its effect on salivary and serum inflammatory markers." Ann Rheum Dis **58**(4): 253-256.

Toda, N., K. Ayajiki, et al. (2000). "Preganglionic and postganglionic neurons responsible for cerebral vasodilation mediated by nitric oxide in anesthetized dogs." J Cereb Blood Flow Metab **20**(4): 700-708.

Togashi, H., M. Sasaki, et al. (1997). "Neuronal (type I) nitric oxide synthase regulates nuclear factor kappaB activity and immunologic (type II) nitric oxide synthase expression." Proc Natl Acad Sci U S A **94**(6): 2676-2680.

Togo, T., O. Katsuse, et al. (2004). "Nitric oxide pathways in Alzheimer's disease and other neurodegenerative dementias." Neurological research **26**(5): 563-566.

Toker, E., S. Yavuz, et al. (2004). "Anti-Ro/SSA and anti-La/SSB autoantibodies in the tear fluid of patients with Sjogren's syndrome." Br J Ophthalmol **88**(3): 384-387.

Toshida, H., D. H. Nguyen, et al. (2007). "Evaluation of novel dry eye model: preganglionic parasympathetic denervation in rabbit." Invest Ophthalmol Vis Sci **48**(10): 4468-4475.

Tsikas, D., R. H. Boger, et al. (2000). "Endogenous nitric oxide synthase inhibitors are responsible for the L-arginine paradox." FEBS Lett **478**(1-2): 1-3.

Turkcapar, N., U. Olmez, et al. (2006). "The importance of alpha-fodrin antibodies in the diagnosis of Sjogren's syndrome." Rheumatol Int **26**(4): 354-359.

Ulbricht, K. U., R. E. Schmidt, et al. (2003). "Antibodies against alpha-fodrin in Sjogren's syndrome." Autoimmun Rev **2**(2): 109-113.

Venturi, E., S. Pitt, et al. (2010). "From Eggs to Hearts: What Is the Link between Cyclic ADP-Ribose and Ryanodine Receptors?" Cardiovascular Therapeutics.

Virág, L., É. Szabó, et al. (2003). "Peroxynitrite-induced cytotoxicity: mechanism and opportunities for intervention." Toxicology letters **140**: 113-124.

Vitali, C., S. Bombardieri, et al. (2002). "Classification criteria for Sjogren's syndrome: a revised version of the European criteria proposed by the American-European Consensus Group." Ann Rheum Dis **61**(6): 554-558.

Vitali, C., S. Bombardieri, et al. (1993). "Preliminary criteria for the classification of Sjogren's syndrome. Results of a prospective concerted action supported by the European Community." Arthritis Rheum **36**(3): 340-347.

Vitali, C., S. Bombardieri, et al. (1996). "Assessment of the European classification criteria for Sjogren's syndrome in a series of clinically defined cases: results of a prospective multicentre study. The European Study Group on Diagnostic Criteria for Sjogren's Syndrome." Ann Rheum Dis **55**(2): 116-121.

Walcott, B. (1998). "The Lacrimal Gland and Its Veil of Tears." News Physiol Sci **13**: 97-103.

Walford, G. A., R. L. Moussignac, et al. (2004). "Hypoxia potentiates nitric oxide-mediated apoptosis in endothelial cells via peroxynitrite-induced activation of mitochondria-dependent and-independent pathways." Journal of Biological Chemistry **279**(6): 4425.

Wanchu, A., M. Khullar, et al. (2000). "Elevated nitric oxide production in patients with primary Sjogren's syndrome." Clin Rheumatol **19**(5): 360-364.

Wang, F., M. W. Jackson, et al. (2004). "Passive transfer of Sjogren's syndrome IgG produces the pathophysiology of overactive bladder." Arthritis Rheum **50**(11): 3637-3645.

Ward, S. D., F. F. Hamdan, et al. (2006). "Use of an in situ disulfide cross-linking strategy to study the dynamic properties of the cytoplasmic end of transmembrane domain VI of the M3 muscarinic acetylcholine receptor." Biochemistry **45**(3): 676-685.

Ward, S. D., F. F. Hamdan, et al. (2002). "Conformational changes that occur during M3 muscarinic acetylcholine receptor activation probed by the use of an in situ disulfide cross-linking strategy." J Biol Chem **277**(3): 2247-2257.

Watanabe, T., T. Tsuchida, et al. (1999). "Anti-alpha-fodrin antibodies in Sjogren syndrome and lupus erythematosus." Arch Dermatol **135**(5): 535-539.

Waterman, S. A., T. P. Gordon, et al. (2000). "Inhibitory effects of muscarinic receptor autoantibodies on parasympathetic neurotransmission in Sjogren's syndrome." Arthritis Rheum **43**(7): 1647-1654.

Weetman, A. P. (2000). "Graves' disease." N Engl J Med **343**(17): 1236-1248.

Wess, J., N. Blin, et al. (1995). "Muscarinic acetylcholine receptors: structural basis of ligand binding and G protein coupling." Life Sci **56**(11-12): 915-922.

Whittingham, S., I. R. Mackay, et al. (1983). "Autoantibodies to small nuclear ribonucleoproteins. A strong association between anti-SS-B(La), HLA-B8, and Sjogren's syndrome." Aust N Z J Med **13**(6): 565-570.

Wink, D. A., K. S. Kasprzak, et al. (1991). "DNA deaminating ability and genotoxicity of nitric oxide and its progenitors." Science **254**(5034): 1001.

Witte, T., T. Matthias, et al. (2000). "IgA and IgG autoantibodies against alpha-fodrin as markers for Sjogren's syndrome. Systemic lupus erythematosus." J Rheumatol **27**(11): 2617-2620.

Wolin, S. L. and J. A. Steitz (1984). "The Ro small cytoplasmic ribonucleoproteins: identification of the antigenic protein and its binding site on the Ro RNAs." Proc Natl Acad Sci U S A **81**(7): 1996-2000.

Wollheim, F. A. (1999). "A humble gentleman at 100. 1951." Clin Exp Rheumatol **17**(6): 648-652.

Worley, P. F., J. M. Baraban, et al. (1987). "Characterization of inositol trisphosphate receptor binding in brain. Regulation by pH and calcium." J Biol Chem **262**(25): 12132-12136.

Xie, Q. and C. Nathan (1994). "The high-output nitric oxide pathway: role and regulation." J Leukoc Biol **56**(5): 576-582.

Xie, Q. W., Y. Kashiwabara, et al. (1994). "Role of transcription factor NF-kappa B/Rel in induction of nitric oxide synthase." J Biol Chem **269**(7): 4705-4708.

Yamaki, H., K. Morita, et al. (1998). "Cyclic ADP-ribose induces Ca^{2+} release from caffeine-insensitive Ca2+ pools in canine salivary gland cells." J Dent Res **77**(10): 1807-1816.

Yoon, Y., J. Song, et al. (2000). "Plasma nitric oxide concentrations and nitric oxide synthase gene polymorphisms in coronary artery disease." Clin Chem **46**(10): 1626-1630.

Zandbelt, M. M., J. Vogelzangs, et al. (2004). "Anti-alpha-fodrin antibodies do not add much to the diagnosis of Sjogren's syndrome." Arthritis Res Ther **6**(1): R33-R38.

Zhang, X., J. Wen, et al. (1999). "Ryanodine and inositol trisphosphate receptors are differentially distributed and expressed in rat parotid gland." Biochem J **340 (Pt 2)**: 519-527.

Zhao, Y., P. E. Brandish, et al. (2000). "Inhibition of soluble guanylate cyclase by ODQ." Biochemistry **39**(35): 10848-10854.

Zhou, D., J. A. Ursitti, et al. (1998). "Developmental expression of spectrins in rat skeletal muscle." Mol Biol Cell **9**(1): 47-61.

Zorzato, F., J. Fujii, et al. (1990). "Molecular cloning of cDNA encoding human and rabbit forms of the Ca^{2+} release channel (ryanodine receptor) of skeletal muscle sarcoplasmic reticulum." J Biol Chem **265**(4): 2244-2256.

Zoukhri, D., R. R. Hodges, et al. (1998). "Lacrimal gland innervation is not altered with the onset and progression of disease in a murine model of Sjogren's syndrome." Clin Immunol Immunopathol **89**(2): 126-133.

Zoukhri, D., E. Macari, et al. (2006). "c-Jun NH2-terminal kinase mediates interleukin-1beta-induced inhibition of lacrimal gland secretion." J Neurochem **96**(1): 126-135.

Zucchi, R. and S. Ronca-Testoni (1997). "The sarcoplasmic reticulum Ca^{2+} channel/ryanodine receptor: modulation by endogenous effectors, drugs and disease states." Pharmacol Rev **49**(1): 1-51.